The Hong Kong Polytechnic University

Department of Applied Biology & Chemical Technology

CERULOPLASMIN AND CERULOPLASMIN HOMOLOGUE HEPHAESTIN IN THE BRAIN: REGULATION OF EXPRESSION AND ROLE IN IRON TRANSPORT

YANZHONG CHANG

A THESIS SUBMITTED IN PARTIAL FULFILMENT OF THE REQUIREMENTS FOR THE DEGREE OF DOCTOR OF PHILOSOPHY

November 2003

CERTIFICATE OF ORIGINALITY

I hereby declare that this thesis in my own work and that, to the best of my knowledge and belief, it reproduces no material previously published or written nor material which has been accepted for the award of any other degree or diploma, except where due acknowledgement has been made in the text.

.....(Signed)

YANZHONG CHANG

.....(Name of Student)

Abstract of thesis entitled 'Ceruloplasmin and ceruloplasmin homologue hephaestin in the brain: regulation of expression and role in iron transport'

Submitted by

Yanzhong Chang

For the degree of Doctor of Philosophy

At the Hong Kong Polytechnic University in November 2003

ABSTRACT

Ceruloplasmin (CP) is a copper-containing ferroxidase that is essential for normal iron homeostasis. Whereas CP in plasma is produced and secreted by hepatocytes, recent study has shown that a glycosylphosphatidylinositol (GPI)-anchored form of CP is expressed on the surface of astrocytes in the brain. The precise biological role of CP remains unclear despite decades of investigation. Hephaestin (Heph) is a newly identified membrane-bound multi-copper ferroxidase necessary for iron egress from intestinal enterocytes into the circulation. The molecule is highly homologous to CP (50% identity, 68% similarity) and, significantly, all the residues involved in copper binding and disulfide bond formation in CP are conserved in Heph. Studies in this thesis demonstrated the presence of CP and identified for the first time, Heph protein synthesis in the rat brain. We determined the effects of iron status and age on expression of CP and Heph genes in different rat brain regions. We also studied the role of CP in iron release in C6 glioma cells and obtained stronger evidence for its proposed role in brain iron metabolism. In order to detect the specificity of regulation in different organs *in vivo* and *in vitro*, the effect of iron status on

iron-related metabolism proteins (ferroportin1, FP1; transferrin receptor, TfR) was examined in rat hearts and C6 glioma cells was examined. In addition, the regulation of CP, Heph, divalent metal transporter 1 (DMT1), FP1 and TfR expression by gamma-aminobutyric acid (GABA), glutamate and L-DOPA in C6 glioma cells was investigated. Studies in the thesis, also ascertain for the first time, the possibility that neurotransmitters regulate the iron metabolism though control of iron transport proteins. This thesis consists of 9 chapters, beginning with a general introduction, followed by the methodology section, and 6 chapters on results, and ends with a general discussion.

LIST OF PUBLICATIONS

JOURNAL PAPERS

1. Ke Y, Chan YY, **Chang YZ**, Qian ZM (2003) Post-transcriptional expression of DMT1 in the heart of rat. *Journal of Cellular Physiology*. 196(1):124-130. IF [Rank]: 4.845 [6/73]

2. **Chang YZ**, Yuan QP, Qian ZM (2003) Transferrin and transferrin receptor system and drug transport and delivery. *Chinese Science Bulletin* 48(3): 213-218. IF [Rank]: 0.570 [19/48]

3. **Chang YZ**, Duan SL, Qian ZM (2003) Transferrin receptor 2: current knowledge. *Progress in Biophysics & Biochemistry* 30(4): 533-537. IF [Rank]: 0.160 [259/266, 61/66]

4. Jiang DH, Ke Y, **Chang YZ**, Ho KP, Qian ZM (2002) Distribution of ferroportin1 protein in different regions of developing rat brain. *Developmental Neuroscience* 24(2-3): 94-98. IF [Rank]: 2.118 [89/197]

5. Chen YM, Qian ZM, Zhang J, **Chang YZ**, Duan XL (2002) Distribution of constitutive nitric oxide synthase in the jejunum of adult rat. *World Journal of Gastroenterology* 8(3): 537-539. IF [Rank]: 2.532 [13/45]

6. Xie JX, Tsoi YK, **Chang YZ,** Ke Y, Qian ZM (2002) Effects of ferroxidase activity and species on ceruloplasmin mediated-iron uptake by BT325 Cells. *Molecular Brain Research* 99(1): 12-16. IF [Rank]: 2.309 [76/197]

7. **Chang YZ,** Qian ZM (2002) Ceruloplasmin and brain iron metabolism. *Progress in Physiological Science* 生理科学进展 33(2): 101-105.

8. **Chang YZ,** Yuan QP, Zhou B, Qian ZM (2003) Hepcidin and iron homeostasis. *Chinese Journal of Endocrinology and Metabolism.* 中华内分泌代谢杂志 (In press).

9. Yu P, **Chang YZ,** Qian ZM (2003) Recent advances in research on stimulator of iron transporter (SFT) *Progress in Physiological Sciences.* 生理科学进展 (In press)

10. Kang YM, **Chang YZ,** Qian ZM (2003) HFE and hereditary hemochromatosis. *Chinese Journal of Pathophysiol.* 中国病理生理杂志 (in press)

11. **Chang YZ,** Ke Y, Wang XY, Ho KP, Qian ZM (2003) Iron-dependent transcriptional regulation of hephaestin expression in rat brain. *Journal of Neuroscience* (Submitted).

12. Ke Y, **Chang YZ,** Ho KP, Qian ZM (2003) Iron-independent and Age-dependent Expression of the two mRNA Isoforms of Divalent Metal Transporter 1 in Different Brain Regions of Rats. *Journal of Biological*

Chemistry (Submitted).

13. **Chang YZ,** Ke Y, Ho KP, Qian ZM (2003) Expression of ceruloplasmin homologue Hephaestin in different regions of developing brain in rats. *Molecular Brain Research* (Submitted).

14. **Chang YZ,** Ke Y, Wang XY, Ho KP, Qian ZM (2003) Effects of neurotransmitters on transferrin receptor, DMT1, ferrportin1 and hephaestin in the brain of rats. (In preparation)

15. **Chang YZ,** Ke Y, Wang XY, Ho KP, Qian ZM (2003) Effects of iron status on ferrportin1, ceruloplasmin and hephaestin in rat heart. (In preparation)

16. **Chang YZ,** Ke Y, Ho KP, Qian ZM (2003) Effects of levodopa on the expression of transferrin receptor, DMT1, and ferrportin1 and iron uptake in C6 glioma cells. (In preparation)

17. **Chang YZ,** Ke Y, DKL Lee, KP Ho, Qian ZM (2003) Effect of age and variations in dietary iron on Ceruloplasmin gene expression in rat brain. (In preparation)

18. **Chang YZ,** Ke Y, Qian ZM (2003) Regulation of ceruloplasmin gene expression by iron status and low concentration of ceruloplasmin evoke the iron uptake in C6 glioma cell. (In preparation)

CONFERENCE PAPERS

1. **Chang YZ,** Ke Y, Daniel KL Lee, Ho KP, Agnete Svendsen, Xie JX, Wang J, Yuan QP, Zhou B, Loh CN, Wang Q, Li J, Wen ZM, Du JR, Li FY, Qian ZM (2003) Effect of iron on expression of ceruloplasmin homologue hephaestin in cultured rat astrocytes. *The 3rd National Congress of Neurosciences, Qiandao, PRC, Sept. 2003*

2. **Chang YZ,** Ke Y, Daniel KL Lee, Ho KP, Agnete Svendsen, Yuan QP, Zhou B, Loh CN, Wang Q, Li J, Du JR, Xie JX, Li FY, Qian ZM (2003) Expression of ceruloplasmin homologue Hephaestin in Developing Rat Brain. *The 3rd National Congress of Neurosciences, Qiandao, PRC, Sept. 2003*

3. Ke Y, **Chang YZ,** Daniel KL Lee, Ho KP, Wang Q, Agnete Svendsen, Qian ZM (2003) Effects of ceruloplasmin on iron uptake by brain neuronal cells. *The 3rd National Congress of Neurosciences, Qiandao, PRC, Sept. 2003*

4. Ke Y, Ho KP, **Chang YZ**, Xie JX, Daniel KL Lee, Du JR, Agnete Svendsen, Yuan QP, Zhou B, Loh CN, Wang Q, Li J, Wang J, Wen ZM, Li FY, Qian ZM (2003) Iron-independent and Age-dependent Expression of DMT 1 (Nramp2/DCT1) in Different Brain Regions of Rats. *The 3rd National Congress of Neurosciences, Qiandao, PRC, Sept. 2003*

5. Qian ZM, **Chang YZ,** Ke Y, Agnete Svendsen, Daniel KL Lee, Yuan QP, Zhou B, Wang Q, Du JR, Ho KP (2003) Iron-dependent transcriptional Expression of

the Ceruloplasmin Homologue Hephaestin in Rat Brain. *The 3rd National Congress of Neurosciences, Qiandao, PRC, Sept. 2003*

6. Ho KP, Agnete Svendsen, **Chang YZ,** Ke Y, Xie JX, Daniel KL Lee, Yuan QP, Zhou B, Loh CN, Wang J, Li J, Du JR, Wang Q, Wen ZM, Li FY, Qian ZM* (2003) Expression and Distribution of the Ceruloplasmin Homologue Hephaestin in the Brain: A Immunohisto- chemistry Study. *The 3rd National Congress of Neurosciences, Qiandao, PRC, Sept. 2003*

7. Ho KP, Ke Y, **Chang YZ,** Xie JX, Daniel KL Lee, Du JR, Agnete Svendsen, Yuan QP, Zhou B, Loh CN, Wang Q, Li J, Wang J, Wen ZM, Li FY, Qian ZM* (2003) Effects of Dietary Iron on Expression of Ceruloplasmin in Rat Brain. *The 3rd National Congress of Neurosciences, Qiandao, PRC, Sept. 2003*

8. Chen YM, Duan XL, **Chang YZ,** Ke Y, Du, JR, Daniel KL Lee, Agnete Svendsen, Xie JX, Yuan QP, Zhou B, Ho KP, Loh CN, Wang Q, Li J, Wang J, Wen ZM, Li FY, Qian ZM* (2003) Effects of intracellular iron and NO on Expression of Ferroportin 1 in PC 12 cells. *The 3rd National Congress of Neurosciences, Qiandao, PRC, Sept. 2003*

9. Daniel KL Lee, **Chang YZ,** Ke Y, Ho KP, Agnete Svendsen, Yuan QP, Zhou B, Loh CN, Xie JX, Qian ZM* (2003) Ceruloplasmin Expression in Developing Rat Brain. *The 3rd National Congress of Neurosciences, Qiandao, PRC, Sept. 2003*

10. Agnete Svendsen, **Chang YZ,** Ke Y, Xie JX, Daniel KL Lee, Ho KP, Wang Q, Du, JR, Yuan QP, Zhou B, Loh CN, Li J, Wang J, Wen ZM, Li FY, Qian ZM* (2003) Effects of Iron on Expression of Ferroportin1 and Hephaestin in Rat Heart. *The 3rd National Congress of Neurosciences, Qiandao, PRC, Sept. 2003*

11. Ke Y, Duan XL **Chang YZ,** Jiang DH, Yuan QP, Li HY, Jiang H, Qian ZM* (2002) Expression of mRNAs of hephaestin and duodenal cytochrome b in rat brain. The 3rd FAONA (Federation of Asian-Oceanian Neuroscience Societies) Congress, Seoul, Korea (Sept. 28- Oct. 2, 2002), *Experimental Neurobiology* 11(2): 62.

12. Duan XL, **Chang YZ,** Ke Y, Jiang D, Yuan Q, Li H, Chan Y, Ho KP, Qian ZM* (2002) Distribution of ferroportin1 protein in different brain regions of developing rat. The 3rd FAONA (Federation of Asian-Oceanian Neuroscience Societies) Congress, Seoul, Korea (Sept. 28-Oct. 2, 2002), *Experimental Neurobiology* 11(2): 63.

13. **Chang YZ,** Ke Y, Jiang DH, Yuan QP, Li HY, Jiang H, Duan XL, Qian ZM* (2002) Expression of ceruloplasmin mRNA and iron level in developing rat brain. The 3rd FAONA (Federation of Asian-Oceanian Neuroscience Societies) Congress, Seoul, Korea (Sept. 28-Oct. 2, 2002), *Experimental Neurobiology* 11(2): 69.

14. Ke Y, **Chang YZ,** Duan XL, Qian ZM* (2002) Brain iron misregulation: one of initial causes of neurodegenerative disorders. *The 9th National Congress of*

Biophysics, Dalian, PRC (26-30 May) S5-2 pp89.

15. Ke Y, **Chang YZ,** Chan YY, Wang K, Qian ZM* (2001) Effect of iron status on DMT1 expression in different area of rat brain. *The 34th International Congress of Physiological Sciences*, Christchurch, New Zealand (26-31 August) ID No. 1050.

16. **Chang YZ,** Chan YY, Ke Y, Wang K, Qian ZM* (2001) Developmental expression of ceruloplasmin in rat brain. *The 34th International Congress of Physiological Sciences*, Christchurch, New Zealand (26-31 August) ID 359.

ACKNOWLEDGEMENTS

The investigations described in this thesis were carried out in the Laboratory of Iron Metabolism in the Department of Applied Biology and Chemical Technology (ABCT), The Hong Kong Polytechnic University.

I am especially indebted to my Chief Supervisor, Dr. Zhong Ming Qian, for his outstanding guidance, sincere encouragement, and helpful advice throughout the course of this work. It would have been impossible for me to complete this thesis without everything he did. I am also grateful to my co-supervisor, Dr. Kam-Len Daniel Lee, for his encouragement and valuable suggestions.

I am much indebted to the Departmental Research Committee of ABCT Department and the Research Committee of the Hong Kong Polytechnic University for giving me a Research Scholarship and supporting my study in this university.

I would like to thank Dr. Thomas Leung for providing the Fluostar Galaxy fluorescence plate reader to measure iron uptake experiment, Mr. CH Cheung, Miss Seral Yang and all other technicians in the Applied Biology Section of the Department of ABCT for their valuable technical assistance. I would also like to thank Dr. Ya Ke, Ms. Ying Ying Chen, Dr. Filly Cheung, Mr. Da He Jing, Mr. Yan Min Chen and Ms. Xiao Yun Wang and all other colleagues in our research group for their kind help and strong support.

With all my heart, I would like to thank my grandmother Wen Qing Si for her moral support, my parents, my wife, Shu-E Zhao, my son, Shi He Chang and my young brother and sister for their unconditional love, endless encouragement and understanding. I am also grateful to my primary school teacher, Juan Yun Sun, Prof. Yun Hui Gu and all people who encouraged and supported throughout my life.

CONTENTS

CHAPTER 1

INTRODUCTION

1.1 INTRODUCTORY STATEMENT

The aim of this chapter is to provide a general introduction to this thesis. Ceruloplasmin (CP, or the sky-blue protein) was first isolated from pig serum by Holmberg and Laurell in 1948. It is an alpha-2 glycoprotein with approximately 132 kDa molecular mass and produced by hepatocytes in the liver and secreted into the serum. CP is expressed by astrocytes in the brain, cerebellum, retina and by the epithelial cells of the choroids plexus. An alternatively spliced, glycosylphosphatidylinositol (GPI)-anchored form of CP is expressed on the surface of astrocytes. It is widely accepted that CP has an important role in iron release from the brain neuronal cells based on the original suggestion by Oskai et al. and clinical studies on aceruloplasminemia. However, the accumulated evidence shows that CP functions in brain iron metabolism, both in iron efflux from and in iron influx into the brain cells, via its ferroxidase activity. Hephaestin (Heph) is found to encode a protein with a single predicted membrane-spanning domain and extensive homology to CP. In the intestine, Heph suggests that it acts in conjunction with Ferroportin1 (FP1), or metal transporter protein-1 (MTP1) to transport iron across the basolateral membrane. FP1 is found on the basolateral side of mouse duodenal enterocytes, and several other cell types including neuron cells. DMT1 (also Nramp2/DCT1/SLC11A2) is a divalent metal transporter found in duodenal

enterocytes. Mutations in DMT1 seen in *mk* mice with microcytic anemia cause defects in iron transport from the lumen of the gut into enterocytes, and from plasma transferrin into erythroid precursors. A mammalian ferric reductase, duodenal cytochrome b (Dcytb/Cybrd1) was cloned recently from mouse duodenum and proposed to function as a ferric reductase, which converts ferric iron to ferrous iron. DMT1 can transports non-heme, ferrous iron into the enterocytes of the gut. Although much is known about iron absorption and efflux in enterocytes in the gut, the mechanisms controlling iron homeostasis in neural cells in the central nervous system (CNS) is still not well understood.

1.2 CERULOPLASMIN

CP is a copper-containing ferroxidase that is essential for normal iron homeostasis. Whereas CP in plasma is produced and secreted by hepatocytes, in the brain a GPI-anchored form of CP is expressed on the surface of astrocytes and leptomeningeal cells (Patel and David, 1997; Mittal et al., 2003). Loss-of-function mutations in the CP gene will induce hereditary aceruloplasminemia. Until now the effect of CP on iron metabolism has not been established (Qian and Ke, 2001).

1.2.1 Molecular Structure of Ceruloplasmin

1.2.1.1 Constitution of Ceruloplasmin

The human CP consist of a single polypeptide chain of 1046 residues and 4 asparagine-linked oligosaccharide chains (Takahashi et al., 1984). It has an

isoelectric point of about 4.4 and an absorption peak at 605 nm (Shreffler et al., 1967). The reported molecular weights are very similar, ranging between 100-135 kDa (Table 1-1). With advanced technology, the molecular weight of human CP was confirmed to be 132 kDa (Takahashi et al., 1984). At the same time, SDS-PAAG electrophoresis demonstrated that human serum (from adults and newborns) contains three CP-immmunoreactive polypeptides with apparent molecular weights of 200, 135, and 115 kDa; their concentrations were proportional to total oxidase activity (Sato et al., 1990). Serum CP isoforms with varying molecular weight were revealed in other studies (Chowrimootoo et al., 1996; Davis et al., 1996). SDS-electrophoresis and Western-blot analysis revealed two bands corresponding to 132 and 125 kDa, respectively.

The rat CP molecular weight determined by a molecular sieve column was 124 kDa (Manolis and Cox, 1980). CP of other species was also studied, such as pig (Ryden, 1972), rabbit (Morell et al., 1968; Ryden, 1972; Mainero et al., 1996), horse (Ryden, 1972; Medda et al., 1987), sheep (Calabrese et al., 1988), bovine (Calabrese et al., 1981), chicken (Starcher and Hill, 1966; Machonkin et al., 1999) and goose (Hilewicz-Grabska et al., 1988). These CP molecular weights are indicated in table 1-1.

1.2.1.2 X-ray Crystal Structure

The human CP is in general less complex structurally than oligomeric blue oxidases (Saenko et al., 1994) and is unique in being able to oxidize both organic and inorganic substrates (Gitlin et al., 1992).

Table 1-1. The relative molecular weight of CP from different species

Source	Relative molecular	References
Human	160 000	Kasper and Deutsch 1963
	110 000	Ryden 1972
	134 000	Ryden and Bjork 1976
	135 000	Noyer et al. 1980
	130 000	Arnaud et al. 1988
	132 000	Takahashi et al. 1984
Rat	124 000	Manolis and Cox 1980
	131 000	Weiner and Cousins 1983
	126 000	Ryan et al. 1992
Pig	102 000	Ryden 1972
Horse	106 000	Ryden 1972
	115 000	Medda et al. 1987
Goose	121 000	Hilewica-Grabska et al. 1988
Chicken	133 000	Stevens et al. 1984
	140 000	Calabrese et al. 1988
Bovine	125 000	Calabrese et al. 1981
Rabbit	106 000	Ryden 1972
	125 000	Mainero et al. 1996
Sheep	130 000	Calabrese et al. 1988

In 1976, Ryden and Bjork first postulated that the copper atoms in the protein are distributed as two type 1 or 'blue' coppers, one type 2 ('non-blue'), one type 3 (binuclear) centers. A unique type 4 (mononuclear) Cu^{+} has also been postulated to fulfill the total complement. Type 1 copper is responsible for the unusually strong electronic absorption around 600nm and is paramagnetic. Type 2 copper is essentially silent in the optical spectrum, but contributes to the EPR spectrum with a

lineshape quite typical of regularly coordinated tetragonal complexes (Musci et al., 1993b). Moreover, it is shielded from the aqueous environment (Saenko et al., 1994). Type 3 copper consists of a pair of metal ions, antiferro-magnetically coupled to give an EPR-silent species. It absorbs in the near-UV region of the electronic spectrum, giving a shoulder around 30nm (Musci et al., 1993a). The X-ray structure of human serum CP has been solved at a resolution of 3.1 Å. The structure reveals that the molecule is comprised of six plastocyanin-type domains arranged in a triangular array. There are six copper atoms: three form a trinuclear cluster sited at the interface of domains 1 and 6. And there are three mononuclear sites in domains 2,4, and 6. Each of the mononuclear coppers is coordinated to one cysteine and two histidine residues, and those in domains 4 and 6 also coordinate to a methionine residue. In domain 2, the methionine is replaced by a leucine residue, which may form van der Waals-type contacts with the copper. The trinuclear center and the mononuclear copper in domain 6 form a cluster essentially the same as that found in ascorbate oxidase, strongly suggesting an oxidase role for CP in the plasma (Fig. 1-1) (Musci et al., 1999; Zaitsev et al., 1999; Qian and Ke, 2001).

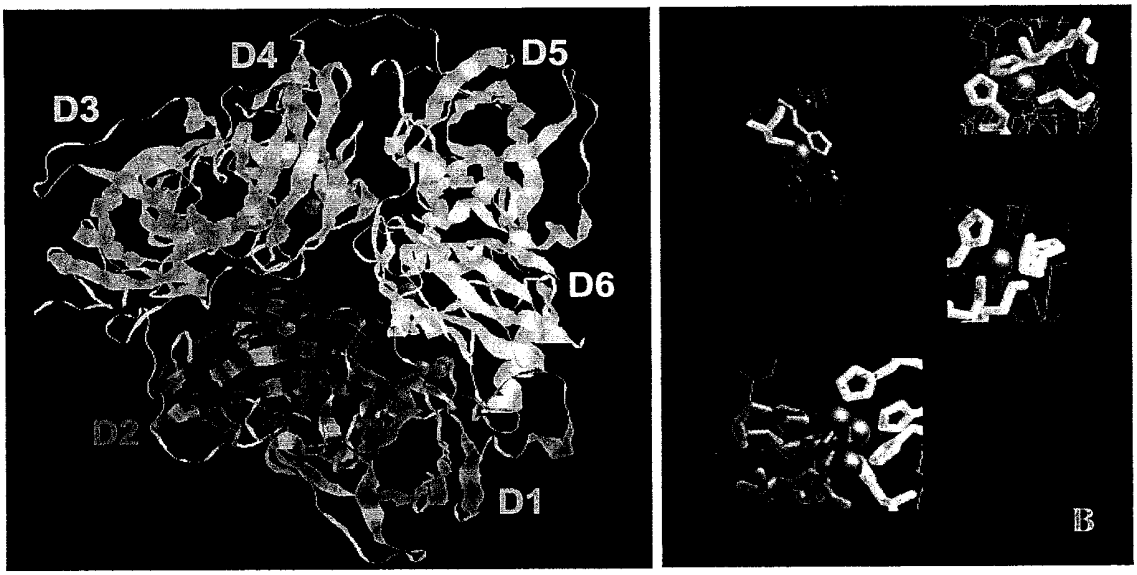

Fig. 1-1. The X-ray crystal structure of human serum ceruloplasmin. A: The six domains are shown in different colors and coppers are shown as red. B: Copper binding sites in ceruloplasmin. (From Qian anz Ke, 2001)

1.2.1.3 Forms of Ceruloplasmin

There are two forms of CP. One is the secreted form (Klomp and Gitlin, 1996; Loeffler et al., 1996) as mentioned above. Another one is the glycosylphosphatidylinositol (GPI)-anchored form of CP (Patel and David, 1997; Salzer et al., 1998; Fortna et al., 1999). The reported molecular weights of the GPI-anchored CP in astrocytes, Schwann cells, and Sertoli cells were 140 kDa (Salzer et al., 1998) and 135 kDa (Fortna et al., 1999) respectively. The mature GPI-CP protein has 1065 amino acids compared with 1040 amino acids for secreted ceruloplasmin (Fig. 1-2). The C-terminal 5 amino acids of secreted CP are replaced with 30 alternative amino acids. The alternative stretch of 30 amino acids is predominantly non-polar, as it is for all known GPI-anchored proteins, with a large fraction of hydrophobic residues (Fig. 1-2). In addition, this stretch of amino acids contains, proximally, a potential site for GPI anchor addition. GPI anchors are added to a small amino acid (denoted the ω amino acid) upstream of the non-polar C-terminal signal peptide, with concomitant cleavage of the signal peptide (Udenfriend and Kodukula, 1995). The first amino acid of the alternative peptide, the alanine, is a good candidate for the ω position. GPI anchor addition also requires small amino acids immediately following the ω amino acid, which are denoted the ω^{+1} and ω^{+2} amino acids. The serines immediately following the alanine are ideal candidates for these positions. Thus, it appears that this alternatively spliced CP with its alternative C-terminal tail satisfies all the known requirements for GPI anchor addition (Patel et al., 2000).

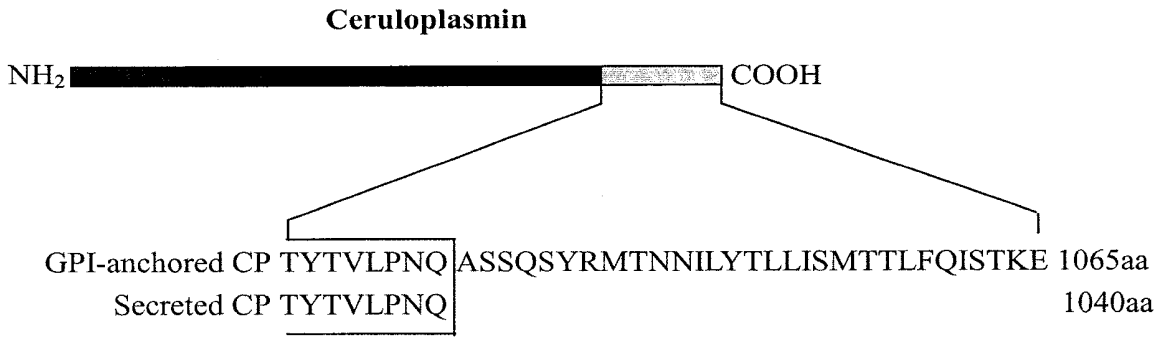

Fig. 1-2. Compare of the C-terminal of GPI-anchored CP and Secreted CP

1.2.2 Ceruloplasmin Synthesis and Distribution

1.2.2.1 Secreted Ceruloplasmin

CP is synthesized in a variety of organs such as the testes, placenta, yolk sac (Aldred et al., 1987b), heart (Linder and Moor, 1977), uterus, lung (Fleming and Gitlin, 1990), lymphocytes (Pan et al., 1996), mammary gland (Jaeger et al., 1991) and synovium (Dixon et al., 1988). But the main synthesis tissue is liver. The hepatocytes synthesize and secrete CP (secreted from) into the circulation and the concentration is about 350μg/ml serum (Lamb and Leake, 1994).

Factors reported to cause changes in the synthesis of CP are copper, hormones and leucocytic endogenous mediator (Weiner and Cousins, 1983). Copper does not affect the rate of synthesis or secretion of apoceruloplasmin (apoCP) (Nakamura et al., 1995), but failure to incorporate copper during biosynthesis results in an unstable protein lacking oxidase activity (Percival and Harris, 1990; Gitlin et al., 1992). In addition, the presence of copper in CP was reported to increase its longevity in the serum of animals (Weiner and Cousins, 1983).

Sertoli cells (Fortna et al., 1999) and placental cells (Danzeisen et al., 2000) express the GPI-anchored CP. This form of CP may have a role of enhancing the iron uptake by the seminiferous tubule in the male and in fetal circulation in pregnancy.

1.2.2.2 Ceruloplasmin in the Central Nervous System

Recent studies show that the mammalian brain has the ability to express CP. In 1988, Mollgard et al (Mollgard et al., 1988) investigated the distribution and possible origins of plasma proteins in the human embryonic and fetal brain at different stages of development. They localized CP expression to astrocytes and neurons in the brain. Zahs et al (Zahs et al., 1993) characterize the CP is synthesized and secreted by cultured rat glial cells. Recently, Gitlin and colleagues (Klomp et al., 1996; Klomp and Gitlin, 1996) analyzed CP gene expression in human and murine CNS. They revealed abundant CP gene expression in specific populations of glial cells associated with the brain microvasculature, surrounding dopaminergic melanized neurons in the substantia nigra and within the inner nuclear layer of the retina. The data presented by others (Patel and David, 1997; Salzer et al., 1998; Patel et al., 2000) shows that the CP detected in the central nervous system by these investigators is predominantly the GPI-anchored form of CP. RNase protection analysis shows that the GPI-anchored form, produced within the brain, is the major form of CP in this organ. The GPI-anchored form and serum CP have ferroxidase activity. Since serum CP does not cross the Blood-Brain Barrier (BBB) and the levels of the secreted form of CP in the cerebrospinal fluid (CSF) are extremely low (1μg/ml, (Del Principe et al., 1989); 1.566μg/ml, (Loeffler et al., 1994). GPI-anchored form of CP is a major functional form. The leptomeningeal cells, which cover the surface of the brain, also express GPI-CP. The expression of GPI-CP on the surface of these cells increases with postnatal development and is regulated *in vitro* by cell density, time in culture and various extracellular matrix molecules (Mittal et al., 2003).

1.2.3 Functions of Ceruloplasmin

1.2.3.1 Physiological Functions of Ceruloplasmin

The precise physiological function of CP remains controversial, although many workers tend to consider the protein multifunctional (Percival and Harris, 1990; Saenko et al., 1994). At least four main functions have been attributed to CP: in copper transport, ferroxidase activity, amine oxidase activity and as an antioxidant in the prevention of the formation of free radicals in serum (Zaitsev et al., 1999) and in CSF (Mittal et al., 2003). The following points summarize the physiological functions attributed to CP.

1) The ferroxidase activity is considered pivotal in mobilizing iron for transport via the protein transferrin (Tf) (Saenko et al., 1994) (detailed explain to see 1.2.3.2).

2) Its ferroxidase activity also eliminates free iron from the plasma, thereby protecting blood and membrane lipids from peroxidative damage. This is supported by its ability to protect phospholipids in vascular walls and erythrocyte membranes from peroxidation as well as DNA from scission. Thus, it acts as antioxidant defense (Saenko et al., 1994). Moreover, it can partially protect rat heart against myocardial injury induced by oxygen free radicals (Chahine et al., 1991).

CP's antioxidant effect may involve:

A. Donating copper to tissues for the synthesis of copper containing antioxidant

enzymes;

B. Directly scavenging superoxide anions; or

C. Oxidatively incorporating Fe^{2+} into Tf or serum ferritin, thus rendering the iron redox inert.

The last function is of particular importance because CP can oxidize the ferrous complex back to the less reactive ferric state. Moreover, it effectively catalyzes the oxidation of Fe^{2+} while directly reducing molecular oxygen ($O_2^{\cdot}$, $OH^{\cdot}$, H_2O_2), which are potentially deleterious to biomolecules (Ryan et al., 1992). However, the findings that heat-denatured CP was also able to inhibit some Fe^{2+} dependent radical formation lead to the argument that the chain-breaking antioxidant effect of CP is independent of its catalytic ferroxidase activity (Atanasiu et al., 1998). Other researchers have pointed out that CP "denaturation" does not always imply "inactivation", as far as the oxidase activity is concerned (Calabrese et al., 1988). Thus the ferroxidase activity is still important for CP's antioxidant effect.

Sever as an antioxidant; CP can inhibit lipid peroxidation induced by iron and copper ions (Olson and Holtzman, 1980; Gutteridge, 1983; Saenko et al., 1994). In the latter, protection is attributed to non-specific copper-binding sites on the CP molecule (Gutteridge, 1983). CP inhibits only those lipid peroxidations that are induced by a chemical redox system (Olson and Holtzman, 1980; Gutteridge, 1983; Miura et al., 1993; Saenko et al., 1994). No antioxidant effect of CP is observed when free radicals are formed in the absence of redox processes, e.g., upon illumination with UV-light (Al-Timimi and Dormandy, 1977; Saenko et al., 1994). This antioxidant property of CP may be of particular importance in protecting the brain from damage

by active oxygen radicals. Since the brain contains a large amount of polyunsaturated fatty acids and metabolizes at a very high rate, it is very susceptible to free radical attacks (Beard et al., 1993a).

During a variety of disease and stress states, human serum CP levels increase. Therefore, plasma CP has been a diagnostic marker for assessing the prevalence of brief inflammations that often accompany certain cancers, brain tumors (Casaril et al., 1989; Senra Varela et al., 1997), rheumatoid arthritis, tuberculosis, hypoxia, psoriasis, biliary cirrhosis and liver diseases. It is also noted that CP level will rise during pregnancy (Wolf, 1982; DiSilvestro et al., 1988; Saenko et al., 1994). CP is extremely susceptible to oxidative modification *in vitro* and this may add to the susceptibility to proteolytic attacks (Arnaud et al., 1988; Calabrese et al., 1988). Such susceptibility has been a major obstacle in the study of the physicochemical characteristics of the protein. It is well known that once purified, CP easily undergoes conformational changes that lead to irreversible modifications of its spectroscopic properties (Musci et al., 1990).

3) As the major copper-containing component of plasma, CP is a donor of copper to extrahepatic tissues;

4) Its amine oxidase activity has the potential to control levels of biogenic amines in plasma, cerebral, spinal and interstitial fluids. It is suggested that CP regulates fluid levels in the catalytic activity of CP on CNS amines, such as dopamine, adrenaline and serotonin. However, a role for CP in the metabolism of these substances has not been established. Moreover, since the pH optimum for

CP-catalyzed oxidation of adrenaline, p-phenylendiamine, catechol and dimethy-p-phenylendiamine is close to 5 (Ryan et al., 1992), and a higher pH results in a sharp decline in activity, it is unlikely that CP regulates these amines *in vivo* (Saenko et al., 1994). However, other researchers have suggested CP could have significant physiological impact on the brain cells. They based on the reactions at which CP produces (DHI)-melanin from 5,6-dihydroxyindole and THP-melanin from tetrahydropapaveroline at pH 7.4 (Rosei et al., 1998).

5) With sequence homology to blood clotting factors V and VIII and an ability to bind to platelets, CP may take part in blood clotting or its regulation (Saenko et al., 1994; Pan et al., 1995);

6) As a deaminase;

7) With superoxide dismutase-like activity (Goldstein et al., 1979; Aldred et al., 1987b), CP can inhibit superoxide-induced lipid peroxidation, but apparently does not possess superoxide dismutase activity (Gutteridge, 1983; Weiner and Cousins, 1983);

8) As an acute phase protein in the inflammatory response (Aldred et al., 1987b; Fleming et al., 1991);

9) For tissue angiogenesis (Gitlin et al., 1992); and

10) As an endogenous neuronal depolarizing factor. CP induced a rapid and sustained

membrane depolarization in neuroblastoma cells. The depolarizing effect of CP was not due to an enhanced Ca2+ or Na+ influx but seemed to result from a reduced K+ efflux since CP significantly inhibited a TEA-sensitive delayed rectifier K+ channel (Wang et al., 1995b).

Many of the projected functions of CP are related to the six copper atoms bound to the peptide chain. Copper centers in CP have been the focus of much of the research on this protein. Also, it is postulated that the limiting step in a CP-catalyzed reaction is a function of the 'blue' copper center and not the affinity of the substrate for its binding site on the protein (Zaitsev et al., 1999).

1.2.3.2 Ceruloplasmin Ferroxidase Activity and Iron Transport

A unique feature of CP is its ability to oxidize Fe^{2+} to Fe^{3+} (Kawanami et al., 1996). Osaki et al. first demonstrated the ferroxidase activity of CP in 1966 (Osaki, 1966). It has been stated that iron is the best substrate for CP (Ryan et al., 1992). As a substrate, Fe^{2+} has the lowest apparent K_m and the highest V_{max} of any of CP's multiple substrates. At neutral pH, CP increases the rate of the non-enzymatic oxidation of serum Fe^{2+} in humans by 10- to 100-fold. It catalyzes the oxidation of 4 atoms of Fe^{2+} with the concomitant production of water from molecular oxygen. This prevents the free radical formation that occurs during spontaneous ferrous oxidation (de Silva and Aust, 1992).

$$4Fe^{2+} + O_2 + 4H^+ \xrightarrow{CP} 4Fe^{3+} + 2H_2O$$

Another role of CP may be to facilitate loading of iron into ferritin. Investigators have proposed that the mechanism by which iron is placed into ferritin is catalyzed by CP and found that ferritin plus CP is an effective 'antioxidant'.

When Tf is present, it binds the ferric product and thus protects it from subsequent reduction. The presence of both CP and Tf in the plasma normally provides considerable antioxidant protection by preventing iron-induced free radical formation (Saenko et al., 1994; Logan, 1996). Human cells store iron in the ferric state in ferritin and haemosiderin. When the body needs iron, the ferric iron is reduced and moved to the outside of the cells. Because spontaneous ferrous oxidation cannot provide a sufficiently large supply of ferric iron for binding to Tf and subsequent distribution to the body, CP-catalyzed oxidation is still required (Logan, 1996).

Thus, by catalyzing the oxidation of Fe^{2+}, CP promotes the incorporation of iron into Tf and into ferritin. A specific ability of CP to stimulate iron mobilization from the stores in the liver of copper-deficient animals may be related to its powerful ferroxidase activity and links CP with iron metabolism. At the same time, the ferroxidase activity removes 'free' or unbound Fe^{2+} and Fe^{3+} from caches in cell membranes or serum, preventing their participation in free-radical generating reactions (Fig. 1-3).

Thus, the 'free iron' concentrations in the plasma are related to the copper-binding properties and ferroxidase activities of CP. Because copper atoms in CP have no

access to O_2 through diffusion, CP must protect cells from this the progenitor of free radical reactions through other mechanisms. As mentioned above, CP is capable of increasing the rate of incorporation of iron into Tf and ferritin, effectively eliminating unbound iron in plasma as fast as it forms. This putative and protective role of the ferroxidase activity in antioxidant action of CP that extends from membrane lipids to DNA has been confirmed by a number of laboratories (Saenko et al., 1994).

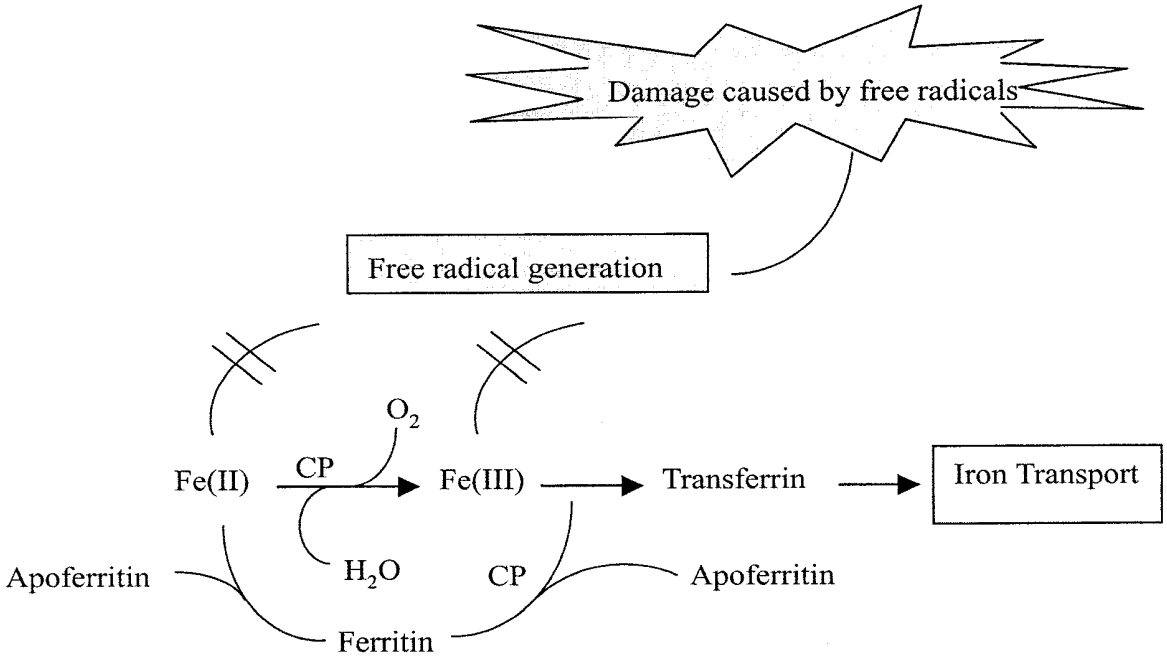

Fig. 1-3. The role of ferroxidase activity of ceruloplasmin in iron transport and in the prevention of free radical processes involving Fe(II) or Fe(III). Ceruloplasmin catalyzes oxidation of Fe(II) to Fe(III) in presence of O2 (which undergoes four-electron reduction to H_2O without oxygen redicals released), which enables Fe(III) to attached to transferrin or to ferritin. CP removes unbound Fe(II) and Fe(III) from cell membranes or serum thus preventing their articipation in free-radical generating reactions.

1.2.4 Regulation of Ceruloplasmin Gene Expression in the Brain

1.2.4.1 Ceruloplasmin Gene

The CP gene was mapped to chromosome 8 in humans (Koschinsky et al., 1987) and chromosome 2 in rats (Miura et al., 1993). The human CP gene region spanned about 50 kb and was composed of 19 exons and 18 introns. The lengths of exons and introns range from 107 to over 267 bp and from 0.44 to 10.0 kb, respectively. The translation initiation codon and the termination codon were located in exons 1 and 19, respectively. The nucleotide sequences of the introns are in the region around the intron/exon boundaries for 24-220 bp. All the sequences around the intron/exon boundaries were consistent with the 5' and 3' consensus sequences for splice junctions of transcribed genes. Putative lariat sequences identified between -17 and -42 nucleotides from the 3' splice junction for all 18 introns (Daimon et al., 1995). The nucleotide of CP mRNA is about 3321bp (NM-000096).

Rat CP nucleotide is 3700 bp (NM-012532). The derived amino acid sequence of rat CP is 93% homologous to the corresponding human sequence and contains a 19-amino acid leader peptide plus 1040 amino acids of mature protein. Southern blot analysis indicates that the CP gene exists as a single copy in the rat haploid genome (Fleming and Gitlin, 1990). The GPI-anchored form of CP mRNA is consists of 3535bp nucleotides (AF202115). The GPI-anchored form of CP is generated by alternative RNA splicing. The splicing occurs downstream of exon 18 and replaces the C-terminal 5 amino acids of the secreted form with an alternative 30 amino acids that signal GPI anchor addition (Patel et al., 2000).

1.2.4.2 Ceruloplasmin Gene Expression in the Brain

Systemic research on CP gene expression in the brain has appeared in recent papers (Klomp et al., 1996; Klomp and Gitlin, 1996). RNA blot analysis and RNase protection studies demonstrate CP-specific transcripts in the cerebellum, cortex, basal ganglia, corpus callosum and substantia nigra of the human brain, and biosynthetic studies reveal CP synthesize and secrete in these same regions. *In situ* hybridization of central nervous system tissue utilizing CP cRNA probes reveals abundant CP gene expression in specific populations of glial cells associated with the brain microvasculature, surrounding dopaminergic melanized neurons in the substantia nigra and other regions of the human brain, i.e. sections of globus pallidus with myelinized fibre bundles. In the caudate nucleus, CP-specific transcripts were detected in ependymal cells lining the lateral ventricle and in glial cells in the subependymal glial membrane. In endothelial cells and neurons, no CP mRNA detected. Taken in the context of the clinical and pathological features observed in patients with aceruloplasminemia, these data reveal that glial cell-specific CP gene expression is essential for iron homeostasis and neuronal survival in the human CNS.

In the rat brain, abundant CP gene expression was also detected in the retina and the brain regions (cortex, cerebellum, and midbrain.) as well as the epithelium of the choroid plexus. The cell-specific expression of CP mRNA in the adult brain was detected in epithelial cells of the pia-arachnoid, the ependymal cells lining the ventricles, the choroid plexus and astrocytes in close association with basal ganglia cerebral microvasculature. However, some astrocytes not obviously associated with

the microvasculature were found to express CP mRNA but in no specific signal observed in neurons.

Analysis of primary cell cultures confirmed that astrocytes express CP mRNA and biosynthetic studies revealed synthesis and secretion of CP by glial but not neuronal cells (Zahs et al., 1993; Klomp et al., 1996; Patel et al., 2000).

The evidence indicate that a membrane-associated, GPI-anchored form of CP is expressed by leptomeninges: (1) cell surface staining with the mAb1A1 is markedly reduced after cultured cells or tissue sections of the brain were incubated with PI-PLC; (2) the presence of the mRNA for GPI-CP detected by RT-PCR; and (3) metabolic labeling of leptomeningeal cells followed by immunoprecipitation with mAb1A1 yielded a 135-kDa band, providing evidence that GPI-CP is synthesized by leptomeningeal cells (Mittal et al., 2003).

1.2.4.3 Regulation of Ceruloplasmin

At present, the mechanism of regulating CP gene expression in the brain is not very clear. In peripheral the factors of inflammation (Gitlin, 1988; Fleming et al., 1991), interferon, IFN-γ (Mazumder and Fox, 1999; Sampath et al., 2003), endotoxin (Yang et al., 1996) and ovarian cancers (Hough et al., 2001) can lead to increased CP gene expression. This supports ceruloplasmin's critical role in host defense against oxidative damage, infection and injury (Yang et al., 1996). Interleukin (IL)-1 can regulate the serum CP (Cousins and Leinart, 1988). IL-1beta can also increase CP mRNA expression and induce two CP peaks at 8 and 20 h, while IL-6 has little effect

in HepG2 cells (Daffada and Young, 1999). Transcript-selective translational silencing by gamma interferon is directed by a novel structural element in the CP mRNA 3' untranslated region (Sampath et al., 2003). Administration of the synthetic glucocorticoid hormone, dexamethasone (2 μg/g body wt), to rats resulted in an increase in CP mRNA on Days 3-7 that was accompanied by an increase in serum CP activity that reached statistical significance on Day 10. Exogenous thyroxin (T4) (2 μg/g body wt) significantly increased CP mRNA 24 hours after administration. Serum CP activity was also significantly elevated by the early neonatal administration of T4. Furthermore, gestational hypothyroidism resulted in a significant decrease in CP activity after postnatal Day 3. These data suggest a role for thyroid hormone and possibly glucocorticoids in the normal developmental regulation of CP (Fitch et al., 1999). Thomas et al. showed that the CP RNA level is closely related to the estrous cycle; there is the maximum expression of CP at estrous (Thomas et al., 1995). An increased rate of CP synthesis was also found in study of the developmental in mice lung (Yang et al., 1996), in the liver during ontogenesis (Puchkova et al., 1994). Insulin was also observed to function as a bidirectional, condition-dependent regulator of hepatic cell CP expression was also observed (Seshadri et al., 2002).

The neonatal rat pups were injected with 2 μg 13-cis-retinoic acid (RA)/g body wt on postnatal day (PND) 1. Serum CP activity and hepatic CP mRNA were measured over the next 3 weeks in RA-treated and vehicle-treated controls. Serum CP activity increased 2.5-fold 24 h after RA administration. However, hepatic CP mRNA was not elevated during this period, suggesting that the action of RA on CP activity was the result of post-transcriptional changes (Song and Levenson, 1997). Retinoid can

also induce delayed CP gene expression in vascular smooth muscle cells. Therefore the CP gene was considered a retinoid-response gene (Chen et al., 2001).

A number of factors can induce change in CP gene expression. However, little is known about the cellular and molecular mechanism(s) involved. Mukhopadhyay et al. reported that iron chelators increase CP mRNA expression and protein synthesis in human hepatocarcinoma HepG2 cells. Furthermore, the increase in CP mRNA is due to the increased rate of transcription. They cloned the 5'-flanking region of the CP gene from a human genomic library. A 4774-base pair segment of the CP promoter/enhancer driving a luciferase reporter was transfected into HepG2 or Hep3B cells. Iron deficiency or hypoxia increased luciferase activity by 5 to10-fold compared with untreated cells. Examination of the sequence showed three pairs of consensus hypoxia-responsive elements (HREs). Deletion and mutation analysis showed that a single HRE was necessary and sufficient for gene activation. The involvement of hypoxia-inducible factor-1 (HIF-1) was shown by gel-shift and supershift experiments that showed HIF-1alpha and HIF-1beta binding to a radiolabeled oligonucleotide containing the CP promoter HRE. These results are consistent with *in vivo* findings that iron deficiency increases plasma CP and provide a molecular mechanism that may help to understand these observations (Mukhopadhyay et al., 1998; Mukhopadhyay et al., 2000).

In the CNS, the change of CP expression is found in the study of neurodegenerative disorders (NDs). In Alzheimer's disease (AD) hippocampus, entorhinal cortex, frontal cortex, and putamen, Parkinson's disease (PD) hippocampus, frontal, temporal, and parietal cortices, and Huntington's disease (HD) hippocampus, parietal

cortex, and substantia nigra the mean CP concentrations were significantly increased vs. elderly normal controls (Loeffler et al., 1996). In PD disease, the ferroxidase activity reduced in CSF (Boll et al., 1999). But in AD the CP of CSF is increased (Loeffler et al., 1994). The inflammation can also induce an increasing the brain CP gene expression (Kalmovarin et al., 1991). The optic nerve crush increased CP gene expression. The possible role of CP in inhibiting reaction oxygen species in the retina after injury was suggested (Levin and Geszvain, 1998; Chen et al., 2003b). The neurotransmitter has a relationship with brain CP and iron. In L-DOPA treated PD patients, CP concentration in the CSF increases about 40% (Boll et al., 1999). The expression of GPI-CP on the surface of leptomeningeal cells increases with postnatal development and is regulated *in vitro* by cell density, time in culture, and various extracellular matrix molecules (Mittal et al., 2003).

In the present study, great attention will be paid to the regulation of CP gene expression in brain and brain cells.

1.3 HEPHAESTIN

1.3.1 Hephaestin Gene and Sex-linked Anemia

Sex-linked anemia (*sla*) is an X-linked disorder of the mouse that is characterized by a microcytic, hypochromic anemia (Bannerman and Cooper, 1966). Early studies indicated that the anemia was due to iron deficiency rather than to a problem with erythroid cell development (Edwards and Bannerman, 1970), and this was supported by the demonstration that the anemia could be completely corrected by the parenteral

administration of iron (Bannerman and Cooper, 1966). In contrast, the anemia was refractory to oral iron treatment. The differential response to parenteral and oral iron suggested that these mice had a defect in intestinal iron absorption, and subsequent studies showed that this was indeed the case (Pinkerton and Bannerman, 1967). Affected animals are able to absorb iron from their diet across the luminal brush border normally, but the subsequent transfer across the basolateral membrane and into the circulation is impaired (Manis, 1971). As a result, iron accumulates in the intestinal epithelial cells and is subsequently lost from the body when these cells are sloughed at the tip of the villus. Body tissues other than the small intestine are deficient in iron in the *sla* mouse (Russell, 1979). Early studies indicated that the *sla* gene lay on the position close to the microsatellites DXMit16 and DXMit96 based on the analysis of intraspecific crosses (Anderson et al., 1998). These mapping data were refined further by ancestral chromosome mapping and by analyzing a mouse strain with a translocation in the candidate region (Vulpe et al., 1999). The Heph gene was a CP homolog that mapped to a region of the human X chromosome that was syntenous with the *sla* region in the mouse. Subsequent analysis revealed that this gene was deleted in the *sla* mouse and that exons 10 and 11 were missing (Vulpe et al., 1999). This deletion segregated perfectly with the *sla* anemia.

1.3.2 Characteristic of Hephaestin

Hephaestin is highly homologous to CP (50% identity, 68% similarity) and, significantly, all the residues involved in copper binding and disulfide bond formation in CP are conserved in Heph (Vulpe et al., 1999). Unlike CP, however, Heph is an integral membrane protein with a single membrane-spanning domain at

its C-terminus. The well-defined domain organization of CP appears to be conserved in Heph and Syed *et al.* have proposed a structure for the protein based on available crystal structure for CP (Syed et al., 2002). CP has a ferroxidase activity that likely facilitates iron export from the reticuloendothelial system and various parenchymal cells to the plasma (Lee et al., 1968; Harris et al., 1999), and it is very likely that Heph plays a similar role in intestinal enterocytes. The defect in Heph in *sla* mice is a large in-frame deletion that removes a number of highly conserved residues, including several involved in copper binding and disulfide bond formation (Vulpe et al., 1999). Thus the truncated Heph protein that these mice produce would be expected to exhibit negligible or severely reduced ferroxidase activity. In addition, Heph from both an intestinal cell line and enterocytes is capable of oxidizing paraphenylenediamine (PPD), like CP in plasma. These data combined with the *sla* phenotype suggest that Heph is a multicopper oxidase that plays a central role in whole body iron homeostasis due to its involvement in intestinal iron export at the basolateral membrane of duodenal enterocytes (Chen et al., 2003a).

1.3.3 Distribution and Role of Hephaestin

The expression pattern of Heph is unique among molecules of iron homeostasis. It is expressed in a limited number of tissues, but is found at high levels throughout the small intestine and intestine cell line (Thomas and Oates, 2002; Fleet et al., 2003; Linder et al., 2003), to a lesser extent in the colon, and weakly in a few other tissues such as brain, spleen, lung and placenta (Vulpe et al., 1999; Frazer et al., 2001). The high expression of Heph in the duodenum is consistent with it playing a primary role in intestinal iron transport, and this is a feature it shares with other important

intestinal iron transport molecules including DMT1, FP1 and Dcytb (Gunshin et al., 1997; Abboud and Haile, 2000; Donovan et al., 2000; McKie et al., 2000; Frazer et al., 2001; McKie et al., 2001; Frazer et al., 2003). Within each region of the intestine, Heph expression is restricted to the differentiated cells of the villus and it is not expressed at an appreciable level in the intestinal crypts (Vulpe et al., 1999; Frazer et al., 2001; Stuart et al., 2003). This again is consistent with a role in intestinal iron transport as this function is restricted to the differentiated enterocytes. The subcellular distribution of Heph is intriguing. Immunohistochemical studies have shown that the protein is located at an intracellular, supranuclear site, rather than on the plasma membrane (Frazer et al., 2001; Simovich et al., 2002). It is possible that there is an intracellular reservoir of Heph from which protein is trafficked to the basolateral in times of high iron demand, such as under iron deficient conditions. Alternatively, Heph may function in the oxidation of iron at an intracellular site. More detailed localization and functional studies are required to resolve these issues.

Heph has only a single transmembrane domain, so it also is unlikely to be able to transport iron itself. The FP1 is expressed at high levels on the basolateral membranes of intestinal epithelium expected to be involved in iron efflux. But no studies have yet demonstrated a clear interaction between Heph and FP1 in the small intestine (Anderson et al., 2002a).

Other CP homologues may also be involved in cellular iron export in other tissues. The placenta is an organ that must vectorially transport large amounts of iron to meet the demands of the growing fetus, and although CP has been suggested to play a role in this process, it was not able to stimulate iron release from a placental cell line

(Danzeisen et al., 2000). However, an endogenous CP-like protein with ferroxidase activity could be detected in these cells. Like Heph, this molecule appears to be membrane bound, but its smaller size suggests that it is a novel protein. The other intriguing characteristic that the placental oxidase shares with Heph is an intracellular, perinuclear location, but the precise compartment to which it localizes has yet to be identified (Danzeisen et al., 2000; Danzeisen et al., 2002).

1.3.4 Regulation of Hephaestin Gene Expression

Because the Heph mRNA does not possess an IRE structure, the transcription is thought to be important for the regulation of Heph gene expression. Studies in rodents have shown that the expression of Heph mRNA is increased to a small degree under iron deficient conditions and decreased with iron loading (Frazer et al., 2001; Sakakibara and Aoyama, 2002). However, no iron-dependent regulation of the Heph gene expression was observed in hereditary hemochromatosis (HHC) patients (Rolfs et al., 2002). Recent study showed that Heph and FP1 expression responds to systemic rather than local signals of iron status (Chen et al., 2003a; Frazer et al., 2003). The change of Heph protein response to iron status is larger than mRNA, so the post-translational modification of Heph may play a significant role (Anderson et al., 2002a). Taken together, however, the current evidence suggests that Heph is not highly regulated in response to iron requirements. The small amount of regulation observed also needs to be considered against the background of a high basal expression of Heph.

A further point worth considering is the possible regulation of Heph by intracellular

copper levels. Studies in Caco-2 cells have shown an increase of Heph mRNA with copper loading (Han and Wessling-Resnick, 2002) and the placental oxidase is also stimulated by copper (Danzeisen et al., 2002), but the physiological relevance of these observations needs to be clarified. No other factor affecting the Heph expression study was observed.

1.4 PROTEINS RELATED TO IRON METABOLISM

1.4.1 Transferrin

Tf is an 80 kDa glycoprotein that is capable of binding 2 iron atoms. The polypeptide chain is arranged in two lobes, respectively representing the N-terminal and C-terminal halves of the molecule (Anderson et al., 1987). When devoid of iron, a Tf lobe takes an 'open-jaw' conformation with domains separated. Upon binding iron, the domains undergo a rigid rotation to enclose their iron-binding site (Gerstein et al., 1993), thereby guarding the bound iron from hydrolysis and too-facile release. A distinctive, even defining feature of transferrins is the dependence of iron binding upon concomitant binding of a synergistic anion, normally carbonate. Protonation of the anion, resulting in its expulsion from the harboring protein, is probably a critical event in iron release *in vivo* as *in vitro* (el Hage Chahine and Pakdaman, 1995). These two features provide for the tight but reversible binding of iron by transferrins, thus accounting for the 100–200 cycles of iron transport and release displayed by the human protein during its lifetime in the circulation.

Tf is synthesized primarily in the liver and secreted into the serum (Morgan, 1983);

all nonheme iron in the circulation is bound to Tf. Only about 30% of Tf binding sites are occupied, so most of the protein is free of iron. Tf is relatively abundant in the CSF. It is made in the brain by the choroid plexus and oligodendrocytes, which are supported by evidence that both have the ability to secrete Tf (Kluge et al., 1986; Aldred et al., 1987a; Bloch et al., 1987; Dwork et al., 1988). The neurons (Mollgard et al., 1987; Dwork et al., 1988) and certain types of astrocytes (Dwork et al., 1988; Qian et al., 1999a; Qian et al., 2000) are also expression the Tf. Expression of Tf mRNA in rat oligodendrocytes is iron-independent and changes with increasing age (Moos et al., 2001).

1.4.2 Transferrin Receptor and Transferrin Receptor 2

Transferrin receptors (TfR) provide for controlled access of Tf to cells. Transferrin-bond iron (Tf-Fe) uptake or Tf and TfR mediated-endocytosis has been considered to be the main route for cellular iron accumulation (Qian et al., 2002). Two kinds of receptors have been described. The first and much more studied of these is now known as transferrin receptor 1 (TfR1) but, before the discovery of transferrin receptor 2 (TfR2), it was simply designated the TfR. TfR2 is a newly described receptor, which is mainly expressed in liver (Kawabata et al., 1999).

1.4.2.1 Molecular Characterization and Expression of TfR and TfR2

The human TfR is encoded by a single gene of about 32 kb located on chromosome 3, giving rise to a major 5 kb mRNA species. The entire human TfR gene contains 19 exons. The human TfR mRNA has a coding region of 2280 nucleotides and an

unusually large 3' untranslated region (UTR) of about 2500 nucleotides. The most important feature of this mRNA lies in a conserved fragment in the 3'UTR that encompasses five stem-loop structures containing the iron responsive elements and the rapid turnover determinant. This regulatory region is critically involved in the iron-dependent regulation of the receptor mRNA degradation (Ponka and Lok, 1999). TfR protein is comprised of two disulfide-bonded identical 90 kDa subunits, each bearing three asparagine-linked and one threonine-linked carbohydrate chains. TfR is expressed by all iron-requiring cells, including the neuronal cells, and is far more abundant than TfR2. The first 61 amino acids of each subunit form its cytoplasmic domain, and lead to a membrane-anchoring hydrophobic sequence of residues 62–89 that spans the lipid bilayer once. The remainder of the protein, bearing the Tf recognition sites, lies in the exocytic region. Each subunit contains a protease-like domain, a sandwich of two β-sheets combined with a helix along an open edge, and a third, helical domain (el Hage Chahine and Pakdaman, 1995). Tf binds to the receptor in 2:2 (Tf:TfR subunit) stoichiometry (Enns and Sussman, 1981).

The human TfR2 gene comprises 18 exons, extends 21 kb, and maps to chromosome 7q22 (Kawabata et al., 1999). A mouse TfR2 was identified in 2000 and the mouse gene was found to map to chromosome 5 (Fleming et al., 2000). A 2.9 kb mRNA encodes the full length form (TfR2-) of human TfR2, which is predicted to be a type II transmembrane protein with an 80 amino-acid transmembrane domain, and an extracellular domain comprising residues 105-801. The alternatively spliced form (TfR2-β) lacks exons 1, 2 and 3, which likely results in a truncated protein missing the entire transmembrane and cytoplasmic domains. It remains to be seen if TfR2-β is present in the cytoplasm of cells. The extracytoplasmic domain has the greatest

identity as well as similarity with TfR (45% and 66%, respectively). TfR2-α has a number of similarities to TfR. These include the presence of the motif YQRV, which may function as a signal for endocytosis, a protease-associated domain (PA domain), and the presence of cell attachment sequences (RGD motifs). It has yet to be determined if the internalization signal is functional and whether the RGD sequences are the binding sites for Tf, as has been shown for TfR (Subramaniam et al., 2002). Unlike TfR, which is ubiquitously expressed, expression of TfR2 is predominantly in liver and liver-derived cell lines (Fleming et al., 2000; Kawabata et al., 2001), but is also found in human erythroid/myeloid cell lines (Kawabata et al., 1999; Vogt et al., 2003) and platelets (Hannuksela et al., 2003). Using specific peptide antiserum *in situ* detected the duodenal localization of a class 1 HLA molecule involved in hereditary hemochromatosis (HFE) and TfR2 in humans and mice that was restricted to crypt cells. This finding provides evidence for a novel mechanism for the regulation of iron balance in mammals (Griffiths and Cox, 2003).

1.4.2.2 Regulation of TfR and TfR2 Gene Expression

Both transcriptional and post-transcriptional regulation plays an important role in the control of TfR expression. Transcriptional regulation may play a more significant role in tissue- or stage-specific regulation. Earlier studies of nuclear run-on and reporter gene assays demonstrated that at least a portion of the reciprocal regulation of the TfR mRNA levels by iron is mediated at the transcriptional level. Transcriptional regulation is also involved in serum/mitogenic stimulation of TfR expression, in the TfR induction during T and B lymphocyte activation, in the enhanced TfR expression by SV40 viral infection, in the decrease of TfR during

terminal differentiation of myeloid and lymphoid leukemic cell lines, and also in the marked increase of TfR during erythroid differentiation (Ponka and Lok, 1999). A minimal region of about 100 bp upstream from transcriptional start site was shown to drive both basal as well as serum/mitogenic stimulation of the promoter activity (Miskimins et al., 1986; Owen and Kuhn, 1987; Casey et al., 1988). This region contains putative regulatory elements similar to AP-1 and SP-1. Due to the five similar IRE motifs identified within the 2.7 kb 3'UTR of TfR mRNA, regulation is achieved via iron regulatory proteins (IRPs) and IREs. At low intracellular iron levels, both IRP1 and IRP2 bind to the stem loop IREs and protect the mRNA from degradation. At high intracellular iron concentrations, IRP1 binds iron, rendering it unable to bind mRNA. IRP2 is oxidized, ubiquitinated and degraded via proteasomes. The TfR mRNA with no IRP bound to it is rapidly degraded, resulting in low steady state levels of TfR mRNA. Consequently, less TfR is synthesized (Aisen et al., 2001).

The TfR2 transcript lacks IRE(s), so its expression is not sensitive to iron status (Fleming et al., 2000; Kawabata et al., 2000). TfR2 is normally expressed in the iron-overloaded liver of hemochromatosis (Fleming et al., 2000), aceruloplasminemia (Yamamoto et al., 2002) and desferrioxamine (DFO) treated Chinese hamster ovary (CHO) cells (Tong et al., 2002), so regulation of TfR2 may be via the cell cycle accommodating the needs of proliferating cells (Kawabata et al., 2000). During post-ischemic rat liver reperfusion, TfR2 mRNA levels were also enhanced (Tacchini et al., 2002).

1.4.2.3 Transferrin Receptor in the Brain

Immunocytochemical methods initially demonstrated the presence of TfR on capillary endothelial cells (Jefferies et al., 1984), and binding studies have shown Tf mediated transport of iron into these cells (Pardridge et al., 1987). TfR are also present in neurons (Giometto et al., 1990). The distribution of TfR shows a unique distribution with high densities in the cerebral cortex, hippocampus, amygdala, and certain brain-stem nuclei in both rat (Hill et al., 1985; Mash et al., 1990) and man (Morris et al., 1989). This pattern of distribution appears to reflect the iron requirement of specific neuronal groups (Morris et al., 1990), and may explain why previous studies (Hill et al., 1985; Morris et al., 1989) have shown an inverse relationship between the distribution of iron and TfR densities with, for example, very high iron levels in the globus pallidus, a low TfR density region.

The brain obtains iron via a Tf-TfR interaction at the level of the BBB, and both neurons and glia acquire iron via Tf (Fishman et al., 1987; Pardridge et al., 1987; Crowe and Morgan, 1992; Moos and Morgan, 2000). TfR is a key component of the iron regulatory system. In the adult nervous system, TfR has received relatively little attention and even less information exists on the expression and distribution of TfR during development. The density of TfRs on the brain microvasculature is 6-10 fold higher in adult human brains compared to the brain parenchyma. Autoradiographic studies reveal a heterogeneous distribution of TfRs in the adult brain; areas associated with motor function express a relatively higher density than non-motor areas (Hill et al., 1985; Mash et al., 1990; Kalaria et al., 1992).

In a preliminary analysis of TfR density during development, TfR density was low at birth (15.2 fmol/mg protein) and increased 4 fold (67 fmol/mg protein) by PND 18, with the level of receptor stabilized in adulthood (3 months of age). The low level of TfRs at birth in the presence of high concentration of Tf and iron suggests a negative feedback relationship (Mash et al., 1990). The cellular distribution of TfR and factors that regulate TfR expression require additional investigation because of changes, which occur with age and following injury and the possibility that TfR density may be an indicator of neuronal respiratory activity (Mash et al., 1990). Resent study showed the developmental regulation is mediated at the post-transcriptional level (Moos and Morgan, 2002).

1.4.3 Divalent Metal Transporter 1

Divalent metal transporter 1 (DMT1) has four names. Natural resistance associated macrophage protein 2 (Nramp2) was the name assigned when it was first found as a DNA sequence with an unknown function, but clearly related by sequence similarity to Nramp1 (Vidal et al., 1995). Divalent cation transporter 1 (DCT1) was proposed (Gunshin et al., 1997) after mRNA expression cloning made it a likely candidate for the apical, duodenal iron transporter. Almost instantly the apical iron transport role was established when Fleming et al. (Fleming et al., 1997) identified a G185R mutation in the corresponding gene of the microcytic (*mk*) mouse because it clearly has a defect in uptake of iron from the lumen of the gut (Edwards and Hoke, 1972). Soon after, Fleming et al. (Fleming et al., 1998) found the identical mutation accounted for the phenotype of the Belgrade (*b*) rat extending the function of the gene to exit of Fe^{2+} from endosomes during the Tf cycle and leaving little doubt

about the major role of the transporter in intestinal iron uptake. Andrews (Andrews, 1999b) agreed that the name should be changed, and proposed DMT1. OMIM (http://www3.ncbi.nlm.nih.gov/omim) now uses solute carrier family 11, member 2 (SLC11A2), a choice that may turn out to be the final one; but this thesis will use DMT1.

In recent years, the study of DMT1 has advanced rapidly. Two mRNA isoforms differ in the 3' UTR: DMT1+IRE has an IRE (Iron Responsive Element) but DMT1-IRE lacks this feature. The difference is in the distal 18 or 25 amino acid residues after shared identity for the proximal 543 residues. DMT1+IRE appears to serve as the apical iron transporters in the lumen of the gut; DMT1-IRE is mainly exit of iron from endosome. Studies on the role of DMT1 in the brain have proposed that dysfunction in DMT1 is likely to contribute to the etiology of certain neurodegenerative diseases. How DMT1 contributes to brain iron misregulation remains unclear, so elucidating the mechanisms of neuronal loss and the relationship of DMT1 with a selective neuronal loss in PD and in other NDs such as AD is very useful.

1.4.3.1 Characteristic of DMT1 Gene and Protein

The DMT1 gene is on the 12q13 of human chromosome (Vidal et al., 1995) and mouse chromosome 15 (Andrews and Levy, 1998). The human DMT1 consists of 17 exons spread over more than 36 kb (Lee et al., 1998). The DMT1 genes of murine and rat have a similar structure. There are at least two different splice forms, encoding alternative carboxy-termini and alternative 3'-UTR (Fleming et al., 1998;

Lee et al., 1998). One form contains an IRE in its 3' untranslated regions (3'-UTR), which is similar to IREs found in the 3' untranslated region of the TfR mRNA. This suggests that DMT1 protein expression may be controlled post-translationally by intracellular iron concentration. Another form does not contain a recognizable IRE.

The DMT1 protein is highly hydrophobic, with 12 predicted transmembrane domains. Both amino- and carboxy-termini are predicted to be within the cytoplasm. There is a substantial extracellular loop with predicted asparagine-linked glycosylation sites between transmembrane domains 7 and 8. Mutations in transmembrane domain 4 have been shown to interfere with DMT1 protein function. Several groups have begun to examine whether the ±IRE species are differentially expressed and whether they localize differently within cells (Canonne-Hergaux et al., 1999; Beaumont, 2000; Roth et al., 2000; Tabuchi et al., 2000). There are four isoforms of rat DMT1. In the C-terminal there are two isoforms variants: The –IRE's, associated with the absence of an IRE in the 3'UTR of the mRNA and encodes a 561-amino-acid protein (Gunshin et al 1997), and the +IRE mRNA is associated with its presence and encodes a 568-amino-acid protein (Gunshin et al., 1997; Fleming et al., 1998; Lee et al., 1998). The initial 543 residues appear to be common for the two forms of the protein although the C-terminal 18 or 25 amino acid residues differ as result of splicing a different exon at this region. More recently, two N-terminal variants were identified: One originates with an MV sequence as originally reported (Gunshin et al., 1997; Fleming et al., 1998) and one starts with 31 amino acid residues proximal to that sequence (Hubert and Hentze, 2002). The longer peptide specie has a potential nuclear localization signal (NLS) motif within it. The N-terminal isoforms are due to an alternative exon to exon 1; investigators have

dubbed the new sequence 1A (the old becoming an untranslated 1B and the next exon remaining as 2) so exon 1A predicts 29 additional residues for human DMT1 and 31 for rat DMT1. Antisera have been raised that recognize a ~90-116 kDa DMT1 protein which can be deglycosylated to a ~50-55 kDa protein (Gruenheid et al., 1999; Tabuchi et al., 2000). The latter mass is closer to the predicted molecular weight based on amino acid composition of DMT1. However, other groups have generated specific antisera that recognize a ~65-66 kDa species; these antibodies appear to block iron transport activity, suggesting that this antigen is a true transporter protein (Conrad et al., 2000; Roth et al., 2000; Tandy et al., 2000). It is possible that cell-type specific glycosylation patterns may account for such differences in mass profile.

1.4.3.2 Expression and Regulation of DMT1 Gene

Northern-blot analysis revealed that DMT1 prominently expressed in proximal intestine, followed by kidney, thymus and brain, and is faintly present in the testis, liver, colon, heart, spleen, skeletal muscle, lung, bone marrow, stomach and all tissues examined. In the kidney and thymus, two strong bands at ~ 3.5 kb and ~4.5 kb were detected, indicating that two isoforms mRNA exist in those tissue (Gunshin et al., 1997). *In situ* hybridization study showed cellular localization of DMT1 mRNA in intestine, kidney, testis, thymus and brain. In the small intestine, DMT1 is highly expressed in enterocytes lining the villus, especially in the crypts and lower segments of the villus, but not at the villus tips. Again, a proximal-to-distal gradient of expression is evident in the small intestine. In the kidney, DMT1 mRNA labeling is most prominent in S3 proximal tubule segments, suggesting that it is involved in

the reabsorption of divalent cations. In the testis, DMT1 mRNA is expressed in the Sertoli cells of seminiferous tubules, and was more abundant in those tubules containing mature spermatocytes. In the thymus, DMT1 labeling is positive in cortical, but not medullary, thymocytes. In the brain, DMT1 mRNA is found in neurons, glial and ependymal cells (Gunshin et al., 1997; Burdo et al., 2001). A qualitative examination of sagittal sections indicates that most neurons express DMT1 mRNA at low levels. More prominent labeling is present in densely packed cell groups, such as the hippocampal pyramidal and granule cells, cerebellar granule cells, the preoptic nucleus and pyramidal cells of the piriform cortex, and in moderate amounts in the substantia nigra (Burdo et al., 2001; Wang et al., 2002).

Each DMT1 isoform exhibits a differential cell type-specific expression patterns and distinct subcellular localizations. Epithelial cell lines predominantly express DMT1A, whereas the blood cell lines express DMT1B. In HEp-2 cells, GFP-tagged DMT1A is localized in late endosomes and lysosomes, whereas GFP-tagged DMT1B is localized in early endosomes. Using site-directed mutagenesis, a Y (555) XLXX sequence in the cytoplasmic tail of DMT1B has been identified as an important signal sequence for the early endosomal-targeting of DMT1B. In polarized MDCK cells, GFP-tagged DMT1A and DMT1B are localized in the apical plasma membrane and their respective specific endosomes. Disruption of the N-glycosylation sites in each of the DMT1 isoforms affects their polarized distribution into the apical plasma membrane but not their correct endosomal localization. This data indicate that the cell type-specific expression patterns and the distinct subcellular localizations of two DMT1 isoforms may be involved in the different iron acquisition steps from the subcellular membranes in various cell types

(Tabuchi et al., 2002).

DMT1 gene expression is regulated in response to iron status. Rats that were made iron deficient had markedly increased DMT1 mRNA in intestinal epithelial cells and cell line and iron sufficient rat had markedly decreased levels (Gunshin et al., 1997; Han et al., 1999; Martini et al., 2002; Frazer et al., 2003). The basis of this regulation has not yet been fully defined. The putative promoter of the human DMT1 gene contains several potential metal response elements, suggesting that there may be transcriptional regulation in response to metal levels (Lee et al., 1998). It is likely that there is also post-transcriptional regulation (Gunshin et al., 2001; Ke et al., 2003). The IRE sequence found in the 3' untranslated region of one of the two alternative splice forms of DMT1 mRNA binds iron regulatory protein *in vitro* and appears to respond to cellular iron levels. Under low iron conditions, IRPs bind to the IREs in the 3'UTR of DMT1 mRNA and protect the mRNA from degradation, and lowers mRNA stability when iron is abundant. It has been shown IRP can bind to a 3'UTR stem-loop in DMT1+IRE mRNA *in vitro* (Guerrini et al., 1998; Wardrop and Richardson, 1999). Therefore, DMT1 expression is likely to be modulated by IRP-IRE at the post-transcriptional level. Other mechanism may be involved in the regulation of DMT1 gene expression. It has been demonstrated that the 5' regulatory region of human DMT1 contains a single interferon (IFN)-γ regulatory element, three potential SP1 binding sites, two potential Hif-1 binding sites, and five potential metal response elements, all of which may play some role in the regulation of this molecule (Lee et al., 1998). Wardrop and Richardson showed there was a sevenfold increase in the expression of the 2.3 kb DMT1 mRNA transcript when compared with the control, but little effect on the DMT1 3.1 kb transcript in RAW264.7

macrophage cell line after incubation with LPS/IFN-γ. These results indicate differential regulation of the two transcripts. They suggest that Nramp2 mRNA expression can be influenced by factors other than Fe levels in macrophages (Wardrop et al., 2002). However, the regulation of DMT1 gene expression is still not fully understood.

1.4.3.3 Functions of DMT1

In the microcytic anemia (*mk*) mice and Belgrade (*b*) rats have naturally occurring mutations of DMT1 gene that result in defects in the transport of iron from the gut lumen into the absorptive enterocytes, and from plasma Tf into erythroid precursors (Fleming et al., 1997; Fleming et al., 1998). The results indicated affects iron transport (Su et al., 1998). As a divalent metal transporter, DMT1 was identified by functional cloning in Xenopus lavis oocytes as an electrogenic metal transporter of broad substrate specificity, transporting Fe^{2+}, Zn^{2+}, and other ions (Gunshin et al., 1997). In duodenal iron uptake, Fe^{3+} made soluble by gastric acid, is reduced to Fe^{2+} presumably by Dcytb (McKie et al., 2001) or a similar reductase on the apical surface and enters the brush border via DMT1. Because DMT1 may act as a proton symporter, one assumes that Fe^{2+} uptake is facilitated by the mildly acidic pH expected in the proximal duodenum. DMT1 is found on the apical surface of the enterocyte (Canonne-Hergaux et al., 1999; Trinder et al., 2000). This location is consistent with the finding (Knopfel et al., 2000) that divalent cation transport activity is associated with brush-border membrane vesicles. Like this form of TfR-independent iron transport in the brush border, it is possible that the TfR-independent iron transport via DMT1 is present in other tissue.

The second role of DMT1 is mediated iron transport across endosome. Tf-TfR mediated iron uptake is a main route in the cell (Qian and Wang, 1998). Once Fe is released from Tf, it must cross the endosomal membrane, probably via a membrane-bound transporter that is recruited from the cell surface. A number of recent studies have shown that the transporter is DMT1. Using erythroid precursor cells of anemic Belgrade rat with mutation in DMT1, Fleming et al found that these cells could take up iron into an endosomal compartment by receptor-mediated endocytosis of diferric Tf bound to TfR, but they were subsequently unable to export iron from the endosome into the cytoplasm. As a result, endosomal iron was returned to the cell surface and released and very little was retained for hemoglobin synthesis (Fleming et al., 1998). DMT1 can be expressed on the endosomal membrane and co-localizes with Tf to export iron from the endosome into the cytoplasm of the cell (Su et al., 1998; Tabuchi et al., 2000). In their study, DMT1 showed clear colocalization with FITC-Tf both at the plasma membrane and in recycling endosomes. Canonne-Hergaux et al suggest that DMT1 is coexpressed with TfR in erythroid cells. Experiments with isoform-specific anti-DMT1 antiserum strongly suggest that it is the non-iron-response element containing isoform II of DMT1 that is predominantly expressed by the erythroid cells. These results provide further evidence that DMT1 plays a central role in iron acquisition via the transferrin cycle in erythroid cells (Canonne-Hergaux et al., 2001a). The evidence strongly supports the role of DMT1 in transporting Fe^{2+} into the cytoplasm after acidification of the Tf-positive endosome.

1.4.3.4 DMT1 and Brain Iron Metabolism

The cellular localization of DMT1 and its functional characterization suggest that DMT1 might play a role in physiological iron transport in the brain. The discovery of DMT1 in neurons, astrocytes and ependymal cells in adult rat brain supports the idea (Burdo et al., 2001). The presence of DMT1 within the endothelial cells lining the blood vessels suggests that iron can be removed from the endosome within the endothelial cell. Whether this iron is for use by the endothelial cell or is then transported into the brain remains to be determined. The presence of DMT1 on astrocytes also indicates the involvement of this protein in iron transport into the brain. Astrocytes have end-feet that envelop the vasculature (Xu and Ling, 1994) and DMT1 has a polar expression in astrocytes; it is found only in the process associated with the BBB and occasionally into the soma of the astrocytes (Burdo and Connor, 2003). To investigate the role of DMT1 in brain iron transport, the Belgrade (*b*) rat, which has a defect in DMT1 (Fleming et al., 1998), has been examined. The iron staining is decreased in Belgrade (*b*) rat brains compared to normal (Burdo et al., 1999) and the decrease in iron status is also detectable with magnetic resonance imaging (MRI) (Zywicke et al., 2002). ^{59}Fe uptake in Belgrade rat brains is only 10% that of normal, while ^{125}Tf uptake is 40% that of normal after peripheral injection of ^{125}I-Tf-^{59}Fe (Farcich and Morgan, 1992). DMT1 has recently been found to be moderately expressed in the neurons of the substantia nigra in patients with PD, which correlates to abnormal iron deposition in the same area of the brain. This suggests that DMT1 may be responsible for the increased iron accumulation in PD and may play a role in the etiology of certain NDs (Andrews, 1999b). This might be the cause of the increased iron content in the brain regions and might thereby

contribute to neuronal death by inducing the production of harmful reactive oxygen species (ROS) (Andrews, 1999b). In the brain, NTBI will be acquired by neuronal cells or other brain cells, probably via DMT1- or trivalent cation-specific transporter (TCT)-mediated mechanisms (Qian and Shen, 2001). Therefore, further analysis of the functions of DMT1 within the CNS may be of value in elucidating the mechanisms of neuronal loss in PD and other neurodegenerative disorders where abnormalities in iron metabolism have been demonstrated.

1.4.4 Ferroportin1

Ferroportin1 is a newly discovered molecule that may play a role in iron export. Recently, several groups have isolated a putative iron export molecule within several months of each other (Abboud and Haile, 2000; Donovan et al., 2000; McKie et al., 2000). This protein was first named iron-regulated transporter 1 (IREG1) by McKie et al (McKie et al., 2000). Subsequently, the same molecule was also named ferroportin1 (FP1) (Donovan et al., 2000), and metal transport protein 1 (MTP1) (Abboud and Haile, 2000). In this thesis, this molecule will be referred to as FP1. This protein is expressed in the villus cells of the small intestine and on the basolateral surface of polarized epithelial cells. The gene mutation developed a hypochromic anaemia (Donovan et al., 2000), which suggests that FP1 be involved in iron export. Therefore, mild mutations resulting in differences in the activity of FP1 may modify the severity of diseases associated with iron overload, including hemochromatosis, aceruloplasminemia and porphyria cutanea tarda (Roy and Andrews, 2001).

1.4.4.1 Characteristic of Ferroportin1 Gene and Protein

The human FP1 gene encompasses 20 kb of DNA, comprises 8 exons and maps to 2q32. FP1 encodes a zebrafish basolateral membrane protein of 571 amino acid residues with multiple transmembrane domains, expressed in the yolk sack (Donovan et al., 2000). Mouse FP1 cDNA encodes a protein 570 amino acids in length with a predicted mass of 62 kDa. This protein is extremely well conserved in humans, mice and rats, showing >90% homology. Human FP1 shows little homology to the iron importer DMT1, although uncharacterized FP1-related proteins were found in Arabidopsis and C. elegans.

Further analysis of the FP1 protein by McKie et al (McKie et al., 2000) showed a putative NADP/adenine-binding site and basolateral localization signal present at its C-terminus. The NADP/adenine-binding sequence of FP1 comprises an IFVCGP motif that is also found in yeast ferric reductase and the neutrophil oxidoreductase gp91-phox. This suggests that FP1 may have a reductase activity involved in iron transportation. Both Fe^{2+} and Fe^{3+} are known to exist in complex equilibrium within cells and the conversion between these redox states may be important in terms of transportation and sequestration (St Pierre et al., 1992; Richardson and Ponka, 1997). Indeed, the export of Fe^{3+} from cells may involve the conversion of Fe^{3+} to Fe^{2+} by the reductase region of FP1 and this should be investigated further. The last four amino acids (TSVV) of FP1 comprise a T/S-X-V/L PDZ target motif that is readily recognised by postsynaptic density-95 (PSD-95)/discs large (Dlg)/zona occludens-1 (ZO-1) (PDZ) proteins. PDZ proteins are thought to be involved in the basolateral localization of proteins containing this target motif. Sequence analysis of FP1

mRNA revealed the presence of an IRE in its 5' untranslated end. The 5' IRE sequence of FP1 is well conserved in humans, mice and zebrafish. Similar 5' IREs occur in transcripts encoding ferritin, erythroid-5-aminolevulinate synthase and mitochondrial aconitase (Richardson and Ponka, 1997).

1.4.4.2 Expression and Regulation of FP1 Gene

FP1 was expressed at the basolateral membrane of villus enterocytes within the duodenum, particularly at the tip of the villus rather than the crypt. However, while FP1 is expressed in the duodenum, it is not produced in either the jejunum or ileum. Other important sites of iron metabolism where FP1 expression occurs are the liver and spleen. These tissues are involved in scavenging iron from senescent erythrocytes. Immunostaining of these tissues revealed the expression of FP1 in the cytoplasm of Kupffer cells, the cell surface of hepatocytes lining sinusoids and splenic macrophages in mice. Macrophages and Kupffer cells found in the spleen or liver, respectively, readily engulf senescent erythrocytes to release the iron following haemoglobin degradation. FP1 is not expressed on plasma membranes of macrophages. However, it may still be a vital component for iron export. For instance, cytoplasmic FP1 may be involved in the transportation of iron into acidic cellular vesicles that may release iron at the cell surface via exocytosis (Abboud and Haile, 2000; Donovan et al., 2000). The FP1 was observed in human and rodent lung cells at both the protein and mRNA levels (Yang et al., 2002). The FP1 was also detected in the basal surface of placental syncytiotrophoblasts. The expression of FP1 in placental tissue is highest during the third trimester of pregnancy and is developmentally regulated. This suggests a possible role for FP1 in iron transport

from the mother to the developing fetus. Other tissues where FP1 was expressed include the large intestine, heart, skeletal muscle and, kidney, testis, megakaryocytes and the decidua of the pregnant uterus (Abboud and Haile, 2000).

FP1 mRNA contains an IRE in the 5'UTR. IREs are sequences that form stable stem-loop structures capable of binding the IRP. Cells depleted of iron contain higher levels of IRPs, which form stable complexes with the IRE. Unlike the IRE in 3'UTR of DMT1+IRE and TfR genes, when an IRE is present in the 5' end of the mRNA, the complex of IRE/IRP will prevent mRNA translation. However, in contrast to IRP-IRE theory, it was reported that iron-deficiency (induced via a low Fe diet) induces FP1 expression in duodenal enterocytes, while in iron-replete mice (induced by i.m. Fe-dextran injection) showed lower expression (Abboud and Haile, 2000). These results suggest the presence of an IRE-independent pathway that controls the expression of FP1 in enterocytes. Another IRE-independent pathway was also observed where placental cells in iron-depleted mice showed no changes in the expression of FP1 (Gambling et al., 2001). In contrast to the expression of FP1 in enterocytes and placental cells, the molecule was regulated in accordance to IRP-IRE theory in Kupffer cells of the liver (Abboud and Haile, 2000). Other studies showed transient transfection of cells with a FP1 construct without an IRE motif, demonstrating expression of the molecule at the plasma membrane (McKie et al., 2000). In addition, these cells were found to contain higher levels of IRE-IRP binding and decreased amounts of ferritin protein, indirectly suggesting that the cells became iron-deplete upon overexpression of FP1. Together, these results suggest complex tissue-specific regulation of FP1 that may be related to various functions of the molecule in different cell types.

1.4.4.3 Functions of Ferroportin1

Functional studies of FP1 demonstrate that ferroportin1 mediates iron efflux across membranes by a mechanism that requires an auxiliary ferroxidase activity (Donovan et al., 2000; McKie et al., 2000). Iron efflux studies were conducted to further evaluate the iron export function of FP1. Donovan et al demonstrated that the efflux of iron by FP1 required apotransferrin (apoTf). In contrast, McKie et al showed that iron efflux by FP1 did not require apoTf, but CP instead. Although contradictory results were obtained from these studies, both authors were able to show that FP1 may play a role in iron export in the *Xenopus* expression model. Collectively, the evidence obtained from FP1 efflux and expression studies suggests the important role FP1 plays in iron absorption. However, the expression of FP1 in the cytoplasm of Kupffer cells and enterocytes suggests the possibility that FP1 may be involved in the intracellular trafficking of iron between the cytosol and organelles. The detection of FP1 in placental syncytiotrophoblasts and decidual cells of the pregnant uterus suggests that FP1 may play a role in the transfer of iron from mother to embryo. Recently, a mutation in FP1 has been associated with the development of autosomal dominant hemochromatosis type 4 (Bomford, 2002).

In the past, there was speculation concerning the existence of a Fe exporter at the basolateral membrane of enterocytes. The recent discoveries of FP1 and Heph have given us an insight into Fe export from duodenal enterocytes. However, the link between these molecules and the mysterious labile Fe pool remains unclear. It can be speculated that the release of Fe from its chaperone may require Heph. Heph may

interact with the Fe chaperone to facilitate Fe transfer to FP1. Once transported, Fe^{2+} may then be released into the circulation and oxidized by CP (Le and Richardson, 2002).

1.4.4.4 Ferroportin1 and Brain Iron Metabolism

Through immunohistochemical analysis, FP1 expression has been found in most brain regions. Its staining in the normal rat is highest in the hippocampus, cortex, cerebellum, thalamus, and striatum, with lesser staining in the substantia nigra and subcortical white matter. Within the cortex, the cell bodies and apical dendrites of pyramidal neurons are intensely immunoreactive. In both the striatum and thalamus, FP1 is most predominant in neurons. Within the hippocampus, granule cells and pyramidal cells are immunopositive for FP1. Neurons in the habenular necleus stain strongly for FP1 but there is no FP1 detectable in the ependymal cells. In the subcortical white matter, oligodendrocytes are FP1 positive. There is no pattern of distribution to the immunoreactive oligodendrocytes like that observed for iron and ferritin. In the cerebellum, Purkinje cell bodies and dendrites stain moderately for FP1. In the hindbrain, several nuclei, including the interposed, cochlear and dentate nuclei stain intensely for FP1. Neither ependymal cells nor blood vessels throughout the brain react positively for FP1. In the Belgrade rats, staining for FP1 is decreased. There was no difference in any cell type staining among any of the groups examined. Immunoblot analysis of FP1 levels in brain homogenates indicated no difference in FP1 levels among any of the groups. The FP1 staining pattern suggests some export of iron from oligodendrocytes. Iron release from oligodendrocytes was previously thought to be mediated by Tf (Espinosa de los Monteros et al., 1990), but recent data

indicate that Tf in oligodendrocytes is not secreted (de Arriba Zerpa et al., 2000). Thus, FP1 may be involved in the mechanism for iron release (Connor et al., 1995; Burdo et al., 1999; Burdo et al., 2001).

Western blot annlysis showed the existence of FP1 in the rat brain, including the cortex, hippocampus, striatum and substantia nigra. The findings also showed that age has a significant effect on the expression of FP1 protein in the four brain regions. These data imply that FP1 might play a role in brain iron metabolism. The process of iron transport across the BBB is very similar to that of iron transport across the cells lining the gut. In the BBB, iron first crosses the apical membrane of the capillary endothelium probably by Tf/TfR pathway, and then iron, possibly also in the form of Fe^{2+}, crosses the basolateral membrane and enters into the interstitial fluid or CSF of the brain. The molecular mechanism underlying Fe^{2+} transport across the basolateral membrane of the BBB cells remains a mystery. However, based on the similarity of the two processes and the proposed function of FP1 in duodenal enterocytes, FP1 might function as an iron exporter of the BBB cells. As an iron exporter, FP1 might also play a role in iron release from some brain cell types, keeping an iron balance within the cells. The possibilities need further study (Qian and Shen, 2001; Jiang et al., 2002; Qian et al., 2002).

1.4.5 Duodenal Cytochrome B (Dcytb)

Dcytb, along with FP1 and DMT1, were among the first clones identified as candidate genes involved in iron absorption due to their very high expression in duodenum and the fact the mRNAs were all highly induced by iron deficiency,

hypoxia and hypotransferrinaemia. The protein sequence of Dcytb revealed itself as a close homologue of cytochrome *b*561 (McKie et al., 2001).

The Dyctb molecule has 6 transmembrane domains and may contain a di-heme center vital for electron transport. Dcytb shares a 45–50% homology to cytochrome b561, an enzyme involved with regeneration of ascorbic acid from dehydroascorbate (Okuyama et al., 1998). The putative binding sites for the cytochrome b561 substrates (*i.e.* ascorbate and dehydroascorbate) are partially conserved in Dcytb, suggesting a possible interaction with these or similar molecules. There is little homology between Dcytb and plant and yeast ferric reductases described by others. However, the amino terminal is virtually identical to the amino terminal of cytochrome b558 (p30) derived from plasma membranes of rabbit neutrophils (Escriou et al., 1994). In accordance with a role for Dcytb in iron absorption, iron deficiency and hypoxia induced a marked increase in the expression of this molecule in the duodenum at both the mRNA and protein levels.

Dctyb is localized prominently in the brush-border membrane of mature enterocytes, where iron absorption occurs at maximum rates (McKie et al., 2001), and in the plasma membrane of the HeLa and Caco-2 cell lines. The presence of Dcytb was also confirmed by RT-PCR in liver tissues and by western blot analysis in spleen samples from CD1 mice. Furthermore, Dcytb expression is pronounced along the brush border of enterocytes near the tip of the villus. Dcytb, as the brush border membrane reductase, performs its function in response to the iron status of the organism (Latunde-Dada et al., 2002).

Microinjection of *Xenopus* oocytes with Dcytb cRNA or transfection of intestinal cell lines with Dcytb resulted in a marked increase in ferric reductase activity compared to the controls. Taken together, it has been suggested that Dcytb may be linked to the mechanism involved in the transport of iron from the gut lumen across the enterocyte and into the blood: Dcytb reduces Fe^{3+} complexes in the intestinal lumen to the labile Fe^{2+} form that can then be transported by DMT1. The Fe^{2+}, once internalized, is then probably specifically targeted (via chaperones?) to FP1.The intermediate acceptors that bind the internalized iron within the enterocyte remain unknown. The molecule Heph may be involved. Once at the external surface of the enterocyte, the Fe^{2+} may then be oxidized by the action of the serum ferroxidase CP, and the Fe^{3+} bound by Tf.

Dcytb mRNA and protein levels were raised in Fe-deficient duodenum (McKie et al., 2001; Dupic et al., 2002). RT-PCR shows enhanced expression of Dcytb and DMT1 in Fe-deficient duodenal sample from CD1 mice. Similarly, duodenal reductase activity measured with the electron acceptor, nitro blue tetrazolium, was increased in hypoxic conditions. The activity localises near to the villus tip as shown for Dcytb protein. However, Fe status does not appear to modulate Dcytb expression in the liver and spleen (Latunde-Dada et al., 2002). Apart from the obligatory requirement for ferric ion reduction prior to its absorption in the mammalian gut, the presence of ferric reductases is imperative for intracellular redox changes in the transit of Fe ions between compartments in peripheral tissues. The role of Dcytb in the intestinal absorption of Fe is confirmed by its increased levels in Fe-deficiency, hypoxia, and in hypotransferrinemic (hpx) mice by independent stimulators of Fe absorption (McKie et al., 2001; Frazer et al., 2002). Large oral doses of iron will rapidly

decrease the expression of the mRNAs (Frazer et al., 2003). While Dcytb has no definable IRE, its regulation might be controlled by yet unidentified mammalian transcription factors perhaps similar to the iron-inducible transcriptional regulator, Aft1p, which controls the yeast ferric reductases enzymes FRE1 and FRE2 (Yamaguchi-Iwai et al., 1995; McKie et al., 2001).

Dcytb was shown to have ferric reductase activity in the duodenal mucosa. It was also found in other tissues such as the spleen and liver, and may exist in the brain, leucocytes and erythrocytes. This implies a wider physiological role of Dcytb than just in duodenal Fe absorption.

1.5 HEPCIDIN AND IRON METABOLISM

Iron is an essential element for nearly all-living organisms (Aisen et al., 2001). It is a key functional component of oxygen-transporting and storage molecules (e.g. hemoglobin and myoglobin) and of many enzymes that catalyze the redox reactions required for the generation of energy (e.g. cytochromes), the production of various metabolic intermediates and for host defense (e.g. NADPH oxidase). Humans and other vertebrates strictly conserve iron by recycling it from senescent erythrocytes and from other sources. The loss of iron in a typical adult male is so small that it can be met by absorbing only 1-2 mg of iron per day(Andrews, 1999a). In comparison, the total body iron in an adult male is 3000-4000 mg and the daily iron requirement for erythropoiesis is about 20 mg. Such conservation of iron is essential because many human diets contain just enough iron to replace the small losses. However, when dietary iron is more abundant, absorption is appropriately attenuated.

Important homeostatic mechanisms prevent excessive iron absorption in the proximal small intestine and regulate the rate of iron release from macrophages involved in recycling (Andrews, 1999a).

Analysis of iron metabolism in human diseases and animal models suggests several major influences (Andrews, 1999a) that determine how much iron is absorbed from food and how much recycled iron is released from macrophages. Iron requirements of bone marrow erythropoiesis stimulate iron absorption in the small intestine while excessive iron stores (accumulated predominantly in the liver) provide an inhibitory signal. Both of these responses are homeostatic under most conditions.

Since the sites of iron absorption, recycling, storage and utilization are distant from each other, it is reasonable to expect that iron-regulatory hormones must exist to account for the observed interactions between these compartments, and that inflammatory substances may also be involved in iron regulation. However, the molecular basis of these signals was elusive for many years, until a series of converging and often serendipitous discoveries of hepcidin provided the long sought opening (Ganz, 2003).

1.5.1 Cell Iron Metabolism

The mechanisms involved in cellular iron transport and in the regulation of intracellular iron balance is very important because it is the basis of body iron metabolism.

1.5.1.1 Cellular Iron Uptake

Extracellular iron must be carried across cellular membranes so that it can be incorporated into the many cellular heme and non-heme iron-containing proteins to exert its roles. There are two iron transport mechanisms involved: Tf-TfR dependent iron transport and Tf-TfR independent iron transport.

1.5.1.1.1 Tf and TfR Dependent Iron Uptake (Fig 1-4)

The Tf-Fe uptake or Tf and TfR mediated-endocytosis is considered to be the main route for cellular iron accumulation. In general, the Tf and TfR dependent iron transport process can be divided into seven main steps (Qian and Tang, 1995; Qian and Shen, 2001; Li and Qian, 2002): 1) Binding: Tf-Fe binds to the extracellular portion of TfR on the cellular membrane, which is a simple physiological process independent of cell metabolism. 2) Internalization or endocytosis: Fe-Tf-TfR complexes are clustered together and localized in clathrin-coated pits, which eventually bud off to form coated vesicles called endosomes or receptorsomes. 3) Acidification: the intravesicular pH is lowered to about 5-6 by the activity of H^+-ATPase on the membrane of the endosomes. 4) Dissociation and reduction: intravesicular acidification induces the release of iron (Fe^{3+}) from Tf and its reduction to Fe^{2+} within the endosomes. 5) Translocation: iron (Fe^{2+}) is transported through the membrane of the endosomes to the cytoplasm. DMT1 has been recently proposed to be involved in this process, but the precise mechanism remains unclear. 6) Cytosolic transfer of iron into intracellular compounds: after translocation from endosome to cytoplasm, iron is shuttled by ATP or AMP, which transfers iron to the

sites that need iron for physiological activity, e.g. haem synthesis, electron transport in mitochondria etc., or to ferritin for storage. 7) Return of Tf-TfR complex to the plasma membrane: endosomes containing Tf-TfR return to the plasma membrane. The apotransferrin is replaced by new Tf-Fe molecules from extracellular fluid and the uptake process is repeated. Apotransferrin released form the receptor returns to the plasma or surrounding solution (Qian and Tang, 1995; Qian et al., 2002).

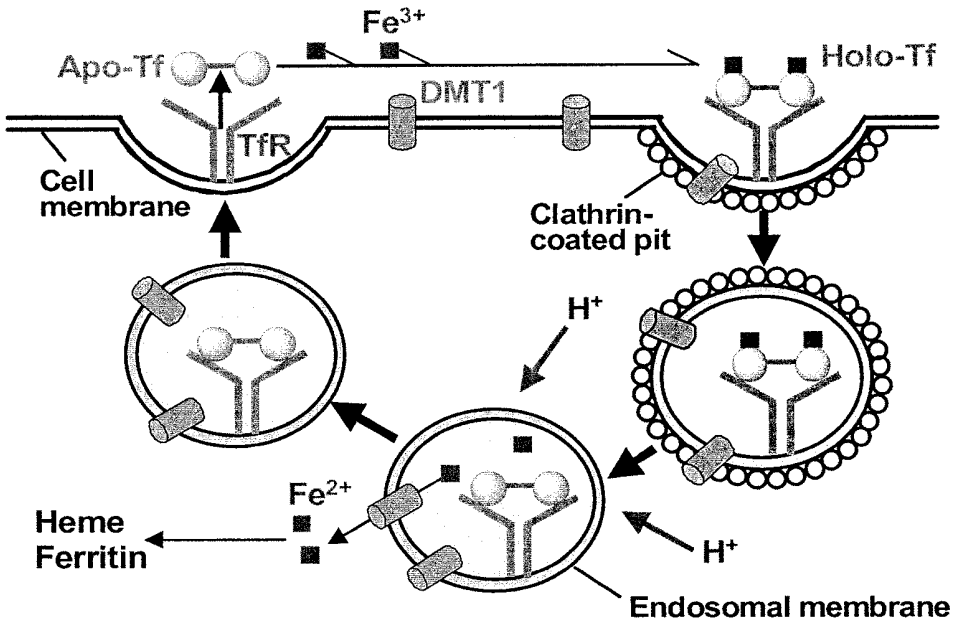

Fig. 1-4. The pathway of cellular iron uptake from Tf via TfR mediated endocytosis.

1.5.1.1.2 Tf and TfR Independent Iron Uptake (Fig. 1-5)

There is strong evidence that cells must also express a Tf and/or TfR-independent iron transport system. For example, mice and humans lacking Tf, while anemic, show iron overload in parenchymal tissues such as liver and spleen. Similarly, when iron enters plasma in excess of the Tf binding capacity (as seen in hereditary hemochromatosis), iron is cleared from plasma by uptake into parenchymal tissues. Further, Tf receptor knockout mice die at the embryonic stage, but there is some tissue development, suggesting a second iron uptake mechanism (Levy et al., 1999). Tf-TfR independent iron uptake drew considerable attention about ten years ago. Results from Morgan's group show that reticulocytes can take up iron when incubated with $FeSO_4$ dissolved in isotonic sucrose (Morgan, 1988; Qian and Morgan, 1992). The process is efficient and leads to iron uptake into heme. More interestingly, the process disappears as reticulocytes mature, and it is very closely associated with the disappearance of the TfR (Qian and Morgan, 1990, 1991, 1992). Iron uptake by this route is not associated with TfR but dependent on reduction of iron to the ferrous state and then across the membrane by an iron carrier (Qian and Morgan, 1992; Qian and Tang, 1995; Trinder et al., 1996).

DMT1 has recently been isolated in microvillous membrane vesicles of the upper small intestine (Fleming et al., 1997; Gunshin et al., 1997). It is considered as a membrane iron carrier protein and mediates Tf and TfR independent ferrous iron transport through enterocytes (Fleming et al., 1998). Dietary iron in the lumen of the gut is predominantly in the ferric form, but it must first be reduced to the ferrous

form before it can be utilized. Dcytb is a strong candidate for this brush border ferrireductase (McKie et al., 2001). The membrane transporter DMT1 then facilitates the transport of ferrous iron across the brush border membrane. Little is known about the trafficking of iron through the cell, but it requires the intracellular protein Heph and likely involves the ferroxidase activity of this molecule. Basolateral transfer to the body is thought to be mediated by the membrane iron exporter FP1 that is strongly expressed in the duodenum. Iron that enters the circulation is loaded onto Tf for transportation to the body tissues. Molecules that have been strongly implicated in the regulation of iron absorption are the hemochromatosis protein HFE, the TfR2, and the antimicrobial peptide hepcidin (Nicolas et al., 2001). Each of these is most strongly expressed in the liver (Kawabata et al., 1999; Frazer et al., 2001; Pigeon et al., 2001).

Another pathway, independent of TfR but not Tf, is available for iron uptake from Tf in the human melanoma cell or CHO cells lacking TfR but transfected with p97 (Kennard et al., 1995; Jefferies et al., 1996). This pathway may involve transfer of iron from Tf or simple chelators to GPI-p97, and hence to the cell interior by an endocytic route that is less sensitive to the effect of weak bases but more accessible to hydrophilic chelators than the receptor-mediated pathway.

The Tf independent iron uptake may be mediated by gelatinase-associated lipocalin (NGAL). Lipocalins are a large group of proteins that are related more in structure than sequence and which bind small molecules. Lipocalins have been implicated in the transport of small organic molecules such as retinol, prostaglandins, fatty acids and oderants. NGAL banding iron is internalized into endosomes and, like Tf, is

recycled. However, the detailed mechanism is not clear (Kaplan, 2002). Besides, other routes are maybe involved in the Tf and/or TfR independent iron uptake.

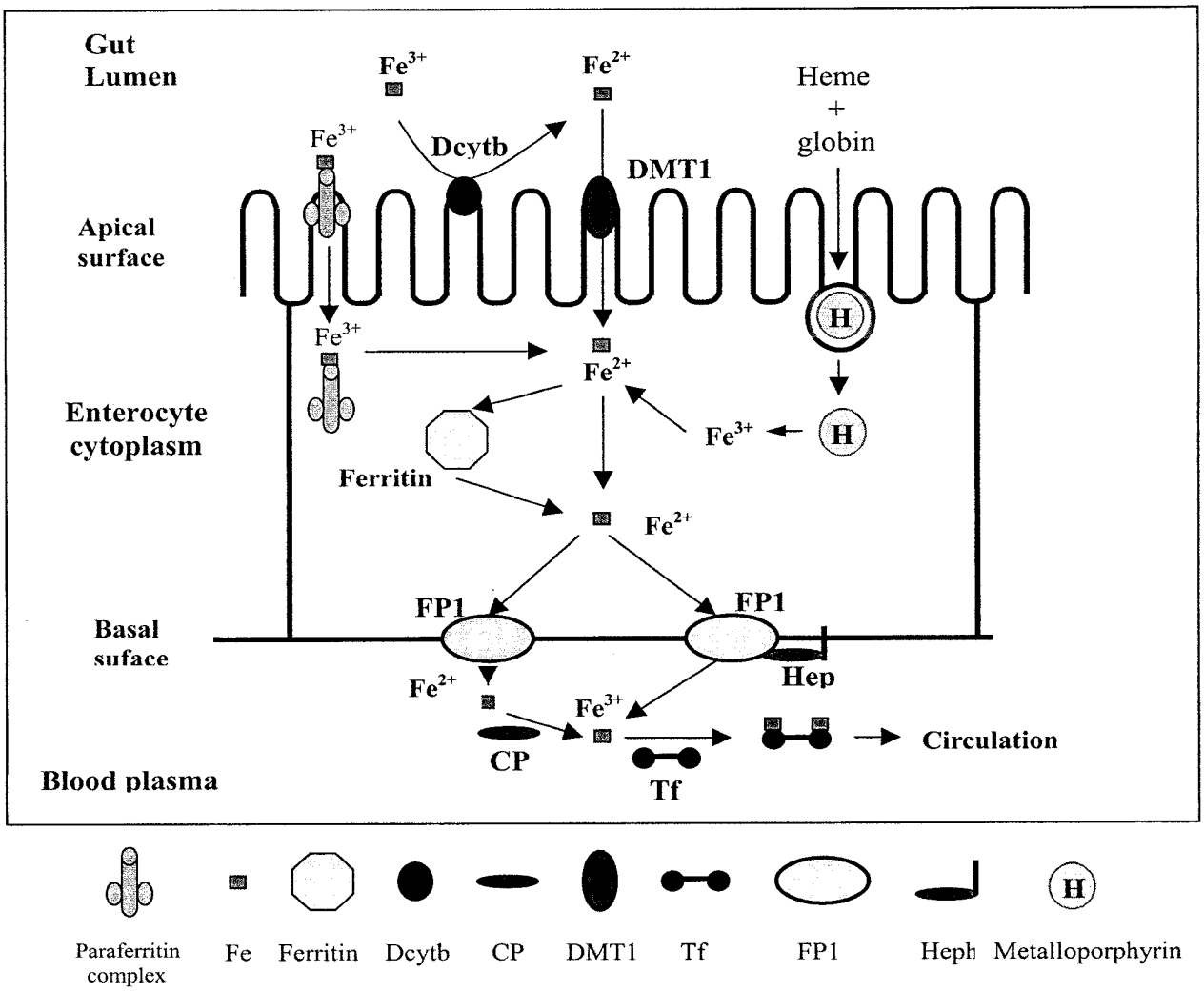

Fig. 1-5. Pathways of heme and non-heme iron uptake and transport in the intestine. Fe^{3+} is reduced by Dcytb forming Fe^{2+}, Fe^{2+} in the intestinal lumen is transported across the apical surface by DMT1. Fe^{3+} and Fe^{2+} can also enter absorptive enterocytes via a pathway mediated by paraferritin complex, consisting of β-integrin, mobilferrin and flavin mono-oxygenase. Heme is processed in the gut lumen and enters enterocytes as an intact metalloporphyrin (H). Mechanism of heme iron transport is not well defined, probably mediated by an endocytic pathway. Once inside the cytoplasm, heme is degraded by heme oxygenase to release inorganic iron. Once inside the cell, iron can either be stored in ferritin or transported across the basolateral membrane by FP1. The species of iron that is exported by FP1 is not known, but the need for ferroxidase activity to load iron onto Tf indicates that it is probably Fe^{2+}. FP1 and Heph may work together in the absorptive enterocyte. In other cell types, FP1 may work with CP to load iron onto Tf. Abbrevs: DMT1, divalent netal transporter; CP, ceruloplasmin; Tf, transferrin; FP1, ferroportin 1; Heph, hephaestin; Dcytb, duodenal cytochrome b.

1.5.1.2 Iron Efflux

Intracellular iron balance is dependent not only upon the amount of iron taken up and sequestered but also upon the amount of iron released from cells. However, we know very little about the pathway through which iron is released from cell and the molecules involved in regulating the rate of iron efflux from cells (Kaplan, 1996). The FP1 is a protein discovered to mediate iron export. The CP is a critical protein that affects on iron release from the cell (Qian and Ke, 2001). FP1 may associate with Heph or CP to regulate iron efflux, but the mechanisms remain to be defined.

1.5.2 Hepcidin and Body Iron Homeostasis

Maintaining normal iron homeostasis is essential for the organism, as both iron deficiency and iron excess are associated with cellular dysfunction. Recently, several lines of evidence have suggested that hepcidin; a peptide mainly produced by the liver, plays a major role in the control of body iron homeostasis.

1.5.2.1 Hepcidin

During sudies of antimicrobial properties of various human body fluids, Park et al. isolated a new peptide from urine (Park et al., 2001), and named it hepcidin, based on its site of synthesis (the liver, hep-) and antibacterial properties *in vitro* (-cidin). Independently, Krause et al. isolated the same peptide from plasma ultrafiltrate (Krause et al., 2000), and named it LEAP-1 (liver-expressed antimicrobial peptide).

1.5.2.1.1 Structure of Hepcidin

Two forms of human hepcidin of 20- (hepc-20) and 25- (hepc-25) amino acids (aa) were isolated from urine (Park et al., 2001) and blood ultrafiltrate referred to as LEAP-1 (Krause et al., 2000). These peptides were chemically synthesized and shown to be active *in vitro* against bacteria and fungi. The major hepcidin form was a cationic peptide with 25 amino acid residues and 4 disulfide bridges. Surprisingly, and unlike other antimicrobial peptides, hepcidin sequences were remarkably similar among various mammalian species, and searches of expressed sequence tag (EST) databases also identified several clearly related fish hepcidins. In humans, the peptide is derived from the C-terminus of an 84-amino-acid prepropeptide, encoded by a 0.4 kb mRNA generated from three exons of a 2.5 kb gene on chromosome 19. As judged by mass spectrometry, electrophoretic migration in acid-urea PAGE, retention on C18 reverse-phase HPLC columns and reactivity with anti-hepcidin antibody, the natural and synthetic forms were identical. Hunter et al. analyzed the synthetic forms by nuclear magnetic resonance spectrometry (Hunter et al., 2002) and established their connectivity and solution structure (Fig. 1-6). The molecule is a simple hairpin whose two arms are linked by disulfide bridges in a ladder-like configuration. One highly unusual feature of the molecule is the presence of disulfide linkage between two adjacent cysteines near the turn of the hairpin. Compared to most disulfide bonds, those formed between adjacent cysteines are stressed and could have a greater chemical reactivity. Like other antimicrobial peptides, hepcidin displays spatial separation of its positively charged hydrophilic side chains from the hydrophobic ones, a characteristic of peptides that disrupt bacterial membranes.

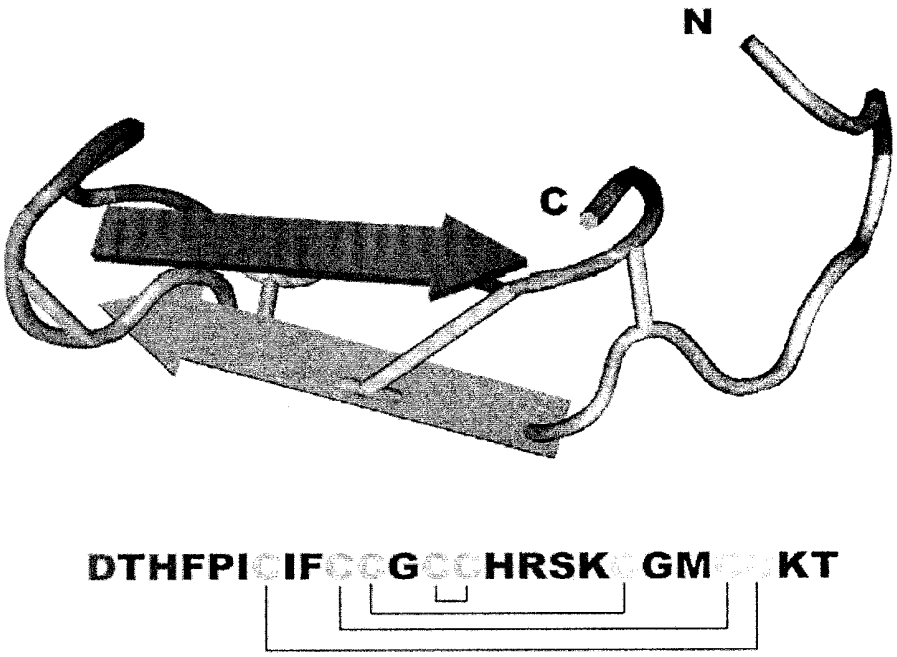

Fig. 1-6: Amino acid sequence and a cartoon model of the major form of human hepcidin. The amino and carboxy termini are labeled as N and C respectively. Disulfide bridges are in yellow, basic amino acids in blue, and acidic in red. The pattern of disulfide linkages between the 8 cysteines is also shown in the amino acid sequence. (From Ganz T et al, 2003)

1.5.2.1.2 Expression and Regulation of Hepcidin

Current literature suggests that hepcidin signals the body's iron requirements to the intestine, and its predominantly hepatic expression and apparent regulation by liver-iron concentration has prompted suggestions that hepcidin is the mediator of iron absorption (Fleming and Sly, 2001a; Nicolas et al., 2001). However, several studies have now shown that hepcidin expression can be altered by anemia, hypoxia, inflammation (Nicolas et al., 2002) and Tf saturation (Frazer et al., 2002).

Iron loading induces hepcidin: The connection between hepcidin and iron metabolism was first made by Pigeon et al. (Pigeon et al., 2001) during studies of the hepatic responses to iron overload. The hepcidin mRNA was induced not only by dietary or parenteral iron overload but also by treatment of the mice with lipopolysaccharide. Moreover, β_2-microglobulin knockout mice, a murine model of hemochromatosis, showed increased levels of hepcidin mRNA on normal diet but not a low iron diet. These results clearly indicated that hepcidin was regulated by iron as well as immune stimuli.

Induction of hepcidin by infection and inflammation: In the meantime, the connection between hepcidin and infection/inflammation was also becoming clearer. Shike et al. showed that in white bass liver, infection with the fish pathogen *Streptococcus iniae* increased hepcidin mRNA expression 4500-fold (Shike et al., 2002). In another study by Nicolas et al., injections of turpentine, a standard inflammatory stimulus, into mice induced hepcidin mRNA 4-fold and led to 2-fold decrease in serum iron (Nicolas et al., 2002). The hypoferremic response to

turpentine-induced inflammation was absent in the USF2/hepcidin-deficient mice, indicating that this response is fully dependent on hepcidin. Nemeth et al. assayed urinary hepcidin peptide in patients with anemia due to chronic infections or severe inflammatory diseases, and observed as much as 100-fold increases in hepcidin excretion (adjusted for urinary creatinine), with smaller increases in patients with less severe inflammatory disorders (Nemeth et al., 2003). Urinary hepcidin also increased about 100-fold in patients with iron overload from transfusions for sickle cell anemia or myelodysplasia. Hepcidin excretion correlated well with serum ferritin that is also increased by both iron loading and inflammation. Studies of the effect of iron or cytokines on isolated primary human hepatocytes (Nemeth et al., 2003) revealed that hepcidin mRNA was induced by lipopolysaccharide and strongly induced by monokines from monocytes exposed to lipopolysaccharide. Among the cytokines, IL-6, but not IL-1α or TNF-α, strongly induced hepcidin mRNA. Surprisingly, exposure of hepatocytes to iron-saturated Tf or to ferric ammonium citrate not only failed to induce hepcidin mRNA but suppressed it. These findings indicated that hepcidin production by hepatocytes is indirectly regulated by both infection and iron. Infections, in particular by pathogen-specific macromolecules like lipopolysaccharide, probably act on macrophages, including hepatic Kupffer cells, to induce the production of IL-6, and the cytokine in turn induces the production of hepcidin mRNA in hepatocytes (Nemeth et al., 2003). In aggregate, the increase of hepcidin production due to inflammation and the ability of transgenic or tumor-derived hepcidin to suppress erythropoiesis by iron starvation strongly suggest that hepcidin is the key mediator of anemia of inflammation. However, it remains to be shown that hepcidin peptide administration to mice or humans will cause iron sequestration and iron-limited erythropoiesis.

Suppression of hepcidin by anemia or hypoxia: In addition to iron stores and inflammation, anemia and hypoxia also affect iron metabolism. These stimuli would be expected to decrease hepcidin production and remove the inhibitory effect on iron absorption and iron release from macrophages so that more iron is available for compensatory erythropoiesis. Several investigators (Weinstein et al., 2002) (Nicolas et al., 2002) confirmed that these effects indeed take place. Anemia induced by mouse mutations that restrict the uptake of iron in the small intestine (*sla* and *mk* mice) showed markedly decreased hepatic hepcidin mRNA. Anemia induced by phlebotomy, or by hemolysis from phenylhydrazine, also suppressed hepatic hepcidin mRNA. Importantly, the suppressive effect of hemolytic anemia was seen even in iron-overloaded mice, suggesting that the suppression of hepcidin by anemia has a stronger effect than the stimulation of hepcidin by iron overload. This hierarchy of effects could explain why iron overload commonly develops with certain hemolytic disorders. However, these observations do not explain why iron overload occurs much more commonly in intramedullary hemolysis than in peripheral hemolysis or nonhemolytic anemias.

Effect of Tf saturation on hepcidin expression: Frazer et al. have demonstrated a positive correlation between Tf saturation and hepcidin expression, suggesting that the level of Tf-bound iron in the bloodstream may be regulating the hepatic expression of hepcidin (Frazer et al., 2002). A possible detection mechanism for Tf saturation is suggested from the study of inherited disorders of iron metabolism. Mutations in TfR2 result in tissue iron overload, indicating that this molecule plays a role in the regulation of iron homeostasis (Camaschella et al., 2000; Roetto et al., 2001; Fleming et al., 2002). Its ability to bind Tf (Kawabata et al., 1999) makes it an

ideal candidate to detect Tf saturation and a regulator of hepcidin expression. HFE, the gene defective in most hemochromatosis patients (Feder et al., 1996), is another candidate, as it interacts with TfR1 and could, therefore, detect a signal from Tf. More direct evidence of the involvement of HFE in the regulation of hepcidin levels has recently come from their laboratory, where analysis of liver biopsies from hemochromatosis patients has revealed a reduction in hepcidin expression despite hepatic iron loading (Bridle et al., 2003). Similar results were seen in HFE knockout mice. The remarkable similarity in the iron loading phenotypes of mice and/or humans with disruptions in HFE, TfR2, or hepcidin is highly consistent with their participation as components of the same regulatory network.

1.5.2.2 Hepcidin Regulation of Iron Homeostasis

1.5.2.2.1 Hepcidin Reflecting the Body Iron Level (Fig. 1-7)

The Tf saturation of serum is a key signal to the hepcidin reflecting. Townsend and Drakesmith proposed the mechanism for the detection of Tf saturation by HFE and TfR2 (Townsend and Drakesmith, 2002). The results showed that the HFE (Frazer et al., 2001), TfR2 (Kawabata et al., 1999), and hepcidin (Pigeon et al., 2001) are highly expressed in the liver.

Tf exists in the serum in three forms: diferric Tf, monoferric Tf, and apotransferrin (Leibman and Aisen, 1979). The distribution of iron between diferric Tf and monoferric Tf is dependent on Tf saturation such that a lowering of Tf saturation shifts the ratio of the two forms in favor of monoferric Tf (Huebers et al., 1984). For

example, the ratio of diferric Tf to monoferric Tf is 1:2 at a Tf saturation of 30% but 1:5 at 15% saturation. All three forms of Tf can bind to TfR1 at the cell surface, although diferric Tf has a 4-fold greater affinity than monoferric Tf and a 24-fold greater affinity than apotransferrin (Young et al., 1984). This, along with the increased iron content of the diferric form, results in more efficient iron delivery from diferric Tf than from monoferric Tf under normal conditions (Huebers et al., 1985). However, the proportion of iron delivered from monoferric Tf increases as Tf saturation decreases (Huebers et al., 1985). Under normal conditions there is sufficient iron-bearing Tf in the circulation to totally saturate the entire cell surface TfR1 in the body (Cazzola et al., 1985). Therefore, in this state, the Tf saturation determines the ratio of diferric to monoferric Tf that is bound to its receptor at any one time.

The hemochromatosis protein HFE has also been shown to bind to TfR1 *in vivo* (Parkkila et al., 1997; Waheed et al., 1999). In addition, the binding site for HFE on TfR1 overlaps with that of Tf (West et al., 2001). This means that there would be competition between Tf from the circulation and HFE on the cell surface for binding to TfR1. The intrinsically higher affinity of Tf for TfR1 (West et al., 2001) makes it reasonable to assume that diferric Tf can outcompete HFE for TfR1, binding more efficiently than monoferric Tf, although it has proved difficult to measure the relative affinities experimentally (West et al., 2001).

Based on this assumption, Frazer proposed a model for the regulation of hepcidin expression (Frazer and Anderson, 2003). The free HFE on the cell surface (i.e., HFE not bound to TfR1) transmits a signal to the nucleus to stimulate the production of

hepcidin. However, when HFE binds to TfR1, the signal is abrogated. The competition between HFE and diferric Tf for binding to TfR1 will determine the amount of free HFE on the cell surface and consequently the level of hepcidin produced. In a normal individual, approximately 30% of the iron binding sites on Tf are occupied (Huebers and Finch, 1987), and at this level of saturation the majority of receptor-bound Tf will be in the diferric form (Huebers et al., 1985). Thus the competition between HFE and Tf for TfR1 binding would favor Tf. This would leave a proportion of HFE molecules free on the hepatocyte surface to stimulate hepcidin production.

As body iron stores decrease, several events occur that shift the competition in favor of HFE binding to TfR1: (1) Tf saturation decreases; (2) the ratio of diferric Tf to monoferric Tf shifts in favor of monoferric Tf; (3) cell surface TfR1 expression increases; and (4) Tf levels increase. Thus more HFE is able to bind to TfR1 and the signal to synthesize hepcidin is reduced, leading to a decrease in circulating hepcidin levels and an increase in intestinal absorption. The opposite would occur during iron overload when Tf saturation is high and the cell surface expression of TfR1 is low. The competition would greatly favor the binding of diferric Tf and result in increased free HFE at the cell surface. In addition, the reported stimulation of HFE expression in iron-loaded cells (Han et al., 1999; Byrnes et al., 2000) would increase the amount of free HFE at the cell surface and, subsequently, the expression of hepcidin. In hemochromatosis, aberrant HFE function would prevent the induction of hepcidin expression despite TfR1 being saturated with diferric Tf. This would reduce hepcidin expression and lead to the inappropriately increased iron absorption seen under this condition.

The binding of diferric Tf to TfR2 produces a signal to increase the expression of hepcidin in a similar manner to unbound HFE. Since TfR2 does not appear to bind to HFE (West et al., 2001), it is unlikely to signal through this molecule. In this case, as the level of diferric Tf falls, TfR1 would out compete TfR2 for diferric Tf binding, as TfR1 has a 25-fold greater affinity for diferric Tf than its homolog (West et al., 2000). This would reduce the signal for hepcidin synthesis and, as a result, stimulate absorption. When iron levels increase, the resultant lowering of TfR1 expression would shift the competition in favor of TfR2, causing an increase in hepcidin production and a decrease in absorption. A recent study has also shown that diferric Tf raises TfR2 expression and causes a redistribution of TfR2 to the cell surface (Deaglio et al., 2002), further increasing hepcidin production when iron levels are high.

This model places the regulation of hepcidin expression under the dual control of HFE/TfR1 and TfR2. A mutation in either gene would reduce the signal to express hepcidin and result in the inappropriately increased iron absorption that is seen in hemochromatosis. The remaining functional molecule would continue to regulate absorption, although basal absorption would occur at a higher rate.

However, many questions need to be explained. Direct exposure of murine (Pigeon et al., 2001) or human (Nemeth et al., 2003) hepatocytes to ferric iron, with or without serum, or of human hepatocytes to iron saturated Tf (Nemeth et al., 2003) did not induce hepcidin mRNA, and at higher concentrations of iron suppressed it. This suggests that iron-sensing may take place in other cell types. How the free HFE

or saturation of TfR2 transmit a signal to the nucleus to stimulate the production of hepcidin is unclear although Ganz has proposed that it causes the release of IL-6 and possibly other signals that act on hepatocytes to induce the synthesis and secretion of hepcidin (Ganz, 2003).

1.5.2.2.2 How Does the Hepcidin Regulate Iron Transport (Fig. 1-7)

The molecules that mediate the transport of non-heme iron in enterocytes have been elucidated in this thesis introduction. Nicolas et al. (Nicolas et al., 2001) proposed that hepcidin interacts with receptors on the crypt cells of the duodenum and dictates the amount of iron absorbed by these cells once they have matured and migrated to the villus. However, in all situations studied thus far, hepcidin expression shows a close inverse correlation with iron absorption. This is equally true in the case of a rapid stimulus (e.g., the acute phase response) or a delayed stimulus (e.g., enhanced erythropoiesis) for iron absorption (Nicolas et al., 2002). The close temporal relationship between variations in hepcidin levels and intestinal transporter expression strongly suggests a direct effect of hepcidin on mature enterocytes. Fazer et al (Frazer and Anderson, 2003) demonstrated that expression of iron transport molecules is altered simultaneously in all mature enterocytes, and not progressively as newly differentiated cells emerge from the crypts, strongly supporting this proposal.

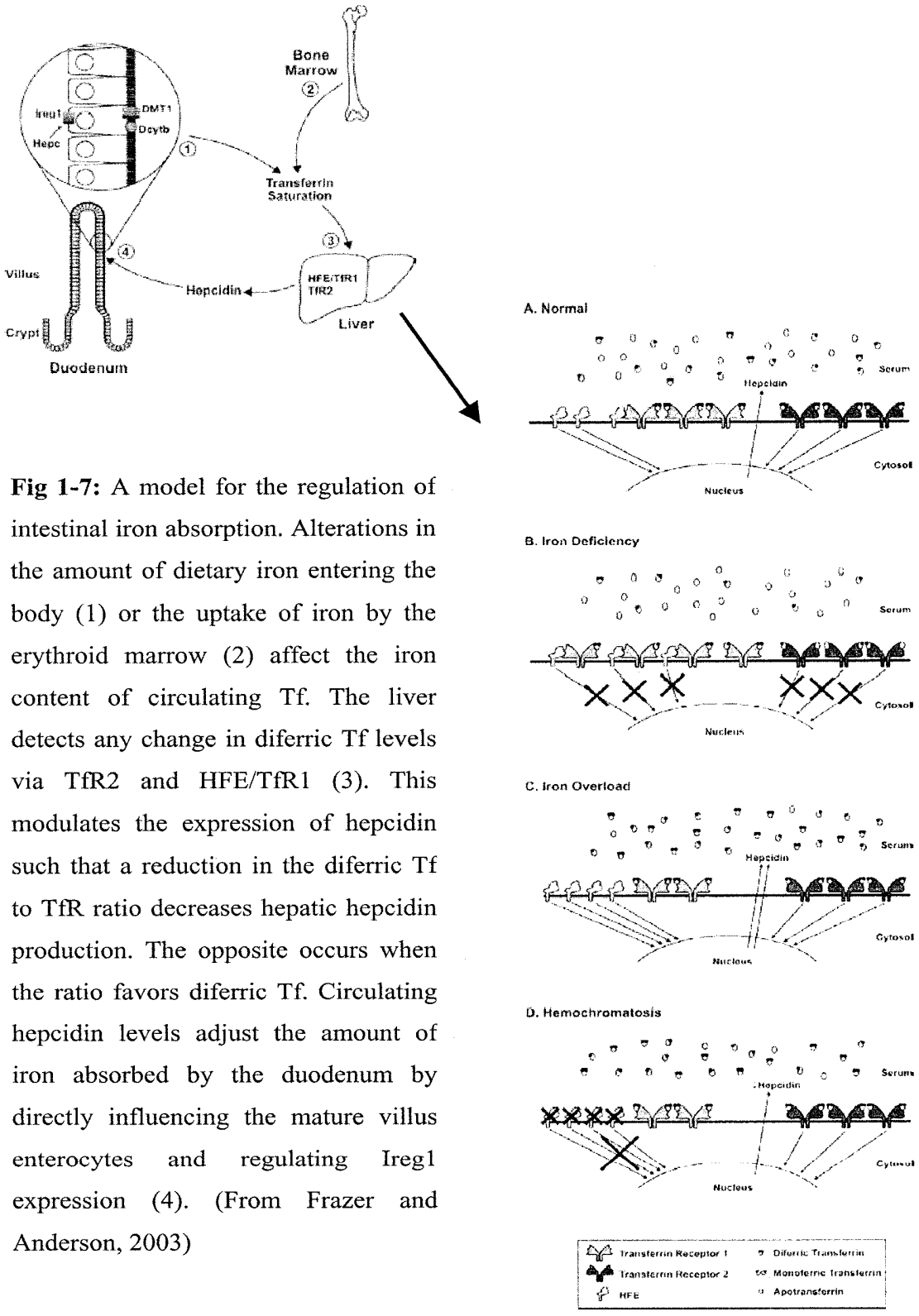

Fig 1-7: A model for the regulation of intestinal iron absorption. Alterations in the amount of dietary iron entering the body (1) or the uptake of iron by the erythroid marrow (2) affect the iron content of circulating Tf. The liver detects any change in diferric Tf levels via TfR2 and HFE/TfR1 (3). This modulates the expression of hepcidin such that a reduction in the diferric Tf to TfR ratio decreases hepatic hepcidin production. The opposite occurs when the ratio favors diferric Tf. Circulating hepcidin levels adjust the amount of iron absorbed by the duodenum by directly influencing the mature villus enterocytes and regulating Ireg1 expression (4). (From Frazer and Anderson, 2003)

1.5.3 Hepcidin and Brain Iron Metabolism

Because the brain resides behind BBB and has multiple regions with differing metabolic requirements, a variety of cell types with specialized functions and hence specialized iron requirements, it is possible that there is a system of regulating brain iron homeostasis. However, the mechanism by which the brain acquires iron or how the mechanism is regulated is poorly understood. The mechanism for iron uptake and transport across the endothelial cells lining the blood vessels, the regulation of iron uptake of specific brain region and where the brain iron is released must be considered. The role of hepcidin in body iron metabolism implies specific factor(s) like hepcidin may also be involved in iron homeostasis in the brain.

1.6 BRAIN IRON METABOLISM

Despite years of investigation, it is still not known why iron levels are abnormally high in some regions of the brain in NDs. Also, it is not clear whether iron accumulation in the brain is an initial event that causes neuronal death or is a consequence of the disease process. We propose that iron and iron-induced oxidative stress constitute a common mechanism that is involved in the development of neurodegeneration. Also, we suggest that, at least in some NDs, brain iron misregulation is an initial cause of neuronal death and that this misregulation might be the result of either genetic or non-genetic factors (Qian and Shen, 2001; Ke and Ming Qian, 2003).

1.6.1 Iron Distribution and Regulation

Iron is relatively abundant in brain tissue. Unlike other organs, iron has a highly characteristic localization and uneven distribution in the brain when compared to other metals. Hallgren and Sourander in 1958 found the iron content in globus pallidus, red nucleus, putamen and substantia nigra are higher than the iron levels in the liver, the main site of iron metabolism in the body (Gerlach et al., 1994). Indeed, iron is present in the basal ganglia at a concentration equal to that in the liver (Hu and Connor, 1996). Biochemical and histochemical analysis (Dwork et al., 1988; Connor and Benkovic, 1992; Morris et al., 1992) indicate that white matter is a major site of iron concentration throughout the brain. Recent MRI mapping of iron distribution in the brains of children and adolescents also shows that the highest concentrations of iron occur in the globus pallidus, caudate nucleus, putamen, and substantia nigra while the cortex and cerebellum contain substantially lower concentrations.

At the cellular level, iron was found in many cell types of the CNS (central nervous system), including neurons, oligodendroglia, microglia and astrocytes. It has been suggested iron is distributed to different cell types in the brain in a heterogeneous fashion. The majority of the cells that contain iron are oligodendrocytes (Hill and Switzer, 1984; Dwork et al., 1988; Gerber and Connor, 1989). Histochemical analysis shows similar results in human, monkey, rat and mice brain tissue (Connor et al., 1990; LeVine and Macklin, 1990; Morris et al., 1992). Even in iron-rich areas, such as the caudate-putamen, substania and deep cerebellar nuclei, it is the oligodendrocytes that stain robustly for iron (Benkovic and Connor, 1993). The

report that 80% of the iron in the brain is found in myelin fractions has led to the proposal that iron may play an important role in myelination and/or oligodendrocytes are involved in iron regulation in the brain. Neuronal iron staining is characteristically different from that seen in oligodendrocytes. Neurons, particularly pyramidal neurons in the cerebral cortex and hippocampus, have small punctatum of iron reaction in their somata that increases in density with age in rats (Benkovic and Connor, 1993). One additional cell type staining prominently for iron is the tanycyte that lines the third ventricle. The epithelial cells of the choroid plexus within the ventricles also stain intensely for iron. These cells may be involved in iron transport between the brain and the cerebrospinal fluid.

Brain iron distribution changes during development. Iron uptake into the brain is a continual process throughout life (Hu and Connor, 1996). In human and rat brains, iron increases with age and reaches its maximum values at the age of 30-40 years and 4-5 weeks postnatal respectively. Hallgren and Sourander measured the iron in 16 different brain regions and their changes with age (Gerlach et al., 1994). They found that in healthy adult brains, the total iron concentrations in globus pallidus, substantia nigra, and red nucleus are higher than in normal human liver (about 20mg iron/100g fresh weight for these gray matter regions vs. 13mg iron/100 g fresh weight for liver). If total iron concentration of the brain is considered, it is the lowest at birth and increases throughout life. Roskams (Roskams and Connor, 1994) analyzed iron in the brain of the same animals throughout development. In his study the brain was dissected into cerebral cortex, cerebellum-pons, and midbrain. Iron levels increase in each brain region into adulthood, but are lower in the aged group compared to the adult group. In the cerebral cortex, the levels of iron are

three times higher at postnatal 2 day than at any other time. In the adult group, the highest levels of iron are in the cerebellum-pons, whereas during development, concentrations in the cortex and midbrain are higher than in the cerebellum.

1.6.2 Roles of Brain Iron

Neurons and glia require iron in many aspects of their cell physiology (Hu and Connor, 1996). It has been argued that iron is likely to be especially critical in the brain because neurons are dependent upon iron-inducing oxidative aerobic metabolism (Connor and Benkovic, 1992). Iron serves as an essential component of numerous cellular enzymes. These include the cytochrome oxidases, a number of enzymes in the citric acid cycle, ribonucleotide reductase (the rate-limiting step for DNA synthesis), and NADPH reductase. With respect to neurological activity, the availability of iron is crucial for brain cell viability (Beard et al., 1993a). Iron is involved in the function and synthesis of dopamine, serotonin, catecholamines, and possibly γ-aminobutyric acid (GABA) and myelin formation (Beard et al., 1993a). It is the key component of the heme in cytochrome proteins, permitting mitochondrial electron transfer during cellular respiration. Moreover, iron is involved in the synthesis and degradation of fatty acids and cholesterol and is likely to have an important role in both myelinogenesis and myelin maintenance (Connor and Benkovic, 1992). A number of physiological functions listed in Table 1-2 have been attributed to brain iron.

Table 1-2. Biological functions of brain iron

1. Catalytic role in enzymatic processes
A. Tricaboxylic cycle enzymes
Succinate dehydrogenase [a]
Aconitase [a]
B. Oxidative phosphorylation enzymes, e.g., cytochrome oxidase C [a]
C. Amino acid and neurotransmitter metabolism enzymes
Phenylalanine hydroxylase [a]
Monoamine oxidase (MAO) [a]
Aldehyde oxidase
Aminobutyric acid transaminase
Glutamate dehydrogenase
2. Effect on D2 receptor function
3. Effect of other neurotransmitters
γ-Aminobutyric acid
Serotonin
Opiate-peptides
4. Role in peroxidation, oxidation and hydroxylation reactions
5. Other possible functions (not established)
Role in protein synthesis
Role in maintenance of the BBB
[a] Brian enzyme levels remain unchanged in iron deficiency.

1.6.3 Brain Iron Metabolism

Iron misregulation in the brain plays a part in neuronal death in some NDs, such as AD, PD and HD and Hallervorden-Spatz Syndrome (HSS). Iron misregulation in the brain may have genetic and non-genetic causes. The disrupted expression or function of proteins involved in iron metabolism increases the concentration of iron in the

brain. Disturbances can happen at any of several stages in iron metabolism (including uptake and release, storage, intracellular metabolism and regulation). Increased brain iron triggers a cascade of deleterious events that lead to neurodegeneration (Ke and Ming Qian, 2003).

1.6.3.1 Iron Transport Across BBB

Adult mammals absorb iron through the duodenum. Ferric iron is reduced by Dcytb (McKie et al., 2001) or ferrous in the intestinal lumen and transported across the apical surface by DMT1. Ferric and ferrous iron can also enter absorptive enterocytes via a pathway mediated by paraferritin complex, consisting of β-integrin, mobilferrin, and flavin mono-oxygenase. Heme is processed in the gut lumen and enters enterocytes as an intact metalloporphyrin (H). The mechanism of heme iron transport is not well defined, probably mediated by an endocytic pathway. Inside the cytoplasm, heme is degraded by heme oxygenase to release inorganic iron (Lieu et al., 2001). Once inside the cell, iron can either be stored in ferritin or transported across the basolateral membrane by FP1 (Donovan et al., 2000). The species of iron exported by FP1 is not known, but the need for ferroxidase activity to load iron on to Tf indicates that it is probably Fe^{2+}. FP1 and Heph may work together in the absorptive enterocyte in other cell types; FP1 may work with CP, a soluble ferroxidase, to load iron on to Tf (Kaplan and Kushner, 2000; Burdo and Connor, 2003) (Fig. 1-8).

The brain possesses a special barrier system that excludes plasma proteins, metals and polar substances from gaining free access to the brain interior. As a number of

transition metals are essential to normal brain function, the brain ensures their transport from the circulation by specialized mechanisms of transport. To date, however, the mechanisms of iron transport across the BBB have not been completely clarified. Accumulated evidence suggests that the Tf/TfR pathway may be the major route of iron transport across the luminal membrane of the capillary endothelium (Malecki et al., 1999; Moos et al., 2000), and that iron, possibly in the form of Fe^{2+}, crosses the abluminal membrane and enters the interstitial fluid (IF), although the molecular events of this process are unknown (Fig. 1-8). The evidence shows that the uptake of Tf-bound iron (Tf-Fe) by TfR-mediated endocytosis from the blood into the cerebral endothelial cells is no different from the uptake into other cell types (Bradbury, 1997). This process includes several steps: binding, endocytosis, acidification and dissociation, and the translocation of iron across the endosomal membrane, probably by a DMT1-mediated process (Gunshin et al., 1997; Fleming et al., 1998). Most of the Tf will return to the luminal membrane with TfR, while the iron crosses the abluminal membrane by an undetermined mechanism. Recent studies show that FP1/Heph and/or Heph-independent [perhaps is FP1-CP (GPI-anchored CP or CSF CP)] iron-export systems might play a key role in Fe^{2+} transport across the basal membrane of enterocytes in the gut (Vulpe et al., 1999; Donovan et al., 2000; Kaplan and Kushner, 2000). It is unknown at present if these two systems have the same role in Fe^{2+} transport across the abluminal membrane of the BBB as in enterocytes. The expression of Heph in the BBB has not been clarified and is worth investigating. Another proposed mechanism for Fe^{2+} transport across abluminal membrane involves astrocytes. The astrocytes probably have the ability to take up Fe^{2+} from endothelial cells through their end feet processes on the capillary endothelia (Malecki et al., 1999; Oshiro et al., 2000). In addition to the Tf/TfR

pathway, it has been suggested that the LfR/Lf and GPI-anchored p97/secreted p97 pathways might play a role in iron transport across the BBB (Faucheux et al., 1995; Malecki et al., 1999; Qian and Shen, 2001). It is also possible that a small amount of iron might cross the BBB in the form of intact Tf-Fe complex by receptor-mediated transcytosis (Moos and Morgan, 1998b).

After the iron has been transported across the BBB, it is likely to bind quickly to the Tf secreted from the oligodendrocytes and choroid plexus epithelial cells (Bradbury, 1997; Moos and Morgan, 1998b) (Fig. 1-8). Data from several experiments reveal that the iron concentration exceeds that of the binding capacity of Tf in the cerebrospinal fluid (CSF) and IF. Because the affinity of Tf with iron is the highest compared with other iron transporters (the equilibrium constant for formation of diferric Tf is more then 10^{10} times that of ferric citrate), Fe^{3+} in CSF and IF will bind to Tf first. Unlike Tf found in blood, Tf in CSF and IF is fully saturated with iron. The excess iron will bind to other transporters. Hence, it is possible that there are two forms of iron transport in CSF and IF in the brain: Tf-Fe and non-Tf-bound iron (NTBI). The latter probably includes citrate-Fe^{3+} or Fe^{2+}, ascorbate-Fe^{2+}, and albumin-Fe (2+ or 3+) and also Lf-Fe^{3+} and secreted p97-Fe^{3+}. If the remaining NTBI in CSF is in the oxidized form, Fe^{3+}, it will be bound almost completely to citrate because the complex has an equilibrium constant Log K ~11.4. If it is present as Fe^{2+}, it will be bound rather more loosely to citrate with an equilibrium constant log K ~4.5. Low concentrations may be present in complex with ascorbate (log K~2) and a finite concentration as free Fe2+ (10^{-8} to 10^{-7} *M).*

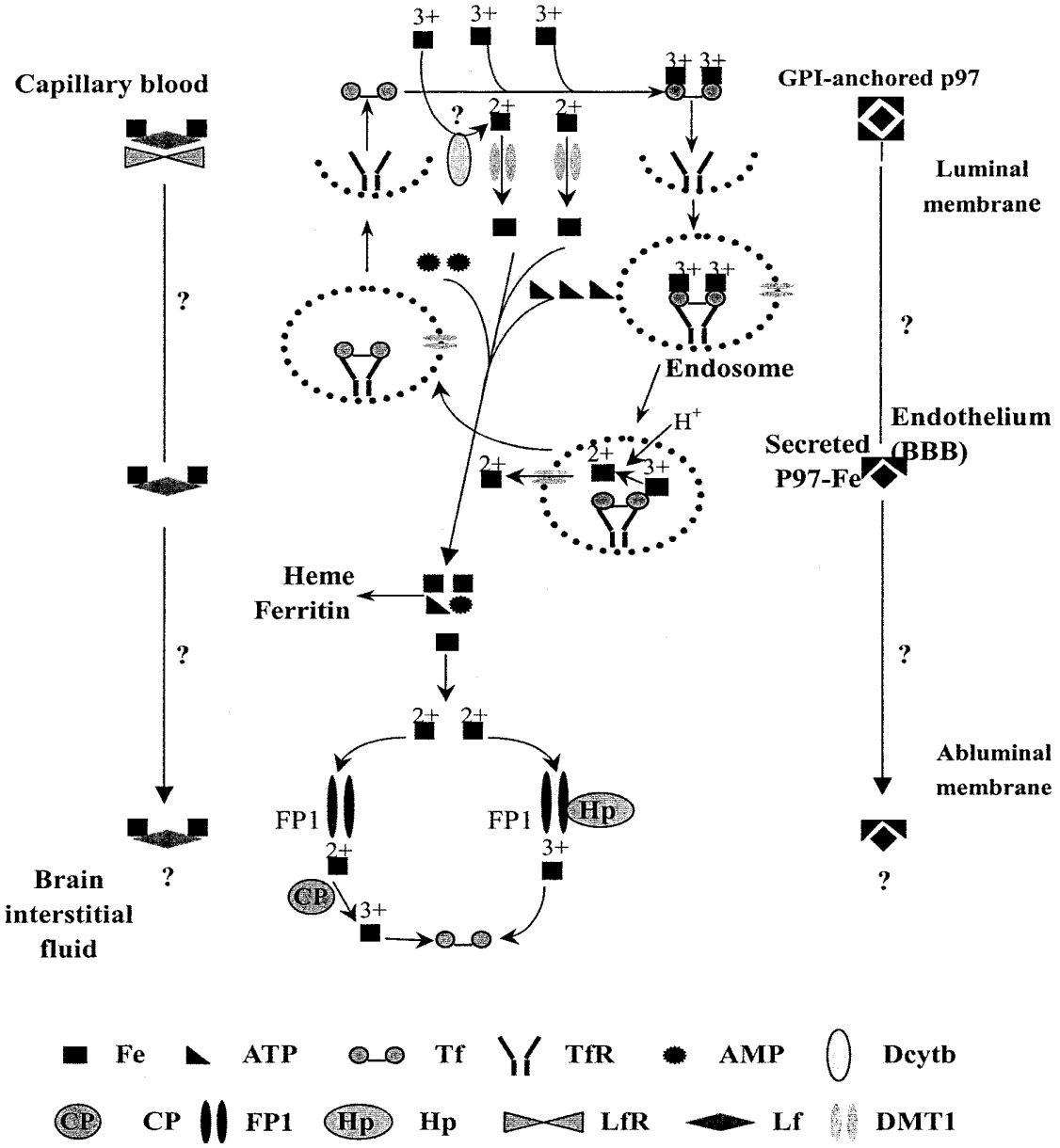

Fig. 1-8. Proposed scheme for iron transport across the BBB. The Tf-TfR pathway might be the major route of iron transport across the luminal membrane of the BBB. Tf-Fe uptake by endothelial cells is similar in nature to the uptake into other cell types. DMT1 might play a role in the translocation of iron from endosome to cytosol. Iron (Fe^{2+}) probably crosses the abluminal membrane via FP1-Heph and /or Heph independent [perhaps is FP1-CP (GPI-CP or CSF CP)] export systems. LfR-Lf and GPI-anchored p97-secreted-p97 pathways might also be involved in iron transport across the BBB; however, further study is needed. Abbreviations: BBB, brain-blood barrier; Tf, transferrin; TfR, transferrin receptor; CP, ceruloplasmin; DMT1, divalent metal transporter; FP1, ferroportin 1; Heph, hephaestin; Dcytb, duodenal cytochrome b; Lf, lactoferrin; LfR, lactoferrin receptor; NTBI, non-transferrin-bound iron; Tf-Fe, transferrin-bound iron.

1.6.3.2 Iron Uptake and Release in Brain Cells (Fig. 1-9)

It is acknowledged that Tf-TfR mediated endocytosis is the main pathway of iron uptake by most extraneural organs cells. In the brain, TfR is found to be widely distributed on both membrane of glial cells and neurons, and the mechanism of Tf-TfR mediated pathway was first identified by Swaiman and Machen in the cultured mammalian cortical neurons and glial cells (Swaiman and Machen, 1985). It demonstrated that iron uptake in cortical neuronal and glial cell cultures could be inhibited by the lysosomotropic agents ammonium chloride and methylamine, raising the possibility that iron transport to brain cells is Tf-mediated just like in other tissues. Qian et al. also detected Tf-bound iron uptake pathway in cultured cerebellar granule cells (Qian et al., 1998).

Based on the accumulated information, however, it is highly likely that Tf-dependent iron uptake is not the only route in brain cell, nor is TfR expression the only factor determining iron uptake by brain cells. The following evidence support this possibility: 1) Photomicrograph study shows, amazingly, that there is little overlap in the distribution of TfR and iron. Except for the interpeduncular nucleus, no other iron-rich area of the brain had an abundance of TfRs, and the areas with dense TfRs had little or no stainable iron. 2) Some iron transporters were newly found in the brain: Two putative iron transporters, DMT1 and SFT (stimulator of Fe Transport) have been identified in some neurons and postnatal astrocyte. CP, which has been postulated as the critical ferroxidase for over 30 years, was found in the astrocyte and suggested its involvement of iron uptake and release in brain cells. LfR is found

to increase within the neurons of the pathological brain areas in PD, where neuronal loss is greatest and iron accumulation is heaviest. p97, first identified on melanoma cells, is also found in a subset of reactive microglia associated with senile plaques in AD brain, where there are high levels of iron and the iron storage protein ferritin.

The Tf-independent iron uptake, perhaps via LfR or GPI-anchored p97-mediated processes, will take up the Lf-Fe and secreted p97-Fe (Malecki et al., 1999). NTBI will be acquired by neuronal cells or other brain cells, probably via DMT1 or trivalent cation-specific transporter (TCT)-mediated mechanisms (Fig. 1-9) (Attieh et al., 1999). However, the mechanisms are unknown.

In addition, little is known about molecules involved in iron release from the brain cells. The results of clinical and CP gene knockout mice support CP involvement in iron release (Gitlin, 1998; Harris et al., 1999). However, our previous study (Qian et al., 2001a) and Fox group results (Mukhopadhyay et al., 1998; Attieh et al., 1999) exhibited the role of CP in iron uptake. Recent evidence also shows that the FP1 is expressed in rat brain (Jiang et al., 2002). The expression of Heph gene in the brain is worth studying. Whether the Heph-FP1 export pathway (like in duodenum) plays a role in the brain is still a matter of debate (Ke and Ming Qian, 2003). So, elucidating the regulation and expression of iron metabolism-related proteins and brain iron metabolism is a worthwhile and realistic goal.

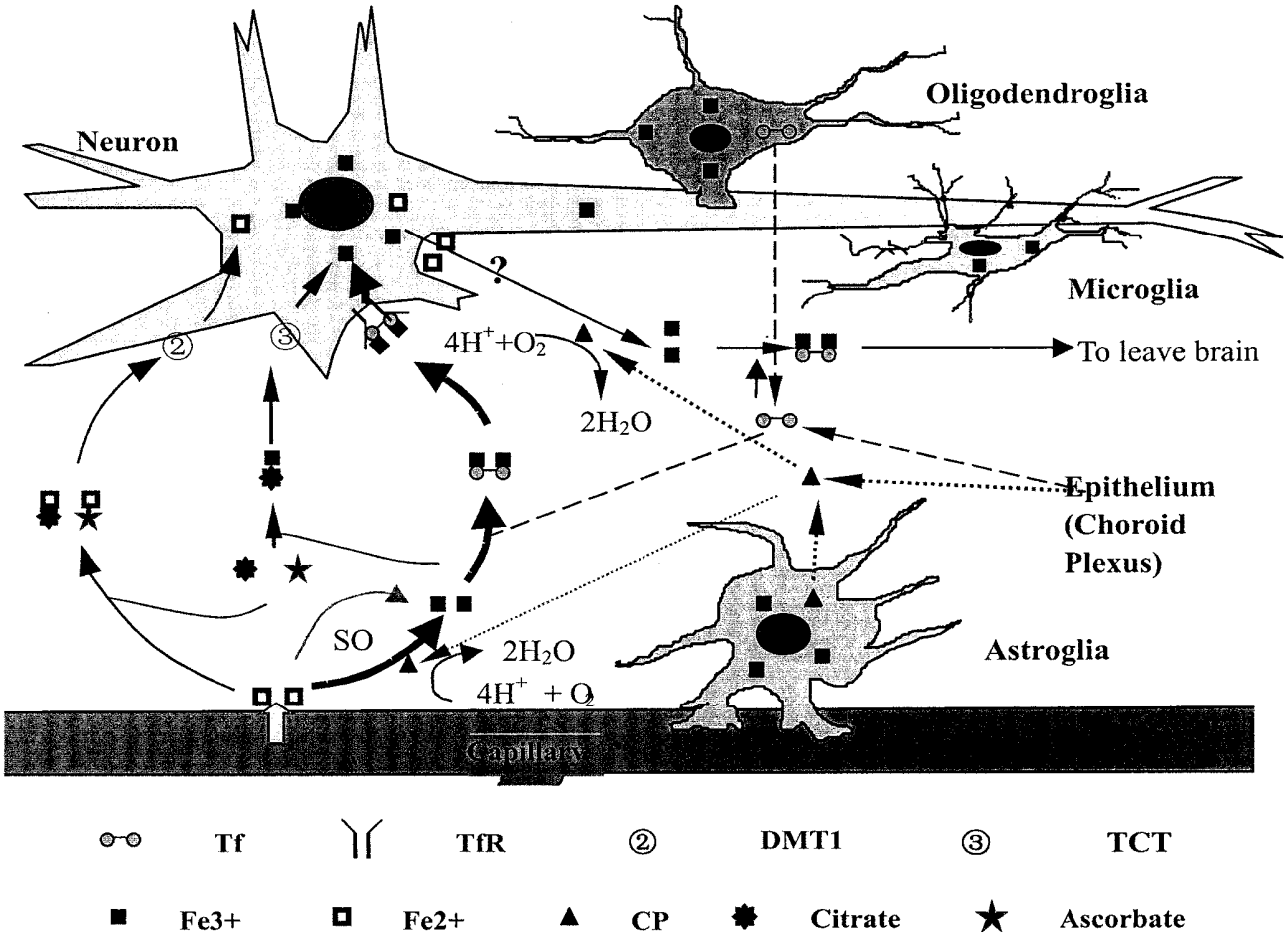

Fig. 1-9. The suggested role of ceruloplasmin in iron uptake by neuronal cells in the brain. CP may play a role in both in iron efflux from and in iron influx into the brain cells via its ferroxidase activity. It is also possible that the involvement of CP in iron uptake is more important physiologically than its role in iron efflux. CP may be necessary for Fe^{2+}, after it crosses the abluminal membrane of the BBB to be oxidized to Fe^{3+}. A small amount of Fe^{2+} might be oxidized to Fe^{3+} via spontaneous oxidization (SO) activity. The Fe^{3+} can than bind to transport carrier Tf in the cerebrospinal fluid and interstitial fluid that is secreted from the oligodendrocytes and choroids plexus epithelial cells and be acquired by neurons (or microglia and other relevant brain cells) via TfR-mediated endocytosis. NTBI (including citrate-Fe^{3+} or –Fe^{2+}, ascorbate-Fe^{2+}, and albumin-Fe^{2+}or Fe^{3+}) will be acquired by neuronal cells (or other brain cells) probably via DMT1 or TCT-mediated mechanisms. CP may be also involved in iron egress from neuronal cells to extracellular fluid. It has been hypothesized that iron, probably in the form of Fe^{2+}, is presented to the surface of the brain cell and then oxidized to Fe^{3+} by CP and combined with Tf in extracellular fluid for eventual excretion. The relevant mechanisms have not been determined. Abbreviations: Tf, transferrin; TfR, transferrin receptor; CP, ceruloplasmin; DMT1, divalent metal transporter; TCT, trivalent cation-specific transporter; NTBI, Non-Tf-bound iron.

1.6.4 Iron and Neurodegenerative Diseases

Iron plays a crucial function in the brain. However, an imbalance in brain iron will inevitably cause some neurological disorders.

Iron deficiency after birth irreversibly affects the content and distribution of iron within the brain and that causes neurotransmitter and behavioral changes (Beard, 2003), which alter neurotransmission involving dopamine, the major neurotransmitter of the extra pyramidal system of the brain (Beard et al., 2003). In human infants, iron deficiency anemia is known to be associated with psychomotor delays, which involve language and body balance. Insufficient iron levels during early postnatal development also result in mental and motor impairments that then persist into adulthood (Gordon, 2003).

In contrast to iron deficiency, a high concentration of free ionic iron may readily induce reactive oxygen species to initial lipid peroxidation of cellular membranes via Fenton-type reactions and increase the oxidative stress in susceptible brain areas such as the frontal and temporal cortex, the key target areas for neuronal degeneration, and senile plaque and neruofibrillary tangle formation. Abnormal iron accumulation in brain has been described for several NDs including PD, AD, and HSS (Qian and Shen, 2001; Sipe et al., 2002). These diseases seriously affect the quality of later life for millions of people and represent a disastrous condition. The table 1-3 lists the neurological diseases and their associated alterations in iron status.

Table 1-3. Neurological diseases and their associated alterations in iron status.

Neurological disease	Involvement of iron
Tardive dyskinesia	Increased striatal iron
Hereditary hemochromatosis	Increased iron in choroid plexus and pituitary, basal ganglia. Presence of mutation influences onset/incidence of AD
Aceruloplasminemia	Increased basal ganglia and CSF iron
Restless legs syndrome	Decreased plasma and CSF ferritin Increased CSF transferrin Decreased iron in substantia nigra and putamen
Huntington's disease	Increased iron in striatum, occurs presymptomatically
Freidreich's ataxia	Increased mitochondrial iron in striatum and cerebellum Mutation in frataxin Loss of ferritin receptors in periplaque white matter Increase ferritin in CSF
Multiple sclerosis	Iron in oligodendrocytes exacerbates oxidative stress Treatment with chelators or antioxidants decreases symptoms and pathology in animal models
Parkinson's disease	Iron accumulation in substantia nigra, striatum, and in neuromelanin-containing cells Decreased levels of ferritin in substantia nigra, caudate, putamen
Alzheimer's disease	Iron accumulation in brain regions associated with neurodegeneration Ferritin decreased in areas that accumulate iron Increased iron in amyloid plaques Changes in Iron Regulatory Protein (IRP) distribution and activity TfR decreased in hippocampus
Hallervorden-Spatz	Iron accumulation in globus pallidus, substantia nigra
Neuroferritinopathy	Iron and ferritin accumulation in the basal ganglia Low serum ferritin levels

1.6.4.1 Parkinson's Disease

PD patients have increased iron content in brain tissue, particularly, in the form of ferric iron (Sofic et al., 1988). The Tf/iron ratio is decreased in the globus pallidus and caudate of PD patients, suggesting defect in iron mobilization (Loeffler et al., 1995). The number of ferrotransferrin binding sites is increased, probably due to increased iron uptake by dopaminergic nerves or brain microvessels. The ultimate cause of neuronal death in patients with PD is not clear, but a growing body of evidence indicates that increased oxidative stress is one of the main culprits. However, whether oxidative stress is a primary or secondary event is unclear. Because iron enhances the formation of free radicals and generation of oxidative stress in cells, it may to play a central role in the development of PD and other NDs.

The selective damage to melanin-containing substantia nigra neurons in PD is possibly initiated by the interaction between iron and neuromelanin, resulting in the accumulation of ferric iron. Substantia nigra neurons may be at special risk of damage by free radicals because of their dopamine metabolism. Dopamine auto-oxidation leads to the formation of hydrogen peroxide as a byproduct and, if not effectively detoxified by glutathione, hydrogen peroxide may potentially induce the generation of highly reactive hydroxyl radicals in the presence of excess iron. The amount of neuromelanin, formed by polymerized oxidized dopamine, seems to direct the vulnerability of neurons. To investigate the process of neurodegeneration, oxidative stress induced by the neurotoxins 6-hydroxydopamine and N-methyl-4-phenyl-1,2,3,6-tetrahydropyridine has been used in animal models. Radical scavengers and iron chelators are found to be neuroprotective. Because the pathogenesis of PD involves several cellular processes and metabolic pathways, including dopamine metabolism, nitric oxide synthesis, activation of calcium

channels, and inflammatory processes with activated $NF_{\kappa}\beta$ and cytotoxic cytokines, treating PD with agents that prevent iron accumulation has get to achieve desirable results (Grunblatt et al., 2000; Koutsilieri et al., 2002).

L-dopa, through its decarboxylation to dopamine, remains the most effective therapy for the treatment of PD symptoms. However, despite almost 30 years of clinical experience, doubts remain as to whether L-dopa adversely affects the progression of the illness by accelerating nigral cell degeneration (Jenner and Brin, 1998). The issue of L-dopa toxicity was initially raised because of its potential to cause long term adverse effects (dyskinesias and motor fluctuations), which are not observed in untreated patients (Simuni and Stern, 1999). These can become so disabling that surgical treatment becomes the only apparent option for restoring any quality of life (Krack et al., 2000). This concept is based on the relative ease of oxidation of levodopa and the generation of toxic reactive oxygen species (Graham, 1978). The enzymatic oxidation of L-dopa to dopamine and its metabolism by monoamine oxidase B (MAO-B) give rise to the formation of hydrogen peroxide (H_2O_2), which may be mildly toxic. H_2O_2 can also be converted by iron-mediated Fenton reactions to produce the more toxic hydroxyl radical (OH ·), which can induce oxidative damage. Examination of postmortem tissues taken from patients who died of PD has shown increased levels of iron in the substantia nigra (Jenner and Brin, 1998). From the past several years' study, iron and iron-induced oxidative stress constitute a common mechanism that is involved in the development of neurodegeneration, at least in some NDs. Brain-iron misregulation is an initial cause of neuronal death and that this misregulation might be the result of either genetic or non-genetic factors (Qian and Shen, 2001). Therefore, alterations in iron and complex I may be related

to drug treatment, although there was no inhibition of complex I activity in patients with multiple-system atrophy who were treated with L-dopa (Schapira et al., 1990; Gu et al., 1997). Whether there is correlation between the iron increase and L-DOPA treatment in the brain cell is an important question to be elucidated.

1.6.4.2 Alzheimer's Disease

β-amyloid deposits, the hallmarks of AD, contain advanced glycosylation end products and copper and iron ions. The formation of covalently cross-linked, high molecular weight, β-amyloid peptide oligomers is accelerated by the presence of micromolar amounts of copper and iron ions (Loske et al., 2000). The amount of ferritin iron in basal ganglia is increased in AD at its onset, suggesting that the accumulation of iron might have a role in the pathogenesis of the disease (Bartzokis and Tishler, 2000). Iron has been shown to accumulate in Alzheimer's disease without a concomitant increase in ferritin. The lack of increase in the amount of translated ferritin might be due to the fact that iron-regulating protein 1 seems to form more stable complexes with the iron-responsive elements of ferritin and TfR1 mRNA in the brain of AD patients than of healthy individuals, resulting in an inhibition of ferritin translation (Pinero et al., 2000a). The pool of free iron might thus be increased, leading to enhanced vulnerability to oxidative damage. Indeed, AD is characterized by signs of major oxidative stress in the neocortex, with simultaneous deposition of β-amyloid proteins. This metalloprotein converts molecular oxygen into hydrogen peroxide by reducing copper or iron, potentially leading to the generation of free radicals through the Fenton reaction (Lynch et al., 2000). The connection between iron metabolism and AD is further supported by the

fact that the C2 Tf allele is more frequently associated with patients with AD than with controls. Because the presence of the C2 Tf allele in patients with AD seemingly shifts the onset of the disease to an earlier age, Tf might be involved in the pathogenesis of AD (van Rensburg et al., 2000).

1.6.4.3 Other Brain Disorders

In addition to PD and AD, a number of brain disorders are associated with disruptions in iron homeostasis in the brain. In HSS (Swaiman, 1991; Gerlach et al., 1994; Swaiman, 2001) it has been reported that large amounts of iron are deposited in the globus pallidus and pars reticulata of the substantia nigra. Postmortem examination of HSS patients found grossly rust-colored basal ganglia, suggesting large amount of iron storage. In HD (Gerlach et al., 1994), there is an increase in iron content in the caudate nucleus but not in the substantia nigra. There is also no elevation in brain ferritin content in the substantia nigra or elsewhere. In contrast to HD, increased ferritin content of the substantia nigra is found in Steel-Richardson-Olszewski's disease (Gerlach et al., 1994). In addition, there are increases in the concentration of iron in the caudate nucleus and putaman. The above studies reflect that an abnormal increase in iron content in some brain areas plays an important role in the pathogenesis and development of these disorders.

It is not known how and why iron accumulates in the substantia nigra and globus pallidus in normal circumstances and why its concentration is further exaggerated in these regions in patients with NDs. Because of the current lack of understanding of iron regulation in the brain, it is difficult to ascertain whether changes in iron levels

or in the histological distribution of iron reported in many of these diseases is in response to the disease state or part of the pathogenesis. Since the imbalance of brain iron can causes the above-mentioned neurological disorders, regulating the optimal level of iron in the brain seems to be a very important function. The importance of elucidating the role(s) of iron-relevant proteins in the maintenance of brain iron homeostasis is thus clear (Connor and Benkovic, 1992).

1.7 NEUROTRANSMITTER AND BRAIN IRON METABOLISM

In the CNS, neurotransmitters are of paramount importance for normal physiological function. The distribution of iron is correlated with some specific neurotransmitters, for example GABA, glutamate and dopamine. Injection of a GABA degradation inhibitor resulted in decreased substantia nigra pars reticulata iron staining two days later. Following the microinjection of excitatory amino acids, kainate or quinolinate, to the anterior olfactory nucleus/ventral striatal region, an increase in histochemical iron concentration was observed in the ipsilateral ventral pallidum, the globus pallidus and the substantia nigra pars reticulata. After microinjection of ibotenate or quisqualate to the nucleus basalis of Meynert, iron also accumulated in pars reticulata of substantia nigra. These results provided the direct evidence of correlation between the neurotransmitter and iron metabolism.

1.7.1 The Overlap Distribution of the Iron and Neurotransmitters

In humans, increased iron concentrations in the substantia nigra and accompanying substantia nigra neuronal loss occur in several NDs, including HSS, multiple system atrophy and progressive supranuclear palsy (Dexter et al., 1991; Gibb, 1991). Iron was also significantly increased in the globus pallidus AD and PD (Loeffler et al., 1995). The striatum and the substantia nigra are two key components in the motor circuit linked relevance to movement disorders. As the previous study exhibited, the substantia nigra and globus pallidus receive substantial innervation from the neostriatum, a considerable amount of which is GABAergic, and also receive excitatory (glutamatergic) efferents from the subthalamic nucleus (STN) (Wichmann and DeLong, 1996, 1999). Synaptic GABA is taken up by nerve ending GABAergic perikarya or by glial cells. Once taken up, GABA is transaminated by GABA-transaminase, producing succinate semialdehyde and glutamate (Hill, 1985). Glutamate is a highly abundant neurotransmitter in the striatum. The striatum receives major glutamatergic projections from most cortical areas (McGeorge and Faull, 1989) and also from the thalamus (Lapper and Bolam, 1992). Release of dopamine from terminals of the nigrostriatal projection appears to modulate the activity over the two pathways: transmission over the direct pathway is facilitated via dopamine D1 receptors and transmission over the indirect pathway is inhibited via dopamine D2 receptors. The overall effect of striatal dopamine release is to reduce basal ganglia output, leading to increased activity of thalamocortical projection neurons (Wichmann and DeLong, 1996, 1999). There is considerable overlap in

substantia nigra pars reticulata and globus pallidus that receive a dense GABAergic and glutamatergic projections and intense iron accumulated.

1.7.2 The Neurotransmitters Regulating the Iron Concentration in the Brain

Previous studies investigating the potential relationship between GABA and brain iron, Hill (Hill, 1985) injected an inhibitor of GABA degradation into either the globus pallidus or adjacent neostriatum or directly into the substantia nigra of the rat brain. These resulted in decreased the iron concentration in the substantia nigra pars reticulata, ipsilateral ventral pallidum and globus pallidus two days later. Direct injection into substantia nigra reduced iron in the injection site. These results provide the first evidence that the histochemical level of brain iron is related to GABA utilization/metabolism. Shoham et al. (Shoham et al., 1992) reported that microinjection of excitatory amino acids, kainate, or quinolinate to the anterior olfactory nucleus/ventral striatal region led to an increase in histochemical iron concentration in the ipsilateral ventral pallidum, the globus pallidus and the substantia nigra pars reticulata. After microinjection of ibotenate or quisqualate to the nucleus basalis of Meynert, iron also accumulated in the pars reticulata of substantia nigra. Increased iron accumulation, compared to that in the contralateral side, was stable for months after a single microinjection. In the basal ganglia distal from the site of EAA injection, the morphological changes of iron accumulation were not observed. Sastry and Arendash (Sastry and Arendash, 1995) further investigated the effects of denervation of striatal/pallidal inputs to globus pallidus/substantia nigra on iron levels in the globus pallidus/substantia nigra, and on

the pathology of those regions. Between one week and one-month post-lesioning, comprehensive neostriatum/globus pallidus lesions induced a progressive increase in both iron staining of substantia nigra zona reticularis and iron concentration of substantia nigra. These results suggest that loss or dysfunction of striatonigral/striatopallidal GABAergic neurons in several NDs may result in an increase or redistribution of nigral iron to cause loss of substantia nigra neurons. However, the mechanism by which neurotransmitters induce iron accumulation is not understood.

1.7.3 The Relationship Between the Neurotransmitters and Iron Transport Protein

Recent studies have demonstrated the presence of a number of iron transport proteins in the brain: GPI-CP, FP1, DMT1, HFE. However, the functions of those proteins in brain iron metabolism do not understood.

Intracellular iron balance depends on the amount of iron taken up as well as on the amount of iron released by the cell (Qian and Wang, 1998; Qian and Shen, 2001). The membrane TfR mediated endocytosis or internalization of the complex of Tf bound iron and the TfR is the major route of cellular iron uptake (Li et al., 2002; Li et al., 2003b). DMT1 may be involved in the transport of iron from endosome to cytosol under physiological conditions (Su et al., 1998; Tabuchi et al., 2000; Touret et al., 2003). DMT1 may also play an important role in iron transport across the apical surface of human intestinal Caco-2 cells (Tandy et al., 2000) and rat duodenal enterocytes (Trinder et al., 2000) via Tf-independent iron uptake. CP is an abundant

plasma protein synthesized mainly in hepatocytes. A role for CP in iron efflux was first suggested in the 1960s, based on the observation that the ferroxidase activity of CP promoted iron incorporation into Tf (Osaki et al., 1966). This suggestion is supported by aceruloplasminemia (Gitlin, 1998) and animal model of aceruloplasminemia (Harris et al., 1999). Recent gene-mapping studies have identified a CP homologue; Heph is expressed predominantly in the small intestine (Vulpe et al., 1999). Heph facilitates the transport of iron from enterocyte to plasma, but is not a membrane transporter. FP1 was recently identified as a duodenal iron export molecule (Donovan et al., 2000). The basolateral membrane of the duodenum is the primary iron regulatory site. FP1 and Heph may work together in iron transport from the enterocytes into the circulation. In other cell types, FP1 may work with CP to load iron on to Tf to enhance iron release from the cell (Fleming and Sly, 2001b).

However, we known very little about the relationship between neurotransmitters and iron transport proteins, although some of investigation have focused on the influence of neurotransmitters on the iron concentration. It is very important to study the role of neurotransmitters in the regulation of the brain iron metabolism, and further understand the pathogenesis of NDs.

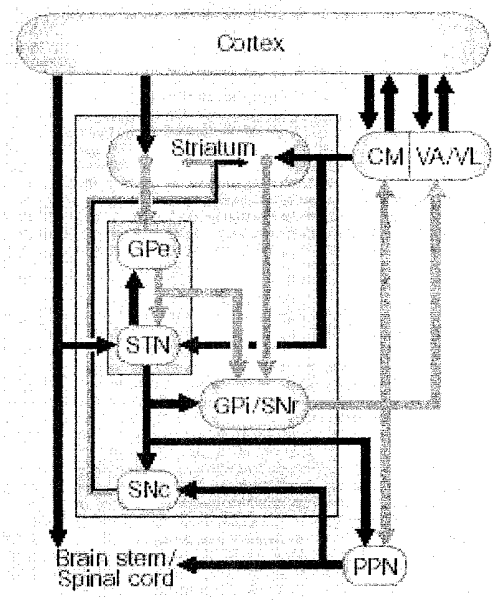

Fig. 1-10. The basal ganglia/thalamo-cortical circuitry (simplified). The basal ganglia (blue box) consists of the striatum, the external and internal segments of the globus pallidus (Gpe and GPi, respectively), the pars compacta and pars reticulata of the substantia nigra (SNc and SNr, respectively), and the subthalamic nucleus (STN). These structures are linked via a complex network of excitatory and inhibitory connections (shown as red and grey arrows, respectively). Their external connections include cortical areas, the thalamic centromedian (CM), ventral anterior (VA) and ventral lateral (VL) nuclei, and the pedunculopontine nucleus (PPN). The GPe/STN 'pacemaker' circuitry proposed by Plenz and Kitai3 is shown inside the green box. (From Wichmann and DeLong, 1999)

1.8 OBJECTIVES

This thesis will investigate some important aspects of brain iron homeostasis and brain iron transport proteins.

1.8.1 Part 1

This study aims to:

1) Identify the distribution of CP and the CP homologue Heph in the brain *in vivo* and determine its expression in various cell types and regions of the brain; study the effect of age and iron status on CP and Heph expression and examine the correlation of iron content and gene expression in developing rat brain areas.
2) Determine the effect of iron status on CP and Heph expression *in vitro*, and the role of low concentration of secreted CP and GPI-CP on iron uptake and release in C6 glioma cells.

These two sets of results will elucidate the role of CP in the brain cell iron metabolism, explain how CP enhances cell iron uptake or release and increase understanding of how CP and Heph gene expression is regulated in the brain and brain cells.

1.8.2 Part 2

To determine whether the regulation of CP and Heph expression is organ and tissue specific, the effect of age and iron status on CP and Heph expression in the heart was also investigated. Studies show that iron-mediated injury may play an important role in the development of a number of cardiovascular diseases. In the part 2, we also analyze the iron status regulates the FP1, TfR, CP, Heph and DMT1 gene expression and propose a role for these genes in heart iron homeostasis.

1.8.3 Part 3

Neurotransmitter and iron metabolism is discussed. Neurotransmitter is very important for the normal metabolism of CNS. The striatum and the substantia nigra are two key components in the motor circuit linked to movement disorders such as PD and AD. As the previous study showed, the substantia nigra and globus pallidus receive a substantial innervation from the neostriatum, a considerable amount of which being GABAergic and also receiving excitatory (glutamatergic) efferents of the subthalamic nucleus (STN). Glutamate is a highly abundant neurotransmitter in the striatum. Release of dopamine from terminals of the nigrostriatal projection occurs in striatum. In this study, the effect of GABA and Glutamate on CP, Heph, FP1, DMT1 and TfR expression in the C6 glioma cells and the role of L-DOPA in regulating TfR, DMT1 and FP1 expression and ferrous iron uptake will be investigated. This results support the possibility that L-dopa adversely affects the progression of PD by accelerating nigral cell degeneration.

The findings obtained from these studies not only advance our knowledge of these newly identified iron transport proteins on brain iron homeostasis, but also provide information on the mechanisms of neuronal injury in a number of human NDs.

CHAPTER 2

MATERIALS, APPARATUS AND METHODS

2.1 MATERIALS

2.1.1 Reagents and Analysis Kits

2-mercaptoethanol	Bio-Rad Technology Ltd., USA
[α-^{32}P]dCTP	Amersham Biosciences, England
ABC Reagent kit	VECTOR, Brulingame, USA.
ABI PRISM BigDye Terminator reaction kit	Perkin Elmer, USA
Acrylamide, electrophoresis grade	Bio-Rad Technology Ltd., USA
Advantage™ RT-for-PCR Kit, Cat# K1402-2	Clontech Laboratories Inc., USA
Agarose standard low-*Mr*	Bio-Rad Technology Ltd., USA
Ammonium persulphate	Bio-Rad Technology Ltd.,
Apo-transferrin (Rat)	Sigma Chemical Co. USA
Aprotinin	Sigma Chemical Co. USA
Bathophenanthroline disulfonic (BP)	Sigma Chemical Co., USA
Bromophenol blue	Bio-Rad Technology Ltd., USA
Calcein acetoxymethyl ester (calcein-AM),	Molecular Probes, The Netherlands
Ceruloplasmin (human)	Sigma Chemical Co., USA

Coomassie blue R-250	Bio-Rad Technology Ltd, USA
Coomassie Brilliant Blue G 250	Bio-Rad Technology Ltd, USA
DAB kit	VECTOR, Brulingame, USA.
Desferrioxamine (DFO)	Sigma Chemical Co., USA
DMEM medium	Invitrogen, CA, USA
ECL Western blotting analysis system (RPN 2108)	Amersham Pharmacia biotech, USA
EDTA	Sigma Chemical Co., USA
Ethidum bromide	Bio-Rad Technology Ltd.,USA
Ethanol (100 %, 96 %)	Lab-Scan Ltd., Ireland
ExpressHyb hybridization solution	Clontech (Palo Alto, CA), USA
$FeCl_3$	Sigma Chemical Co., USA
Ferric ammonium citrate (FAC)	Sigma Chemical Co., USA
Ferrous Ammonium Sulfate (FAS)	Sigma Chemical Co., USA
Fetal bovine serum	Invitrogen (Carlsbad, CA), USA
Glycerol	Bio-Rad Technology Ltd., USA
Glycine	Bio-Rad Technology Ltd., USA
Hank's balance salt solution	Invitrogen, CA, USA
HEPES	Sigma Chemical Co., USA
Hybond-N, Molecular Probes	Amersham Pharmacia biotech, USA
Iron and total iron binding capacity kit	Sigma Chemical Co., USA
Leupeptin	Sigma Chemical Co., USA
Methanol	Lab-Scan Ltd., Ireland
$MgNO_3$	Sigma Chemical Co., USA
Micro Spin G-50 columns	Amersham Biosciences, England
N'N'-bis-methylene-acrylamide	Bio-Rad Technology Ltd., USA

Nitric acid	Lab-Scan Ltd., Ireland
Nitrilotriacetic acid (NTA)	Sigma Chemical Co., USA
Nonidet P-40	Sigma Chemical Co., USA
Paraformaldehyde	Sigma Chemical Co., USA
Penicillin-streptomycin	Invitrogen (Carlsbad, CA), USA
PMSF	Sigma Chemical Co., USA
Prestained protein marker	Bio-Rad Laboratories, CA, USA
Prime-a-Gene labeling system	Promega, WI, USA
Pure nitrocellulose membrane	Bio-Rad Laboratories, CA, USA
Rneasy Mini Kit, Cat# 74104	QIAGEN Ltd., Germany
SDS	Bio-Rad Technology Ltd., USA
Sodium deoxycholate	Sigma Chemical Co., USA
Sodium orthovanadate	Sigma Chemical Co., USA
TEMED	Bio-Rad Technology Ltd., USA
Thapsigargin (TG)	Sigma Chemical Co., USA
Thioglycollic acid	Sigma Chemical Co., USA
Trichloraacetic acid	Sigma Chemical Co., USA
Tris	Bio-Rad Technology Ltd., USA
Trizol® Reagent	Invitrogen (Carlsbad, CA), USA
Trypsin	Invitrogen (Carlsbad, CA), USA
Tween 20	Sigma Chemical Co., USA
Mouse anti-Mouse Ceruloplasmin purified antibody	BD Transduction Laboratories, USA
Mouse anti-rat CD71 monoclonal antibody	BD Bioscience, USA
Rabbit anti-Mouse Hephaestin antibody	Alpha Diagnostic International, Inc., USA
Rabbit anti-Rat DMT1+IRE antibody	Alpha Diagnostic International, Inc., USA

Rabbit anti-Rat DMT1-IRE antibody	Alpha Diagnostic International, Inc., USA
Rabbit anti-mouse FP1 antibody	Alpha Diagnostic International, Inc., USA
Mouse anti-Rat GFAP monoclonal antibody	Boehringer-Mannheim, USA
Rabbit anti-human β-actin polyclonal antibody	Sigma Chemical Co., USA

2.1.2 Apparatus

ABI PRISM 310 Genetic Analyzer	PE Applied Biosystems, USA
Autoclave (model HA-30)	Hirayama manufacturing, Japan
Boiling water bath	Grand Instruments, USA
Flow cytometer	Coulter Epics, USA
Fluostar Galaxy fluorescence plate reader	BMG, Durham, NC, USA
Freezing microtome (model CM1510)	Leica, Germany
GeneAmp® PCR System 9700	PE Applied Biosystems, USA
Incubator (model TC2323)	Shel LAB, USA
Lumi-imager, Model	Bio-Rad Technology Ltd., USA
Microcentrifuge	Eppendorf, Germany
Micro-hematocrit centrifuge and reader	Hawksley, Australia
Minigel apparatus	Bio-Rad Technology Ltd.,USA
Mini-protein II Electrophoresis Cell	Bio-Rad Laboratories Inc.,USA
Molecular Biology Assistant	PE Applied Biosystems, USA
pH meter (Model 701 digital)	Orion research, USA
Phosphorimager	Molecular Dynamics, CA, USA
Power supply	Bio-Rad Technology Ltd., USA
Rotor–stator homogenizer	IKA-Labortechnik., Germany

Sonicator, Branson Sonifier 250	Branson Inc., USA
Leica microscope (Model DRIMB)	Leica Germany
Luminar flow cabinet (model Nu-425-400E)	Nuair Inc., USA
Nikon E400 light microscope	Nikon, Japan
UV cross-linker	Fisher, USA

2.1.3 Animal

In this project, rats are used to investigate CP and Heph expression in the brain. The use of animals was approved by the Department of Health of Hong Kong and the Animal Ethics Committee of The Hong Kong Polytechnic University. The rats were supplied by the Animal House of The Hong Kong Polytechnic University. To eliminate the existence of any sex-related differences in the response of iron metabolism, the male Sprague-Dawley rats were selected in all of experiments. All the animals were housed in pairs in stainless steel rust-free cages at 21±2℃. The rooms were in a light-dark cycle of 12 hours of light (7:00 to 19:00) and 12 hours of dark (from 19:00 to 7:00).

2.1.3.1 Diet and Experiment Design

To detect the expression of proteins relevant to brain iron metabolism in different developing rat brains or other tissue, male SD rats at PND 7, 21, 63, and 196 were used. All the animals were fed the Laboratory Rodent Diet (PMI, Brentwood, MO. Catalog# 5001, containing protein 28%, fat 12.1%, fiber 5.3%, Carbohydrate 59.8% and 270 ppm iron) ad libitum and plenty of distilled water was supplied at all times.

Rats obtained at 21 days of age (after weaning) were fed with a diet with three levels of iron. The animals in the control group (CN) were fed with the Basal Purified Diet (containing protein 19%, fat 10%, fiber 4.3%, Carbohydrate 60.6% and 60ppm iron) (PMI, Catalog# 7024). The animals in the high iron group (HF) were fed with the Basal Purified Diet supplied with 2.5% carbonyl iron (PMI, Catalog# 43784). The animals in the low iron group (LF) were fed with Low Iron Purified Diet containing no added iron (PMI, Catalog# 7444) (residue of 10mg Fe/kg diet). These diets were given ad libitum to rats for 6-8 weeks. By this time, body iron stores were altered, as determined by measurement of serum iron and liver iron stores.

2.1.3.2 Animal Sacrifice and Sample Collection

For RT-PCR, Northern blot and Western blot analysis, animals were anesthetized with 1% pentobarbital sodium (40mg/kg body weight, i.p.). After perfusion with ice-cold phosphate-buffered saline (Milli-Q water prepared and DEPC treated, pH 7.4) though the left ventricle, the brain was rapidly removed and immediately dissected into four brain regions: cortex, hippocampus (Hippo), striatum and substantia nigra (SNigra) according to modified methods published by Focht et al. (Focht et al., 1997). The hearts and liver were also rapidly removed, blotted dry, and weighed. The weighed aliquots were rinsed with cold saline to remove blood, and used directly. The remaining tissues was wrapped with aluminum, and immediately frozen below –70℃ for store after treatment with fluid nitrogen.

For the haematology analysis at the end of the study, the rats were anesthetized with

1 % pentobarbital sodium (40 mg/kg body weight, i.p.). After animals were decapitated, blood samples were collected from the trunk into heparinized syringes and aliquots were taken immediately for hemoglobin (Hb) concentration and hematocrit (Hct) determination. The remaining blood was cooled to 4℃ and centrifuged 3,000 g for 10 min at 4℃, and plasma was removed and frozen at -20℃ before analysis for iron or total iron-binding capacity (TIBC).

For immunohistochemistry, 9 week-old normal adult rats were deeply anaesthetized and perfuse through the left cardiac ventricle with normal saline, followed with a fixative solution consisting of 4% paraformaldehyde in 0.1M phosphate buffer (pH 7.4), and then put the tissue into the solution of sucrose. After the tissue was sedimentation, the tissue slices were cut with freezing microtome.

2.2 GENERAL METHODS

2.2.1 Cell Culture

2.2.1.1 Cell Culture Medium, Solutions and Reagents

(1) **Milli-Q water**

All the solutions for cell culture and medium were made with Milli-Q water.

(2) **Cell culture medium (Invitrogen, CA, USA)**

Dulbecco's Modified Eagle Medium (DMEM), powder (Catalogue Number: 12800)

D-MEM/F-12, powder, 1:1 (Catalogue Number: 12400)

G-5 Supplement (100X) (Catalogue Number: 17503)

Fetal Bovine Sera (FBS), qualified, heat inactivated

(3) **Cell culture solution**

Phosphate-Buffered Saline (PBS) (1×), liquid (Catalogue Number: 20012) pH 7.2 ± 0.05 (Invitrogen, CA, USA)

Hank's Balanced Salt Solution (HBSS) (1×), liquid (Catalogue Number: 14175) (Invitrogen, CA, USA)

Trypsin (2.5%, 10×) (Invitrogen, CA, USA)

Trypan blue solution (Fluka, Buchs, Switzerland)

2.2.1.2 Trypan Blue Staining of Cell

(1) Cell were placed in complete medium without serum and diluted to an approximate concentration of 1×10^5 to 2×10^5 cells per ml. 0.5 ml of this cell suspension was placed in a screw cap test tube, to which was added 0.1 ml of 0.4% Trypan Blue Stain.

(2) The solution was mixed thoroughly and allow to stand 5 min at 15-30℃.

(3) A hemocytometer was filled with cell solution for cell counting. Non-viable cells observed with the stain, and viable cells were not stained.

2.2.1.3 Cryopreservation of Cells

(1) The cultured cells were detached from the substrate using dissociation agents. This was done as gently as possible to minimize damage to the cells.

(2) The detached cells were placed in a complete growth medium and established a viable amount of cells.

(3) The re-suspended cells was centrifuged at ~200 ×g for 5 min and withdrawn the supernatant down to the smallest volume without disturbing the cells.

(4) The cell pellet was resuspended in freezing cold medium to a concentration of 5 × 10^6 to 1 × 10^7 cells/ml.

(5) Aliquot of the cells solution were placed into cryogenic storage vials. The vials were put on ice or in a 4℃ refrigerator, and freezing began within 5 min.

(6) The cells were slowly frozen at a rate of 1℃/min. This could be done by programmable coolers or by placing the vials inside an insulated box placed in a -70℃ to -90℃ freezer, then transferred for storage in liquid nitrogen.

2.2.1.4 Thawing of Cryopreserved Cells

Cryopreserved cells are fragile and require gentle handling. The cells were thawed quickly and placed directly into complete growth medium. If cells were particularly sensitive to cryopreservation (DMSO or glycerol), they were centrifuged to remove cryopreservative and then placed into growth medium.

The following were suggested procedures for thawing cryopreserved cells.

(1) Remove cells from storage and thaw quickly in a 37℃ water bath.

(2) Place 1 or 2 ml of frozen cells in ~25 ml of complete growth medium. Mix very gently.

(3) Centrifuge cells at ~80 × g for 2 to 3 min.

(4) Discard supernatant.

(5) Gently resuspend cells in complete growth medium and perform a viable cell

count.

(6) Culture the cells. Cell density should be at least 3 x 10^5 cells/ml.

Direct Plating Method:

- ✓ The cells from storage are thawed quickly in a 37℃ water bath.
- ✓ The thawed cells are directly placed in a flask with complete growth medium. 1 ml of frozen cells was added to 10 to 20 ml of complete medium to make a suspension cell density of with an at least 3 × 10^5 cells/ml.
- ✓ The cells are cultured for 12 to 24 hours, and the medium replaced with fresh complete growth medium to remove cryopreservatives.

2.2.1.5 C6 Glioma Cell Culture

C6 Glioma cell line was obtained from the American Type Culture Collection (ATCC). The cells were grown in Dulbecco's modified Eagle's medium (DMEM/Glutamax; Life Technologies), supplemented with 10% (vol/vol) heat-inactivated fetal bovine serum and 100U/ml of sodium penicillin G and 100 μg/ml of streptomycin sulfate. The medium was changed every 3 days. The subculture was prepared by removing the medium, adding 1-3 ml of fresh 0.25% trypsin or 2mM EDTA solution (for protein extraction) for several minutes, and the trypsin solution removed. The culture was allowed to stand at room temperature for 10 to 15 minutes. Fresh medium was added, aspirated and dispensed until the cells were detached. Then the cells were transferred to a 15 ml centrifuge tube containing 3-5 ml of fresh medium and centrifuged at 1000 rpm for 5 minutes at 4℃. The supernatant was discarded and the pellet triturated in 2 ml of fresh medium. The cell

number was determined by trypan blue exclusion under the microscope, and the required number of cells placed into the flasks (for maintenance), and in 6-well plates or 96-well plates. All the apparatus and mediums used for cell culture were sterilized before use. For certain immunocytochemistry experiments, the iron transport assay, the cells were replanted in serum-free DMEM or HBSS solution.

2.2.1.6 Primary Astrocyte Culture

(1) Preparation of buffers and medium:

EBS

Solution A: 50ml EBS + 2mg DNase + 0.15g BSA

Solution B: 50ml EBS + 2mg DNase + 0.15g BSA

Solution C: 80g NaCl + 29g $Na_2HPO_4 \cdot H_2O$ + 2g KCl + 2g KH_2PO_4+ 1000ml ddH_2O

Solution D: 200ml solution C + 1g trypsin+ 0.3946g EDTA + 1.7g NaCl (10×, 0.5% Trypsin)

Solutions A and B were freshly prepared, and sterilized with syringe filter of 0.22 μm pore size and heated to 37℃. Solutions C and D were sterilized using a 0.22 μm Millipore membrane and stored at –20℃.

Medium A: DMEM without L-valine, with L-glutamine, supplemented with 187mg/L D-valine.

Medium B: Medium A supplemented with 0.1mg/ml L-valine, 0.33mg/ml L-glutamine, 2.5% of penicillin/streptomycin solution (v/v) and 10% (v/v) FCS.

Medium C: F12 combined 1:1 with Medium A supplemented with 2.5% (v/v) Penicillin/streptomycin and 1% G5 if the G5 is 100x.

All the mediums were adjusted to pH 7.6, sterilized by filtering and stored at 4℃.

(2) Tissue separation and cell culture

The cells were prepared from the brains of newborn rats using established methods of our laboratory (Qian et al., 1999a; Qian et al., 2000).

(A) The surface of the flask was covered with 5μg/ml of Poly-L-lysine solution for 30min, and dried under UV light for about 2 hours.

(B) Infant rats (2-PND, 3-4 rats per dissection) were anaesthetized by hypothermia by placing them in an ice bath for 2-4min. This procedure also served to cool the brain tissue. The skin of the head and neck was cleaned and disinfected with 75% alcohol prior to sacrifice. The animals were rapid decapitated with large surgical scissors at the level of the foramen magnum.

(C) Three cerebral cortices were used. The brain-tissue was placed into three separate 50 ml tubes containing 15ml of Solution B and incubated at 37℃ with gentle agitation for 15min.

(D) Equal volumes (15ml) of medium was changed twice, and the mixture pipetted into the 15ml Solution B and incubated. Solution B was added to the mixture to terminate the trypsinization. After centrifugation at 250g for 1min, the supernatant was discarded and the pellet triturated in 5ml of Solution A.

(E) A further 10ml of Solution A was added. In the latter experiments, cell fragments were gently and repeatedly pipetted without foaming until there was no visible cell debris. The tissue was allowed to settle for about 10ml. The supernatant (10ml) was removed into a collecting tube. 10 ml of Solution A was added. The supernatant was removed again to the collecting tube again after 10min.

(F) Step e) was repeated.

(G) The final mixture was spun at 250g for 5min, the supernatanted and 10ml of Medium B was added to the pellet. The pellet was dispersed gently and then resuspended completely by trituration.

(H) The number of cells was counted by using a cell-counting chamber and cell density was determined with 0.2% trypan blue in PBS. The cells were plated in 75cm^2-flasks and the average density should be 2×10^5 cells/cm^3.

(I) The plated cells were incubated in a 5% CO_2 incubator at 37℃. The culture medium was changed after three days. On the 4th day Medium B was placed with Medium C and changed at 3 days intervals thereafter.

(J) After 9-10 days of culture, the cells were prepared to subculture according to Berhard et al (1992). 10ml of 0.05 Solution D was added to each 75cm^2-flask and incubated for 7min at 37℃. The solution was decanted and 10ml of Medium B was added to terminate the trypsinization. The cells were triturated gently, counted and seeded at approximately 4×10^4 cells/cm^2 in 35mm dish and culture in CO_2 incubator at 37℃ until the day of the use.

(3) Identification of Astrocytes

Cultured astrocytes were identified by the immunocytochemistry of GFAP described by Manthorpe et al. (Manthorpe et al., 1979).

Cells were seeded out (1×10^5) onto the glass coverslips (Sigma, USA) contained within the wells of 6-well culture plates (Corning NY) and maintained as described in the culture of Astrocytes. At confluence, the growth medium was removed and the cells processed for immunocytochemical analysis by using the method described in the thesis, with the following modifications: the primary antibodies used consisted of

mouse anti-GFAP monocolone at 1:100 dilution of the solutions provided, the secondary antibody consisted of biotinylated goat anti-mouse IgG at a dilution 1:2000.

2.2.2 Methods of Molecule Biology

2.2.2.1 RNA Preparation

Total RNA was isolated from brain tissue or other tissues using RNeasy Mini Kit (Qiagen) for RT-PCR and using Trizol® Reagent for Northern blot analysis according to the manufacturer's instructions. The relative purity of isolated RNA was assessed spectrophotometrically and the ratio of A260 nm to A280 nm exceeded 1.8 for all preparations or 28S RNA bands = twice the amounts of the 18S RNA.

2.2.2.2 RT-PCR

(1) **Principle:**

RT-PCR is a powerful technique for mRNA analysis. It is semi-quantitative technique. The advantages of this technique include its versatility, sensitivity and rapid turn-around time. The main point of this technique is to amplify specific complementary cDNA fragments from limited amounts of RNA. This technique includes two major steps: (1) First-strand synthesis of RNA to generate a heterogeneous population of cDNA molecules. (2) Subsequent amplification with sequence-specific primers yields a homogeneous population of the specific cDNA of interest.

(2) **Procedure:**

Total RNA (1μg) was reverse transcribed in a 20 μl reaction using Advantage RT-for-PCR kit (Clontech) with oligo dT primers according to the manufacturers' instructions. The primers for RT-PCR of proteins of interest were based on the cDNA sequences obtained from GeneBank. Amplification was performed with initial denaturation at 94℃ for 3 min, followed by optional cycles at 94℃ (45 s), 60 ℃ (45 s), and 72℃ (2 min), and a single final extension at 72℃ for 7 min, using the GeneAmp® PCR System 9700. The reaction mixture lacking reverse transcriptase was used as a negative control and β-actin cDNA was amplified simultaneously as the internal control. The PCR products were analyzed on a 1.6 % agarose gel using LumiAnalyst Image Analysis software (Roche, Mannheim, Germany). The expected sizes for the positions of interest are shown in the following table. CP and Heph genes expression values were normalized for β-actin expression and expressed in units relative to controls. Other PCR products were for production the ^{32}P-labeled probes. PCR products were purified by using a QIAEX II gel extraction kit (Qiagen) and eluted into 10mM Tris HCl (pH 8.0). In order to verify the sequence of the cDNA fragments, sequencing was performed using a fluorescent-tagged dideoxy chain termination method, and analyzed with an ABI Prism™ 310 Genetic Analyzer (PE Applied Biosystems Inc., Foster City, CA, USA).

2.2.2.3 Northern Blot

(1) **Principle:**

Northern blot is the most widely used method to analyze the expression of eukaryotic mRNA. This technique not only permits identification of mRNA expression, but also demonstrates of mRNA size. The most obvious advantage of Northern blot is its ability to reflect the amount of mRNA expression directly. It is semiquantitative, but is comparably insensitive and cumbersome, requiring microgram quantities of purified poly(A) + RNA and utilizing specific probes recognizing electrophoresed filter transferred mRNA.

(3) **The sequences of primers:**

Gene	**Primar**	**5' 3'**	**Position**	**Size (bp)**	**Accession**
CP	Forward	ATTACATCGCTGCCGAGGAGA	1133-1153	386	L33869
	Reverse	GGAGGCTTGCTTTGAGGAACG	1498-1518		
Heph	Forward	AAGGCAGAGGATGGAATCAG	3659-3678	543	AF246120
	Reverse	CGAACATGGAGAGGACACTC	4182-4201		
β-actin	Forward	GGTCACCCACACTGTGCCCATCTA	2268-2291	263	V01217
	Reverse	GACCGTCAGGCAGCTCACATAGCTCT	2507-2530		
DMT1	Forward	TATCTAGATGACCAACAGCC	1697-1716	335	AF029757
-IRE	Reverse	ATCTTACCCAAACTGGCACG	2012-2031		
DMT1	Forward	CTGAGCGAAGATACCAGCG	1755-1773	386	AF008439
+IRE	Reverse	GGAGCCATCACTTGACCACAC	2572-2592	838	
FP1	Forward	AATGGGAACTGTGGCCTTCA	1298-1317	436	AF394785
	Reverse	AGTTCATGGAGTTCTGCACAC	1714-1733		
TfR	Forward	GAGTTCACTGACATCATCAA	5-24	570	M58040
	Reverse	CAATCCAGATGACTGAGATG	556-574		

Note: To ensure RT-PCR was performed within the linear range of amplification, different amplification cycles were selected. For TfR, anneal temperature was substituted for 52℃.

In this experiment, total RNA was isolated from the brain tissue cell culture. 20-30 μg of the total RNA was heat denatured and then electrophoresed in 1% agarose and 2.2M formaldehyde gels. After electrophoresis, RNA was transferred to a nylon membrane (hybond^{+}, Amersham) in 10 x SSC using the capillary blotting method. The RNA was then cross-linked to the membrane using a UV-crosslinker. The membranes were hybridized with the [α-^{32}P]dCTP labeled probes. After serials of wishing, radioactivity was detected by phosphorimager and quantified using ImageQuant software (Molecular Dynamics, Sunnyvale, CA).

(2) **Generation of Specific Probes:**

Probes were labeled with ^{32}P using the Prime-a-Gene labeling system (Promega, WI, USA), [α-^{32}P]dCTP (Amersham Biosciences) and then purified by a Micro Spin G-50 column (Amersham Biosciences) as manufacturer's instructions. The sequence of probes corresponding to positions 1133-1518 of CP (Genbank, L33869), 3659-4201 (Genbank, AF246120) of Heph, 1755-2592 (Genbank, AF008439) of DMT1+IRE, 1697-2031 of 1697-2031 (Genbank, AF029757) of DMT1-IRE, 1298-1733 (Genbank, AF394785) of FP1 and 5-574 (M58040) of TfR and 2268-2530 (Genbank, V01217) of β-actin cDNAs used were obtained by cloning RT-PCR products of total RNA prepared from the brain of rats, and their identities were confirmed by sequencing.

(3) **Procedure:**

(A) Electrophoresis:

All solutions were treated with 0.1% DEPC for 12h, and the glassware and instruments were baked in the oven at 180℃ for 8h or more. The electrophoresis tank was treated with detergent solution, rinsing with ddH_2O, drying with 70% ethanol, filling with 3% H_2O_2 for 10min at RT, and finally rinsed with DEPC-treated water.

a) Prepared 1 % agarose gel according the standard operation.

a	Agarose 0.35g	Boil until thoroughly solved and cool to 60℃, then add c, d, and e.
b	DEPC-treated water 30.57ml	
c	10 × FA gel buffer 3.5ml	Setting at RT for about 30minn
d	Formaldehyde 0.63ml	
e	Ethidium bromide (10mg/ml) 0.3 μl	

- Sample preparation: the RNA samples were added to the 5 × RNA loading buffer and denatured by incubating for 3-5 min at 65℃, immediately chilled on ice.

b) Electrophoresis:

- The gel was equilibrated in 1 × FA gel running buffer for at least 30min.
- The denatured samples were added to the wells of the gel, and the gel electrophoresed at 60V until the bromophenol blue dye migrated approximately 2/3 of the way through the gel (2~3h).

c) Transfer: (Capillary elution)

- The gel was rinsed several times with DEPC-water in order to remove the formaldehyde and then soaked in the 10 × SSC for 45min.
- The transfer membrane mode was established according to the following illustration:

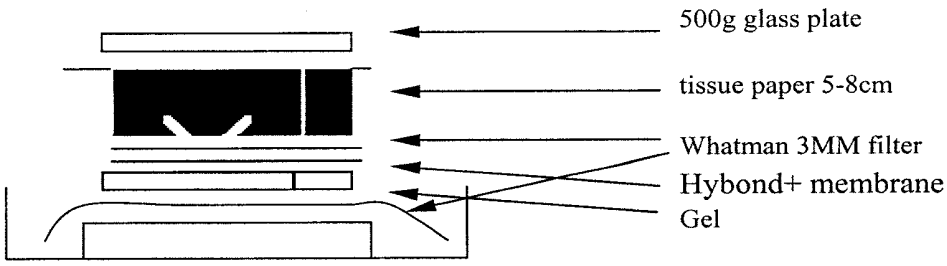

- The 10× SSC was added to the tank and transferred for 16-18 hours at RT. When the paper towels were wet, they were replaced with dry paper.

When the transfer was complete, the Hybond+ membrane was placed on a dry sheet of 3MM paper marked the positions of the gel slots on the membrane. The total RNA was crosslinked under UV-light.

(B) Hybridization:

a) Before the hybridization, the ExpressHyb Solution was warmed at 68℃, and stirred well to completely dissolve any precipitate.

b) The membranes were prehybridized in ExpressHyb Solution (10×10cm membrane in a minimum total volume of 5 ml) with continuous shaking at 68℃ for 60 min in a hybridization oven.

c) The radioactively labeled cDNA probe was put in 95–100℃ water bath and denatured for 5 min, and then chilled quickly on ice.

d) The radio-labeled probe was added to 5 ml of fresh ExpressHyb and mixed

thoroughly.

e) The radio-labeled cDNA probe was added into the tubes, all air bubbles were removed from the container and the tubes incubated with continuous shaking at 68℃ for 16 hr.

f) After the hybridization, the membrane was rinsed several times in 2× SSC containing 0.05 % SDS solution at room temperature and washed for 30–40 min with continuous agitation, replacing the wash solution several times. If the radioactivity was very high, the membrane was washed in 0.1× SSC containing 0.1 % SDS or 2× SSC containing 0.1 % SDS with continuous shaking at 50-65 ℃ for 10-60 min with one change of fresh solution. The radioactivity was monitored regularly.

g) The membrane was removed, the excess wash solution shaken off and then covered with plastic wrap and exposed to phosphor screen at RT for 3-24 hr.

(C) The probe was removed from the blot as outlined below.

The membrane was put into 90–100℃ sterile H_2O/0.5% SDS solution and incubated for 10 min, shaking frequently. After allowing the H_2O to cool, the blot was removed and air-dried before placing into a plastic bag. The membrane can than be stored at –20℃ until needed.

2.2.2.4 Protein Preparation and Determination

(1) Protein Preparation

Tissue samples were homogenized in RIPA buffer containing 0.15mM NaCl, 10mM NaPO4, 1% Nonidet P-40, 0.5% sodium deoxycholate, 0.1% SDS, 1mM PMSF, 1

μg/ml aprotinin, 1 μg/ml leupeptin, 1 μg/ml pepstatin, 1mM sodium orthovanadate and 1% Triton X-100, and sonicated. The cell culture samples were washed with ice-cold PBS, lysed with Tris buffer containing 1% Triton X-100, 0.1% SDS, 1 mM PMSF and protease inhibitors (pepstatin 1μg/ml, aprotinin 1μg/ml, leupeptin 1μg/ml), and then supersonic using Soniprep 150 (MSE Scientific Instruments, England) 3×10s. After centrifugation of homogenate at 10,000 × g for 30 min at 4℃, the supernatant was collected as crude cytosolic fraction.

(2) **Protein Determination (Protein assay kit, Bio-Rad, USA)**

(A) The dye reagent was prepared by diluting 1 part Dye Reagent Concentrate with 4 parts distilled, deionized (DDI) water. This filtered was through Whatman #1 filter to remove particulates. This diluted reagent may be used for approximately 2 weeks when kept at room temperature.

(B) Five dilutions (40, 80, 120, 160, 200 μg/ml) of a protein standard were prepared which is representative of the protein solution to be tested.

(C) 100 μl of each standard and sample solution was placed into a clean, dry test tube; 5.0 ml of diluted dye reagent was added into each tube and vortexed. The sample solutions were assayed in duplicate.

(D) The samples were incubated at room temperature for at least 5 minutes. Because absorbance will increase over time, samples should incubate at room temperature for no more than 1 hour.

(E) Absorbance was measured at 595 nm.

The protein concentration was adjusted to 2-4mg/ml and the fractions (containing 40 μg protein) in aliquots stored at –70℃.

2.2.2.5 Western Blot

(1) **Principle**

Western- or immunoblotting is a commonly employed technique for the detection of protein antigens in complex mixtures. It is highly sensitive can detect as little as picograms of protein with antibodies of known specificity. Samples are first separated by SDS-polyacrylamide gel electrophoresis. The separated proteins are then transferred to a membrane. These membranes are incubated with an antibody specific for the protein of interest that binds to the protein band immobilized on the membrane. The antibody is then visualized with a detection system that is usually based on a secondary protein binding to Ig chains, which are linked to chemiluminescent substrate reaction.

(2) **Procedure:**

(A) Polyacrylamide gel electrophoresis and transfer

a) Polyacrylamide gel electrophoresis

Forty micrograms total protein were diluted in 2× sample buffer (50 mM Tris, pH 6.8, 2% SDS, 10% glycerol, 0.1% bromophenol blue, and 5% β-mercaptoethanol) and heated for 5 min at 95℃ before SDS-PAGE on a 10% gel for FP1, DMT1+IRE, DMT1-IRE, TfR and 7.5% gel for CP, Heph. Electrophoresis was conducted by running the stacking gel at 100V for about 15-20 min and running the separating gel at 200V for about 40-50 min.

b) Transferring gel

- The gel was disassembled from the plates carefully, the stacking gel was removed and the position marked by notching one corner.
- The gel was washed in the transfer buffer for 15 min.
- The NC membrane and the filter papers were cut to fit the dimension of gel size.
- The filter paper and fiber pads were soaked in transfer buffer for at least 15min.
- The cassette was assembled as follows: white (+), fiber pads, filter paper, membrane, gel, filter paper, fiber pads, gray (-). Avoid the bubble by rolling a glass rod.
- The pre-chilled transfer buffer and frozen Bio-Ice cooling Unit was placed in the electrophoresis tank.
- The transfer unit was allowed to stand at 4℃ overnight 12-16h with 30 voltages and gentle agitation.
- After transferring, the blot was put on a clean filter paper, and stained with commassie blue to check the quality of transfer.
- The blots were used immediately or stored.

c) Immunoblotting (ECL western blotting analysis system, RPN 2108)

The membrane was blocked with 5% blocking reagent (Amersham Biosciences, England) in TBS containing 0.1% Tween 20 for 2h at RT or overnight at 4℃. The membrane was rinsed in three changes of TBS-T, incubated once for 15 min and twice for 5 min in fresh washing buffer, and then incubated with primary antibody for 2h at RT or overnight at 4℃, the concentration of primary antibodies was maintained according to the instruction of products. After three washes in washing buffer, the membrane was incubated for 2 hours in horseradish peroxidase-conjugated anti-mouse second antibody (1:5000, Amersham Biosciences,

England) and developed using enhanced chemiluminescence (ECL Western blotting analysis system kit, Amersham Biosciences, England). The blot was detected by Lumi-imager F1 workstation (Roche Molecular Biochemical). The intensity of the specific bands was determined by densitometry with the use of LumiAnalyst 3.1 software (Roche Molecular Biochemical). To ensure even loading of the samples, the same membrane was probed with rabbit anti-human β-actin polyclonal antibody (Sigma-Aldrich, MO) at 1:5000 dilutions.

2.2.3 Methods of Biochemistry and Chemistry

2.2.3.1 Measurement of Hemoglobin (Hb) Concentration

(1) **Principle:**

Blood Hb concentration was measured colorimetrically by the cyanmethaemoglobin method using Drabkin's reagent (Procedure No.525A, Sigma Chemical, St. Louis, MO.). Hb is a complex molecule composed of an iron-containing heme, and the protein globin. The concentration of Hb in solution, i.e. when released from the red cells by haemolysis, can be estimated in various ways such as measurement of its color, the amount of oxygen or carbon monoxide with which it can combine, or by determination of its iron content. The last technique, known as the cyanmethaemogkobin method, is used routinely, as it is simple, rapid and the coloured end product of the reaction is stable.

In this method, potassium ferricyanide (an oxidizing agent) converted the Fe^{2+} iron of haemoglobin to the Fe^{3+} state-methaemoglobin. This was then combined with

cyanide (CN^-) to form cyanmethaemoglobin. This is a stable coloured compound (i.e. unaffected by O2 and CO2 concentrations) and its concentration in solution can be estimated by its absorbance at 540nm in a colorimeter/spectrophotometer.

(2) **Procedure:**

Drabkin's solution

Sodium bicarbonate (1g)+ Potassium ferricyanide (198mg) +

Potassium cyanide (52mg) + Distilled water (1000ml)

(A) 2.5 ml of Drabkin's solution was pipetted into each test tubes and sample tube.

(B) 10 ml of standard human Hb (6g/dl, 12g/dl and 18g/dl) and whole blood was added into test and sample tubes respectively.

(C) The tubes were covered with parafilm and mixed by swirling.

(D) The mixtures were left to stand at room temperature for at least 10 min.

(E) The absorbance of the test sample and the human Hb standard at wavelength of 540 nm were recorded against Drabkin's solution.

(F) The standard curve was plotted and the concentration of each unknown was determined according to the following equation.

(G) Hb conc. (g/100ml)=(A_{540} sample/A_{540} standard)×conc. Standard (g/100ml)

2.2.3.2 Measurement of Hematocrit (Hct)

Hematocrit is determined by centrifugation of blood collected into heparinized microcapillary tubes.

(1) **Materials:**

(A) Microhematocrit capillary tube

(B) Plasticine

(C) Microhematocrit centrifuge (Hawksley, England)

(D) Microhematocrit Reader

(2) **Procedure:**

(A) The microhematocrit capillary tube was filled with blood to 75%~90% of tube length.

(B) The outside of the tube was wiped with parafilm and opposite side was sealed by pushing it into the plasticine.

(C) The tube was placed in a Hawksley microhematocrit centrifuge with the sealed end towards the outside, and centrifuged at 12000rpm for 5min.

(D) After centrifugation, the Hct was read using the Microhematocrit Reader by placing the base of the red cell column on the '0' line, then moving the silver line on the adjuster until it reached the level of red cell/white cell-platelet interface.

(E) The result was expressed as a percentage.

2.2.3.3 Measurement Non-heme Iron

(1) Principle:

Non-heme iron content in the tissues is determined according to published methods (Torrance and Bothwell, 1968). An acid solution is prepared by mixing 20% trichloraacetic acid (TCA) in hydrochloride, which is added to the tissue

homogenates. After mixing and closing the tube with a marble, the content is digested at 65℃ for 20 hr. 0.2 ml acid extract is then transferred into another set of iron-free tubes. Color was developed by adding 1 ml of chromagen solution containing thioglycollic acid, and the absorbance of the solution can be measured in a spectrophotometer at a wavelength of 540 nm against reagent blank. Absorbance of reagent blank at 540 nm against iron-free water is less than 0.010.

(2) **Reagent solutions:**

(A) Bathophenanthroline reagent: 3mM bathophenanthroline disulfonic +1% thioglycollic acid (100% purity)*.

(B) Chromagen solution: bathophenanthroline reagent + saturated sodium acetate + ddH_2O (1:20:20/ v:v:v)

(C) Acid mixture: 6N hydrochloride + 20% trichloraacetic acid (1:1) **

(D) Iron standard: 89μg/dl

* Bathophenanthroline reagent were prepared freshly by first dissolving the 160mg bathophenanthroline in 1ml ddH_2O. After thoroughly dissolved, 1ml thioglycollic acid was added and then the volume was make up to 100ml with DD water.

**100% TCA was prepared by dissolving 500g TCA in 227ml ddH_2O.

(3) **Procedure:**

(A) About 0.1g liver was weighted and cut into small pieces.

(B) 1ml acid mixture was added and mixed thoroughly. Sample: Acid = 1:10 (w/v).

(C) The mixture was kept in the oven at 65℃ for 20 hours.

(D) After cooling to room temperature, 0.2 ml of clear yellow solution was added to

10 ml of chromagen solution reagent, and iron standard (2μg/2ml), was added to 8.2 ml of chromagen solution.

(E) The reaction was allowed to stand for 10 min, and then the absorbance of the solutions at a wavelength of 540 nm was measured.

(F) The concentration of samples was calculated as follows: Non-heme iron (μg/ml) = (A sample/A standard) × 1

2.2.3.4 Serum Iron, UIBC, TIBC Measurement

(1) Principle:

Serum iron and unsaturated iron binding capacity (UIBC) levels are determined by published methods (Persijn et al., 1971). The Tf-bound iron dissociates to form ferrous ions at acid pH and in the presence of reducing agents. The ferrous iron reacts with ferrozine to develop a magenta colored complex with a maximum absorption at 560 nm. The difference in color intensity at this wavelength, before and after addition of ferrozine, is proportional to serum iron concentration.

At alkaline pH (8.1), ferrous iron added to plasma binds specifically with Tf at unsaturated iron-binding sites. Remaining unbound ferrous iron is measured with the ferrozine reaction. The difference between the amount of unbound iron and the total amount added is equivalent to the UIBC. The serum total iron-binding capacity (TIBC) equals the total iron plus the UIBC.

(2) **Materials:**

Iron and total iron binding capacity kit (Sigma)

(3) **Procedure:**

(A) 2.5 ml iron buffer reagent was added to the tubes labeled test, standard and blank for the measurement of serum total iron (A).

(B) In TIBC measurement (B), iron buffer was replaced by UIBC Buffer.

(C) 0.5 ml iron-free water, iron standard and serum were respectively added to tubes and mixed.

(D) The absorbance at 560 nm (A) of test sample and standard vs. blank was recorded as the INITIAL A or INITIAL B.

(E) 50 μL iron color reagent was added in each tubes, mixed thoroughly and placed in water bath at 37℃ for 10 minutes.

(F) The absorbance at 560 nm of test sample and standard vs blank was recorded as the FINAL A or FINAL B.

(G) Calculations:

A (B) test = FINAL A (B) test - INITIAL A (B) test

A (B) standard = FINAL A (B) standard – INITIAL (B) Standard

Serum Total iron (go/dl) = Atest/Astandard × 500.

Serum UIBC (μg/dl) = 500 – (Btest/Bstandard × 500)

Serum TIBC (μg/dl) = Serum Total iron + Serum UIBC

2.2.3.5 Total Iron Measurement (GFAAS method)

(1) **Principle:**

Brain iron analyses are performed using a graphite furnace atomic absorption spectrophotometer (GFAAS, Perkin Elmer SIMAA 6000, Rautaruukki Ltd., Raahe,

Finland). Atomic absorption is a technique based on the unique spectrum of each element. For every element analyzed, characteristic wavelengths are generated in a discharge lamp (hollow cathode lamp) and then absorbed by a cloud or vapor of that element. The amount of absorption is proportional to the concentration of the element vaporized into the light beam.

In this method, brain tissue is pretreated according to modified methods published by Focht et al. 1997. Briefly, different brain areas are taken from rats and homogenized with sonicator. After that, ultra-pure nitric acid is added for sample digestion for two days. The iron concentration of the samples is determined by graphite furnace atomic absorption spectrometry.

(2) **Materials:**

a) 20mM HEPES

b) 3.12 mmol/L nitric acid

c) PBS, pH 7.4

d) $Mg(NO_3)_2$

e) Milli-Q water

(3) **Procedure:**

a) Brian tissue were diluted with HEPES buffer 1:20 (wt/v) and homogenized with a sonicator.

b) A 30μl homogenate was added to an equal volume of ultra-pure nitric acid in a 400μl polypropylene microfuge tube.

c) After being digested for 48 h, the mixture was diluted 1:10~40 with 3.12 mmol/L nitric acid.

d) 50μl portions of standards or samples containing 0.05mg ($MgNO_3$) were taken for iron analyses by using the graphite furnace atomic absorption spectrophotometer. The blanks were prepared using homogenization reagents.

Note:

HGA analytical conditions (for Iron):

Wavelength (nm): 248.3	Pretreatment Temp. (℃): 1400
Slit (nm): 0.2	Atomization Temp. (℃): 2400
Tube/Site: Pyro/platform	
Matrix modifier: 0.05mg $Mg(NO_3)_2$	
Characteristic Mass (pg/0.0044 As): 0.5	

Prepare iron standards by serial dilution of iron storage (1000ppm) with the specified nitric acid (0ppb, 5ppb, 10ppb, 20ppb, 30ppb, 40ppb).

2.2.3.6 MTT Assay

(1) **Principle**

3-(4,5-dimethylathiazlo-2-yl)-2,5-diphenyletertrazolium bromide (MTT) assay was used to investigate the effect of the iron chelators, DFO, BP and $FeCl_3$ on cell growth. This is one of the most common used methods for measuring cell

proliferation and neural cytotoxicity. It is widely believed that MTT is reduced by active mitochondria in living cells (Denizot and Lang, 1986; Liu et al., 1997). Thus, increases obtained in the MTT assay at A570 nm indicate increases in the number of viable cells. It is performed in 96-well microtiter plates. In this study, MTT assay is performed according to Liu et al. (Liu et al., 1997).

(2) **Materials**

(A) 5 mg/ml of MTT solution is prepared by dissolving 50 mg MTT in 10 ml of 0.9% NaCl and warmed at 60℃ to dissolve.

(B) Solubilization solution: 5% iso-butyl alcohol, 10% HCl and 10% sodium dodecyl sulfate.

(3) **Procedure**

(1) The cells of 90 μl (approximately 10^4 cells) per well were plated in DMEM/F12 medium at 37℃.

(2) After 4 hours, 10 μl of chemicals (DFO, BP, $FeCl_3$) at the designed concentrations or PBS as control was added to the wells.

(3) After incubation for 24 hours, 20 μl of 5 mg/ml MTT was added to each well.

(4) 4 hours later, 100 μl of a solubilization solution was added and the absorbance values determined at 570 nm, the next day, using an automatic microtiter plate reader (Bio-Rad Laboratories Inc.). 655 nm was used as the reference wavelength.

2.2.4 Immunocytochemical Methods

2.2.4.1 Immunhistochemical Method

(1) **Principle**

Immunohistochemistry is the localization of antigens in tissue sections by the use of labeled antibodies as specific reagents through antigen-antibody interactions that are visualized by a marker such as fluorescent dye, enzyme, radioactive element or colloidal gold.

With the development of immunohistochemistry techniques, enzyme labels such as peroxidase (Avrameas and Uriel, 1966; Nakane and Pierce, 1967) and alkaline phosphatase (Mason and Sammons, 1978) have been introduced. Since immunohistochemistry involves specific antigen-antibody reaction, it has an apparent advantage over traditional special and enzyme staining techniques that identify only a limited number of proteins, enzymes and tissue structures. Therefore, immunohistochemistry has become a crucial technique in many areas of research.

(2) **Procedure**

(A) Tissue Processing

9-week-old normal adult rats were deeply anaesthetized and perfused through the left cardiac ventricle with normal saline, followed by a fixative consisting of 4% paraformaldehyde in 0.1M phosphate buffer (pH 7.4). The tissue was embedded in OCT and was cut at 10μm thickness on a freezing microtome (Leica), and then mounted on gelatin-coated slides. If not use immediately, the sections were stored at - 80℃ until needed.

(B) Antigen retrieval

A microwave oven was for antigen retrieval. The tissue was heated for 10 min and then cooled for 10 min. this process was repeated another two times. The retrieval solution was citrate buffer at pH 6.0.

(C) IHC Method

The sections were washed in 0.01 M phosphate-buffered saline (PBS) to remove traces of fixative. Endogenous peroxidase was blocked by 0.3% H_2O_2 in methanol for 25 minutes, followed by incubation in 5% normal goat serum for 1 hour at room temperature to block non-specific binding of antibodies. The sections were incubated with the primary antibodies (the concentration of the primary antibody diluted in blocking solution showed in every experiment) for 24 hours at 4 ℃. A biotin-streptavidin detection system was employed with diaminobenzidine as the chromogen. The sections were washed with PBS and incubated with diluted biotinylated secondary antibody (VECTOR, Brulingame, USA) for 60 minutes at 37 ℃. After rinsing in PBS, the sections were incubated with ABC Reagent (VECTOR, Brulingame, USA) for 60 minutes at 37℃, and incubated with diaminobenzidine and H_2O_2 for 5 minutes. As negative control, the same kind of normal animal serum was substituted for primary antibody. 0.01 M PBS was used as a substitute for primary antibody for negative control groups.

When the color was suitable, the slides were rinsed in distilled water 2×5 min. The slides were dehydrated through 70% ethanol and 80% ethanol for 5min, 95% ethanol for 2×5 min and 100% ethanol for 2×5 min and then cleared in xylene for 2×5 min. Finally, the slides were covered with mounting medium and cover slides.

2.2.4.2 Immunocytochemical Methods

(1) **Principle**

Immunocytochemistry is the name given to methods that use antibodies to detect the location of proteins within cells. The antibodies bind specifically to the protein being investigated.

(2) **Procedure**

The primary culture astrocytes and C6 cells were plated on a poly-lysine (Sigma, MO, USA) coated glass slide. When cells reached about 70-80% confluence, they were fixed with 4% paraformaldehyde in 0.1M phosphate buffer (pH 7.4) for 10 min at RT. Following this, the cells were permeabilized with 1% Triton X-100 in PBS for 10 min and further washed in PBS. In order to quench endogenous peroxidase activity, the fixed cells were incubated in a 0.5% solution of hydrogen peroxide in PBS (0.15 M NaCl, and 0.01 M sodium phosphate buffer, pH7.3) for 10 min. Cells were washed in PBS and then incubated in horse serum block for 20 min to prevent nonspecific binding. Cells were washed in PBS and then incubated with the primary antibody for 1 hour at room temperature. Subsequently, the cells were processed using the ABC kit (Vector, Burlingame, CA, USA) and developed with DAB kit (Vector, Burlingame, CA, USA) as per the manufacturer's instructions. As negative control, the same kind of normal animal serum was substituted for primary antibody. Finally, The cells were dehydrated using 70%, 95% and 100% ethanol and xylene. The slides were cover-slipped and viewed under a Nikon E400 light microscope.

2.2.5 Measurement of Cell Iron Uptake and Release with Fluorescence

2.2.5.1 Principle

Calcein-AM (CA-AM, Molecular Probes, Eugene, OR, USA) is a membrane-permeable, nonfluorescent molecule that becomes fluorescent upon intracellular cleavage to calcein (CA, membrane-impermeate) by cytoplasmic esterases (Breuer et al., 1995a). In cell-free systems, calcein binds to both iron (II) and iron (III) with stability constants of 10^{14} and 10^{24}/mol, respectively, and results in quenching its fluorescence (Breuer et al., 1995b). CA is insensitive to calcium and magnesium ions up to 1 mM at physiological pH. In addition, intracellular concentration of other CA-binding molecules is very low and pH in the range of 6.5–7.5 has only a minor effect on CA fluorescence. Taken together, these properties indicate that intracellular CA can sense cell iron dynamically and transmit information regarding changes in cellular labile iron pool (LIP) levels (Epsztejn et al., 1997; Cabiscol et al., 2002). Thus, the appearance of a fluorescent signal was monitored continuously during incubation of a reaction mixture consisting of preloaded CA-AM cells in HEPES-buffered saline (10 mM HEPES, 150 mM NaCl, pH 7.0).

2.2.5.2 CA-AM Loading to the Cells

Calcein was loaded on to the C6 cells according to methods described by Picard et al (Picard et al., 2000) and Barnabe et al (Barnabe et al., 2002). To measure the effect

of CP on iron metabolism, C6 cells were grown to 65-70% confluence, made iron deficient by incubation with 1 mM BP and 1 mM DFO, and made iron sufficient by incubation with 50 μM FAC + 50 μM FAS for 16 hours. When the cells were grown to 80% confluence, they were treated with 600 μU/ml PI-PLC for 60 min at 37℃. Just prior to measurement, the cells were washed three times with medium and incubated with 0.125 μM CA-AM in serum-free medium. After incubation for 10 min at 37℃, excess calcein-AM was removed, the cells were washed twice at 37℃ with Hank's balance salt solution (HBSS, invitrogen, CA), and then maintained in HEPES buffer solution.

To measure the effect of L-DOPA on iron uptake in the cells, C6 cells were grown to 65-70% confluence on poly-l-lysine coated plastic 96-well plates, and then maintained at control and in the presence of 10, 30, 100 μM L-DOPA DMEM medium for 16 hours. Cells were washed twice with medium and incubated with 125 nM CA-AM in serum-free medium. After incubation for 10 min at 37℃, excess calcein-AM was removed, and the cells were washed twice with HBSS.

2.2.5.3 Measurement of Iron Homeostasis

The kinetic fluorescence was measured with the BMG (Durham, NC, USA) Fluostar Galaxy fluorescence plate reader. The equipment was set with λ_{ex} of 485 nm and λ_{em} of 520 nm at 37℃, fluorescence was detected at the bottom of the plate. 100 μl of calcein-loaded cell suspension (approximately 6×10^5 cells) or 100 μl HEPES was added in 96-well plates. The initial baseline fluorescence intensity data was collected, and then the chemicals (FAS, CP, Tf) were added respectively (indicated as Figure

caption) by pipetting 2 μl of stock aqueous solutions into the well and gently mixing the solutions. The changes of calcein fluorescence were measured every 5min for 30 min at 37℃ environment. Data were normalized to the steady-state values of fluorescence before addition of chemicals.

CHAPTER 3

EFFECT OF DIETARY IRON AND AGE ON THE CERULOPLASMIN EXPRESSION IN THE RAT BRAIN

3.1 ABSTRACT

In this chapter, ceruloplasmin (CP) expression in the brain was confirmed with the use of immunohistochemistry. The cell-specific positive staining of CP in the adult brain was mainly detected in glial cells of the brain parenchyma, endothelial cells of microvasculature, ependymal cells lining the ventricles, the choroid plexus, and the leptomeningeal cells, which cover the surface of the brain. However, specific immunoactive staining was rarely observed in neurons. The effects of age and dietary iron status on CP mRNA expression and protein synthesis in different brain regions, including the cortex, hippocampus, striatum and substantia nigra, were investigated. At postnatal days (PND) 7, 21, 63, and 196, the total iron, CP mRNA and protein expression in cortex, hippocampus, striatum and substantia nigra had an influence during development. In the cortex and hippocampus, CP mRNA and protein levels were the lowest at PND7, and then increased to the highest at PND 21 (cortex) or PND63 (hippocampus). But at PND196 the CP mRNA and protein levels decreased, and there was no correlation with the iron concentration. However, in the

striatum and substantia nigra areas, CP mRNA and protein levels were lowest in rat at PND 7, and then increased to the highest at PND196, which significantly correlated with the iron concentration. The CP mRNA and protein levels were not significantly regulated by iron status in the cortex, hippocampus and striatum but there was influence in the substantia nigra. Further analysis of the four brain areas by Western Blotting in low-iron, high-iron and control groups found that CP protein synthesis was affected by iron status. Based on these results, we suggest that CP gene expression pattern is brain region specific and there is a significant relationship between the CP protein synthesis and iron concentration in striatum at different ages, and in substantia nigra both at different ages and iron status.

KEY WORDS:

Ceruloplasmin, Glycosylphosphatidylinositol (GPI)-anchored Ceruloplasmin, Gene Expression, Brain, Iron Metabolism, Cortex, Hippocampus, Striatum, Substantia Nigra, Aceruloplasminemia

3.2 INTRODUCTION

Ceruloplasmin (CP) is a copper-containing ferroxidase that is essential for normal iron homeostasis. Whereas CP in plasma is produced and secreted by hepatocytes, in the brain, a glycosylphosphatidylinositol (GPI)-anchored form of CP is expressed on the surface of astrocytes (Patel and David, 1997). Based on the observation that the ferroxidase activity of CP promoted iron incorporation into transferrin (Tf) (Osaki et al., 1966), clinical studies on aceruloplasminemia (Gitlin, 1998), and animal model

of aceruloplasminemia (Harris et al., 1999) suggest one of the functions of CP is to aid in the release of iron from liver cells and perhaps from cells of other tissues. However, other studies of Mukhopadhyay CK et al. (Mukhopadhyay et al., 1996), and Attieh ZK et al. (Attieh et al., 1999) support the hypothesis that CP plays a role in iron influx into cells. Our study (Qian et al., 2001a; Xie et al., 2002) found that CP plays a role both in iron transport into and out of the brain cells via its ferroxidase activity. It is also possible CP plays a more important physiological role in iron uptake than iron efflux. CP might be necessary for the oxidation of ferrous iron (Fe^{2+}) to ferric iron (Fe^{3+}) after it crosses the abluminal membrane of the blood–brain barrier. Ferric iron (Fe^{3+}) can then bind to Tf, lactotransferrin (LF) or melanotransferrin (p97) in the cerebrospinal fluid and interstitial fluid, and be acquired by neuron, microglia or other relevant brain cells (Qian and Ke, 2001). The precise biological role of CP remains unclear despite many decades of investigation. The regulation of CP gene expression by iron was different between cell culture studies and whole–animal model studies. In HepG2 and K562 cells (Mukhopadhyay et al., 1998; Attieh et al., 1999), CP expression was boosted by iron deficiency and suppressed by increasing levels of iron. In the animal model, however, iron status has little effects on the levels and activity of plasma CP, as well as the expression of its mRNA in rat liver (Huang and Shaw, 2002; Strube et al., 2002; Tran et al., 2002). In the brain, however there were a very few report on the regulation of CP gene expression by iron status. No changes were observed in CP mRNA levels in the HFRT +/- iron-deficient mice brain, but the CP protein levels were increased when compared to the wild-type controls (Thompson et al., 2003). Iron was found to be significantly increased in Alzheimer's disease (AD) globus pallidus and frontal cortex and in Parkinson's disease (PD) globus pallidus (Loeffler et al., 1995). In AD

hippocampus, entorhinal cortex, frontal cortex and putamen, and PD hippocampus, frontal, temporal and parietal cortices, and Huntington's disease (HD) hippocampus, parietal cortex and substantia nigra, the mean CP concentrations were significantly increased compared to normal elderly controls (Loeffler et al., 1996; Loeffler et al., 2001). However, a loss in excess of 1/3 of the CP was observed in both the gray and white matter from the superior temporal gyrus in AD brains compared to age-matched controls (Connor et al., 1993). In PD, ferroxidase activity was reduced in cerebrospinal fluid (CSF) (Boll et al., 1999), but in AD the CP of CSF is increased (Loeffler et al., 1994). Thus, the relationship between CP and iron status in the brain has not been established.

Iron is heterogeneously distributed in the brain of adults, with the highest concentration in the basal ganglia, substantia nigra and deep cerebellar nuclei (Hill and Switzer, 1984). However, the localization of iron in adult rat brains are different from the neonatal and young rats (Benkovic and Connor, 1993); (Focht et al., 1997); (Erikson et al., 1997); (Pinero et al., 2000b). The reason(s) for the change of iron distribution in the developing brain is not clear.

In the present study, the changes of CP gene expression and iron distribution in developing rat hippocampus, striatum and substantia nigra were investigated. The regulation of CP gene expression by variations in dietary iron on rat brain regions was also studied.

3.3 MATERIALS AND METHODS

3.3.1 Materials

Unless otherwise stated, all chemicals were obtained from Sigma Chemical Company, St. Louis, MO, USA. Agarose, Tris, and Ethidium Bromide and prestained protein marker were purchased from Bio-Rad Laboratories, Hercules, CA, USA. 10×PCR buffer, Taq DNA polymerase were from Invitrogen, Carlsbad, CA, USA. Advantage™ RT-for-PCR kit was from Clontech, Palo Alto, CA, USA. RNeasy Mini kit and QIAEX II gel extraction kit were from QIAGEN, Valencia, CA, USA. ECL Western blotting analysis system was from Amersham Biosciences, England. The purified antibodies against CP were purchased from BD Transduction Laboratories, BD Biosciences Pharmingen, USA. The monoclonal antibody against glial fibrillary acidic protein (GFAP) antibody was from Boehringer-Mannheim, Indianapolis, IN, USA. The ABC Reagent and DAB kit were from VECTOR, Brulingame, USA.

3.3.2 Animals and Samples Collection

Male Sprague-Dawley (SD) rats were supplied by the Animal House of The Hong Kong Polytechnic University. All the animals were housed in pairs in stainless steel cages at 21 ± 2℃ and provided free access to food and water. Rooms were in a cycle of 12 hours of light (7:00 to 19:00) and 12 hours of dark (from 19:00 to 7:00). All of the normal animals for studying the effects of ageing were fed the Laboratory Rodent Diet (PMI, Brentwood, MO. Catalog# 5001) ad libitum, and shavings and plenty of distilled water was supplied at all times. To study the regulation of CP gene expression by variations in dietary iron, male SD rats obtained at 21 days (after

weaning) were fed with three levels iron diet. The animals in the control group (CN) were fed with the Basal Purified Diet (containing 60mg Fe/kg diet) (PMI, Catalog# 7024). The animals in the high iron group (HF) were fed with the Basal Purified Diet with 2.5% carbonyl iron (PMI, Catalog# 43784). The animals in the low iron group (LF) were fed with Low Iron Purified Diet (PMI, Catalog# 7444) (residue of 10mg Fe/kg diet). These diets were given ad libitum to the rats for 6 weeks. The Hb, Hct, TIBC was measured to confirm the influence of the variations iron diet. The findings indicated that the rats developed iron deficiency and iron overload after six weeks (Table3-1).

On postnatal day (PND) 7, 21, 63, and 196, and 6 weeks various iron level diet feeding, all animals were anesthetized with 1% pentobarbital sodium (40mg/kg body weight, i.p.). After perfusion with ice-cold phosphate-buffered saline (Milli-Q water prepared and DEPC treated, pH 7.4) though the left ventricle, the brain was rapidly removed and immediately dissected into four brain regions: cortex, hippocampus (Hippo), striatum and substantia nigra (SNigra) according to the modified method published by Focht et al.(Focht et al., 1997).

3.3.3 Methods

3.3.3.1 Immunohistochemistry

Nine-week-old normal adult rats were deeply anaesthetized and perfused through the left cardiac ventricle with normal saline, followed by a fixative consisting of 4% paraformaldehyde in 0.1M phosphate buffer (pH 7.4). The sections were cut at 10μm

thickness on a freezing microtome. The sections of brain were washed in 0.01 M phosphate-buffered saline (PBS) to remove traces of fixative. Endogenous peroxidase was blocked by incubating the tissue slices in 0.3% H_2O_2 in methanol for 25 minutes. This was followed by incubation in 5% normal goat serum for 1 hour at room temperature to block non-specific binding of antibodies. The sections were incubated with a 1:50 dilution of the primary purified mouse anti-CP IgG1 (BD Transduction Laboratories, BD Biosciences, USA) for 24 hours at 4℃. This source of antibody is from 233 to 355 immunogen sequence of mouse CP, that is 94.3% conserved in rat. A biotin-streptavidin detection system was employed with diaminobenzidine as the chromogen. The sections were washed with PBS and incubated with diluted biotinylated secondary antibody (VECTOR, Brulingame, USA) for 60 minutes at 37℃. After rinsing in PBS, the sections were incubated with ABC Reagent (VECTOR, Brulingame, USA) for 60 minutes at 37℃, and incubated with diaminobenzidine and H_2O_2 for 5 minutes. 0.01 M PBS was used as a substitute for primary antibody for negative control groups.

3.3.3.2 Total Iron Measurement of Rats Brain

The total iron of the brain analysis was performed using a graphite furnace atomic absorption spectrophotometer (GFAAS, Perkin Elmer, AAnalyst 100). Brain regions were diluted in a ratio of 1:20 (wt/v) for hippocampus, striatum and 1:80 for substantia nigra with HEPES buffer and homogenized with a sonicator (MSE Soniprep 150 Ultrasonic Disintegrator, MSE Scientific Instruments, England). A 50-μl portion of the homogenate was added to an equal volume of ultra-pure nitric acid in a 0.5 ml polypropylene microfuge tube, digested for 48 h at 50℃. The

samples were then diluted to 1:10 for substantia nigra and 1:40 for hippocampus, striatum with 3.12 mmol/L nitric acid for iron analysis using the graphite furnace atomic absorption spectrophotometer. Standard curves ranging from 0 to 40 ppb were prepared by diluting iron standard (1 mg iron/ml, Alpha Products, Danvers, MA) with blanks prepared from homogenization reagents in 0.2 % HNO_3. Standards and digested samples were read in triplicate by injecting 50 µl aliquots, including 0.05 mg $Mg(NO_3)_2$ as matrix modification, into graphite furnace. Absorbance readings at 248.3 nm, slit at 0.2 nm, pretreatment temperature at 1400 ℃, atomization temperature at 2400 ℃ were recorded and used for analysis. All the solutions were prepared with Milli-Q water.

3.3.3.3 RNA Isolation

Total RNA was isolated from hippocampus, striatum and substantia nigra using RNeasy Mini Kit (Qiagen, Valencia, CA) according to the manufacturer's instructions. The relative purity of isolated RNA was assessed spectrophotometrically and the ratio of A260 nm to A280 nm exceeded 1.9 for all preparations.

3.3.3.4 Reverse Transcription (RT) and Polymerase Chain Reaction (PCR)

Total RNA (1µg) was reverse transcribed in a 20µl reaction using Advantage RT-for-PCR kit (Clontech, Palo Alto, CA) with oligo dT primers according to the manufacturer's instructions. The primers for RT-PCR of CP were based on the cDNA sequence reported by Fleming and Gitlin (Fleming and Gitlin, 1990). The

forward primer sequence is 5'- ATTACATCGCTGCCGAGGAGA-3' (1133-1153 nt); the reverse primer sequence is 5'- GGAGGCTTGCTTTGAGGAACG-3' (1498-1518 nt). Amplification was performed (using the GeneAmp® PCR System 9700) with initial denaturation at 94℃ for 3min, followed by 25 cycles at 94℃ (45s), 60℃ (45s), and 72℃ (2min), and a single final extension at 72℃ for 7min. The reaction mixture lacking reverse transcriptase was used as a negative control and β-actin cDNA (5'-primer, 5'-GGTCACCCACACTGTGCCCATCTA-3'; 3'-primer, 5'-GACCGTCAGGCAGCTCACATAGCTCT-3') was amplified simultaneously as the internal control. The PCR products were analyzed on a 1.6% agarose gel using LumiAnalyst Image Analysis software (Roche, Mannheim, Germany). The expected sizes for CP and β-actin are 385bp and 263bp, respectively. Gene expression values were normalized with β-actin expression and expressed in units relative to controls. PCR products were purified by using a QIAEX II gel extraction kit (Qiagen) and eluted into 10mM Tris HCl (pH 8.0). In order to verify the sequence of the cDNA fragments, sequencing was performed using a fluorescent-taged dideoxy chain termination method of Sanger et al(Sanger et al., 1992), then analyzed with an ABI Prism™ 310 Genetic Analyzer (PE Applied Biosystems Inc., Foster City, CA.).

3.3.3.5 Western Blot Analysis

The brain tissue was washed and homogenized in RIPA buffer containing 1% Triton X-100, 0.1% SDS, 1 mM PMSF and protease inhibitors (pepstatin 1μg/ml, aprotinin 1μg/ml, leupeptin 1μg/ml), and then sonicated using Soniprep 150 (MSE Scientific Instruments, England) 3×10 seconds. After centrifugation at 10,000×g for 15 min at 4℃, the supernatant was collected. Protein content was determined using the

Bradford assay kit (Bio-Rad, Hercules, CA). Forty micrograms total protein were diluted in 2× sample buffer (50 mM Tris, pH 6.8, 2% SDS, 10% glycerol, 0.1% bromophenol blue, and 5% β-mercaptoethanol) and heated for 5 min at 95℃ before SDS-PAGE on a 10% gel and subsequently transferred to a pure nitrocellulose membrane (Bio-Rad, CA). After transfer, the membrane was blocked with 5% blocking reagent (Amersham Biosciences, England) in TBS containing 0.1% Tween 20 for 2 hours at RT or overnight at 4℃. The membrane was rinsed in three changes of TBS-T, incubated once for 15 min and twice for 5 min in fresh washing buffer, and then incubated with primary antibody (purified mouse anti CP IgG1, BD Transduction Laboratories, USA), 1:1000 for 2 hours at RT or overnight at 4℃. After three washes in washing buffer, the membrane was incubated for 2 hours in horseradish peroxidase-conjugated anti-mouse secondary antibody (1:5000, Amersham Biosciences, England) and developed using enhanced chemiluminescence (ECL western blotting analysis system kit, Amersham Biosciences, England). The blot was detected using a Lumi-imager F1 workstation (Roche Molecular Biochemical). The intensity of the specific bands was determined by densitometry with the use of LumiAnalyst 3.1 software (Roche Molecular Biochemical). To ensure even loading of the samples, the same membrane was probed with rabbit anti-human β-actin polyclonal antibody (Sigma-Aldrich, MO) at a 1:5000 dilution.

3.3.4 Statistical Analysis

The statistical analyses were performed using SPSS 10.0. Data are presented as mean ± SEM. The difference between means was determined by One-Way ANOVA

followed by a Student-Newman-Keuls test for multiple comparisons. Differences with $P<0.05$ are considered significant. The correlation was analyzed using Pearson's bivariate correlations with the SPSS version 10.0 statistical software program.

3.4 RESULT

3.4.1 Distribution of CP in the Rat Brain

In situ hybridization of central nervous system tissue utilizing CP cRNA probes revealed abundant CP mRNA in specific populations of glial cells and the epithelium of the choroids plexus(Klomp et al., 1996; Klomp and Gitlin, 1996). The major form of CP in the brain is GPI-anchored form(Patel and David, 1997; Patel et al., 2000). Here, immunohistochemistry method was used to detect the CP protein distribution in the rat brain. CP staining was in the cortex (Fig 3-1A, 3-1B), hippocampus (Fig 3-1C), striatum (Fig. 3-1D), substantia nigra (SN, Fig. 3-1E), periventricular (Fig 3-1G, 3-1H, 3-1J), perimicrovasculature (Fig 3-1F) and the choroid plexus (Fig 3-1I) of the adult rat. As with CP mRNA distribution (Klomp et al., 1996; Klomp and Gitlin, 1996; Patel and David, 1997; Patel et al., 2000), the cell-specific positive staining of CP in the adult brain was mainly detected in glial cells of the brain parenchyma, endothelial cells of microvasculature (Fig 3-1F), ependymal cells lining the ventricles (Fig 3-1G, 3-1H, 3-1I, 3-1J), the choroid plexus (Fig 3-1I) and the leptomeningeal cells (Fig 3-1A), which cover the surface of the brain. However, some specific immunoactive staining was rarely observed in neurons. Within the cortex (Fig 3-1B), very strong staining was observed in the entorhinal cortex area. The glial cell membrane was intensely immunoreactive (Fig 3-1A, 3-1B, 3-1C,

3-1D). The immunopositive CP of membrane and fiber of the cells in the SN (Fig 3-1E) was stronger than other brain areas. Periventricular glial cells, choroids plexus and ependymal cells lining the lateral ventricle stained more prominently than other cells.

3.4.2 Total Iron Concentration of the Hippocampus, Striatum, and Substantia Nigra in Developing Rats (Fig 3-2).

Brain structures including cortex, hippocampus, striatum and substantia nigra, isolated from six or seven rat brains at PND 7, 21, 63, and 196. The total iron of the brain regions was measured by using a GFAAS method. As shown in Fig 3-2, regional brain iron concentrations ranged between 171.2±9.5 and 339.2±5.1 nmol iron/mg brain wet weight tissue. The iron concentration of 4 regions showed an upward trend as developing. Within each age group, the iron concentration was highest in the substantia nigra.

3.4.3 Effect of Age on Ceruloplasmin Gene Expression in Rat Brain (Fig 3-3, 3-4)

To test whether the expression of CP was influenced by age, six to seven rats were used in each group at PND 7, 21, 63, and 196. The brain cortex, hippocampus, striatum, and substantia nigra were excised to extract total mRNA for RT-PCR analysis. A 386-bp and a 263-bp fragment from the CP cDNA and β-actin cDNA were amplified and their identity confirmed by DNA sequencing (Fig 3-3A). After being normalized with β-actin, the following results were found: In the cortex and

hippocampus, CP mRNA expression was the lowest at PND7, and then increased to the highest at PND 21 (cortex) or PND63 (Hippocampus), but at PND196 the CP mRNA expression decreased. However, in the striatum and substantia nigra areas, CP mRNA expression was lowest in rat at PND 7, and then increased to the highest at PND196 (Fig 3-3B). Expression of CP protein in the cortex, hippocampus, striatum and substantia nigra of the rat brain during development was analysed by Western blotting (Fig. 3-4), which detected one expected band with an approximate relative molecular weight (*Mr*) of ~150 kDa. The molecular weight of CP was similar to the 135 kDa previously reported in rat brain (Klomp et al., 1996; Patel and David, 1997). Analysis of the bands showed that the protein synthesis of CP in each brain region almost corresponded to the change of its mRNA level in the rats at ages PND 7, 21, 63 and 196. CP protein expression showed no significant difference at PND 21 in the cortex and striatum. At PND 63, the mRNA level was statistically significant in hippocampus and substantia nigra. This suggests that transcriptional regulation in CP gene.

Since iron distribution in the brain changes during brain development, the relationship of CP mRNA and protein expression to regional brain iron concentration was investigated. After plotting the values of CP mRNA and protein expression against brain iron content, the results showed that the value of CP mRNA expression and protein synthesis is strongly positive and significantly correlated to iron content in striatum (r=0.904, P<0.001; r=0.811, P<0.001,) and substantia nigra (r=0.909, P<0.001; r=0.822, P<0.001) respectively.

3.4.4 The Role of Variations Iron Diet on Iron Status of Rats

After a six-week period with various iron diets, the rat body weight, Hb, Hct, TIBC, serum iron Tf saturation and non-heme iron levels in liver was measured. All of the data were significantly different from the control group ($P<0.01$, Table 3-1). The body weight, Hb, Hct, and Tf saturation as well as non-heme iron level of the liver were significantly lower in iron-deficient rats than in control rats. These data suggested that rats fed the iron deficient diet developed iron deficiency with anemia. On the contrary, The Hb, Hct, serum iron, Tf saturation and non-heme iron level in liver were significantly higher in rats on the high-iron diet group than the control ($P<0.01$, Table 3-1). These data show that rats have developed iron overload status.

In order to assess the brain iron status, we also measured iron concentrations in the different brain regions in the control, low-iron and high-iron rat groups using atomic absorption spectrophotometer. Lower iron concentrations were found in low-iron rats, and higher concentrations in high-iron rats compared to the control group (Table 3-2). This implied that iron overload and iron deficiency animal models were successfully developed in each brain areas.

3.4.5 Effect of the Iron Status on CP Gene Expression in the Cortex, Hippocampus, Striatum and Substantia Nigra of Rat Brain

In the HFRT +/- mice brain, the regulation of CP mRNA by iron deficiency was not observed. This might be masked by the use of total RNA derived from whole brain

extracts(Thompson et al., 2003). To investigate the possible role of iron status in transcriptional regulation of CP, we tested whether CP mRNA expression is changed by feeding iron-deficient and iron-surfeit diets in the cortex, hippocampus, striatum and substantia nigra of rat brain. RT-PCR was performed on the tissues from the different brain regions. As illustrated in Fig 3-5A, representative bands on the gel correspond to the expected oligonucleotide size based on the primers used for CP and β-actin. Although iron concentration was significantly decreased in low-iron diet rats and increased in high-iron diet rats to the control, after normalization to β-actin, the results showed that CP mRNA expression was only slightly but no significant increased by iron deficiency status in hippocampus and striatum, only 5% increased in substantia nigra to control group, however, a slightly decreased but no significant difference of CP mRNA expression in hippocampus, striatum and substantia nigra by excess iron diet feeding. To the contrary, in cortex, there was a reverse little change of CP mRNA expression by the iron status (Fig 3-5B). We further analyzed CP protein synthesis in the four brain areas by the Western blot method in low-iron, high-iron and control groups to detect whether protein synthesis was influenced by iron status. CP protein was no significant change in the cortex, hippocampus and striatum in rats on low-iron or high-iron diets. However, there was significant increase and decrease in CP levels in the substantia nigra by iron overload and deficiency status (Fig 3-6). To confirm this result, we examined the expression of TfR mRNA and protein in each brain area. This result indicated TfR expression increased in iron-deficient rat brains, and decreased in the iron-overload rat brains, although the changes appeared at different levels in the different brain regions.

3.5 DISCUSSION

The immunohistochemistry data in this study demonstrate CP immunoactive staining at the cortex, hippocampus, striatum, substantia nigra and strong staining at periventricular area, the brain-CSF (choroid plexus) barrier and the blood-brain barrier. These results correspond with those for CP mRNA expression detected by *in situ* hybridization in rat central nervous system (Klomp et al., 1996). Specifically, in the brain parenchyma, CP staining was mainly observed in glial cells, very slightly in neuron. This is different from the results observed with a CP homologue gene, hephaestin (Heph) distribution (in chapter 4). This data will support the view that CP has a possible role in the brain iron metabolism (Qian and Ke, 2001).

Iron concentrations in various rat brain regions, as determined by flame atomic absorption spectrophotometry in the present study, are similar to those observed by others investigators (Erikson et al., 1997) and Pinero(Pinero et al., 2000b) in corresponding age groups. The relationship of CP mRNA and protein expression to regional brain iron concentration was investigated. The value of CP mRNA expression and protein synthesis did not correlate significantly with iron concentration in the cortex and hippocampus, whereas there was a strong positive and significant relationship between CP expression and iron concentrations in the striatum and substantia nigra.

In neurodegenerative disorders (NDs), not all brain regions showed the increased concentrations of CP consistent with the increased concentrations of iron. CP concentrations in Alzheimer's disease (AD), Parkinson's disease (PD), progressive

supranuclear palsy (PSP), Huntington's disease (HD) substantia nigra, AD, PD, HD caudate and AD, PD putamen were increased by > 90% vs. elderly controls specimens. In AD hippocampus, entorhinal cortex, frontal cortex and putamen, PD hippocampus, frontal, temporal and parietal cortices, and HD hippocampus, parietal cortex and substantia nigra, the mean CP concentrations were significantly increased compared to elderly normal controls (Loeffler et al., 1996). This differed from the results obtained in Conner JR (Connor et al., 1993). The upregulation of CP expression in cultured cells by iron deficiency could be the result of the activation of hypoxia-inducible factor (HIF)(Mukhopadhyay et al., 1998; Attieh et al., 1999). It is now clear that the HIF-1α and HIF-1β bind to the CP gene promoter HRE (Mukhopadhyay et al., 2000). However, in a whole animal model, iron status has little or no influence on the levels of plasma CP and on the expression of its mRNA by the liver (Huang and Shaw, 2002; Strube et al., 2002; Tran et al., 2002). This different result may be due to very low levels of iron achievable only in culture and not *in vivo* (Tran et al., 2002). This could also explain a 'super effect' by an unknown factor like estrogen, which could overcome HIF-1 CP regulation and therefore counteract the iron effect (Laine et al., 2002). In the HFRT +/- mice brain, CP levels were increased compared to wild-type controls. This change was not due to a change in the amount of mRNA, but may be due to an increase production by the choroids plexus (Thompson et al., 2003). The failure to observe any CP mRNA change in iron-deficient conditions may be due to a masking effect from the use of total RNA derived from whole brain extracts (Thompson et al., 2003). We dissected the rat brain to four areas of cortex, hippocampus, striatum and substantia nigra to study the effect of iron status on CP gene expression using PT-PCR and western blot analysis. The data show iron deficiency or overload has a weak effect on the

expression of CP mRNA in those regions. We suppose that the change of brain iron has no effect on the expression of CP mRNA *in vitro*, and it is not due to the use of total RNA to analyze the brain CP mRNA expression. As with mRNA expression, protein levels were not regulated by iron status in cortex, hippocampus and striatum. Surprisingly, the protein level was significantly decreased in iron deficiency and increased in iron overload in the substantia nigra. These results imply there are post-transcriptional and translational mechanisms involved in the regulation of the CP protein. This regulation is related not only with the total iron levels (Mukhopadhyay et al., 1998; Mukhopadhyay et al., 2000) but also the indices of oxidative stress (Loeffler et al., 1996; Chen et al., 2003b). The expression of GPI-CP in the leptomeninges is very low at birth and high in the adult, indicating a higher demand in the mature brain for protection from iron-mediated oxidative stress (Mittal et al., 2003). Results show region-specific differences in iron and oxidative stress in a critical neonatal period in the brain of rats on a high-iron diet. The level of lipid peroxidation in the cerebellum is apparently not influenced by iron supplementation but increases in the substantia nigra and decreases in the striatum (Dal-Pizzol et al., 2001). In the present study, the high-iron diet induced the iron increase in the substantia nigra. The oxidative stress was perhaps also increased, and the CP expression was boosted. In contrast, CP protein synthesis decreased. However, our understanding of the regulation of CP in brain cells *in vivo* or *in vitro* remains rudimentary, and further study is required.

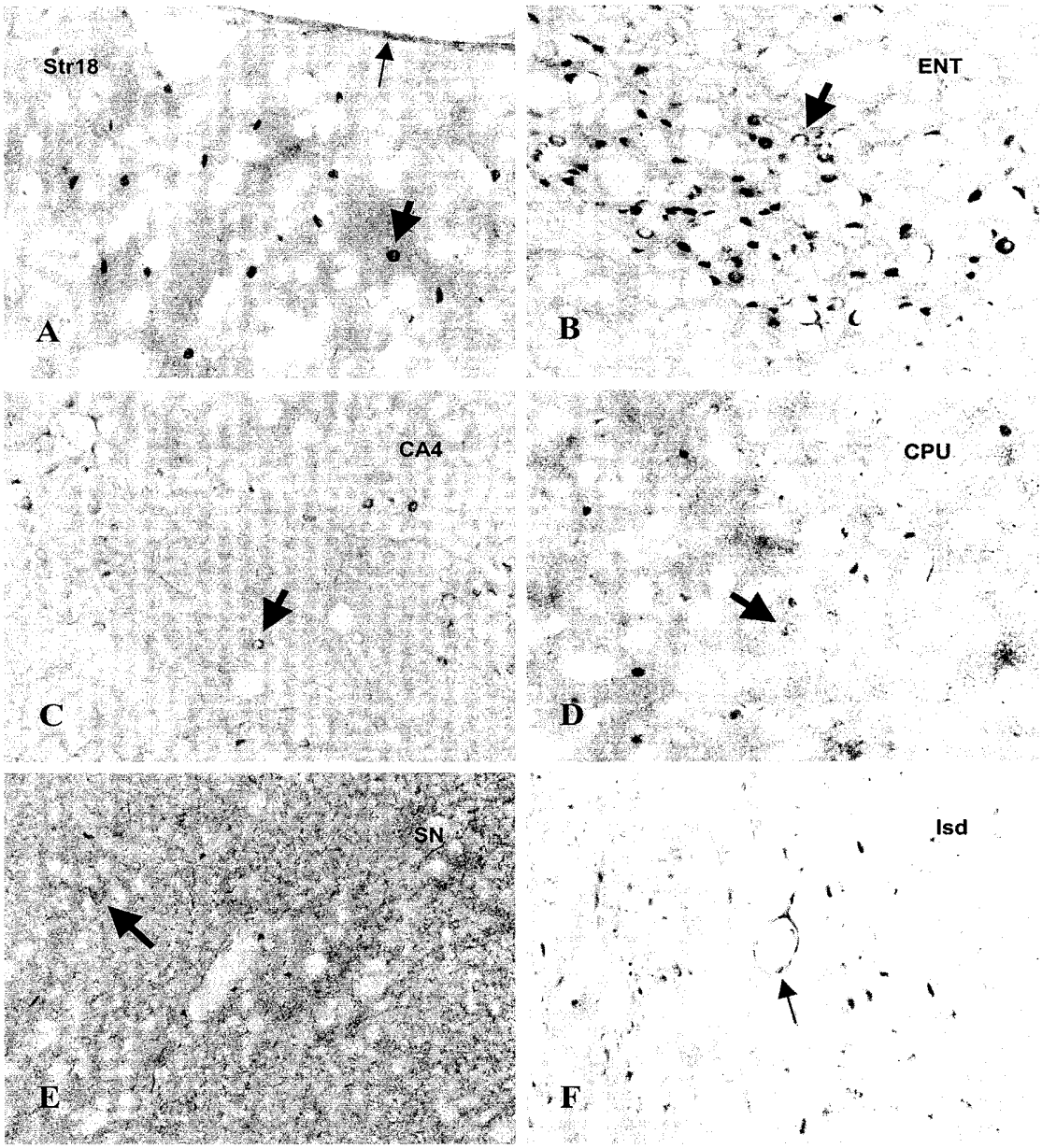
Str18
A
ENT
B
CA4
C
CPU
D
SN
E
lsd
F

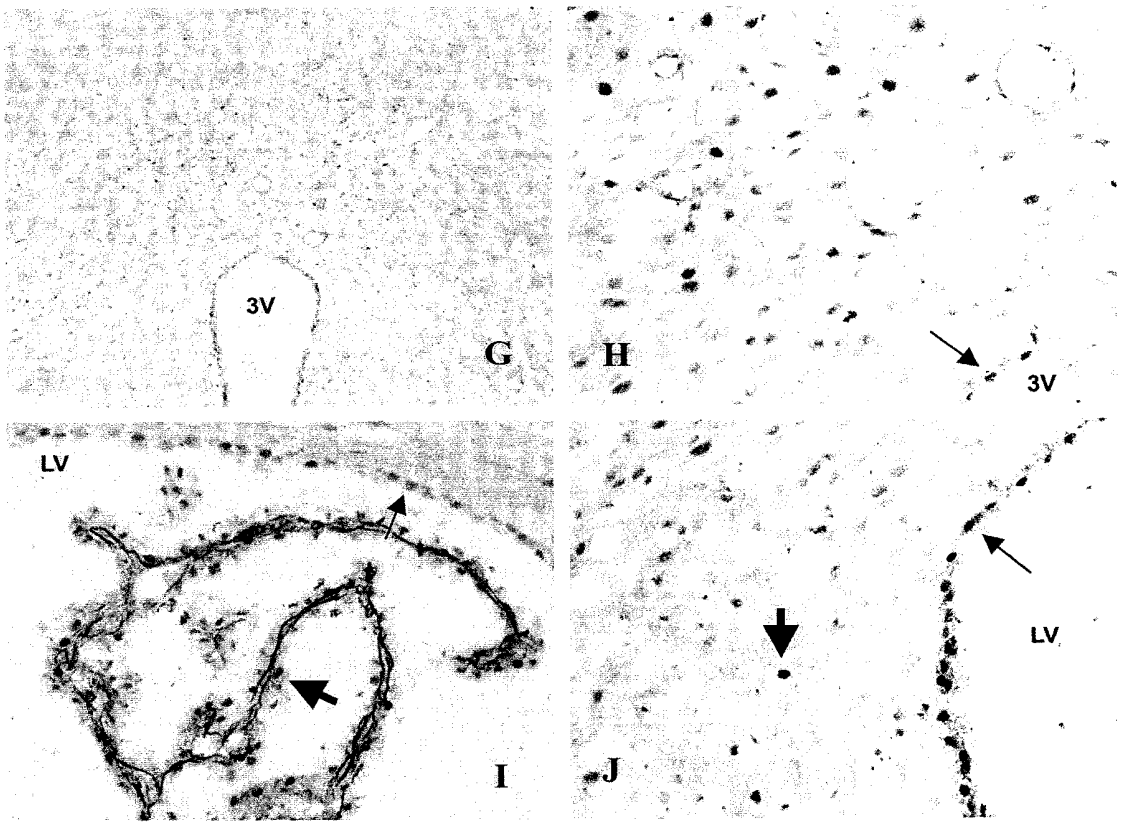
3V
G
H
3V
LV
I
J
LV

Figure 3-1. Immunohistochemical detection of Ceruloplasmin in adult rat brain with specific antibody. The cell-specific positive staining of ceruloplasmin in the adult brain was detected in the glial cells of the brain parenchyma, ependymal cells lining the ventricles, the choroid plexus and the leptomeningeal cells, which cover the surface of the brain. But specific immunoactive staining was rarely observed in neurons. CP staining in the area 18 of striate cortex (**A**, Str18), CA4 of hippocampus (**C**), caudate putamen (**D**, CPU) and heavy staining in the entorhinal cortex (**B**, Ent), the immunoactive-labeled glial cell membrane (fat arrow) and leptomeningeal cells (thin arrow) were indicated. **E**, CP staining in the substantia nigra (SN), was stronger in the membrane and fiber than other areas; heavy staining was observed the oligodendrocyte body (fat arrow). **F**: Section through the lateral septal nucleus (lsd), showed moderately heavily labeled endothelial cells of microvessel (thin arrow). Strong staining in the glial cell (fat arrow) and ependymal cell (thin arrow) was observed in nearly of the third ventricle (**G**, low magnification; **H**, higher magnification) and the lateral ventricle (**J**). **I**: Section through the lateral ventricle and corpus callosum show strong CP staining in the choroid plexus (fat arrow) and the ependymal cells (thin arrow). Original magnifications: ×100 (G), ×400 (A, B, C, D, E, F, H, I, J)

Table 3-1. Hematological variables, liver non-heme iron in the control, iron deficient, and iron overload rats.

	Control (n=6)	Iron deficiency (n=6)	Iron overload (n=6)
Body weight (g)	327 ± 4.27	270 ± 4.48**	340 ± 7.11
Hct (%)	43.50 ± 0.99	17.67 ± 0.99**	48.33 ± 0.67**
Hb (g/dl)	17.96 ± 0.29	5.27 ± 0.38**	19.63 ± 0.30**
Serum iron (mmol/L)	24.67 ± 0.88	3.11 ± 0.53**	48.80 ± 2.11**
TIBC (mmol/L)	67.79 ± 1.29	109 ± 3.27**	69.69 ± 1.34
Transferrin saturation (%)	36.36 ± 0.81	2.93 ± 0.54**	70.20 ± 3.57**
Liver iron (mg/g dry weight)	0.27 ± 0.01	0.07 ± 0.01**	2.66 ± 0.13**

Each value represents sample mean ± SEM of six rats. ** Indicates significant difference at $P < 0.01$ vs. control.

Table 3-2. Regional brain iron concentration of rats with iron-deficiency, iron overload and normal iron (control) diets rats.

	Control (n=6)	Iron deficiency (n=6)	Iron overload (n=6)
Cortex	281.6 ± 6.42	252.8 ± 2.74**	319.1 ± 3.85
Hippocampus	269.1 ± 4.55	221.0 ± 5.25**	322.2 ± 3.06**
Striatum	283.4 ± 9.73	244.6 ± 5.03*	394.4 ± 7.55**
Substantia Nigra	291.6 ± 13.2	226.2 ± 6.26**	347.8 ± 6.63**

Data on iron were presented as mean ± SEM nmol/g wet weight of brain tissue (n=6). *P<0.05, **P<0.01 vs. control.

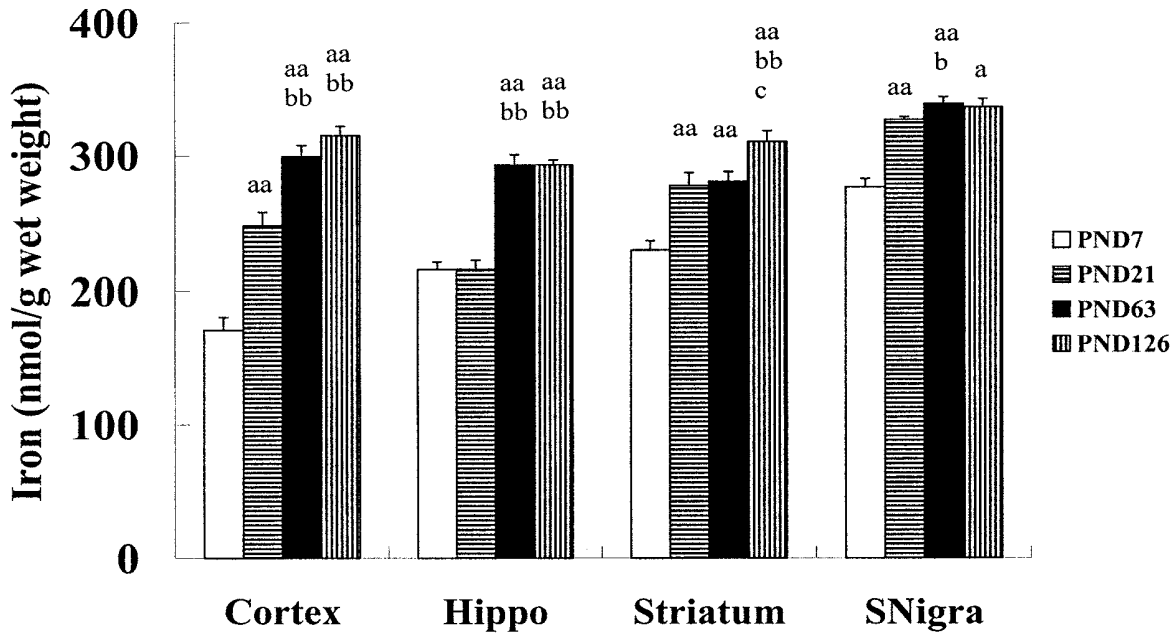

Figure 3-2. Levels of iron in the cortex, hippocampus, striatum and substantia nigra at postnatal days 7, 21, 63 and 126 expressed per unit brain wet weight tissue. Data are presented as mean ± SEM, with n = 6 or 7. Letters above data bars indicate that these groups are statistically different: a: $P<0.05$; aa: $P<0.01$ from PND 7, b: $P<0.05$; bb: $P<0.01$ from PND 21, c: $P<0.05$; cc: $P<0.01$ from PND 63.

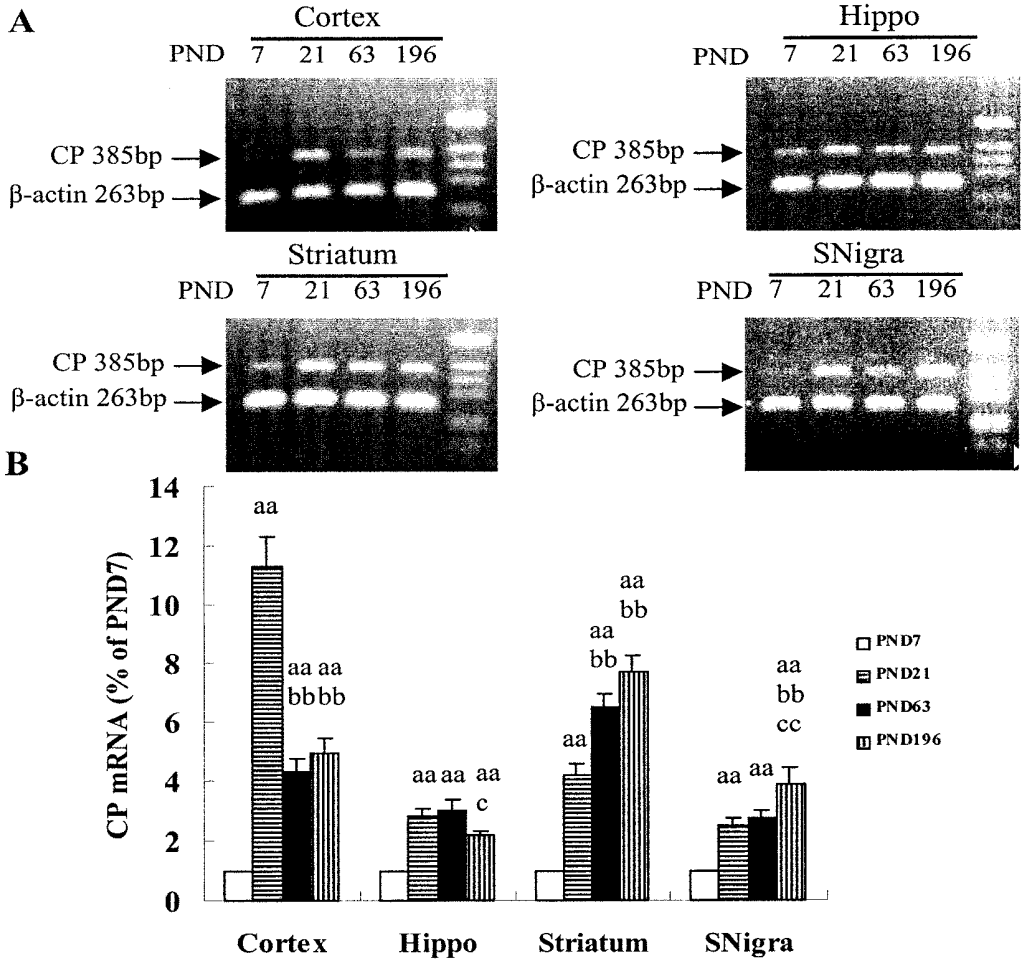

Figure 3-3. Expression of ceruloplasmin (CP) mRNA in the cortex, hippocampus (Hippo), striatum and substantia nigra (SNigra) of rats at the ages of postnatal day (PND) 7, 21, 63 and 196. **A:** A representative experiment of RT-PCR products of CP and β-actin mRNA. The bands on the gel correspond to the expected oligonucleotide size based on the primers used for CP and β-actin. **B:** Expression of CP mRNA was quantified by normalized to β-actin mRNA and expressed as a percentage of PND 7 levels. Data were presented as the mean ± SEM of the values from 6, 7 independent experiments. Letters above data bars indicate that these groups are statistically different: aa: $P<0.01$ from PND 7, bb: $P<0.01$ from PND 21, c: $P<0.05$; cc: $P<0.01$ from PND 63.

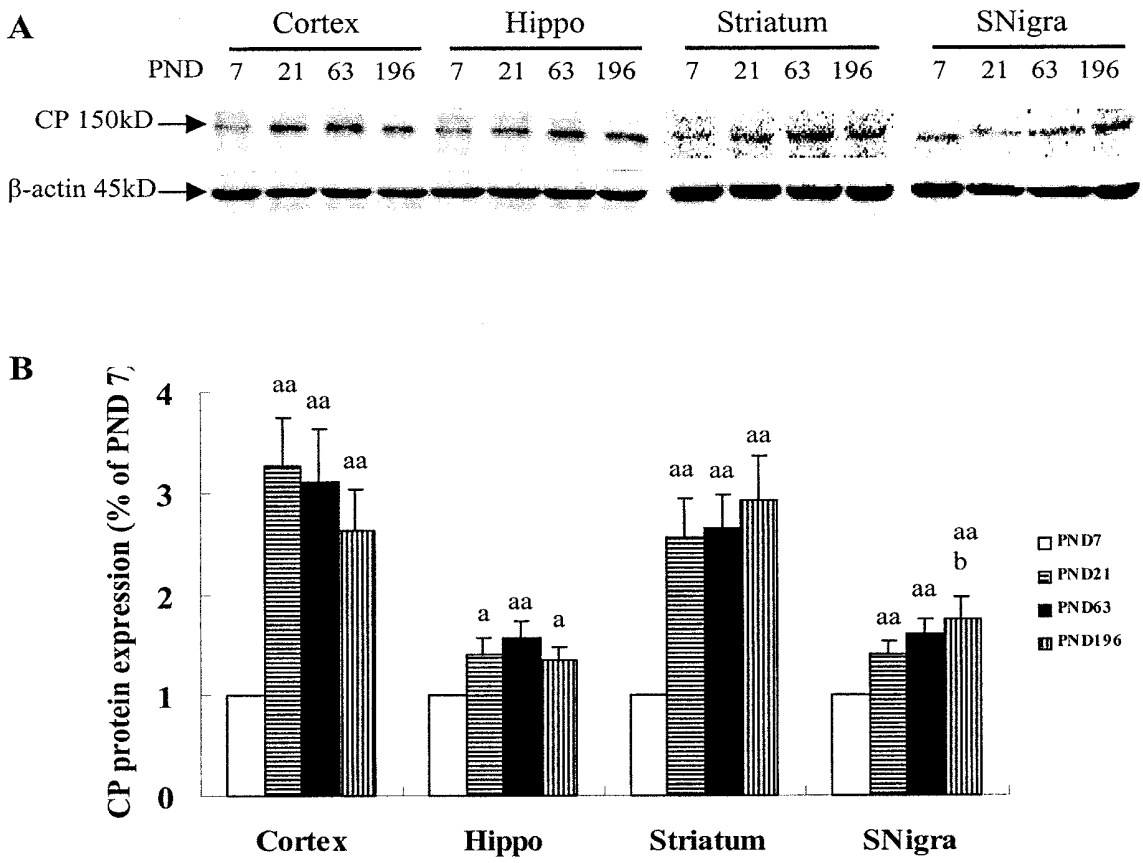

Figure 3-4. Expression of ceruloplasmin protein in rat cortex, hippocampus, striatum and substantia nigra at the ages of PND 7, 21, 63 and 196. Western blot analysis was performed as described in Materials and Methods. **A:** The expected molecular weight of CP ~150 kDa and β-actin ~ 45 kDa bands appearing on each gel. **B:** Quantification of expression of CP protein in the cortex, hippocampus, striatum and substantia nigra of rats at the ages of PND 7, 21, 63 and 196. Expression values were normalized for β-actin and expressed as a percentage of PND 7 level. The data were presented as means ± SEM of 3 to 6 separate experiments. Letters above data bars indicate that these groups are statistically different: aa: $P<0.01$ from PND 7, bb: $P<0.01$ from PND 21, c: $P<0.05$; cc: $P<0.01$ from PND 63.

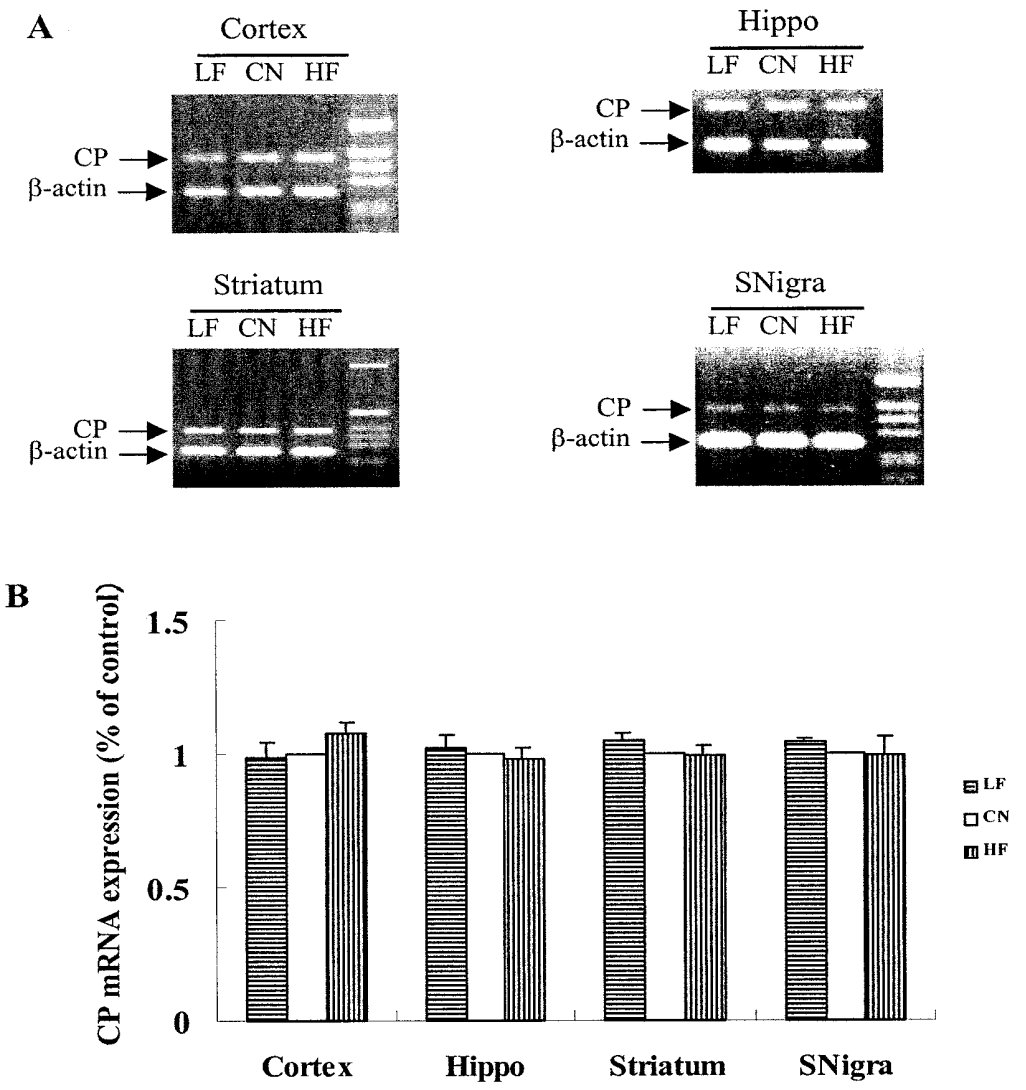

Figure 3-5. Effect of brain iron status on the expression of CP mRNA in cortex, hippocampus, striatum and substantia nigra. RT-PCR products of CP mRNA and β-actin mRNA from the cortex, hippocampus, striatum and substantia nigra of rats fed with iron-deficient (LF), iron-overload (HF) and normal (CN) diet. **A:** The bands on the gel correspond to the expected oligonucleotide size based on the primers used for CP and β-actin. **B:** RT-PCR assay for CP mRNA was performed in duplicate for three samples in each group. Expression values were normalized for β-actin and expressed as percentage of normal levels.

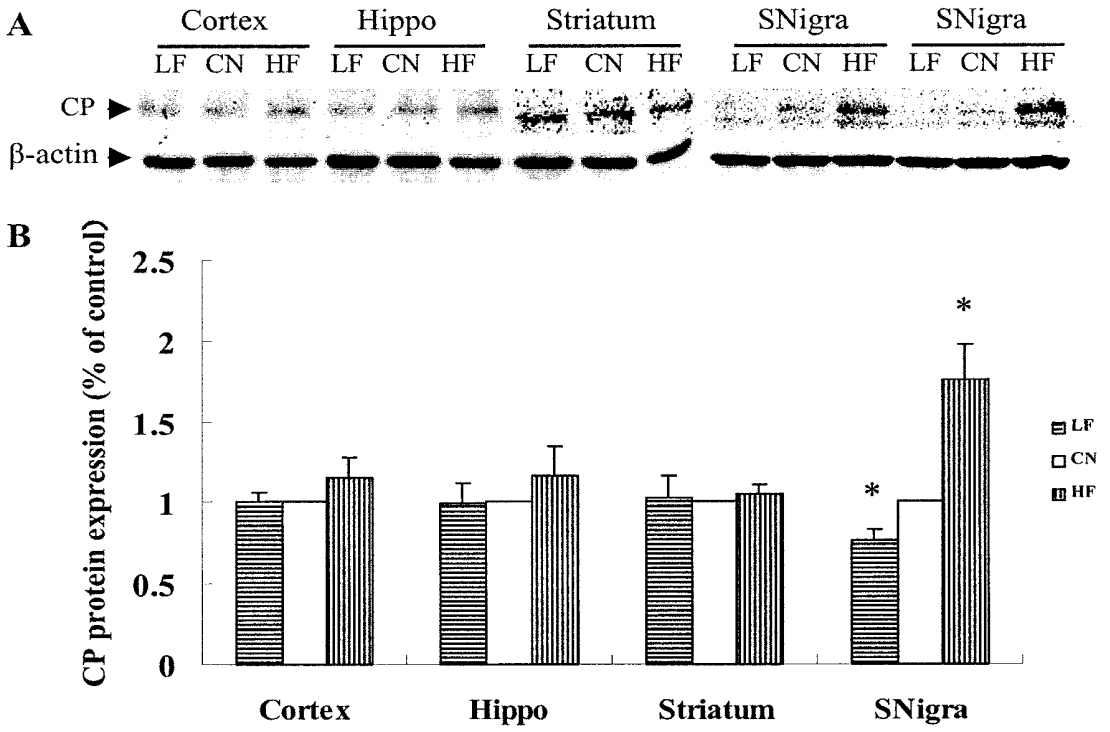

Figure 3-6. Effect iron status on ceruloplasmin protein synthesis in the cortex, hippocampus, striatum and substantia nigra of normal (CN), iron-deficient (LF) and iron-overloaded (HF) rats. The tissue samples were treated as described in Methods. Western blot analyses were performed in duplicate for three samples in each group. A representative sample is showed in **A**. The single band in *M*r of ~150 kDa CP protein and ~45 kDa β-actin protein appearing on each gel. **B:** The results were normalized with β-actin and expressed as a percentage of normal levels. The data are presented as the means ± SEM of 5 or 6 samples. **P*<0.05 vs. control.

CHAPTER 4

THE EXPRESSION OF CERULOPLASMIN HOMOLOGUE, HEPHAESTIN, AND THE EFFECT OF AGE AND IRON IN RAT BRAIN

4.1 ABSTRACT

Excessive iron in the brain in NDs may result from increased uptake as well as decreased release. Currently, little is known about the molecules involved in iron efflux from brain cells. Heph, a newly discovered CP homologue, has been suggested to be necessary for iron egress from the enterocytes into circulation via interaction with ferroportin1. Based on the putative function of Heph in enterocytes, the similarity of the process of iron transport in enterocytes with that in blood-brain barrier (BBB) cells, and the unique location and form of CP expression in the brain, Heph has also been proposed to play a similar role in iron export from BBB cells and other brain cells as in enterocytes. The existence of ferroportin1 in the brain has recently been demonstrated. In this study, we demonstrated that all brain regions examined have the ability to express Heph. At the cellular level, Heph was detected in the body as well as on the membrane of neurons, vascular endothelial cells and ependymal cells. Heph staining was found in the body as well as on the membrane of neurons and vascular endothelial cells. Age and iron dependent regulation of Heph

expression at transcriptional level in different brain regions were observed. These data support a putative role for Heph in iron release from the neurons, BBB cells and probably some other brain cells.

KEY WORDS:

Brain iron metabolism, Hephaestin, Iron transport, Iron release, Brain cells, Transcriptional regulation

4.2 INTRODUCTION

Heph is highly homologous to CP (50% identity, 68% similarity) and, significantly, all the residues involved in copper binding and disulfide bond formation in CP are conserved in Heph (Vulpe et al., 1999). Unlike CP, however, Heph is an integral membrane protein with a single membrane-spanning domain at its C-terminus. The well-defined domain organization of CP appears to be on served in Heph and Syed *et al.* have proposed a structure for the protein based on that available crystal structure for CP (Syed et al., 2002). It has been predicted that Heph, like CP, would possess a ferroxidase activity and this was recently shown to be the case (Anderson et al., 2002a). Sex-linked anaemia (*sla*) mice have a block in intestinal iron transport. Although these mice normally take up iron from the intestinal lumen into mature epithelial cells, the subsequent exit of iron into the circulation is diminished. This is

because a mutation in the Heph gene. The result suggests that Heph is involved in the transfer of iron across the basolateral membrane (Vulpe et al., 1999). CP is a copper-containing ferroxidase that is essential for normal iron homeostasis. Whereas CP in plasma is produced and secreted by hepatocytes, in the brain a glycosylphosphatidylinositol (GPI)-anchored form of CP is expressed on the surface of astrocytes (Patel and David, 1997). Based on the observation that the ferroxidase activity of CP promoted iron incorporation into Tf, clinical studies on aceruloplasminemia (Gitlin, 1998) and animal model of aceruloplasminemia (Harris et al., 1999), a role for CP in iron efflux was suggested. The most likely role for these proteins with ferroxidase activity is to give some direction to membrane iron transport by oxidizing iron to the ferric form after it has traversed the membrane and preventing its transport in the opposite direction.

The mechanisms of iron transport across the blood–brain barrier (BBB) have not been completely clarified. Nonetheless, accumulated evidence suggests that the transferrin–transferrin receptor (Tf–TfR) pathway might be the major route of iron transport across the luminal membrane of the capillary endothelium, although the mechanism for transport across the abluminal membrane has yet to be determined (Qian and Shen, 2001). Because the form of iron transport across this membrane might be ferrous iron, a ferroxidase such as Heph (or CP) might be necessary for ferrous iron to be oxidized to ferric iron, after crossing the basolateral membrane of the BBB cells, so that iron can be carried away by Tf (Qian and Ke, 2001). Based on

the similarity of the transport form of iron across the basolateral membranes (both are ferrous iron), and the existence of ferroportin1 (FP1) and Heph in the brain (Jiang et al., 2002), it is possible that a FP1/Heph or a FP1/CP system may play a role in iron transport across the BBB cells (Qian et al., 2002). Intracellular iron balance depends on the amount of iron taken up as well as on the amount of iron released by the cell. The excessive accumulation of iron in the brain that is found in NDs might result from increased uptake as well as decreased release (Qian and Wang, 1998; Qian and Shen, 2001). Clinical data have demonstrated that there is increased production of some of these iron 'uptake' proteins in some NDs. These clinical findings imply that excessive iron accumulation could be induced by the abnormally increased expression of iron 'uptake' proteins. On the other hand, the increased intracellular iron in the brain can also result from decreased iron release from cells, as in the patients with aceruloplasminemia, because of the absence of expression of CP, currently the only known iron 'release' protein. Decreased CP expression has also been considered as a possible cause for excessive iron accumulation in some other NDs, although no direct evidence has been obtained (Qian and Wang, 1998). However, recent studies of Mukhopadhyay CK (Mukhopadhyay et al., 1998), Attieh ZK (Attieh et al., 1999) and Qian ZM (Qian et al., 2001a; Xie et al., 2002) support the possibility that CP plays a role in iron influx into the cells. CP is not found in neuron of rat brain (Patel and David, 1997), so perhaps there are other proteins in brain tissue, which take the role of CP.

Studies have shown that the expression of Heph mRNA is slightly increased degree under iron deficient conditions and decreased with iron loading in rat intestine (Frazer et al., 2001; Sakakibara and Aoyama, 2002). However, little is known about the distribution and regulation of Heph expression in the brain. In the current studies, we investigate the distribution of Heph in rat brain and determine whether age can influence the Heph expression. Also, the effect of dietary iron on the levels of Heph expression in the brain tissue and iron status on primary astrocyte Heph expression *in vitro* was studied.

4.3 MATERIALS AND METHODS

4.3.1 Materials

Please refer to chapter 3

4.3.2 Animals

Please refer to chapter 2

4.3.3 Methods

4.3.3.1 Primary Astrocyte Cultures and Treated

Primary astrocyte cells were established from the cortex of 2-day-old SD rats as previously reported (Qian et al., 1999a; Qian et al., 2000). Briefly, the brains of rat were removed and the cortex was dissected and counted with a hemocytometer. The cells were cultured in 75 cm^2 flasks, and the average density was 2×10^5 cells/cm^2. The cultured cells were incubated in a 5% CO_2 incubator at 37℃, and the culture medium (Dubelcco's modified eagle medium (DMEM) with L-glutamine, sodium pyruvate, and pyridoxine hydrochloride, containing 10% fetal bovine serum (FBS), penicillin, streptomycin) (Life Technologies, NY) was changed every 3 days. After 9–10 days, the cells were prepared for subculture to remove the O2A lineage cells from the type-1 astrocytes according to Juurlink and Hertz (1992). 10 ml of 0.05% trypsin in Ca^{2+}-Mg^{2+}-free PBS buffer was added to each flask, and the cells incubated for 10 min at 37℃. The solution was then discarded, and 10 ml of DMEM containing 10% FBS was added to terminate trypsinization. The cells were counted and seeded at 4×10^5 cells/cm^2 in 25 cm^2 flasks and cultured in a 5% CO_2 95% air atmosphere in a CO_2 incubator at 37℃. After 5–6 days of plating (subculture), more than 95% of the cells were positively stained with a monoclonal antibody against glial fibrillary acidic protein (GFAP) (Boehringer-Mannheim, Indianapolis, IN), thus being judged as type-1 astrocytes (Fig 4-1). The astrocytes were treated with DFO and FAC in serum free DMEM medium for 24 hours and the cellular proteins were collected.

4.3.3.2 Immunohistochemistry

11-week-old normal adult rats were deeply anaesthetized and perfused through the left cardiac ventricle with normal saline, followed by a fixative, consisting of 4% paraformaldehyde in 0.1M phosphate buffer (pH 7.4). The sections of brain were cut at 10μm thickness on a freezing microtome. These were washed in 0.01 M phosphate-buffered saline (PBS) to remove traces of fixative. Endogenous peroxidase was blocked by 0.3% H_2O_2 in methanol for 25 minutes, followed by incubation in 5% normal goat serum for 1 hour at room temperature to block non-specific binding of antibodies. The sections were incubated with a 1:500 dilution of the primary rabbit anti-mouse Heph antibody (ADI, San Antonio, USA) for 24 hours at 4℃. This antibody source of antigen sequence is 100% conserved in rat. A biotin-streptavidin detection system was employed with diaminobenzidine as the chromogen. The sections were washed with PBS and incubated with diluted biotinylated secondary antibody (VECTOR, Brulingame, USA) for 60 min at 37℃. After rinsing in PBS, the sections were incubated with ABC Reagent (VECTOR, Brulingame, USA) for 60 min at 37℃, and incubated with diaminobenzidine and H_2O_2 for 5 min. 0.01 M PBS was used as a substitute for primary antibody for negative control groups.

4.3.3.3 Total Iron Measurement of Rat Brain Areas

Analysis of total iron in the brain was performed using a graphite furnace atomic absorption spectrophotometer (GFAAS, Perkin Elmer, AAnalyst 100). Brain tissues were diluted 1:20 (wt/v) for cortex, hippocampus, striatum and 1:80 for substantia nigra with HEPES buffer and homogenized with a sonicator (MSE Soniprep 150 Ultrasonic Disintegrator, MSE Scientific Instruments, England). A 50 μl portion of the homogenate was added to an equal volume of ultra-pure nitric acid in a 0.5 ml polypropylene microfuge tube, digested for 48 hours at 50℃, and diluted 1:10 for substantia nigra and 1:40 for cortex, hippocampus, striatum with 3.12 mmol/L nitric acid for iron analysis using the graphite furnace atomic absorption spectrophotometer. Standard curves ranging from 0 to 40 ppb were prepared by diluting iron standard (1 mg iron/ml, Alpha Products, Danvers, MA) with blanks prepared from homogenization reagents in 0.2 % HNO_3. Standards and digested samples were read in triplicate by injecting 50 μl aliquots, including 0.05 mg $Mg(NO_3)_2$ as matrix modification, into graphite furnace. Absorbance readings were recorded at 248.3 nm, slit at 0.2 nm, pretreatment temperature at 1400℃, atomization temperature at 2400 ℃ and used for analysis. All of the solutions were prepared with Milli-Q water.

4.3.3.4 RNA Isolation

Please refer to chapter 3

4.3.3.5 RT-PCR Amplification and Sequence Analysis

Please refer to chapter 2 and 3.

4.3.3.6 Northern Blot Analysis

Thirty micrograms of total RNA were electrophoresed on 1% agarose formaldehyde gels, transferred overnight to Hybond-N (Amersham Pharmacia Biotech, England) membranes with 10× standard saline citrate (SSC), and fixed to the membranes using a UV cross-linker (Fisher). The blots were prehybridized at 65℃ in ExpressHyb hybridization solution (Clontech, CA, USA) for 1hour, then hybridized overnight at 65℃ in the same solution containing ^{32}P-labeled probes using the Prime-a-Gene labeling system (Promega, WI, USA), [α-^{32}P]dCTP (Amersham Biosciences) and purified by a Micro Spin G-50 columns (Amersham Biosciences) as per manufacturer's instructions. Heph and β-actin cDNAs used as probes were obtained by cloning the RT-PCR products of total RNA prepared from the brain of rats, and their identities were confirmed by sequencing. Heph cDNA correspond to positions of 3659-4201nt (Genbank, AF246120). After three 5-10 min washes with 2× SSC containing 0.05% sodium dodecyl sulfate (SDS) at room temperature, the blots were washed in 0.1× SSC, 0.1% SDS with continuous shaking at 50-60℃ for 10 min for several times, radioactivity was detected by Phosphorimager and quantified using

ImageQuant software (Molecular Dynamics, Sunnyvale, CA). For normalization, the blot was stripped and probed again with β-actin probe corresponding to position 474-736 of rat β-actin (Genbank, NM031144). The results were expressed as the ratio to β-actin.

4.3.3.7 Western Blot Analysis

Please refer to chapters 2 and 3.

The primary antibody (rabbit anti-mouse Heph polyclonal antibody, Alpha Diagnostic, USA) is 1:5000 and horseradish peroxidase-conjugated anti-rabbit or anti-mouse secondary antibody (Amersham Biosciences, England) is 1:5000.

4.3.4 Statistical Analysis

Please refer to chapter 3.

4.4 RESULTS

4.4.1 Distribution of Hephaestin in Rat Brain

Heph staining in normal rats was highest in the cortex (Fig 4-2A), hippocampus (Fig 4-2C), striatum (Fig. 4-2E), compact part of substantia nigra (Fig. 4-2G), medial preoptic area (Fig. 4-2I), preoptic suprachiasmatic nucleus (Fig. 4-2J), mammillary

(Fig. 4-2K), with lesser staining in the white matter. Almost all kinds of neural cell were Heph positive. Very weak or no staining was observed in the superficial layers compared to the superficial layers; the deeper layers, the glial cell bodies and the cell membrane and apical dendrites of pyramidal neurons were intensely immunoreactive. Within the hippocampus, the pyramidal cell layer (Fig. 4-2C, 4-2D) was strong immunopositive for Heph. The heavy staining was observed on neuron bodies. While Immunoreactive staining was lighter in the striatum (Fig. 4-2E) than in the cortex and hippocampus, heavily labeled cell membrane and bodies were also observed in this region (Fig. 4-2F). The immunopositive (Fig. 4-2G and 4-2H) Heph was most dominant in neuron bodies of the compact part of substantia nigra. Very little staining was observed in the reticular part of substantia nigra. In the corpus callosum white matter, oligodendrocytes were Heph positive (Fig. 4-2M and 4-2O). Ependymal cells lining the lateral ventricle stained more prominently than other neuronal cells (Fig. 4-2M and 4-2N). Heph was detected in the ependymal cells of the lateral ventricle and third ventricle (Fig. 4-2N and 4-2P). In the superior colliculus, the microvasculature was immunoreactive (Fig. 4-2L).

4.4.2 The Regulation of Hephaestin Gene Expression in Developing Rat Brain

Six to seven rats were used in each group at PND 7, 21, 63, and 196. The brain cortex, hippocampus, striatum, and substantia nigra were excised for RT-PCR

analysis. As illustrated in figure 4-3A, RT-PCR products from the appropriate Heph and β-actin primers each yielded a single major band consistent with the expected number of base pairs for Heph and β-actin. A 543-bp and a 263-bp fragment from the Heph cDNA and β-actin cDNA were amplified and their identity confirmed by DNA sequencing. After being normalized to β-actin, and compared with the adult age group (PND63), the following results were observed: In each brain region, Heph mRNA expression was lowest at PND7, and then increased significantly to the highest expression at PND 21 (hippocampus, striatum and substantia nigra) or PND63 (cortex). After the Heph mRNA reached the highest expression, it remains no significantly change (hippocampus, substantia nigra). However, in the cortex and striatum areas, Heph mRNA expression was significantly decreased at PND196 and at PND63 (Fig. 4-3B). This data implied that age has an effect on the expression of Heph mRNA in the brain and after adult their expression remains steady level.

Our immunohistochemistry data showed heavy Heph immunoactive staining in the cortex, hippocampus, striatum and compact part of substantia nigra. Expression of Heph protein in the rat brain during development was confirmed by Western blot analysis (Fig. 4-4), which detected two bands with approximate relative molecular weight (*Mr*) of ~165 kDa and ~106 kDa. Anderson and coworkers (Frazer et al., 2001), detected a major polypeptide species of molecular mass 155 kDa in rat distal small intestine. 165 kDa molecular weight of Heph protein detected in this study is similar to the molecule observed by Anderson, but the ~106 kDa protein is smaller

than the molecular weight of 155 kDa. Analysis of the band of ~165 kDa revealed it was significantly expressed at PND 21 and PND 63 in each brain region, but almost no band has been observed at PND 7 and PND 196 in all brain areas. The level of Heph protein expression in rat brain areas at PND 21 was significantly higher than PND 63 (Fig. 4-5A). When the amounts of ~106 kDa Heph protein were analyzed using Western blotting, the highest expression of Heph was detected in adult rat brain. The change of Heph protein in each brain region corresponded to the change of its mRNA level in the rats at ages PND 7, 21, 63, 196. However, Heph protein expression appeared distinct from its mRNA expression in the striatum and substantia nigra, where the highest level of its protein expression occurred at PND 63 rather than at PND 21. The level of Heph protein expression at PND 7 appeared to be much lower than that we found in adult rat brain (Fig. 4-5B, Fig. 4-3). We also examined the effect of age on the total expression of Heph protein in rat brain regions (Fig. 4-5C). The data showed that the lowest expression was in PND 7 rat brain, the highest-level expression was in PND 21 rat brain, however, marked decrease protein expression was observed in PND 196 rat brain. After plotting the ~106 kDa Heph gene expression against brain iron content, the results showed that the value of Heph was significantly correlated with iron content in the cortex (r=0.604, P<0.005), Hippo (r=0.514, P<0.02), striatum (r=0.627, P<0.003) and substantia nigra (r=0.677, P<0.016) respectively. In the substantia nigra, the total Heph protein was also significantly correlated with iron content, however, there was

not correlation in other brain areas. The ~165 kDa Heph did not exhibit significant correlation with brain iron concentration.

4.4.3 Total Iron Concentration in the Cortex, Hippocampus, Striatum, and Substantia Nigra of Rats on Varied Diets (Fig. 4-6).

After the rats were fed low, control and high iron diets for 6 weeks, the total iron of the cortex, hippocampus, striatum and nigra showed significant difference. In rats fed with a high iron diet, the iron concentration of the cortex, hippocampus, striatum, and nigra was higher than the control ($p<0.001$, n=6). In rats fed with the low iron diet, the total iron of the four areas is lower than control ($p<0.001$; $p<0.05$ for striatum, n=6). These data indicated that the model of making high iron and low iron in the rat brains was appropriate to our experimental design.

4.4.4 Expression Patterns of Hephaestin Gene in Response to Alterations in Brain Iron Status

Recent studies have shown that ferroportin1–hephaestin (FP1–Heph) and/or Heph-independent iron export systems may play a key role in Fe^{2+} transport across the basal membrane of enterocytes in the gut (Vulpe et al., 1999; Donovan et al., 2000; Kaplan and Kushner, 2000). It is also likely have the same role in Fe^{2+}

transport across the abluminal membrane of the BBB (Qian and Shen, 2001). CP gene expression has not been detected in neurons. However, our immunohistochemistry data showed strong immunoactive staining for Heph in neurons. While the mechanism for the export of iron in neurons is unknown, Heph is likely to have a role in the process. Because iron transport is strongly regulated by iron stores, we examined the effect of altering brain iron status on the expression of Heph gene in the rat brain areas. Representative Northern blot analysis showing the expression of Heph is presented in Fig. 4-7A. One mRNA band with molecular mass ~5 kb was detected with randomly primed ^{32}P-labeled probe for Heph. This molecular weight was in agreement with those was observed in mice intestinal tissue and Caco-2 cells (Vulpe et al., 1999) (Han and Wessling-Resnick, 2002). The level of Heph mRNA was found to increase in the cortex and hippocampus and dramatically decrease in the striatum of rats on a high-iron diet. In contrast, Heph mRNA in iron-deficient rats was significantly decreased in the cortex and hippocampus compared to controls, but significantly increased in striatum (Fig. 4-7B). This was also observed at the protein level, although the difference was not found to be statistically significant in the cortex of iron-deficient rats (Fig. 4-8). The similar pattern was seen for Heph protein expression in substantia nigra in response to iron status (Fig. 4-8).

4.4.5 Effect of the Iron Status on Hephaestin Protein Expression in Primary Astrocytes

Heph protein in cell extracts derived from primary astrocytes treated with 100 μM $FeCl_3$, 1 mM DFO and untreated astrocytes were analyzed using Western blot. As shown in the immunoblot (Fig. 4-9A), a protein band with molecular mass ~106 kDa reacted strongly with the anti-Heph antibody. The molecular mass ~155 kDa reacted slightly with the anti-Heph antibody. There was a $FeCl_3$ and DFO dependent change of this ~106 kDa protein. After being normalized to β-actin, a very significant increase ($p<0.01$) in the intensity of this band was detected in cells exposed to 100 μM $FeCl_3$ compared with control astrocyte culture. Cells exposed to 1 mM DFO showed significant decrease ($p<0.05$) (Fig. 4-9B). This pattern of Heph protein regulated by iron status corresponded to rat brain *in vivo*.

4.5 DISCUSSION

Intracellular iron balance is dependent not only upon the amount of iron uptake by cells but also upon the amount of iron released. The excessive accumulation of iron in the brain found in some NDs may result from increased uptake by as well as decreased release from cells (Qian and Wang, 1998). Over the past decades, considerable research has been devoted to investigating cell iron uptake. However, little is known about the molecules involved in iron efflux from cells and the

relevant mechanisms under physiological conditions. Although CP is widely believed to have a role in iron release from brain cells (Harris et al., 1999), expression of CP in the brain is only observed in those astrocytes surrounding the microvasculature (Klomp et al., 1996). Also, GPI-anchored CP expressed by astrocytes is the predominant form of this protein in the brain (Patel and David, 1997; Patel et al., 2002). The unique location and expression this protein in the brain suggest that CP might be necessary to oxidize Fe^{2+}, after it crosses the abluminal membrane of the BBB endothelial cells probably via FP1 (Jeong and David, 2003), so that the latter can bind to transport carriers (Patel et al., 2000; Qian and Ke, 2001; Qian and Shen, 2001; Patel et al., 2002). Also, these characteristics of CP, together with recent *in vitro* studies on the effect of CP on iron transport in brain glioma cells (Qian et al., 2001a; Xie et al., 2002), suggest CP is unlikely to play a role in iron efflux from other brain cells except for BBB cells and astrocytes. Therefore, there is probably another molecule(s) that has a CP-like role in the brain.

The results in the study provided a direct evidence for the existence of Heph protein in the brain. Heph staining was found in all four regions of the rat brain. At the cellular level, the neuron was the predominant cell type expressing Heph. The expression of this protein was also detected in the glia, vascular endothelial cells and ependymal cells. The existence of Heph protein suggested that this protein might play a physiological role in iron release from these cells. Iron (Fe^{2+}) might be first transported across the membrane of these cells by FP1. Heph, acting as a putative

ferroxidase (Anderson et al., 2002b), might oxidize the Fe^{2+} to Fe^{3+} and subsequently load iron (Fe^{3+}) on to transferrin or some other iron carrier in the brain. Currently, it is unknown whether FP1 exists in glial cells. However, in the case of brain neurons, the existence of FP1 has been demonstrated (Burdo et al., 2001). In this study, we detected heavy Heph staining not only in the cytoplasm but also on the membrane of neurons, which differs from enterocytes, where Heph is predominantly located inside cells and not on the basolateral membrane (Frazer et al., 2001; Anderson et al., 2002b). These data support the hypothesis that an FP1/Heph pathway might mediate iron release from brain neurons. Also it is possible for the pathway to play a role in iron transport across the basolateral membrane of BBB cells, given the presence of Heph detected in this study and our preliminary studies that showed that BBB cells have the ability to express FP1 (unpublished data). However, on study has yet demonstrated a clear interaction between FP1 and Heph, even in the small intestine. Further investigations are needed to confirm the putative role of FP1/Heph pathway in iron release from brain cells.

In the current study, the level of Heph expression in the brain changed during the brain development was found. This suggests that Heph expression in the brain may be age dependent. Moreover, two molecular weights of Heph protein, one ~165 kDa, another ~106 kDa was detected. Analysis of the band of ~165 kDa revealed significant expression at PND 21 and PND 63 in each brain region, but almost no band was observed at PND 7 and PND 196 in all brain areas. The ~106 kDa Heph

protein was detected at PND 21, PND 63 and PND196 but not at PND 7. Therefore, we suggest there are two molecular weights of Heph in rat brain, which appear at different ages. How and why are the two Heph molecules synthesized? Are the two Heph molecules like hepcidin (Ilyin et al., 2003), which was hydrolyzed from one protein molecule? Further study is needed.

In the present study, we also observed iron status had a significant effect on Heph mRNA expression as well as protein synthesis in different brain regions. This finding is different from that in the duodenum where variations in iron status have little effect on Heph mRNA expression (Frazer et al., 2001; Sakakibara and Aoyama, 2002). The lack of response of Heph to iron in the duodenum suggests that Heph may not play a primary regulatory role and may be not rate limiting for intestinal iron transport although it plays a critical role in iron absorption (Anderson et al., 2002b). The more active response of Heph to iron in the brain implies that Heph may play a key role in cellular iron balance and may be essential for iron release from brain cells. In all brain regions, we also found that iron-induced and age-related changes of Heph mRNA expression were very similar to those of Heph protein synthesis. The similar regulation patterns suggest the existence of an iron-dependent-transcriptional regulation. Studies on the duodenum have also demonstrated that regulation of Heph protein in response to variations in iron status is similar to that of the mRNA (Anderson et al., 2002b). These data suggest that Heph is not strongly regulated at the translational level, not only in the duodenum

but also in the brain. Unlike mRNAs for FP1 and some other iron metabolism proteins, the message for Heph does not have an iron-responsive element (IRE). IREs are posttranscriptional regulators of gene expression (Han and Wessling-Resnick, 2002). It might explain why Heph is not regulated at the translational level by IRE. Currently, nothing is known about the mechanisms involved in iron induced-transcriptional regulation of Heph in the brain. Further work is necessary to understand this aspect. An unexpected finding in this study was that the effects of iron status on Heph gene expression in the cortex and hippocampus were different from those in the striatum and substantia nigra. It is not known whether this is due to regional differences in the capacity to manage iron and oxidative stress, and related to uneven distribution of iron in the brain. The reason for the regionally specific effects of iron status on Heph gene expression also needs to be clarified.

To determine the effect of iron status on Heph expression *in vivo*, we studied the regulation of Heph gene expression in primary culture cortical astrocytes. We also detected two major immunoactive bands in response to variations in iron status. The pattern of regulation of Heph is the same as in the cortex and hippocampus. One possible explanation is the astrocytes were originally from cortex. This study suggests that Heph may play a primary regulatory role for brain iron transport both in the BBB and in neuron cell levels.

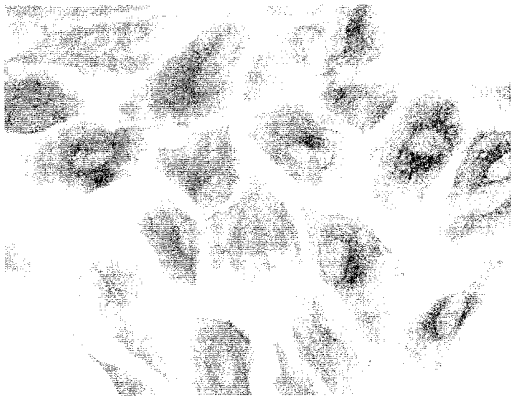

Figure 4-1. Immunocytochemical detection of GFAP expression in astrocytic primary culture. After 2 weeks in culture, more than 95% of the culture was positive for GFAP staining. Magnification 400×

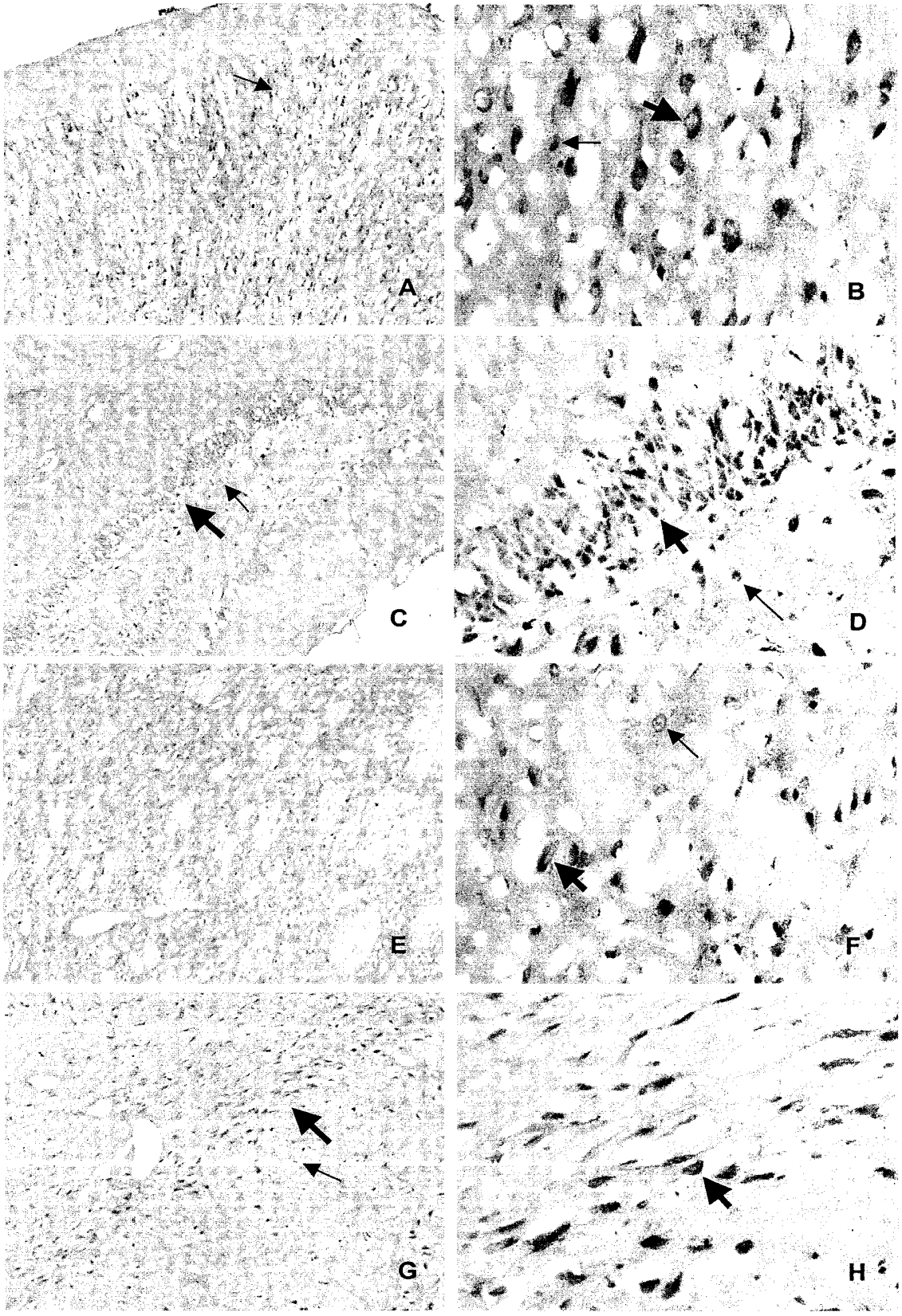
A
B
C
D
E
F
G
H

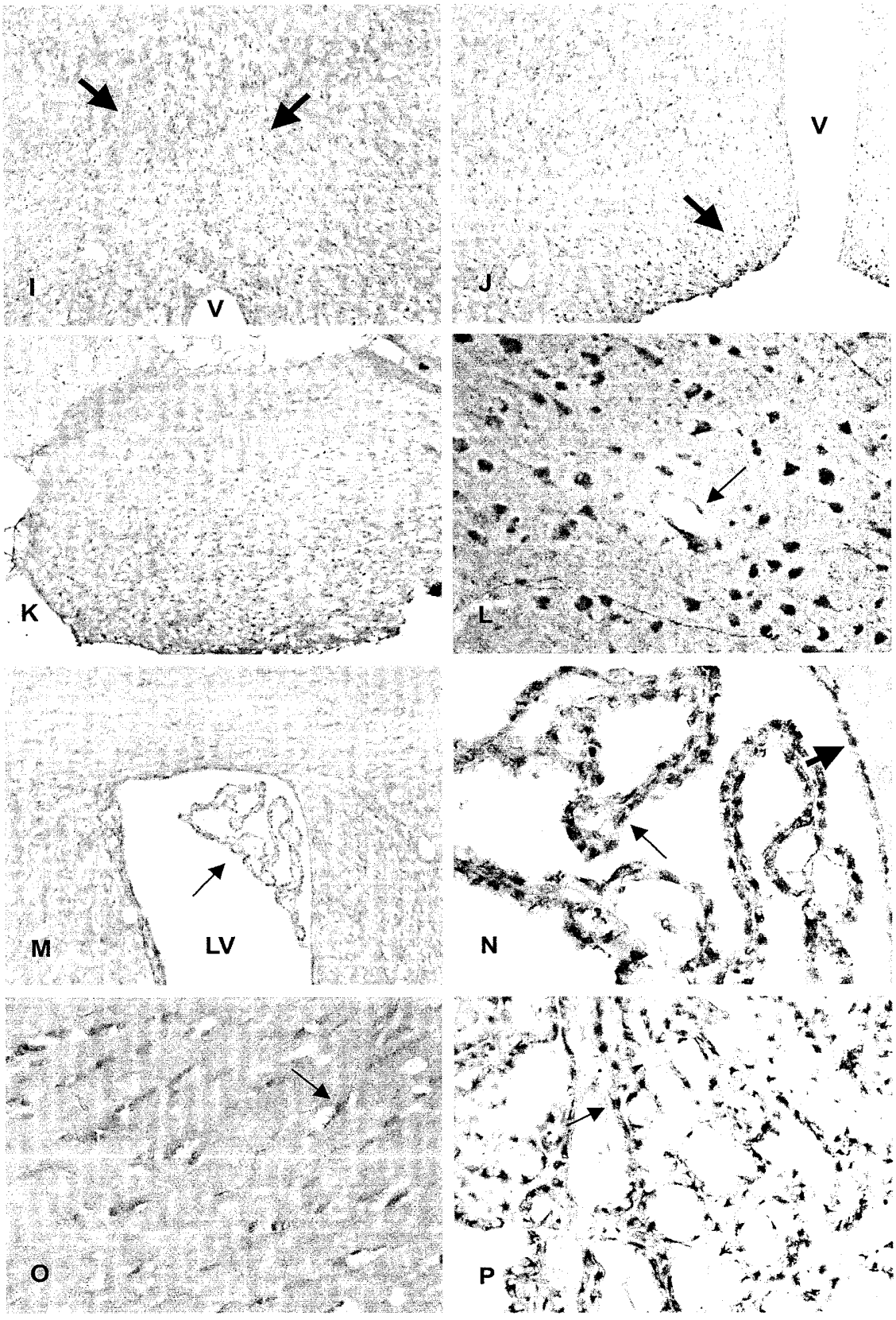
I
V
J
V
K
L
M
LV
N
O
P

Figure 4-2. Hephaestin (Heph) staining in the adult rat brain. **A:** Heph staining in cortex, showing heavy staining in deep layer neuronal cells (thin arrow). **B:** Higher magnification of pyramidal neurons (fat arrow) and glial cells (thin arrow). **C, D:** Heph immunoactive labeled cell bodies of hippocampal pyramidal layer neurons (fat arrow) and glial cells (thin arrow). **E, F:** Heph staining in the striatum. Fat arrow indicates heavy staining in the neuron body and thin arrow indicates the positive staining of the astrocyte membrane. **G:** Neuronal staining in the compact part of substania nigra (fat arrow), and in a few cells in the reticular part of substania nigra (thin arrow). **H:** Higher magnification of the compact part of substantia nigra shows the strong neuron body staining (fat arrow). **I, J, K:** Heavy immunoactive staining in medial preoptic area (I, fat arrow indicated), preoptic suprachiasmatic nucleus (J, fat arrow indicated), mammillary (K). **L:** Section through the superior colliculus showing heavily labeled endothelial cells of microvessels (thin arrow). **M:** Section through the lateral ventricle and corpus callosum, the thin arrow points to strong Heph staining of the choroid plexus. **N:** Higher magnification of ependymal cell staining from cells lining the lateral ventricle (fat arrow). The thin arrow points to the endothelial cells of the choroids plexus in the lateral ventricle and the third ventricle (**P**). **O:** Oligodendrocyte staining for Heph in the corpus callosum white matter. The thin arrow points to a single oligodendrocyte that is positively immunostained for Heph. Magnification 100× (A, C, E, G, V, J, K, M), 400× (B, D, F, H, L, N, O, P).

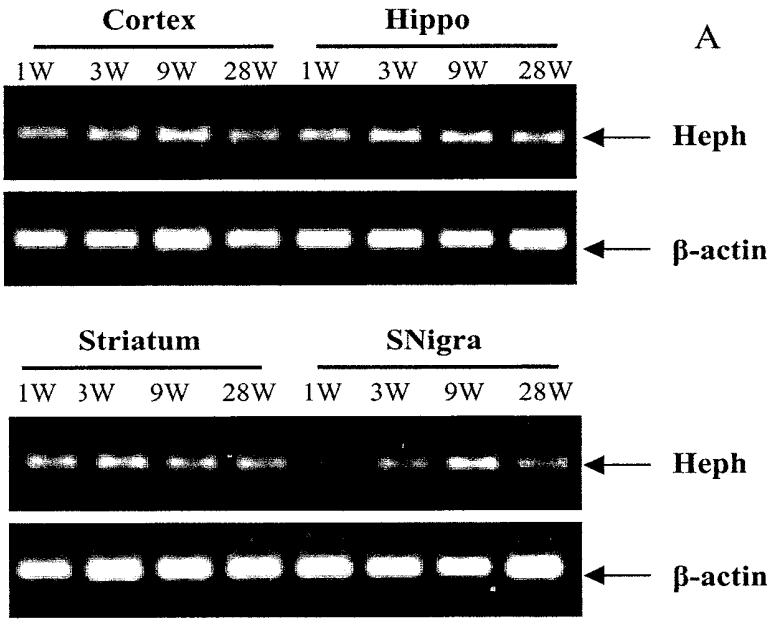
A
Cortex
Hippo
1W 3W 9W 28W 1W 3W 9W 28W
Heph
β-actin
Striatum
SNigra
1W 3W 9W 28W 1W 3W 9W 28W
Heph
β-actin

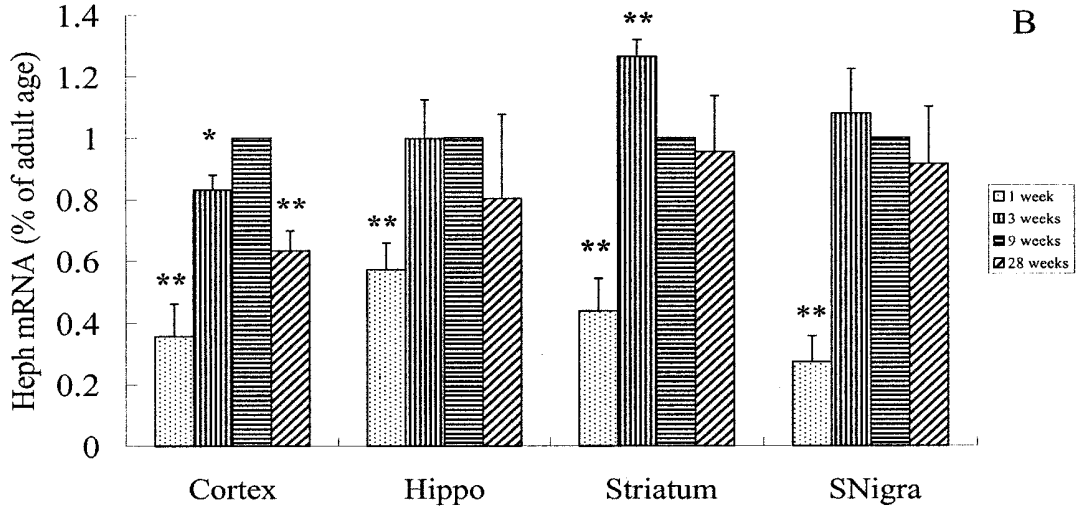
B
Heph mRNA (% of adult age)
1.4
1.2
1
0.8
0.6
0.4
0.2
0
Cortex
Hippo
Striatum
SNigra
1 week
3 weeks
9 weeks
28 weeks

Figure 4-3. Expression of hephaestin (Heph) mRNA in the cortex, hippocampus (Hippo), striatum and substantia nigra (SNigra) of rats at the ages of 1 week, 3 weeks, 9 weeks and 28 weeks. **A:** A representative experiment of RT-PCR products of Heph and β-actin mRNA. The bands on the gel correspond to the expected oligonucleotide size, based on the primers used for Heph and β-actin. **B:** Expression of Heph mRNA was normalized to β-actin mRNA and expressed as a percentage of 9 weeks levels. Data were presented as the mean ± SEM of the values from 6, 7 independent experiments. Different markers above data bars indicate that these groups are statistically different from each other (* $P<0.05$, ** $P<0.01$).

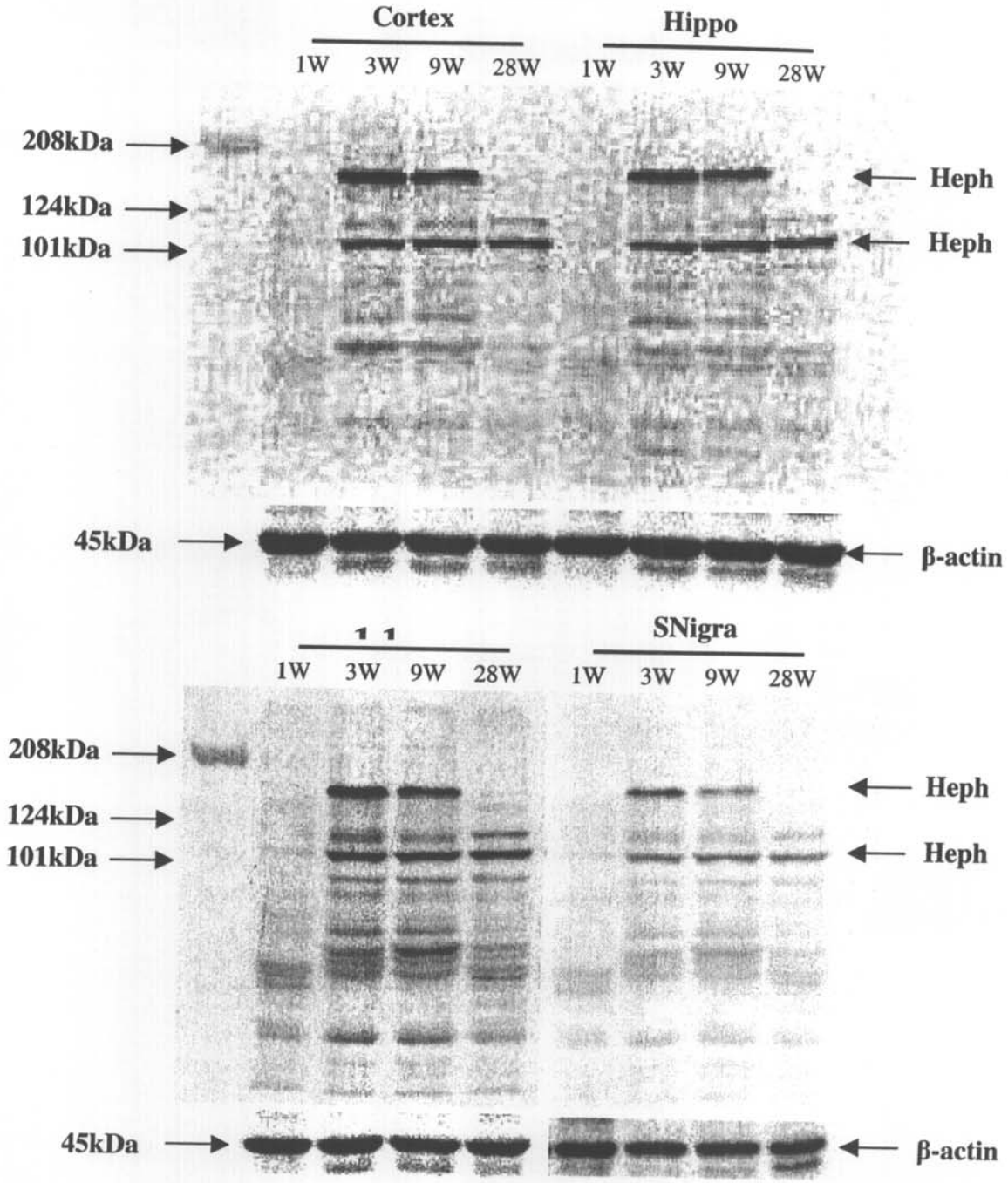

Figure 4-4. Expression of hephaestin (Heph) protein in rat cortex, hippocampus (Hippo), striatum and substantia nigra (SNigra) at the ages of 1 week, 3 weeks, 9 weeks and 28 weeks. Western blots analysis was performed as described in Materials and Methods. Two Heph immunoactive bands in *Mr* ~165 kDa and ~106 kDa appeared on each gel. The β-actin band was also observed that corresponded with the expected molecular weight ~45 kDa.

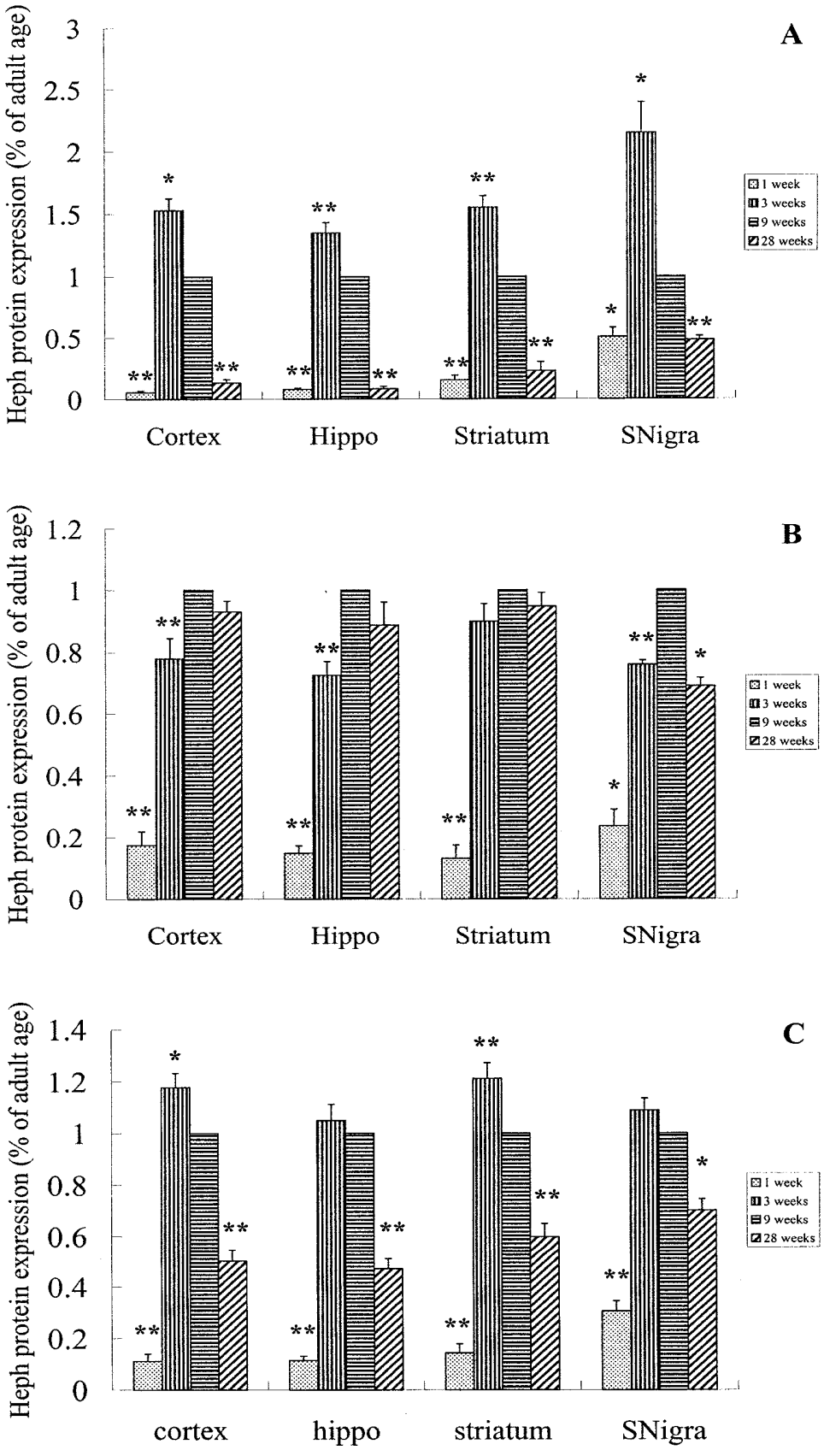
A
Heph protein expression (% of adult age)
3
2.5
2
1.5
1
0.5
0
1 week
3 weeks
9 weeks
28 weeks
Cortex
Hippo
Striatum
SNigra
B
Heph protein expression (% of adult age)
1.2
1
0.8
0.6
0.4
0.2
0
1 week
3 weeks
9 weeks
28 weeks
Cortex
Hippo
Striatum
SNigra
C
Heph protein expression (% of adult age)
1.4
1.2
1
0.8
0.6
0.4
0.2
0
1 week
3 weeks
9 weeks
28 weeks
cortex
hippo
striatum
SNigra

Figure 4-5. Expression of hephaestin (Heph) protein in the cortex, hippocampus (Hippo), striatum and substantia nigra (SNigra) of rats at the ages of 1 week, 3 weeks, 9 weeks and 28 weeks was quantified by Western blot analysis. **A:** Analysis of *Mr* ~165 kDa **B:** ~106 kDa **C:** total levels of Heph protein expression in development rats brain areas. Expression values were normalized with β-actin and expressed as a percentage of the 3-week level. The data are presented as the mean ± SEM of 3 separate experiments. Different letters above data bars indicate that these groups are statistically different from the adult (*P<0.05, **P<0.01).

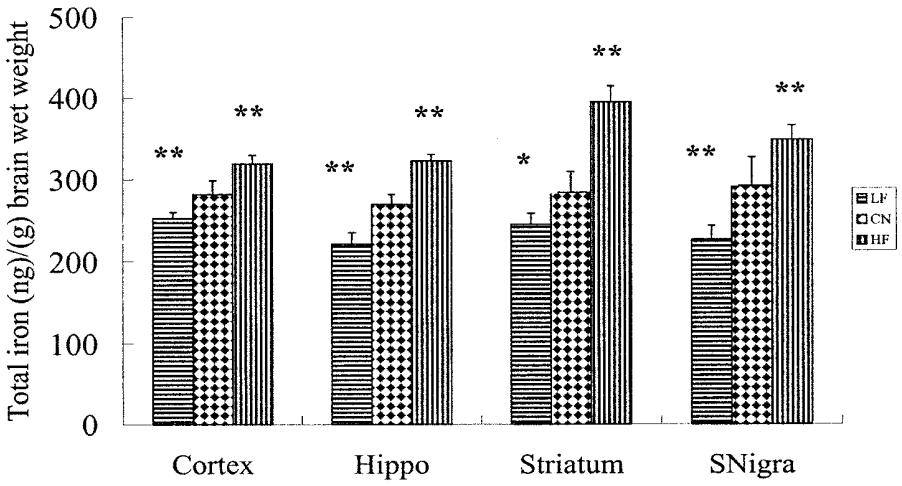

Figure 4-6. Regional brain iron concentration of rats with iron deficient (LF), iron overload (HF) and normal (CN) diets. Data on total iron were presented as the mean ± SEM nmol/g wet weight of brain tissue (n=6). *P<0.05, **P<0.01 vs. control.

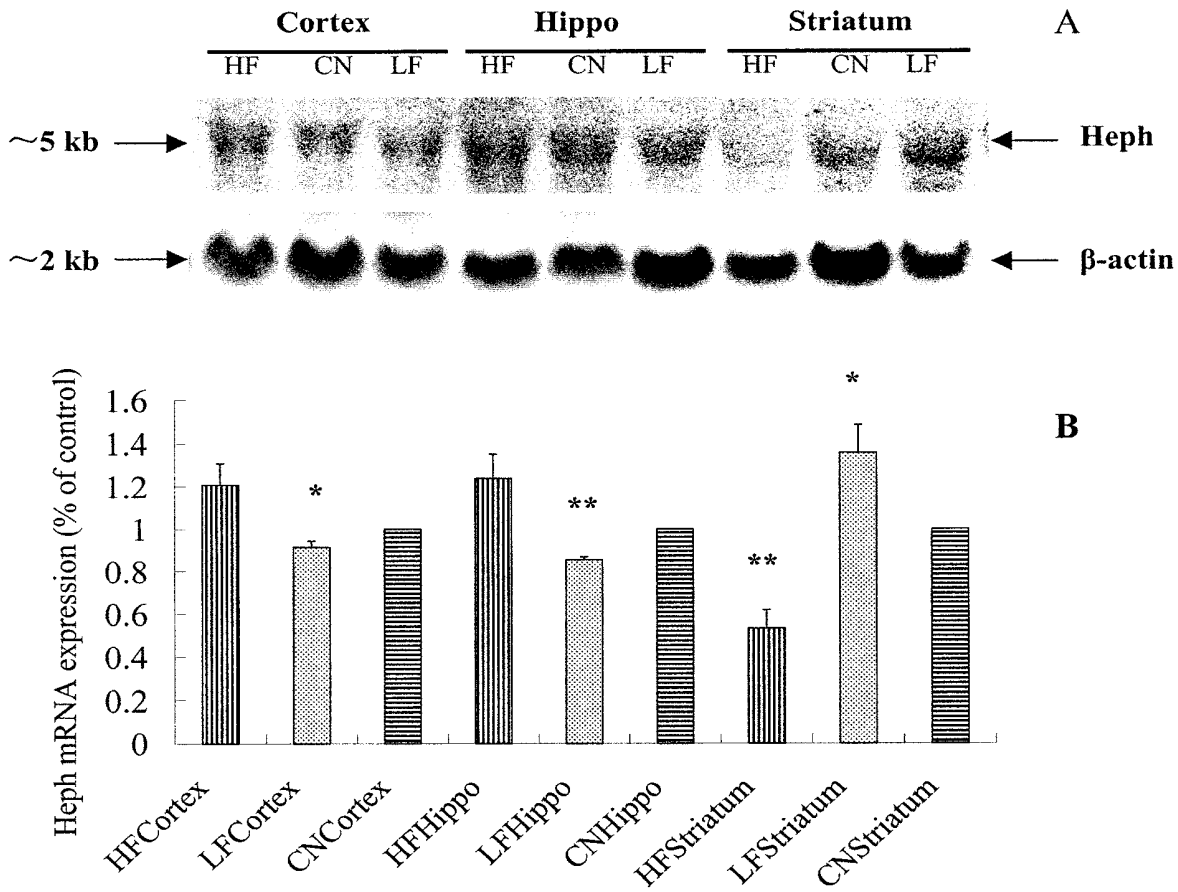

Figure 4-7. Effect of brain iron status on the expression of Hephaestin (Heph) mRNA in the cortex, hippocampus (Hippo), striatum and substantia nigra (SNigra). The Northern blot was hybridized with randomly primed ^{32}P-labeled probe for Heph and exposed to phosphor screen for 12 h for image analysis. To confirm equal loading of RNA in each lane, each blot was rehybridized with ^{32}P-labeled probe for β-actin. **A:** band intensities for ~5 kb and ~2 kb transcripts of Heph and β-actin, respectively. **B:** radioactivity in bands for Heph was quantified using ImageQuant software (Molecular Dynamics) and normalized to values obtained for β-actin and compared with (%) normal diet rats. Data are presented as means ± SEM from 3 independent experiments. *P<0.05, **P<0.01 vs. control.

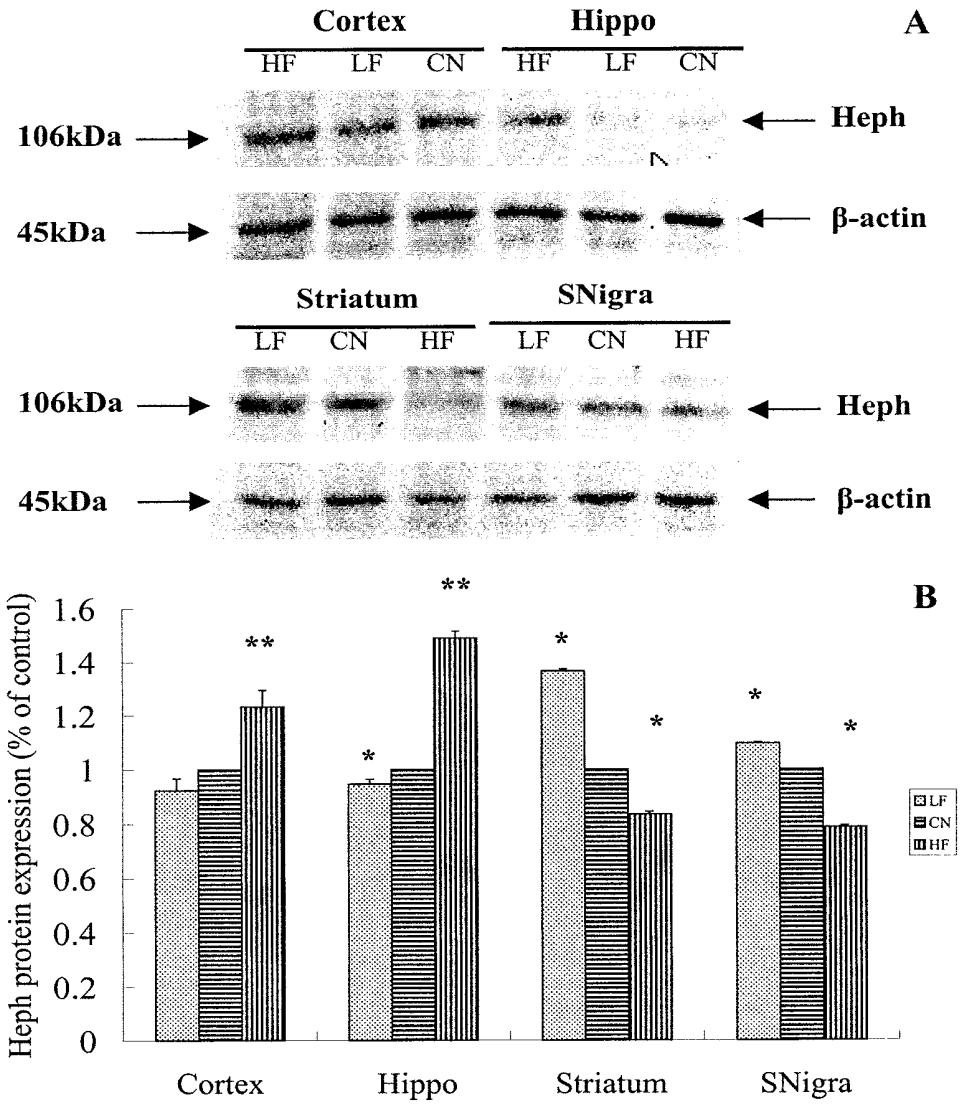

Figure 4-8. Effect iron status on hephaestin (Heph) protein synthesis in the cortex, hippocampus (Hippo), striatum and substantia nigra (SNigra) of normal (CN), iron-deficient (LF) and iron-overloaded (HF) rats. The tissue samples were treated as described in Methods. Western blots were performed as described in Materials and Methods. A representative sample is showed in **A**, The *Mr* of ~106 kDa Heph protein and ~45 kDa β-actin protein appear as a single band on each gel. **B:** The results were normalized for β-actin and expressed as percentage of normal levels. The data are the means ± SEM of 5 or 6 samples. **P*<0.05, ***P*<0.01 vs. control.

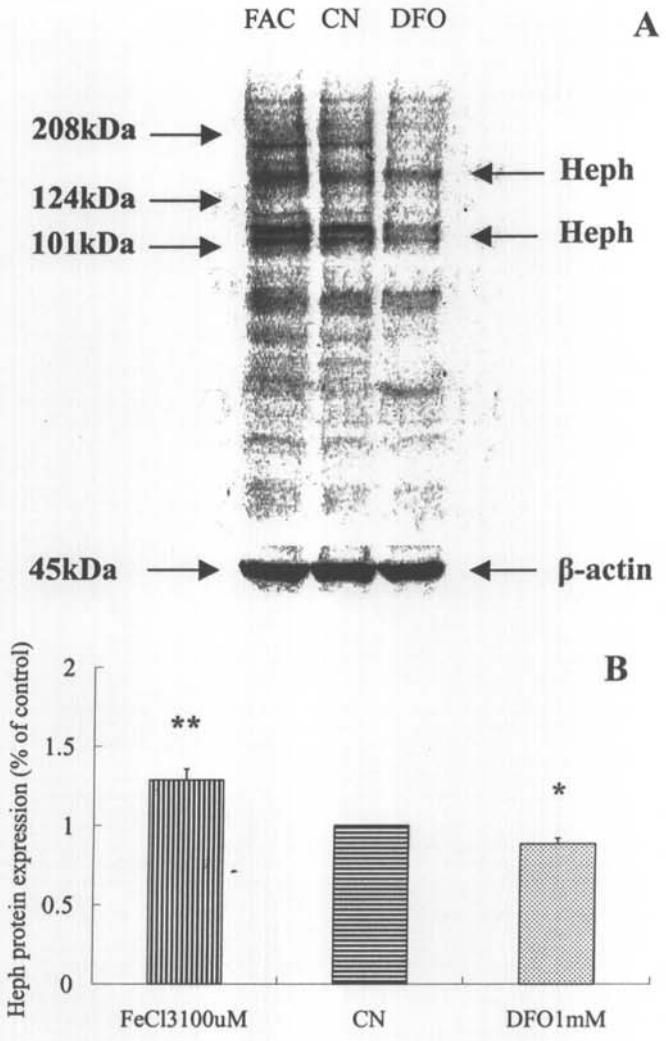

Figure 4-9. Effect of the iron status on hephaestin (Heph) protein expression in primary astrocyte. Western blots were performed as described in Materials and Methods. **A:** A representative sample is showed: a protein band with molecular mass ~106 kDa reacted strongly with the anti-Heph antibody, but one with molecular mass ~155 kDa reacted only slightly with the anti-Heph antibody. The Mr ~45 kDa of single band of β-actin protein also appeared on each gel. **B:** The results were normalized for β-actin and expressed as percentage of control levels. The data are presented as the means ± SEM of 3 independent experiments. **P*<0.05, ***P*<0.01 vs. control.

CHAPTER 5

REGULATION OF CERULOPLASMIN GENE EXPRESSION BY IRON STATUS AND THE EFFECT OF CERULOPLASMIN ON IRON UPTAKE IN C6 GLIOMA CELLS

5.1 ABSTRACT

The experiments of this chapter were designed to investigate the regulation of CP expression *in vitro* by iron status, and the effect of the CP on iron transport in brain cells. *In vivo*, results showed that iron status had no or very little effect on CP gene expression. This study suggests that DFO and 10mM BP increased CP protein synthesis and $FeCl_3$ depressed its synthesis *in vitro* although iron status had no effect on CP mRNA expression *in vivo*. In comparison, $FeCl_3$ decreased and DFO increased both the TfR mRNA and protein. This result implies that the regulation of CP by iron status is at a post-transcriptional level in C6 glioma cells. Our previous data identified that CP enhanced iron uptake in BT325 cell at the concentration of serum level (300 μg/ml); this study supported the role of CP on iron uptake at the CSF concentration (about 2 μg/ml). In the present study, however, we found GPI-CP did not have any influence on iron uptake and release in C6 glioma cells. Based on the findings of this study and chapters 3, 4, it appeared that the regulation of CP and

Heph by iron status in the brain was more complex.

KEY WORDS

Cerulopalsmin, Gene Expression, Iron, Iron Uptake, Iron Release, Transferrin Receptor, DFO, BP

5.2 INTRODUCTION

Ceruloplasmin (CP) is an abundant serum α_2–glycoprotein and consists of a single polypeptide chain of 1046 amino acid residues. CP is mainly synthesized in hepatocytes. Recently, GPI-anchored CP was demonstrated in rat brain, which is mainly expressed by astrocytes (Patel and David, 1997; Salzer et al., 1998; Patel et al., 2000). Human GPI-CP was also cloned recently (Hellman et al., 2002). Humans with mutations of the CP gene (aceruloplasminemia) show iron accumulation in various organs, including the liver and brain, which is noticeable by the age of 45-55 years (Miyajima et al., 1987; Yoshida et al., 1995). CP null mutant mice also show accumulation of iron in the liver and CNS (Harris et al., 1999; Patel et al., 2002). However, despite years of effort, the functions of CP in brain iron metabolism have not been determined. In a previous study (Qian et al., 2001a), we investigated the effect of human CP on iron transport in brain cells using BT325 cells, a glioblastoma cell line. That study was initiated to elucidate the mechanism of CP-mediated iron release from brain cells; however, negative results were obtained. The addition of CP, either at low (25 μg/ml) or high (300 μg/ml) concentrations, did not lead to significant change in iron release from iron-loaded BT325 cells. Although

apotransferrin (apoTf) was shown to have a role in iron release from the cells, the effect of apoTf was not significantly affected by the addition of different concentrations of CP. When the cells were incubated with 1μM $^{59}Fe^{2+}$ in the presence of varying amounts of CP for 30 min at 37℃, CP was found to increase iron uptake. Furthermore, CP was shown to significantly promote iron uptake in not only iron-sufficient but also iron-deficient cells. There was no significant difference in the effects of CP on iron uptake between iron-sufficient and -deficient cells. These results showed that CP had a role in iron uptake rather than release in BT325 cells *in vitro*, similar findings were also reported for HepG2 (Mukhopadhyay et al., 1998) and K-562 cells (Attieh et al., 1999). We also investigated the effect of ferroxidase activity of hCP and different species of ceruloplasmins on CP-mediated iron uptake by the cells (Xie et al., 2002). The cells were incubated for 30 min at 37℃ with 1 μM $^{59}Fe^{2+}$ with or without 150 μg/ml of the untreated and the ferroxidase-defective hCPs (apohCP and heat-inactivated hCP) or different species of CPs (human CP, rabbit CP and bovine CP). The untreated hCP induced a significant increase in iron uptake by BT325 cells, while ferroxidase-defective hCPs with (heat-inactivated hCP) or without cooper ions (apohCP) had no such effect. The untreated hCP significantly increased internalized iron but not membrane-bound iron, implying that hCP stimulated iron entry into the cell rather than increased extracellular binding of iron to the cell surface. All species of CPs could promote iron uptake by the cells and the difference in degree of stimulation among them was insignificant. These results suggest that ferroxidase activity of hCP is essential for hCP-mediated iron uptake process and that CP-stimulated iron uptake is not associated with copper ions in the protein. In addition, the effect of CP on iron uptake by BT325 cells is not species specific. The concentration of soluble CP in the CSF, which is produced by the

choroids plexus and astrocytes, is only about 2 μg/ml (Loeffler et al., 1994). In the present study, we investigated the effect of low concentrations of CP (0, 2, 4, 8 μg/ml) on iron flux in normal, iron-sufficient and iron-deficient brain cells using C6 cells, a rat glioma cell line. Considering the presence of GPI-CP in the C6 glioma cells (Patel and David, 1997), we also determine the role of GPI-CP on the iron uptake.

The regulation of CP gene expression by iron was different in cell culture and in the whole–animal model. In HepG2 and K562 cells in culture (Mukhopadhyay et al., 1998; Attieh et al., 1999), CP expression was enhanced by iron deficiency and suppressed by iron loading. Enhanced CP expression in cultured cells by iron deficiency could be due to the activation of hypoxia-inducible factor (HIF) (Mukhopadhyay et al., 1998; Attieh et al., 1999). It is now clear that the HIF-1α and HIF-1β bind to the HRE of CP gene promoter (Mukhopadhyay et al., 2000). However, there is very little evidence for the regulation of CP gene expression by the iron status in brain cells. In this study, we investigated whether the synthesis of CP was regulated by cellular iron content in C6 glioma cells.

5.3 MATERIALS AND METHODS

5.3.1 Materials

Please refer to chapters 2 and 3.

5.3.2 Methods

5.3.2.1 Cell Culture

Please refer to chapters 2.

When cells reached about 65-70% confluence, the experiments were initiated by changing the medium followed by addition of various concentration bathophenanthroline disulfonate (BP), desferrioxamine (DFO) or iron ($FeCl_3$ or FAC, FAS) as indicated in the figure legends.

5.3.2.2 Immunocytochemistry

C6 cells were plated on a poly-lysine (Sigma, MO, USA) coated glass slide. When they reached about 70-80% confluence, the cells were fixed with 4% paraformaldehyde in 0.1M phosphate buffer (pH 7.4) for 10 min at RT. Following this fixation the cells were permeabilized with 1% Triton X-100 in PBS for 10 min, with further PBS washed afterwards. In order to quench endogenous peroxidase activity, the fixed cells were incubated in a 0.5% solution of hydrogen peroxide in PBS (0.15 M NaCl, and 0.01 M sodium phosphate buffer, pH7.3) for 10 min. Cells were washed in PBS and then incubated in horse serum block for 20 min to prevent nonspecific binding. Cells were washed in PBS and then incubated with 1:50 dilution of the primary purified mouse anti CP IgG1 (BD Transduction Laboratories, BD Biosciences, USA) for 1 hour at room temperature. The source of immunogen sequence is from 233 to 355 of mouse CP, that is 94.3% conserved in rat.

Subsequently, cells were processed using the ABC kit (Vector, Burlingame, CA, USA) and developed using a DAB kit (Vector, Burlingame, CA, USA) according to the manufacturer's instructions. Finally, the cells were dehydrated using 70%, 95% and 100% ethanol and xylene. The slides were cover-slipped and viewed under a Nikon E400 light microscope. Images were obtained using a 40× lens, numerical aperture (NA) 0.75.

5.3.2.3 RNA Purification, Generation of Specific Probes, and Northern Blot Assay

Total RNA isolated from the C6 cells was treated with 1 mM BP, 0.5 mM DFO or 0.1 mM $FeCl_3$ for 16 hours using Trizol reagent (Invitrogen, CA) according to the manufacturer's instructions. Thirty micrograms of RNA from each treatment were electrophoresed on 1% agarose formaldehyde gels, transferred overnight to Hybond-N (Amersham Pharmacia Biotech, England) membranes with 10× standard saline citrate (SSC), and fixed to the membrane using a UV cross-linker (Fisher). The blots were prehybridized at 65℃ in ExpressHyb hybridization solution (Clontech, CA, USA) for 1 hour, then hybridized overnight at 65℃ in the same solution containing ^{32}P-labeled probes using the Prime-a-Gene labeling system (Promega, WI, USA) and [α-^{32}P]dCTP (Amersham Biosciences) as per manufacturer's instructions, the sequence of probes corresponding to positions 1133-1518 of CP (Genbank, L33869) and 5-574 of TfR (Genbank, M58040). After three 5-10 min washes with 2× SSC containing 0.05% sodium dodecyl sulfate (SDS) at room temperature, the blots were washed several times in 0.1× SSC, 0.1% SDS with continuous shaking at 50-60℃ for 10 min. Radioactivity was detected by Phosphorimager and quantified

using ImageQuant software (Molecular Dynamics, Sunnyvale, CA). For normalization, the blot was stripped and reprobed with β-actin probe corresponding to position 474-736 of rat β-actin (Genbank, NM031144). The results were expressed as the ratio to β-actin.

5.3.2.4 Western Blot

Please refer to chapters 2 and 3.

For sample preparation, the control and BP, DFO, $FeCl_3$ treated cells (the concentration as indicated in the legends for 16 hours) were washed with ice-cold PBS (invitrogen, CA), lysed with Tris buffer containing 1% Triton X-100, 0.1% SDS, 1 mM PMSF and protease inhibitors (pepstatin 1μg/ml, aprotinin 1μg/ml, leupeptin 1μg/ml), and then sonicated using Soniprep 150 (MSE Scientific Instruments, England) 3×10 seconds. The mixture was centrifuged for 15 min in 10,000g at 4℃. Protein content of the supernatant was determined using the Bradford assay kit (Bio-Rad, Hercules, CA). Forty micrograms of total protein were diluted in 2×sample buffer (50 mM Tris, pH 6.8, 2% SDS, 10% glycerol, 0.1% bromophenol blue, and 5% β-mercaptoethanol) and heated for 5 min at 95℃ before SDS-PAGE on a 7.5% gel.

5.3.2.5 Calcein Loading of the Cells and Iron Flux Assay

Calcein-AM (CA-AM, Molecular Probes, Eugene, OR, USA) is a membrane-permeate, nonfluorescent molecule that becomes fluorescent upon

intracellular cleavage to calcein (CA, membrane-impermeate) by cytoplasmic esterases (Breuer et al., 1995a). In cell-free system, calcein binds to both iron (II) and iron (III) with stability constants of 10^{14} and 10^{24}/mol, respectively, which results in quenching its fluorescence (Breuer et al., 1995b). CA is insensitive to calcium and magnesium ions up to 1 mM at physiological pH. At the same time, the intracellular concentration of other CA-binding molecules is very low, and pH in the range of 6.5–7.5 has only a minor effect on CA fluorescence. All these properties indicate that intracellular CA senses cell iron dynamically and transmits information regarding changes in the cellular labile iron pool (LIP) levels (Epsztejn et al., 1997; Cabiscol et al., 2002). Thus, the appearance of a fluorescent signal is monitored continuously during incubation of a reaction mixture consisting of preloaded CA-AM cells in HEPES-buffered saline (10 mM HEPES, 150 mM NaCl, pH 7.0).

Calcein loading of the C6 cells and iron flux assay was performed according to Picard et al (Picard et al., 2000) and Barnabe et al (Barnabe et al., 2002). C6 cells were grown to 65-70% confluence, made iron deficient by incubation with 1 mM BP and 1 mM DFO, and made iron sufficient by incubation with 50 μM FAC + 50 μM FAS for 16 hours. When the cells were grown to 80% confluence, they were treated with 600 μU/ml PI-PLC for 60 min at 37℃. Just prior to measurements, the cells were washed three times with medium and incubated with 125 μM CA-AM in serum-free medium, After incubation for 10 min at 37℃, excess calcein-AM was removed, the cells were washed twice with Hank's balance salt solution (HBSS, invitrogen, CA) at 37℃, and then maintained in HEPES buffer solution. For the kinetic fluorescence measurements on the BMG (Durham, NC, USA), a Fluostar Galaxy fluorescence plate reader (λ_{ex} of 485 nm, λ_{em} of 520 nm, 37℃) equipped with

excitation and emission probes was directed to the bottom of the plate. 100 μl of calcein-loaded cell suspension (approximately 6×10^5 cells) and 100 μl HEPES was added to a 96-well plate, and initial baseline fluorescence intensity data was collected. Then 2 μM ferrous ammonium sulfate (FAS) or 30 μg/ml apoTf with/without (2, 4, 8 μM) CP was added (indicated as Figure caption) by pipetting 2 μl of the respective stock aqueous solutions into the wells and gently mixing. The changes of calcein fluorescence were measured in every 5min for 30 min at 37℃. Data were normalized to the steady-state values of fluorescence before addition of the FAS, apoTf and CP.

5.3.3 Statistical Analysis

Statistical evaluation of data was performed by One-Way ANOVA. When differences were detected ($P < 0.05$), means were tested with the Student-Newman-Keuls test for differences between individual means. Data are presented as means ± SEM.

5.4 RESULTS

5.4.1 Localization of Ceruloplasmin Protein in C6 Glioma Cells

GPI-anchored CP is mainly formed in brain astrocytes. We stained C6 cells grown on poly-l-lysine coated coverslips with CP antibodies to determine CP protein by the immunocytochemistry method. Strong immunoactive staining for CP (Fig 5-1) was

observed in the membranes of C6 cells.

5.4.2 Expression of Transferrin Receptor mRNA and Protein in C6 Glioma Cells with Different Iron Status

Expression of the transferrin receptor (TfR) is controlled essentially by post-transcriptional regulation, which is mediated by the interaction between iron regulatory proteins (IRPs) and iron-responsive elements (IREs) located in the 3'-untranslated region (UTR) of TfR mRNA. The classic regulation of receptor expression is accomplished by controlling the level of TfR mRNA (Haile, 1999; Ponka and Lok, 1999). Recnet study demonstrated that the regulation of TfR expression by iron status exists not only on the post-transcriptional level but also on the protein translation level (Tong et al., 2002). In this study, regulation of TfR mRNA expression by different iron status was examined. After treating the C6 glioma cells with DFO and BP for 16 hours, the mRNA increased 9 and 6 times to the control respectively ($P<0.01$, Fig 5-2A, 5-2B). Iron overload suppressed the expression of TfR mRNA about 50% ($P<0.01$, Fig 5-2A, 5-2B). Similarly, regulation of the TfR protein synthesis by iron status was investigated. Protein levels are increased by DFO incubation and decreased by iron overload ($P<0.05$, Fig 5-2C, 5-2D). However, no significant increase by BP incubation was noted ($P>0.05$, Fig 5-2C, 5-2D).

5.4.3 Effect of Iron Status on Expression of Ceruloplasmin mRNA and Protein in C6 Glioma Cells

In our experiments, the TfR mRNA level increased remarkly in the iron deficient C6 glioma cells when treated with the DFO and BP, and decreased in iron overload cells incubated with $FeCl_3$. But Northern blot analysis showed no significant change in the expression of CP mRNA (Fig 5-3). Representative blots showing one mRNA band with expected molecular mass ~3.7 kb of CP are presented in Fig 5-3A. To determine the effect of iron on the synthesis of CP protein, the C6 glioma cells were incubated with the 0, 5, 10 20, 40,100 μM $FeCl_3$ for 16 hours. The cells protein was then extracted for Western blot analysis. A single major band (~150 kDa) was observed with CP antibody that is in good agreement with the expected molecular weight (Fig 5-4A). After being normalize to β-actin, the CP protein was found to decrease with significant induction occurring at concentrations of 10, 20, 40 100 μM (Fig 5-4B). This decrease is iron concentration dependent. Similarly, the regulation of CP protein synthesis by iron deficiency was investigated. Protein levels of CP were not significantly affected by treated with low concentration BP. But 10 μM BP induced an increase in the CP protein level. CP protein levels in C6 glioma cells were significantly increased by incubation with ferric ion chelator DFO (0.3, 0.5, 1.0, 3.0 μM). The results of statistical evaluation showed there was no significant difference between these concentrations.

5.4.4 Effect of Ceruloplasmin on C6 Glioma Cells Iron (II) Uptake

We utilized the fluorescent probe calcein to study the effect of CP on iron uptake in C6 glioma cells. In order to confirm that the calcein method provides a valid measure of ferrous uptake, a base line signal was obtained for normal and no ferrous added cells. This indicated fluorescence was steady in the 30 min recording. After

stabilization of the fluorescence signal, 2 μM FAS was added to normal iron status C6 glioma cells in the absence or presence of varying amounts of CP (2, 4, 8 μg/ml) at 37 ℃, resulting in a slow, time-dependent quenching of intracellular fluorescence. The quenching rate was the fastest within the first 5 min (about 5% of initial fluorescence), and slowed to about 12% of initial fluorescence after 30min. There was no significant difference observed between the total quenching in the control (no CP) group and in groups with differing CP concentrations (P>0.05, Fig 5-5A). The findings imply that low concentrations CP were not able to increase the iron uptake in C6 glioma cells.

We also investigated the effect of CP on iron uptake by iron-deficient and PI-PLC treated brain cells. Iron deficient C6 glioma cells were prepared by incubation with 1 mM Fe^{2+} chelator BP and 1 mM Fe^{3+} chelator DFO for 16 hours in serum-free DMEM medium at 37℃. Before this preparation, the effect of these iron chelators on the growth of C6 glioma cells was investigated by MTT assay. It was found that incubation in 1 mM BP and 1 mM DFO for 12 hours did not significantly inhibit the cell growth (data not presented). Therefore these incubation conditions were used in the preparation. In order to detect the role of the GPI-anchored CP, we removed the GPI-anchored CP from the cell membrane by incubation in 600 μU/ml PI-PLC at 37 ℃ for 30 min. 100 μl of calcein-loaded cell suspension (approximately 6×10^5 cells) and 100 μl HEPES was added to a 96-well plate, and the initial baseline fluorescence intensity data were collected. 2 μM FAS was added to the cells in the absence or presence of varying amounts of CP (2, 4, 8 μg/ml) incubated at 37℃. The quenching of fluorescence was measured at indicated times. For the PI-PLC treated cells, the GPI-anchored CP did not significantly change fluorescence quenching (P>0.05).

This suggests that GPI-CP had no effect on iron uptake from the C6 glioma cells under the experimental conditions. For the iron deficient cells, a significant quenching of fluorescence was observed with the addition of 4, 8 μg/ml CP at 5, 10, 15, 20, 25 min ($P<0.05$) and 30 min (18.8 ± 0.67%; 18.0 ± 0.33%, $P<0.01$) as compared to the control (12.9 ± 0.7%). The addition of 2 μg/ml CP group was found to quench the fluorescence significantly after 10 min. These results showed that low concentration of CP has a role in iron uptake by iron deficient C6 glioma cells (Fig 5-5B).

5.4.5 Effect of Ceruloplasmin on Iron Release Induced by Apo-transferrin from C6 Glioma Cells

Our previous study showed that the addition of different concentrations of CP (25, 75, 150 and 300 μg/ml) did not significantly change the total iron of BT325 cells (Qian et al., 2001a). In the present study, similar results were observed at low concentrations of CP (2, 4, 8 μg/ml) in C6 glioma cells (data not shown). After incubating the cells in apo-transferrin (apo-Tf, 30 μg/ml) for 30 min, the intensity of fluorescence was increased to a high degree (112.4 ± 1.1% of control) in the iron-sufficient group than fluorescence (105.5 ± 0.03%) in the normal iron status group (Fig 5-6). This suggests that apo-Tf affects iron release from iron-sufficient cells. The combined effect of GPI-CP or CP with apo-Tf on iron release from C6 glioma cells was studied. Before the experiments cells were preloaded with 50 μM FAC + 50 μM FAS for 16 hours at 37℃ (Fig 5-6B) or without (Fig 5-6A). The cells were then loaded with 0.125 μM calcein-AM for 10 min and washed 3 times with Hank's buffer solution. After the initial baseline fluorescence intensity data was

collected, varying amounts of human CP (0, 2, 4, 8 μg/ml) with apoTf 30 μg/ml was added by pipetting 2 μl of stock CP and apoTf solution into a 96-well plate and gently mixed. The dequenching of the cytoplasmic calcein by iron release was measured. Exposure of calcein-loaded normal iron status C6 glioma cells to the 30 μg/ml apo-Tf with or without human CP (0, 2, 4, 8 μg/ml) caused weak changes of the dequenching signal compared to the control (30 μg/ml apo-Tf and no CP), though the fluorescence increased about 5% compared to the initial values (before adding the apo-Tf and CP) in each group (Fig 5-6A). For the iron sufficient cells, the 30μg/ml apo-Tf induced marked dequenching of fluorescence but the role of low concentrations CP was similar to that in the normal iron status cells (Fig 5-6B). The findings showed that the low concentrations of CP had no effect on iron release induced by apo-Tf both in normal iron status cells and iron-sufficient cells. No difference was observed in the dequenching of fluorescence in the PI-PLC treated group compared with the control group.

5.5 DISCUSSION

There is very little reported data about the regulation of the CP gene by iron status in brain cells *in vivo* and *in vitro*. In the chapter 3, we investigated the effect of dietary iron on iron status of the rat brain, and found it had no significant effect on expression of the CP mRNA in the cortex, hippocampus, striatum and substantia nigra. CP protein synthesis was significant decrease only in the substantia nigra of the iron-deficient group and increased in the iron-overload group. The results indicate that the regulation of CP is related not only to the total iron level but also to the indices of oxidative stress. Increased expression of CP could help protect the

retina from oxidative stress. Since the retina is exposed to large amounts of ROS produced because of its exposure to focused light, it may require higher levels of antioxidants to combat oxidative stress; the higher CP protein levels was reported in normal retina than in the brain (Chen et al., 2003b). The abundant expression of GPI-CP on the surface of leptomeningeal cells also suggests that the CP protein level is regulated according to the antioxidant defense along the surface of the postnatal CNS, thereby detoxifying the cerebrospinal fluid (CSF) (Mittal et al., 2003). Our findings of lower levels of CP in the substantia nigra of iron deficient rats and higher levels of CP in the substantia nigra of iron sufficient rats are consistent with the regulation of CP by oxidative stress. The regulation of CP gene expression by iron status has been previously reported. Serum CP increases during dietary iron deficiency anemia *in vivo* (Venakteshwara Rao et al., 1975; Iwanska and Strusinska, 1978), and the secreted CP increases in hepatocellular carcinoma line HepG2 cells in iron deficiency *in vitro* (Mukhopadhyay et al., 1998; Mukhopadhyay et al., 2000), suggesting that the iron deficiency upregulated the CP gene expression. It is now clear that the CP promoter contains a hypoxia-inducible factor (HIF)-responsive element. HIF-1 is a helix–loop–helix factor that binds to a number of genes presenting a hypoxia responsive element (HRE) in their regulatory sequence. Hypoxia, or iron chelation are able to induce an increase of HIF-1 which in turn leads to an enhanced transcription of the genes carrying the HRE regulatory sequence and to increased levels of the corresponding proteins (Wang et al., 1995a; Mukhopadhyay et al., 2000). However, recent studies *in vitro* suggest that iron status has little or no influence on either the level of plasma CP, or on the expression of its mRNA by the liver (Huang and Shaw, 2002; Strube et al., 2002; Tran et al., 2002). This disparity may be due to very low levels of iron achievable only in culture and

not *in vivo* (Tran et al., 2002). In the present study, the incubation of C6 glioma cells with 1 mM ferrous chelator BP or 0.5 mM ferric chelator DFO for 16 hours had no effect on CP mRNA expression but increased the TfR mRNA for 6 or 9 times. Yet incubation of 0.1 mM $FeCl_3$ for 16 hours did not depress CP mRNA expression although TfR mRNA was down-regulated by about 0.5 times compare to control. It is worth noting, however, that there appear to be differences in CP protein synthesis relating to iron states. The levels of CP protein were decreased by a maximal of about 25% in C6 glioma cells treated with excess iron for 16 hours. The iron chelator BP did not affect the CP protein synthesis at low concentrations, but 10 mM Bp induced CP protein to increase to 143% of control. 0.3 mM DFO also significantly increased CP protein synthesis. Consistent with our findings, the CP levels increased in the HFRT +/- mice brain compared to the wild-type controls (Thompson et al., 2003). Such change was not due to an increase the amount of mRNA, but probably due to an increase the CP protein synthesis by the choroids plexus (Thompson et al., 2003). Taken together with results from our study of modulation of CP gene expression in rat brain, this indicates the regulation of CP by iron status occurs at the post-transcriptional level. However, the effect of iron status may be masked by other factors such as oxidative stress.

CP ferroxidase activity catalyzes the oxidation of Fe^{2+} to Fe^{3+}, accelerating iron incorporation into apoTf, which may induce cellular iron release (Osaki et al., 1966). Studies on patients with aceruloplasminemia (Harris et al., 1995; Yoshida et al., 1995; Takahashi et al., 1996) and animal model of aceruloplasminemia (Harris et al., 1999; Patel et al., 2002) support this possibility. However, the accumulated evidence shows that addition of CP to cells *in vitro* results in enhanced uptake rather then in

release of non-Tf iron (Mukhopadhyay et al., 1998; Attieh et al., 1999). Our studies show the addition of CP induces the iron uptake in brain BT325 cells. The concentration of CP 30 μg/ml or 300 μg/ml was shown to significantly promote iron uptake in iron-sufficient and iron-deficient brain glioma cells (Qian et al., 2001a). The effect of CP on iron uptake by BT325 cells is not species specific (Xie et al., 2002). CP concentration is about 2 μg/ml in the CSF. In the present study, results showed that the addition of 2, 4 or 8 μg/ml CP did not lead to any significant change in iron release from normal iron or iron-loaded C6 glioma cells. Although apoTf has a significant effect on iron release from iron-loaded cells, the effect of apoTf was not significantly influenced by the addition of different concentrations of CP. These findings were similar to those observed for high concentrations of CP in BT325 cells (Qian et al., 2001a), in HepG2 (Mukhopadhyay et al., 1998) and in K-562 cells (Attieh et al., 1999), suggesting that CP does not affect iron release in either normal iron or iron-loaded C6 glioma cells at the similar concentration in CSF. Furthermore, the addition of 2, 4 or 8 μg/ml CP was shown to increase iron uptake in iron-deficient cells but did not alter iron uptake in normal iron cells. These results were partly similar to our previous findings (Qian et al., 2001a).

The concentration of soluble CP is about 1-2 μg/ml in the human CSF, and likely to contribute only minimally to the ferroxidase activity and iron transport in the CNS. We show here that a low concentration of CP increases the iron influx in iron-deficient C6 glioma cells. This implies the effect of low concentration of CP on the iron metabolism of neuronal cells in the CSF is not been ignored. CP had no effect on iron uptake or release in normal iron cells, indicating its physiological function is to protect from damage, and has little role on iron metabolism in the CSF.

In the CNS, GPI-CP is in astrocytes (Patel and David, 1997; Patel et al., 2000) is essential for iron efflux and not involved in regulating iron influx (Jeong and David, 2003). C6 glioma cells were found to express the CP mRNA and protein. These cells were therefore used to study the effect of GPI-CP on iron uptake. After C6 glioma cells were treated with PI-PLC to eliminate the GPI-CP, no difference was observed in the iron uptake of iron-deficient cells compared with control, and in the iron release of iron-sufficient cells compare with control. The controversial results might be partly due to the difference of cell types used, the damage of PI-PLC, or the time of experiment and other experimental conditions.

Our data show that the physiological concentration CP in CSF has no role in iron release in C6 glioma cells, whether in the iron-overload group or normal iron group. However, CP was found to have a role in iron uptake in iron deficient C6 glioma cells. It is clearly too early to infer from these results that the physiological concentration of CP has a role in cellular iron uptake in the brain and no role in cellular iron release in the brain *in vivo*. However, data from the present and previous studies (Mukhopadhyay et al., 1998; Attieh et al., 1999; Qian et al., 2001a; Xie et al., 2002) at least imply that the traditional view on the role of CP in brain iron metabolism should be reconsidered. In the light of the evidence reported recently, it is highly likely that CP plays a role not only in iron release but also in iron uptake in brain cells. CP in the brain is not expressed in all astrocytes but rather in a unique subpopulation of those glial cells surrounding the microvasculature (Klomp et al., 1996; Klomp and Gitlin, 1996). CP located on these astrocytes is ideally positioned to oxidize the highly toxic Fe^{2+} to Fe^{3+}, limiting the Fe^{2+} concentration in the CSF. This unique location implies that CP is critical for the oxidation of Fe^{2+} to Fe^{3+}, after

it crosses the abluminal membrane of the blood–brain barrier (BBB), to be oxidized to Fe^{3+}, which subsequently bound to transport carriers and be rapidly acquired by brain cells. The mechanisms of iron transport across the BBB are very important for iron balance in the brain. The role of CP increases iron efflux from the cytoplasm of brain capillary endothelial cells to the CSF and interstitial fluid (IF) and then enhance iron uptake of the brain cells (Qian and Shen, 2001). Under physiological conditions, CP has no effect on iron release on astrocytes. But if CP is not a major iron release protein in the brain, what are the key molecules in this process? Recently, two new "iron release proteins", FP1 (Donovan et al., 2000) and Heph (Vulpe et al., 1999), have been identified as being necessary for the export of iron from enterocytes into the blood stream. It has also been suggested that FP1 and Heph may work together in the absorptive enterocyte and that FP1 may work with CP to load iron to Tf (Qian and Shen, 2001). Our previous study has shown that the FP1 is expressed in rat brain (Jiang et al., 2002). In chapter 4, our results indicated that Heph is expressed in the membrane of neurons, ependymal cells and microvasculature. It is possible that the FP1 and Heph play a major role in iron release from the cells in the brain under physiological conditions, but further investigation is needed to provide evidence of this role.

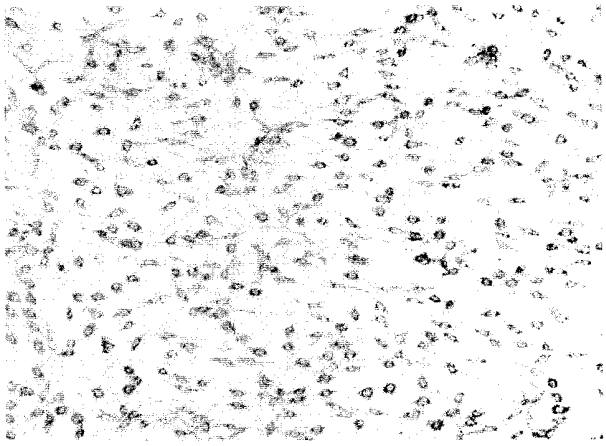

Figure 5-1. Immunocytochemical labeling for ceruloplasmin in C6 glioma cells. The cell surface localization of ceruloplasmin on C6 glioma cells was demonstrated by labeling live cultures with a purified mouse anti ceruloplasmin IgG1 antibody. Original magnifications: × 400.

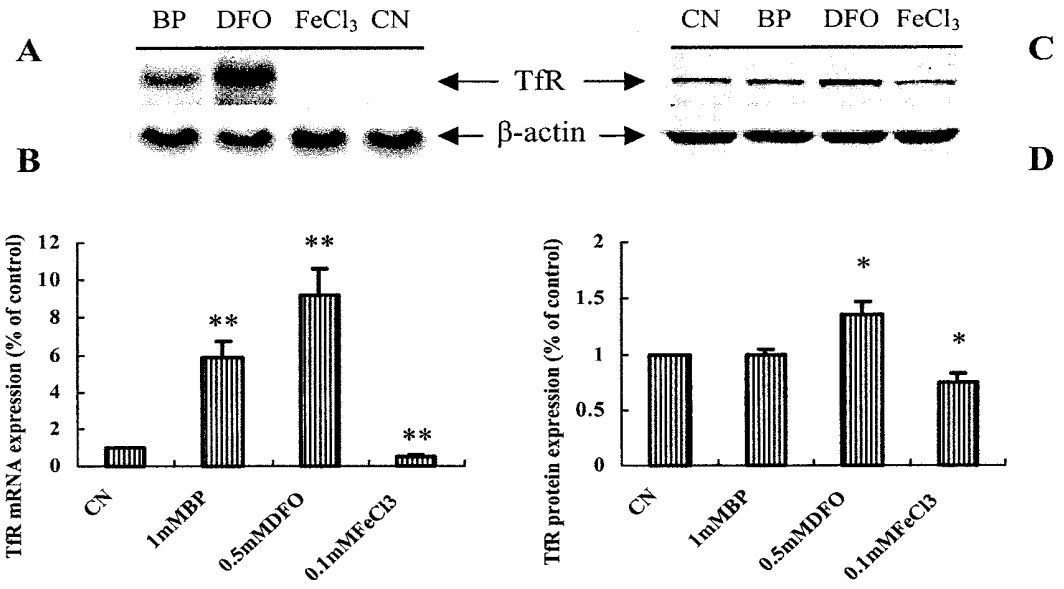

Figure 5-2. The regulation of TfR gene expression by iron states. C6 glioma cells were grown to 65-70% confluence and incubated with Fe^{2+} bathophenanthroline disulfonate (BP) chelator, Fe^{3+} chelator desferrioxamine (DFO) or $FeCl_3$. Northern blot and Western blot analyses were performed as described in Materials and Methods. To confirm equal loading of RNA and protein in each lane, each blot was probed with ^{32}P-labeled probe of β-actin and β-actin antibody. **A:** Band intensities for ~5kb and 2kb transcripts for TfR and β-actin. **C:** Band intensities for 90 kDa and 45 kDa bands for TfR and β-actin. TfR mRNA expression (**B**) and protein synthesis (**D**) values were normalized for β-actin. Data are means ± SEM as % control from 3 independent experiments. Different letters above data bars indicate that these groups are statistically different from each other: $*P < 0.05$, $**P < 0.01$ vs. control.

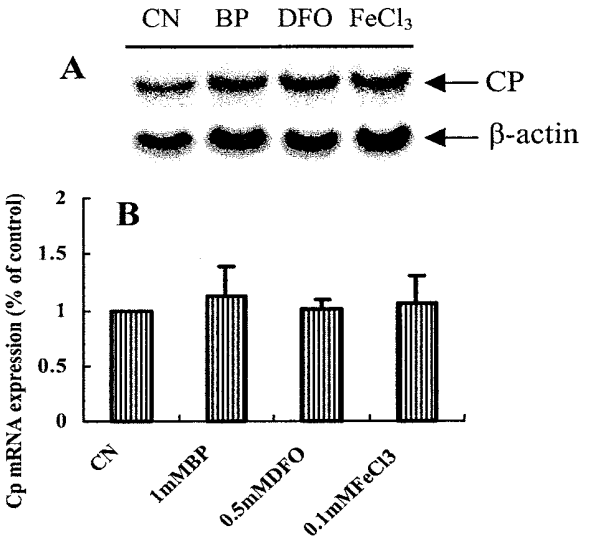

Figure 5-3. Regulation of CP mRNA by iron and iron chelators. C6 glioma cells were treated with 0.1 mM $FeCl_3$ or 1 mM BP or 0.5 mM DFO or with medium alone for 16 hours. Total RNA was harvested with Trizol regent, and equal amounts of total RNA (30 μg) were electrophoresed and transferred to Hybond-N^+ membrane as described in Materials and Methods. The Northern blot was hybridized with randomly primed ^{32}P-labeled probe for CP and exposed to a phosphor screen for 24 hours for image analysis. To confirm equal loading of RNA in each lane, each blot was rehybridized with ^{32}P-labeled probe for β-actin. Shown are band intensities for ~3.7 kb and ~2 kb transcripts for CP and β-actin (**A**). The radioactivity in bands for CP was quantified using ImageQuant software (Molecular Dynamics, Sunnyvale, CA) and normalized to values obtained for β-actin and expressed as percentage of control levels. Data are means ± SEM of 3 independent experiments (**B**).

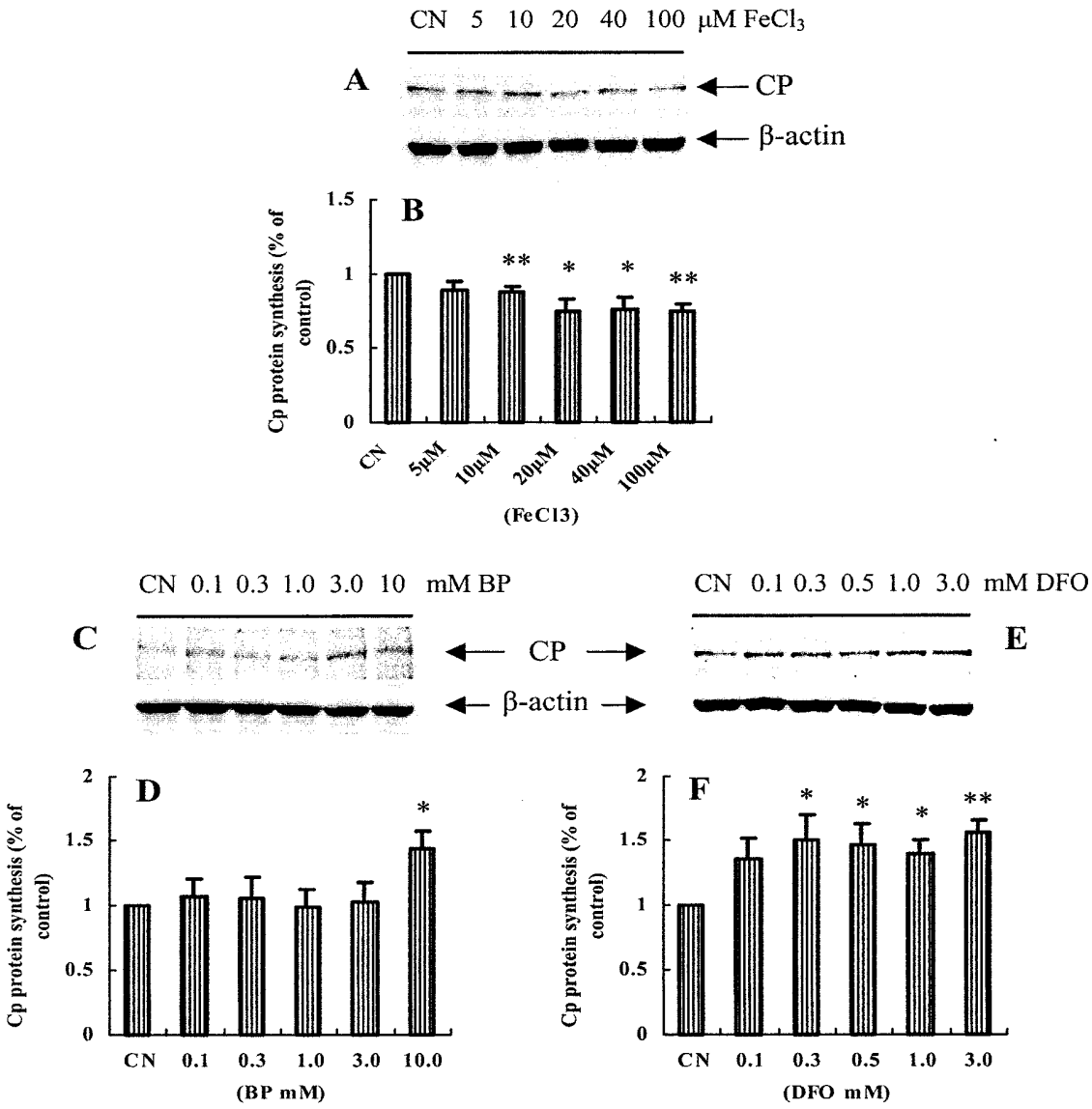

Figure 5-4. Regulation of CP synthesis by iron status. C6 glioma cells were treated with FeCl3 (A, B), BP (C, D) and DFO (E, F) for 16 hours in serum-free DMEM medium. Western blot annlysis was performed as described in Materials and Methods. The *Mr* of ~150 kDa for CP of a single band of CP appearing on each gel, the bands of β-actin on the gel correspond to the expected molecular weight (45 kDa). Values of CP protein synthesis were normalized for β-actin and expressed as % of control levels. Data represent means ± SEM from 3 independent experiments. The letters above data bars indicate that these groups are statistically different from control (*P<0.05, **P<0.01).

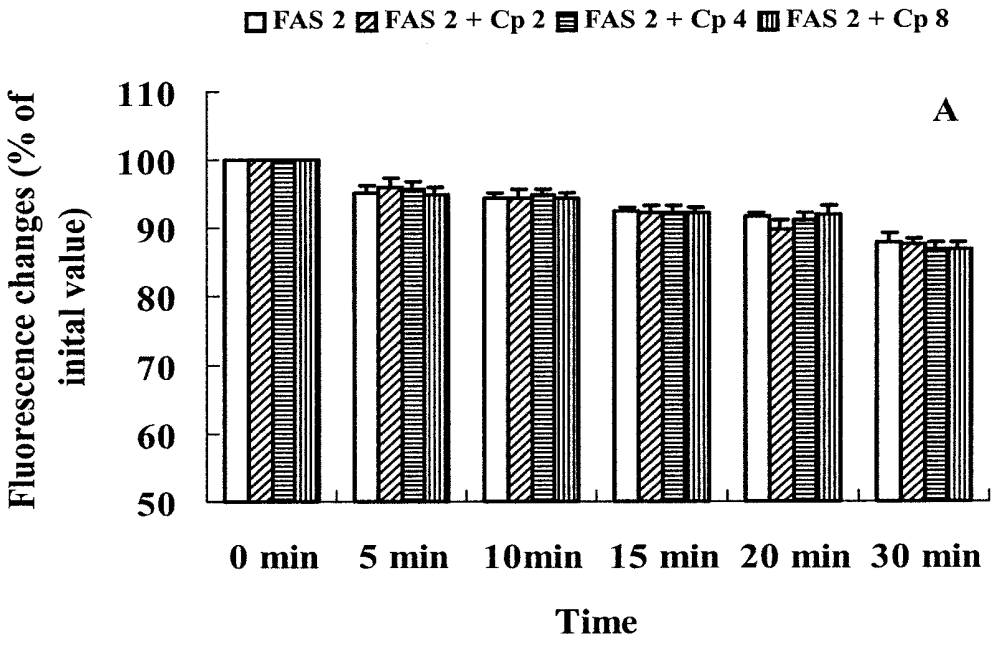
FAS 2
FAS 2 + Cp 2
FAS 2 + Cp 4
FAS 2 + Cp 8
A
Fluorescence changes (% of inital value)
110
100
90
80
70
60
50
0 min
5 min
10min
15 min
20 min
30 min
Time

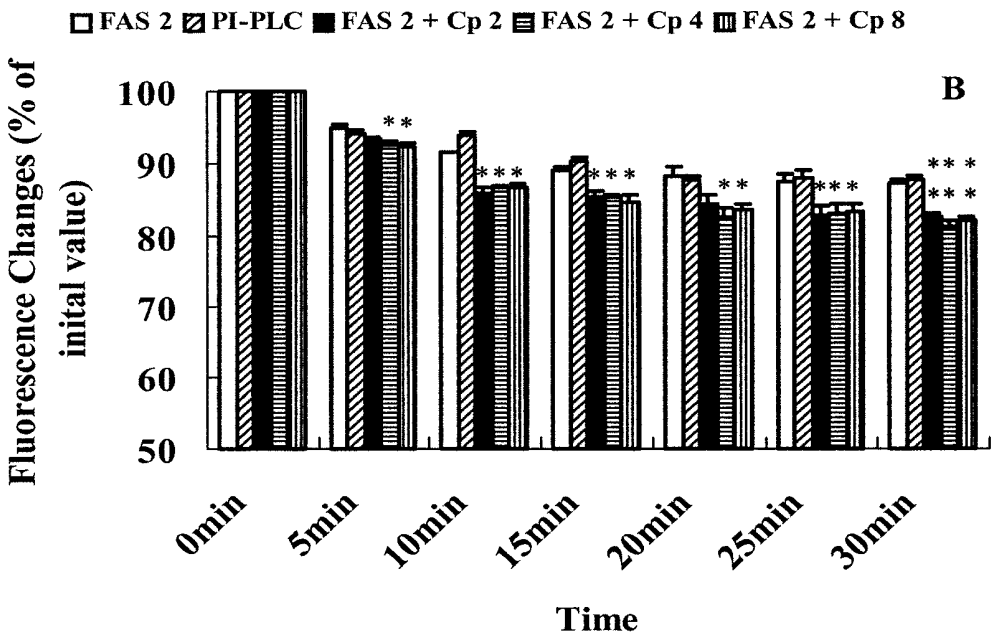
FAS 2
PI-PLC
FAS 2 + Cp 2
FAS 2 + Cp 4
FAS 2 + Cp 8
B
Fluorescence Changes (% of inital value)
100
90
80
70
60
50
0min
5min
10min
15min
20min
25min
30min
Time

Figure 5-5. Effect of CP on iron uptake by C6 glioma cells. Normal iron status cells (**A**) and no GPI-CP cells (**B**) treated with 600 μU/ml PI-PLC, and iron-deficient cells (**B**) treated with 1 mM BP and 1 mM DFO for 16 hours were loaded with 0.125 μM calcein-AM for 10 min. Kinetic fluorescence was measured on the BMG (Durham, NC, USA) Fluostar Galaxy fluorescence plate reader (λ_{ex} of 485 nm, λ_{em} of 520 nm, 37℃) equipped with excitation and emission probes directed to the bottom of a 96-well plate maintained at 37℃. 100 μl HEPES was added and initial baseline fluorescence intensity data was collected. Then varying amounts of human CP (0, 2, 4, 8 μg/ml) with 2 μM FAS were added by pipetting 2 μl of stock aqueous FAS and CP solution into the wells and gently mixing the solution. The quenching of calcein fluorescence by iron was measured as indicated. The change of fluorescence value was normalized as a percentage to the steady-state values of fluorescence before addition of FAS and/or CP. The data represent means ± SEM from 4 independent experiments. Different letters above data bars indicate that these groups are statistically different from normal iron status cells group: $*P < 0.05$, $**P < 0.01$ vs. control.

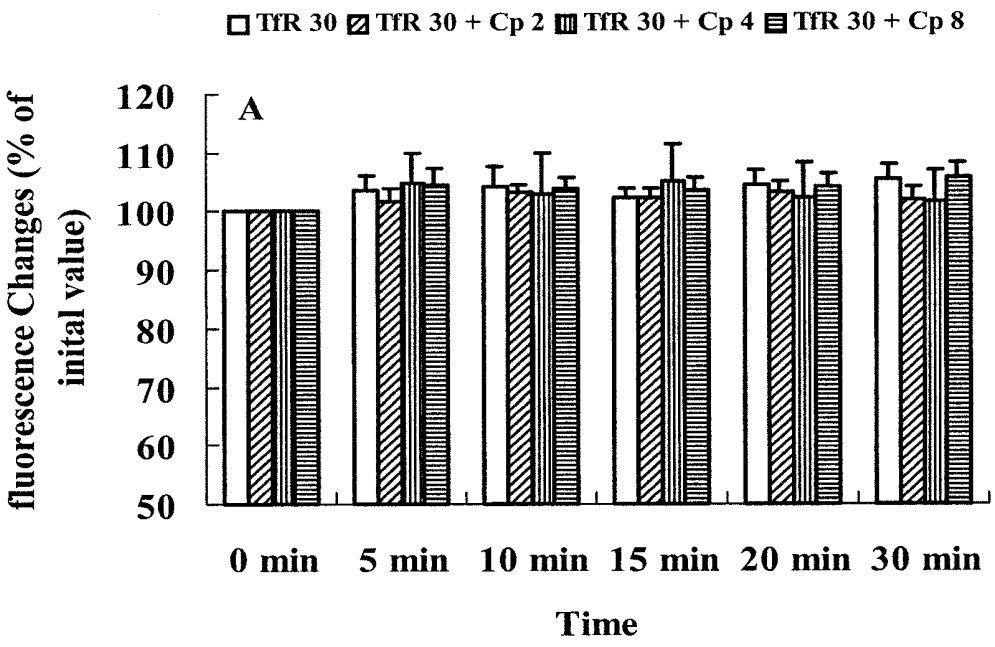
TfR 30
TfR 30 + Cp 2
TfR 30 + Cp 4
TfR 30 + Cp 8
A
fluorescence Changes (% of inital value)
120
110
100
90
80
70
60
50
0 min
5 min
10 min
15 min
20 min
30 min
Time

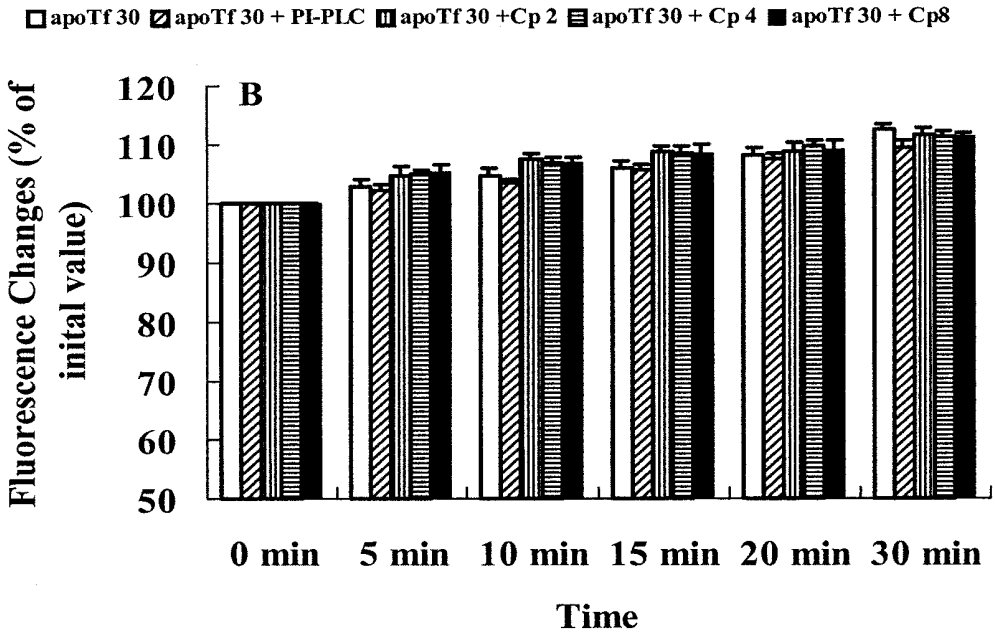
apoTf 30
apoTf 30 + PI-PLC
apoTf 30 +Cp 2
apoTf 30 + Cp 4
apoTf 30 + Cp8
B
Fluorescence Changes (% of inital value)
120
110
100
90
80
70
60
50
0 min
5 min
10 min
15 min
20 min
30 min
Time

Figure 5-6. Effect of CP and apotransferrin (ApoTf) on iron release from C6 glioma cells. (A) Cells without pretreatment (B) cells preloaded with iron by incubation with 50 μM FAC + 50 μM FAS for 16 hours. Before fluorescence measurements, the cells were loaded with 0.125 μM calcein-AM for 10 min and then washed 3 times with Hank's buffer solution. Kinetic fluorescence was measured on the BMG (Durham, NC, USA) Fluostar Galaxy fluorescence plate reader (λ_{ex} of 485 nm, λ_{em} of 520 nm, 37℃) equipped with excitation and emission probes directed to the bottom of a 96-well plate maintained at 37℃. 100 μl HEPES was added and initial baseline fluorescence intensity data was collected. Varying amounts of human CP (0, 2, 4, 8 μg/ml) with or without apoTf 30 μg/ml was then added by pipetting 2 μl of stock aqueous CP and apoTf solution into the wells and gently mixing the solution. The increase in fluorescence induced by iron release was measured as indicated. The change of fluorescence value was normalized as a percentage to the steady-state values of fluorescence before addition of the CP or/and apoTf. The data represent means ± SEM from 3 independent experiments.

CHAPTER 6

THE REGULATION OF FERROPORTIN1, CERULOPLASMIN AND ITS HOMOLOGUE HEPHAESTIN EXPRESSION IN RAT HEART BY IRON STATUS

6.1 ABSTRACT

Recently, the expression of two forms of DMT1 mRNA and protein in the rat heart was firstly reported. These results provided direct evidence that the NTBI uptake by heart cells might be mediated by DMT1. Intracellular iron balance depends on the amount of iron uptake as well as on the amount of iron release by the cell. FP1-Heph and FP1-CP iron export systems might play a key role in Fe^{2+} transport across the basal membrane of enterocytes in the gut or in other tissue. This study provided direct evidence for the existence of Heph and FP1 proteins in the rat heart. On one hand, iron deficiency increased the level of CP and decreased Heph and FP1 gene expression; on the other hand, high iron diet lowers the level of CP protein and increased the Heph and FP1 protein expression. This suggested that the FP1-Heph system plays a key role in heart iron release. It also showed that the regulation of CP and Heph expression by iron was tissue and brain area specific.

KEY WORDS

Ceruloplasmin, Hephaestin, Ferroportin1, MPT1, Transferrin Receptor, Heart, Iron Metabolism

6.2 INTRODUCTION

Iron is an essential trace element in human. As in all cells, heart cells require iron for many aspects of their physiology. On the other hand, iron is an effective catalyst in free radical reaction and excess iron in the heart can be potentially harmful via the generation of reactive oxygen species. Studies show that iron-mediated injury might play an important role in the development of a number of cardiovascular diseases. These include heart ischemia-reperfusion injury (Berenshtein et al., 1997; Chen et al., 2002), hemochromatosis (Pereira et al., 2001; Sullivan and Zacharski, 2001), bata-thalassemia (Aessopos et al., 2001), heart failure (Ide et al., 2001), atherosclerosis (de Valk and Marx, 1999; Haidari et al., 2001), acute myocardial infarction (Tuomainen et al., 1998; Klipstein-Grobusch et al., 1999) and coronary heart disease (Tzonou et al., 1998). Iron may also be involved in the development of cardiotoxicity induced by doxorubicin, an anthracycline antineoplastic agent, via iron-induced oxygen free radicals (Minotti et al., 1998; Minotti et al., 1999; Xu et al., 2001b; Xu et al., 2001a). Clinical investigation demonstrates that iron chelation therapy can significantly alleviate heart reperfusion injury, and the prognosis of thalassemia patients and endothelial function of patients with coronary artery diseases (Horwitz et al., 1998; Horwitz and Rosenthal, 1999; Duffy et al., 2001;

Taher et al., 2001). At present, it is not known how iron increases to a pathological level in the heart. The uptake of NTBI (non-transferrin-bound iron) by heart cells might be a key cause in heart injury because the toxicity of NTBI is much higher than that of Tf-Fe as judged by its ability to promote hydroxyl radical formation. However, decreased iron release by the heart cell is also another important mechanism. Therefore, the study of NTBI uptake and iron release by the heart cells is critical (Qian and Wang, 1998). It will provide important insights into the cause of excessive accumulation of heart iron as well as the pathogenesis of iron-induced heart diseases.

Our earlier studies provide direct evidence for the existence of DMT1 (IRE) mRNA as well as DMT1 (non-IRE) mRNA in the rat heart and demonstrate that the rat heart expresses a high ratio of DMT1 (IRE) to the NTBI uptake by heart cells might be mediated by DMT1 (Ke, 2003). Intracellular iron balance depends on the amount of iron taken up as well as on the amount of iron released by the cell (Qian and Wang, 1998; Qian and Shen, 2001). CP is an abundant plasma protein synthesized mainly in hepatocytes. A role for CP in iron efflux was first suggested in the 1960s, based on the observation that the ferroxidase activity of CP promoted iron incorporation into Tf (Osaki et al., 1966). This suggestion is supported by aceruloplasminemia (Gitlin, 1998) and animal model of aceruloplasminemia (Harris et al., 1999). Recent gene mapping studies have identified a CP homologue, Heph, which is expressed predominantly in the small intestine (Vulpe et al., 1999). Heph facilitates the transport of iron from enterocyte to plasma, but it is not a membrane transporter. Ferroportin1 (also known as IREG1, or MTP1) was recently identified a duodenal iron export molecule (Donovan et al., 2000). The basolateral membrane of the

duodenum is the primary iron regulatory site; FP1 and Heph may work together in iron transport from the enterocytes into the circulation. In other cell types, FP1 may work with CP to load iron onto Tf and enhance iron release from the cell (Fleming and Sly, 2001b).

At present, there is no data to confirm Heph and FP1 mRNA are expressed in the heart. Also, little is known about the regulation of Heph, FP1 and CP mRNA expression and protein synthesis in the heart. Therefore, in the current study, we investigated the Heph, FP1 and CP gene expression in the hearts of rats and analyzed the possible regulation of these genes by dietary iron, and determined whether the regulation of these genes in the heart was distinct from the brain. The understanding of these aspects is fundamental for elucidating the mechanism of iron balance in the heart. Most importantly, data on the expression and regulation of Heph, FP1 and CP in the heart would help explain iron metabolism and the etiology of the iron-related cardiovascular disease and neurological diseases.

6.3 MATERIALS AND METHODS

6.3.1 Materials

Please refer to chapters 2 and 3.

6.3.2 Animals

Please refer to chapters 2 and 3

6.3.3 Methods

6.3.3.1 Sampling of Blood and Tissue

Animals fed on different iron diet, were anesthetized with 1% pentobarbital sodium (40mg/kg body weight, i.p.) and decapitated. Blood samples were then collected into heparinized syringes and aliquots were taken immediately for the determination of Hb concentration and Hct. The serum samples were analyzed for serum iron, total TIBC and Tf saturation (serum iron/TIBC). The hearts were perfused with PBS, excised and rinsed in PBS, blotted dry and weighed according to (Zaman et al., 2001). Portions of the left ventricle were used immediately for total RNA extraction and protein determination. The remaining ventricle and liver were frozen in liquid nitrogen and stored at -70℃, for the measurement of non-heme iron.

6.3.3.2 Immunohistochemistry

Please refer to chapters 2 and 3.

Heart sections were prepared at 10μm thickness perpendicular to the axis of left ventricle with a cryomicrotome (Leica) and placed on glass slides coated with Vectabond (Vector Laboratory).

For the primary antibodies, we use a 1:500 dilution of the rabbit anti-mouse Heph antibody (this antibody source is 100% conserved in rat) and FP1 antibody (ADI,

San Antonio, USA); 1:50 dilution of the purified mouse anti CP IgG1 (BD Transduction Laboratories, BD Biosciences, USA) and mouse anti rat CD71 monoclonal antibody (BD Bioscience).

6.3.3.3 RNA Purification, Generation of Specific Probes, and Northern Blot Assay

Please refer to chapters 2 and 4.

Total RNA was isolated from the left ventricle using Trizol reagent (Invitrogen, CA) according to the manufacturer's instructions. Special ^{32}P-labeled probes corresponding to positions 1298-1733 of FP1 (Genbank, AF394785), 3659-4201 of Heph (Genbank, AF246120), 1133-1518 (Genbank, L33869) of CP and 5-574 of TfR (Genbank, M58040) were generated.

6.3.3.4 Western Blot Analysis

Please refer to chapters 2 and 3.

The concentrations of primary antibodies for blotting are rabbit anti-mouse Heph and rabbit anti-mouse FP1 antiserum (1:5000), purified mouse anti CP IgG1 and mouse anti rat CD71 monoclonal antibody (1:1000).

6.3.4 Analytical methods

Hb concentration was determined by the cyanmethemoglobin method (Qian et al., 1999b; Qian et al., 2001b). Hct was measured using the microhematocrit centrifuge and plasma iron and total iron-binding capacity were determined using commercial kits (Sigma). Non-heme iron concentrations of tissues were measured as described previously (Qian et al., 1999b; Qian et al., 2001b). The results were expressed as means ± SEM. The difference between means was determined by one-way ANOVA followed by a Student-Newman-Keuls test for multiple comparisons. A probability value of $P<0.05$ was taken to be statistically significant.

6.4 RESULTS

6.4.1 Distribution of Ceruloplasmin, Hephaestin, Ferroportin1 and Transferrin Receptor in the Rat Heart

Immunohistochemistry in 3 rats revealed prominent CP (Fig 6-1A), Heph (Fig 6-1B), FP1 (Fig 6-1C) and TfR (Fig 6-1D) staining in the cardiac myocyte of the myocardium. Fig 6-1A shows strong CP immunoactivity in the membrane of the myocyte. As shown in Fig 6-1B, Heph was mainly localized in the membrane of the myocyte (thin arrow) and intercalated disc (fat arrow). TfR immunoactivity was also mainly observed in the membrane of the myocye.

6.4.2 Effect of Iron Diets on Biochemical Parameters

After rats had fed with an iron deficient diet for 6-weeks, the body weight, Hb, Hct,

Tf saturation and non-heme iron levels saturation in the heart were significantly changed compared to the controls ($p<0.01$, Table 6-1). The heart weight and the heart:body weight were higher in iron-deficient rats than in the controls ($p<0.01$). The data suggest that rats on the iron-deficient diet developed iron deficiency with anemia. In the high-iron rats, Hb, Hct, Tf saturation and non-heme iron level in the heart and liver were significantly higher than those in the control rats ($p<0.01$, Table 6-1). The iron content in the heart increased 6-fold above that of the controls. These findings show that a high iron-loaded heart model was successfully developed.

6.4.3 Effect of Iron on Transferrin Receptor mRNA Expression and Protein Synthesis

To test the effect of the iron on gene expression, we firstly analyzed the expression of TfR mRNAs and protein synthesis in the control, low-iron and high-iron rats. The Northern blotting and Western blotting results (Fig 6-2) showed that a high-iron diet leads to an increase in serum iron and heart iron and a significant declined of about 30% of TfR mRNA and 60% of protein to the control. In iron-deficiency models, iron in the heart and serum significantly decreased and the level of TfR mRNA and protein increased remarkably, being about 2.7 folds the mRNA and 2.9 folds the protein respectively, compared to the control rats. These results demonstrated that iron has a significant effect on the expression of TfR in the heart.

6.4.4 Effect of Iron Status on Hephaestin, Ferroportin1 and Ceruloplasmin mRNA Expression and Protein Synthesis

Northern blot analysis was performed to determine the effect of iron on the Heph, FP1 and CP mRNA expression. Representative Northern blots showing the expression of FP1 (Fig 6-3A), Heph (Fig 6-4A) and CP (Fig 6-5A) are presented. Quantified mRNA levels relative to β-actin for each transcript from independent samples are shown in Figure 6-2B, 6-3B and 6-4B. Transcript level of FP1 mRNA was significantly decreased (58 ± 3%) in iron-deficient rats and increased (253 ± 20%) in iron-overloaded rats (Fig 6-3B, all $P<0.01$). In contrast, the level of Heph mRNA decreased dramatically in both iron-deficient (59 ± 5%) and iron-sufficient (75 ± 4%) rat hearts (Fig 6-4B, all $P<0.01$). The level of CP mRNA increased (135 ± 2%) in the iron-deficient rats and decreased (89 ± 5%) in the iron-sufficient rats (Fig 6-5B, $P<0.05$), the similar result was also found in other studies (Mukhopadhyay et al., 1998; Mukhopadhyay et al., 2000),

To determine the effect of iron on the synthesis of FP1, Heph and CP proteins, Western blot analysis was conducted. It was found that the amount of FP1 protein decreased to 74 ± 8% of the controls after the rats were fed with a low-iron diet. After the rats were fed with a high-iron diet, the FP1 protein increased to 230 ± 20% of the controls (Fig 6-3B, all $P<0.01$). The decreased mRNA levels of Heph in rats on iron-deficient and iron-sufficient diets compared to rats on a control diet are reflected in the respective decreases of (77 ± 8% and 63 ± 5%) in Heph protein synthesis (representative blots are shown in Fig 6-4A, the values of the quantity are shown in Fig 6-4B). As shown in Fig 6-5, the regulation of CP protein synthesis is parallel to that of mRNA expression. After the rats were fed with a low-iron diet, the CP protein increased to 142 ± 3% of the controls (Fig 6-5B, $P<0.05$); in the high-iron group the CP protein decreased to 72 ± 3% of controls (Fig 6-5B, $P<0.05$).

These results demonstrate that the iron transporter proteins TfR, FP1, Heph and CP were regulated by the iron status of the cardiac myocyte. However, the pattern of regulation of FP1 and Heph was different from that in the duodenal epithelial cells.

6.5 DISCUSSION

To our knowledge, this is the first report on the expression of FP1 and Heph mRNAs and proteins in the rat heart. Immunohistochemistry, Northern blotting and Western blotting results provide direct evidence for the existence of FP1, Heph, CP and TfR mRNAs and proteins in the rat heart. The strong immunoactivity of CP in the cardiac myocyte cell membrane combined with other results (Reilly and Aust, 1998; Patel et al., 2000) confirm the presence of membrane-bound CP (GPI-anchored form). Heph, encoding a transmembrane-bound CP homologue protein is highly expressed in the villus of the small intestine (Vulpe et al., 1999; Frazer et al., 2001). Our findings show that Heph appeared to be located in the membrane of the myocyte and intercalated disc. The special membrane distribution was also investigated in the K562 erythroleukemia cells and IEC6 rat cells (Simovich et al., 2002), but was found to be different than in villus of the duodenum (Frazer et al., 2001). The subcellular distribution of FP1 is distinctly different in some tissue (Abboud and Haile, 2000). The distribution of TfR in the membrane of myocyte was detected. In addition, iron status was found to have a significant effect on the expression of TfR, FP1, Heph, and CP mRNAs and proteins in the heart.

At present, the mechanisms involved in the regulation of FP1 mRNA expression and protein synthesis are not completely understood. Studies (Abboud and Haile, 2000;

McKie et al., 2000; Martini et al., 2002) have demonstrated that FP1 mRNA expression and protein synthesis in the small intestine are both inversely regulated by iron status in duodenal epithelial cells. However, our findings and the results reported by others imply there may be disparities in FP1 mRNA expression and translation in response to iron status in different organs or tissues. FP1 mRNA and protein are increased in the Kupffer cells and lung cells of iron-replete mice, and suppressed in iron-deprived mice (Abboud and Haile, 2000; Yang et al., 2002). Our results show that iron status has a significant effect on FP1 mRNA expression and protein synthesis in the rat heart. Both mRNA expression and protein synthesis of FP1 increased in iron-overloaded rats and decreased in iron deficient rats, suggesting a transcriptional regulation of the FP1 gene in the cardiac myocyte cells. This is different from our previous findings on the regulation of the DMT1 gene by iron status in the rat heart (Ke, 2003).

FP1, TfR and DMT1+IRE and many other mRNAs encoding proteins involved in iron uptake and storage contain IRE within its 3' or 5'UTR that is a binding site for iron-regulatory protein (IRP). IRE mediates the changes of these proteins' levels in response to iron availability. The binding of IRP to IRE in the 5'UTR of mRNA such as that encoding FP1 causes a decrease in FP1 mRNA translation. An IRE/IRP-dependent iron-regulatory pathway for the FP1 gene appears to be present in the rat heart and in lung cells (Yang et al., 2002). In duodenal entreocytes, however, the iron-regulatory pathway is IRE/IRP-independent (Abboud and Haile, 2000; McKie et al., 2000; Martini et al., 2002; Chen et al., 2003a). In contrast, IRP binding to IRE in the 3' UTR of mRNA like the one encoding TfR enhances mRNAs stability and protein expression. The IRE-IRP mechanism allows for the coordinated

regulation of iron uptake and storage in response to the iron metabolism in most cells. In this study, the regulation of TfR gene is at a transcriptional level. Under low iron status, IRP would bind and stabilize the IRE of TfR mRNA, leading to an increase in TfR mRNA expression and protein synthesis. In addition, the high iron status results in decrease in the IRE/IRP binding and hence destabilization of the TfR mRNA, leading to a suppression of TfR mRNA expression and protein synthesis. At present, very little is known about the mechanisms of Heph regulation. Previous studies showed variations in iron status had a small but no significant effect on Heph expression in the duodenum (Frazer et al., 2001; Rolfs et al., 2002; Yamamoto et al., 2002; Frazer et al., 2003), whereas Sakakibara and Aoyama studies showed dietary iron-deficiency increased Heph mRNA expression in small intestine of rats (Sakakibara and Aoyama, 2002). In a notable study on *sla* mice, cellular iron levels are increased in the intestinal enterocytes yet systemic iron levels are low; the pattern of increased Heph mRNA expression is similar to iron deficient mice, the Heph protein is also up-regulated. Thus, Heph mRNA and protein levels correlate with systemic rather than local iron status (Chen et al., 2003a). Our results showed the Heph mRNA and protein levels are down regulated in both iron overload and iron deficiency in rat heart. The possible explanation is that both systemic and cellular local iron status affect Heph mRNA expression and protein synthesis. The results of the regulation may be according to the physiological function of the cardiac myocyte. High systemic iron depressed the Heph mRNA expression and protein synthesis. However, the exceeding low cellular iron suppressed Heph mRNA and protein in order to reduce the iron efflux. The molecule mechanisms of regulation of CP expression by iron deficiency could be explained by activation of hypoxia-inducible factor (HIF) (Mukhopadhyay et al., 1998; Attieh et al., 1999). It is now clear that

HIF-1α and HIF-1β bind to the CP gene promoter HRE (Mukhopadhyay et al., 2000). Our results also show that iron deficiency enhanced CP mRNA expression and protein synthesis in rat heart while iron surplus suppressed them. However, other reports show iron status has little or no influence on either the levels of plasma CP, or on expression of its mRNA in the liver (Huang and Shaw, 2002; Strube et al., 2002; Tran et al., 2002). These different results may be due to the degree of iron levels achievable in culture and *in vivo*.

Studies show that FP1 plays a role conjunction with Heph in the intestinal absorption of iron, and in conjunction with CP in iron release from the cell in other tissues (Kaplan and Kushner, 2000; Frazer et al., 2001). On the other hand, the DMT1 may play an important role in iron transport across the apical surface of human intestinal Caco-2 cells (Tandy et al., 2000) and rat duodenal enterocytes (Trinder et al., 2000). The membrane TfR mediates endocytosis or internalization of the complex of Tf bound iron, and the TfR is the major route of cellular iron uptake (Li et al., 2002; Li et al., 2003a). Studies on human embryonic kidney (HEK293T) cells suggest that DMT1 may be involved in translocation of iron from endosome to cytosol under physiological conditions (Su et al., 1998; Tabuchi et al., 2000; Touret et al., 2003). Evidence shows that DMT1 may have a role in dependent-dependent iron uptake in some types of cells (Wardrop and Richardson, 1999). It is necessary for cardiac myocytes to balance the iron metabolism ensuring the physiological function of the heart. Based on the above results and present study of DMT1 (Ke, 2003), we propose the following model for cardiac myocyte iron transport (Fig 6-6): High iron stores lead to decreased levels of TfR and DMT1 proteins and minimal TfR-dependent iron absorption. If the level of systemic iron rises so much that it outstrips the range of

physiological regulation, this may induce NTBI uptake -- perhaps mediated by DMT1 -- and induce the heart injury. The high systemic iron and cellular (local) iron increases the FP1 and Heph expression, probably in order to boost iron release from the iron overload cells. But the degree of the iron release is likely to be inhibited by the persistent high systemic iron, which will further increase expression of the two proteins. Iron deficiency significantly enhances the levels of TfR and DMT1, which increases the enterocyte iron uptake. On the other hand, iron deficiency suppresses FP1 protein level, which may prevent iron loss. Nevertheless, the steady low iron levels in the system and cells may result enhance TfR and DMT1 levels and suppress FP1 together with the Heph gene expression, ensuring the physiological function (iron involved) of the cardiac myocyte. However, it has not been determined whether FP1 acts in conjunction with Heph/CP in iron release or on its own in cardiac myoctes. In addition, no definitive studies have been reported to show a role of DMT1 in iron uptake by myocardium. Thus further investigation is needed to clarify the function of TfR, DMT1, FP1, Heph and CP in heart iron metabolism.

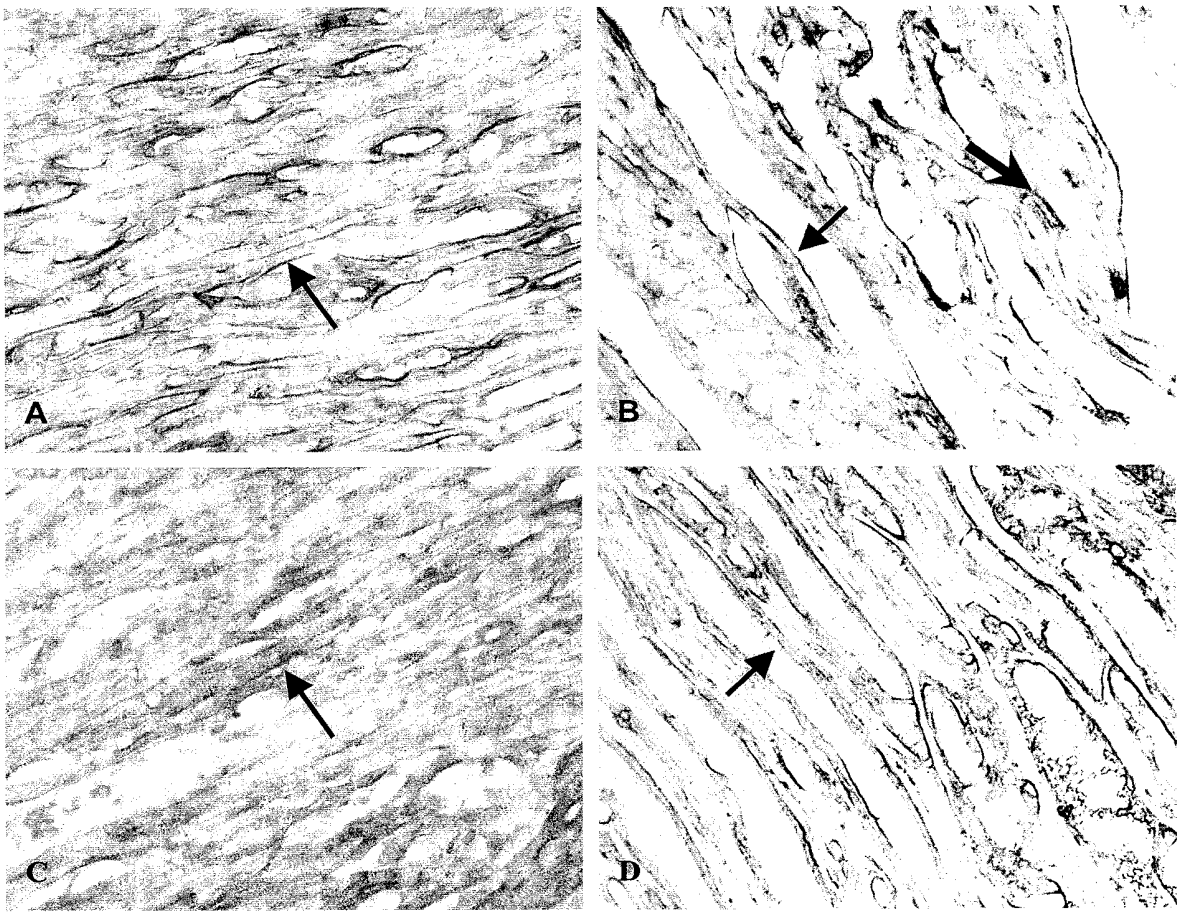

Figure 6-1. Immunohistochemical staining of CP (A), Heph (B), FP1 (C) and TfR (D) proteins in myocardium. An immunohistochemical study using anti-CP, Heph, FP1 and TfR antibodies was performed on left ventricle sections of rat. The cardiac myocyte cell membrane was stained for CP (A), Heph (B), FP1 (C) and TfR (D) proteins (black arrow). Magnifications ×400.

Table 6-1. Hematological variables, liver non-heme iron in the control, iron deficient, and iron overload rats

	Control (n=6)	Iron deficiency (n=6)	Iron overload (n=6)
Body weight (g)	327 ± 4.27	270 ± 4.48**	340 ± 7.11
Hct (%)	43.50 ± 0.99	17.67 ± 0.99**	48.33 ± 0.67**
Hb (g/dl)	17.96 ± 0.29	5.27 ± 0.38**	19.63 ± 0.30**
Serum iron (mmol/L)	24.67 ± 0.88	3.11 ± 0.53**	48.80 ± 2.11**
TIBC (mmol/L)	67.79 ± 1.29	109 ± 3.27**	69.69 ± 1.34
Transferrin saturation (%)	36.36 ± 0.81	2.93 ± 0.54**	70.20 ± 3.57**
Liver iron (mg/g dry weight)	0.27 ± 0.01	0.07 ± 0.01**	2.66 ± 0.13**
Heart iron (mg/g dry weight)	0.073 ± 0.008	0.032 ± 0.003**	0.379 ± 0.016**
Heart weight (g)	1.01 ± 0.05	1.33 ± 0.05**	0.92 ± 0.04
Heart:body weight ($\times 10^{-3}$)	3.02 ± 0.18	4.91 ± 0.26**	2.69 ± 0.13

Each value represents sample mean ± SEM of six rats. ** Indicates significant difference by *t*-test at $P < 0.01$ vs. control.

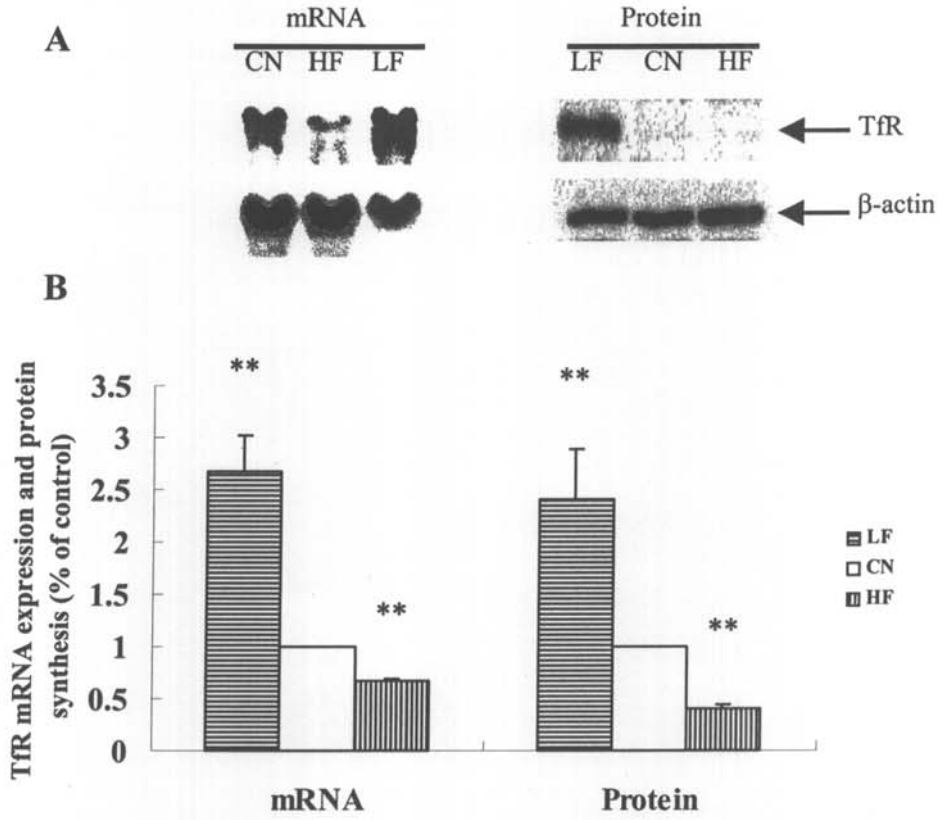

Figure 6-2. TfR mRNA expression and protein synthesis are responsive to iron status of the heart. Northern blot and Western blot analyse were performed on left ventricles from rats fed with control diet (CN), iron-deficient (LF) and iron-overload (HF) diets for 2 months. mRNA blots were sequentially hybridized to probe for TfR and β-actin. The β-actin band was used as a loading control (**A**). Representative blots of TfR and β-actin proteins were shown in (**A**). Relative mRNA and protein levels of Heph were quantified using ImageQuant software for mRNA and LumiAnalyst Image Analysis software for protein and densitometry values were normalized to values obtained for β-actin. Data are presented as means of % control ± SEM from 6 independent experiments. **P<0.01 vs. control (**B**).

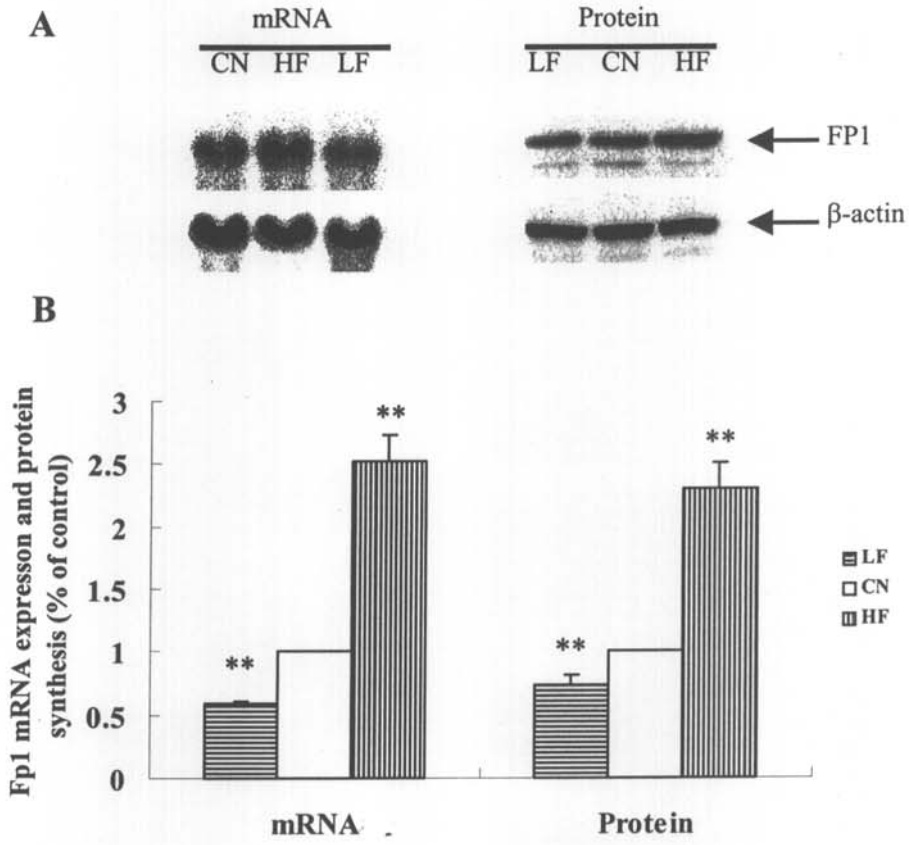

Figure 6-3. FP1 mRNA expression and protein synthesis are responsive to iron status of the heart. Northern blot and Western blot analyse were performed on the left ventricles from rats fed with control diet (CN), iron-deficient (LF) or iron-overload (HF) diets for 2 months. **A:** Representative blots of FP1 and β-actin mRNA and protein. The β-actin band was used as a loading control. **B:** Relative mRNA and protein levels of FP1 were quantified using ImageQuant software for mRNA and LumiAnalyst Image Analysis software for protein and densitometry values were normalized to values obtained for β-actin. Data are means of % control ± SEM from 6 independent experiments. **P<0.01 vs. control.

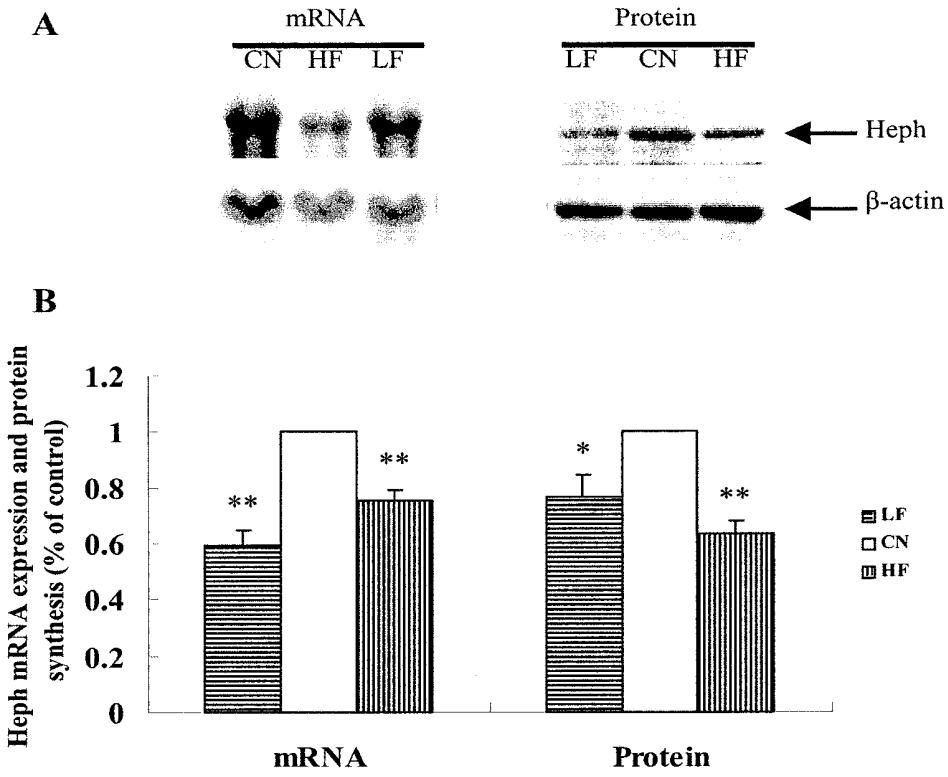

Figure 6-4. Expression of Heph mRNA and protein synthesis in the hearts of the control (CN), iron deficient (LF), and iron overload rats (HF). Northern blot was hybridized with randomly primed ^{32}P-labeled probe for Heph and exposed to a phosphor screen for 12 hours for image analysis, and Western blot analysis was performed as described in Materials and Methods on the left ventricles from rats fed control diet (CN), iron deficient (LF) and overload (HF) diets for 2 months. **A:** Representative blots of Heph and β-actin mRNA and protein. The β-actin band was used as a loading control. **B:** Relative mRNA and protein levels of Heph were quantified using ImageQuant software for mRNA and LumiAnalyst Image Analysis software for protein and densitometry values normalized to values obtained for β-actin. Data are means of % control ± SEM from 6 independent experiments. *P<0.05, **P<0.01 vs. control.

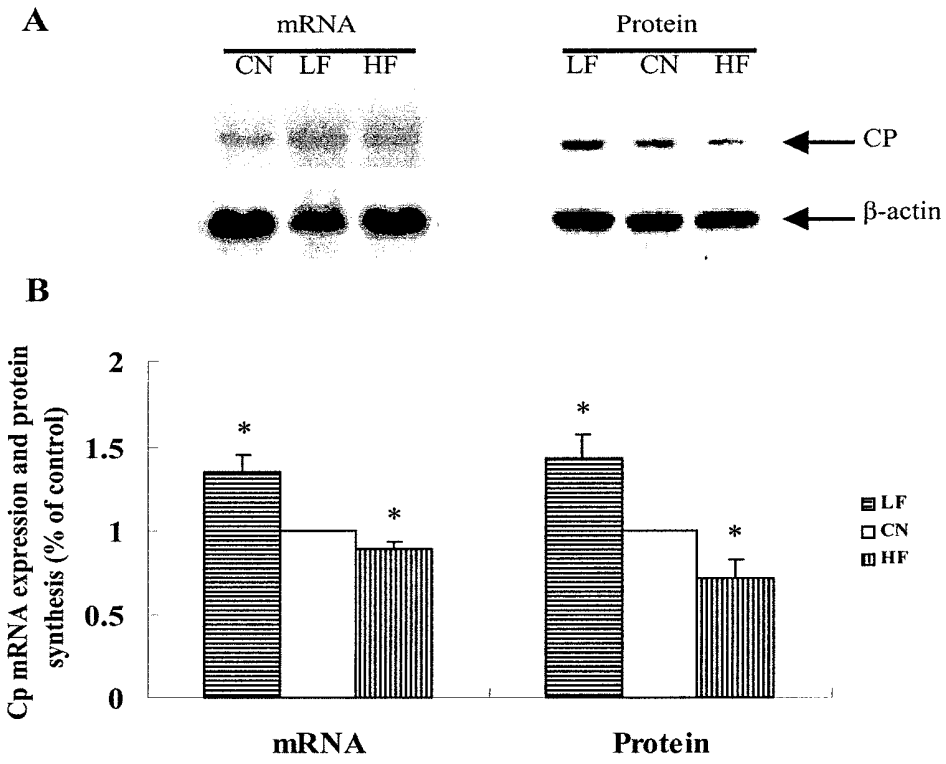

Figure 6-5. Expression of CP mRNA and protein synthesis in the hearts of the control (CN), iron deficient (LF), and iron overload rats (HF). Northern blot was hybridized with randomly primed ^{32}P-labeled probe for CP and exposed to phosphor screen for 12 hours for image analysis, and Western blot analysis was performed as described in Materials and Methods on the left ventricles from rats fed control diet (CN), iron-deficient (LF) and iron-overload (HF) diets for 2 months. **A:** Representative blots of CP and β-actin mRNA and protein. The β-actin band was used as a loading control. **B:** Relative mRNA and protein levels of CP were quantified using ImageQuant software for mRNA and LumiAnalyst Image Analysis software for protein and densitometry values were normalized to values obtained for β-actin. Data are means of % control ± SEM from 6 independent experiments. *P<0.05 vs. control.

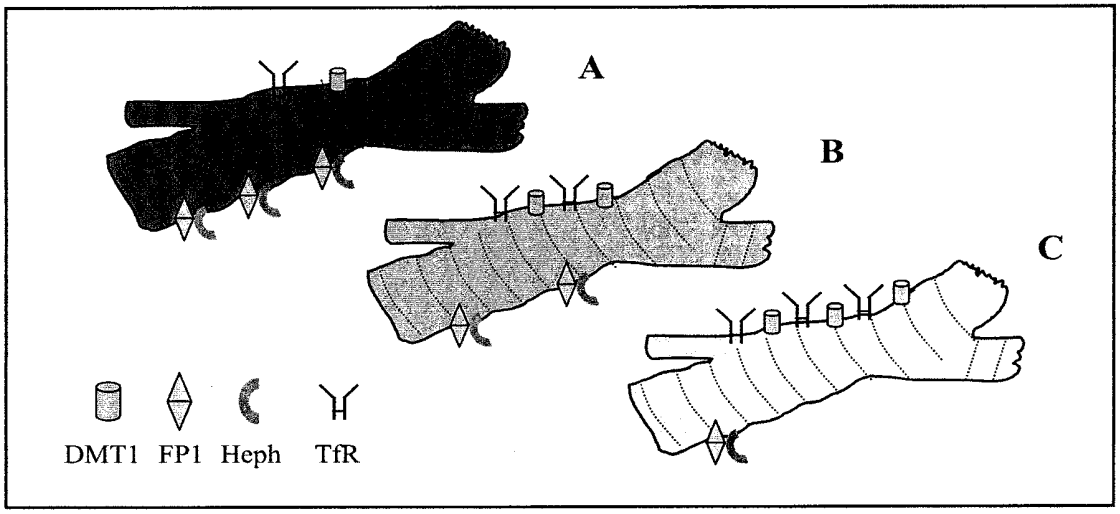

Figure 6-6. A model for iron balance control of cardiac myocyte. **A:** High iron diets lead to an increase in serum iron and iron content in the heart and decreased levels of TfR and DMT1 proteins and minimal iron absorption. When the systemic iron level outstrips the physiological range, it may be induce NTBI uptake perhaps mediated by DMT1. The high systemic iron level and local iron in cardiac myocyte induces an increase in FP1 and Heph expression in order to scavenge the overload iron from the cytoplasm. However, the steady high systemic iron level inhibits the effect of FP1/Heph, so further up-regulated the FP1 and Heph expression. **B:** There is suitable expression of FP1 and Heph in the normal diets fed rats, and the iron uptake and release is in a balanced state. **C:** In iron deficiency models, iron in the heart and serum is significantly decreased and the levels of TfR and DMT1 are remarkably increased, which enhances the enterocyte iron uptake. On the other hand, iron deficiency leads to a decrease of FP1 and Heph protein levels, which may prevent iron release and ensure the physiological function of the cardiac myocyte.

CHAPTER 7

EFFECT OF LEVODOPA ON DMT1, FP1 AND TFR GENES EXPRESSION AND IRON UPTAKE IN C6 GLIOMA CELLS

7.1 ABSTRACT

L-dopa, through its decarboxylation to dopamine, remains the most effective therapy for symptoms of PD. However, despite almost 30 years of clinical experience, doubts remain as to whether L-dopa worsens the illness by accelerating nigral cell degeneration. From the past several years' study, iron and iron-induced oxidative stress constitute a common mechanism that is involved in neuronal death and the development of neurodegeneration. In this study, we investigated the effect of L-dopa on the gene expression of iron uptake related proteins DMT1, TfR and FP1 and the role of L-dopa on iron uptake in C6 glioma cells. DMT1-IRE mRNA and protein expression were up-regulated by L-dopa; the effect was concentration dependent with the optimal concentration of the L-dopa at 10 μM. This regulation of DMT1-IRE gene expression by L-dopa operated at the transcriptional level. However, DMT1+IRE, TfR and FP1 gene expression were not regulated by L-DOPA treatment. In addition, after L-dopa treatment, ferrous uptake was increased

in C6 glioma cells. The data suggests that L-dopa treatment increases the cell iron uptake and perhaps induces the Fenton reactions producing the more toxic hydroxyl radical (OH ·), which lead to the neuron oxidative damage. However, the detailed mechanism requires more study.

KEY WORDS

Levodopa, DMT1, Ferroportin1, Trnasferrin Receptor, Parkinson's Disease, Iron Uptake, Calcein

7.2 INTRODUCTION

The divalent metal transporter 1 (DMT1), also known as natural resistance-associated macrophage protein 2 (Nramp2) or divalent cation transporter 1 (DCT1), is a protein recently shown to play a pivotal role in iron uptake from both Tf and non-Tf sources in different anatomic sites (Andrews, 2000; Wessling-Resnick, 2000). There are at least two different splice forms of DMT1. One form, containing the iron-responsive element (IRE) sequence, encodes a 561-amino-acid protein. Another form does not contain a recognizable IRE and encodes a 568-amino-acid protein (Fleming et al., 1998; Lee et al., 1998). Iron is taken up in most cells by the specific binding of the Fe-binding protein Tf to the TfR on the cell membrane. The roles of Tf and TfR in iron uptake have been well characterized, but the pathway taken by iron after it is released from Tf remains elusive. A number of recent studies have shown that DMT1 can be expressed on the endosomal membrane and acts to export iron from the endosome into the cytoplasm of the cell (Su et al., 1998;

Tabuchi et al., 2000). In the brain, DMT1 mRNA is consistently found in neurons and epithelial cells of the choroid plexus and is present at moderate levels in the substantia nigra (Gunshin et al., 1997; Andrews et al., 1999). The cellular localization of DMT1 and its functional characterization suggest that DMT1 may play a role in physiological iron transport in the brain. It has also been proposed that defects in DMT1 are likely to contribute to the etiology of certain NDs. It has been reported that the affected neurons of the substantia nigra in PD patients have a moderately high expression of DMT1 (Andrews et al., 1999). This may be the cause of the increased iron content in this region and may therefore contribute to neuronal death by inducing the production of harmful ROS (Andrews et al., 1999). TfR is clearly expressed by neurons throughout the CNS. The immunoreactive cell bodies have been mainly confined to the cerebral cortex, hippocampus, habenular nucleus, red nucleus, substantia nigra, pontine nuclei, reticular formation, several cranial nerve nuclei, deep cerebellar nuclei and cerebellar cortex (Moos, 1996). Because Tf in the cerebrospinal fluid (CSF) and interstitial fluid (IF) is fully saturated with iron, excess iron will bind to other transporters. Hence, it is possible that there are two transport forms of iron in the CSF and IF in the brain: Tf and non-Tf-bound iron (NTBI) (Bradbury, 1997; Moos and Morgan, 1998a). Tf–Fe or Lf–Fe, and secreted p97–Fe are respectively taken up by brain cells via TfR- or LfR- and GPI-anchored p97-mediated processes. NTBI is acquired by neuronal cells or other brain cells, probably via DMT1- or trivalent cation-specific transporter (TCT)-mediated mechanisms (Qian and Shen, 2001). Ferroportin1 (FP1) is member of the DMT1 family of metal transporters, and overexpression of FP1 in tissue culture cells results in IRP1 activation and ferritin depletion, indicating a possible role as an iron exporter (Abboud and Haile, 2000). We investigated expression of FP1 protein in different

brain regions in developing male Sprague-Dawley rats, including cortex, hippocampus, striatum and substantia nigra. The results provided direct evidence for the existence of ferroportin1 protein in the rat brain. All brain areas examined have the ability to synthesize ferroportin1 protein. The findings also showed that age has a significant effect on the expression of ferroportin1 protein in the cortex, hippocampus, striatum and substantia nigra of the rat brain (Jiang et al., 2002).

L-dopa, is generally regard as most effective treatment for symptoms of PD. However, despite almost 30 years of clinical experience, doubts remain as to whether L-dopa adversely affects the progression of the illness by accelerating nigral cell degeneration (Jenner and Brin, 1998). The issue of L-dopa toxicity was initially raised because of its potential to cause long-term adverse effects such as dyskinesias and motor fluctuations, which are not observed in untreated patients (Simuni and Stern, 1999). These can become so disabling that surgical treatment becomes the only apparent option for restoring any quality of life (Krack et al., 2000). This concept is based on the relative ease of oxidation of levodopa and the generation of toxic reactive oxygen species (Graham, 1978). The enzymatic oxidation of L-dopa to dopamine and its metabolism by monoamine oxidase B (MAO-B) give rise to the formation of hydrogen peroxide (H_2O_2), which may be mildly toxic. H_2O_2 can also be converted by iron-mediated Fenton reactions to produce the more toxic hydroxyl radical ($OH^{\cdot}$), which can induce oxidative damage. Examination of postmortem tissues taken from patients who died of PD has shown increased levels of iron in the substantia nigra (Jenner and Brin, 1998). Past studies show iron and iron-induced oxidative stress are commonly involved in the development of neurodegeneration. At least in some NDs, brain iron misregulation is an initial cause of neuronal death and

that this misregulation might be the result of either genetic or non-genetic factors (Qian and Shen, 2001). Therefore, changes in iron and complex I may be related to drug treatment, although there was no inhibition of complex I activity in patients with multiple-system atrophy who were treated with L-dopa (Schapira et al., 1990; Gu et al., 1997). In this study, we investigated the effect of L-dopa on the gene expression of iron uptake related proteins DMT1, TfR and FP1 and the role of L-dopa on iron uptake in C6 glioma cells.

7.3 MATERIALS AND METHODS

7.3.1 Materials

Please refer to chapters 2 and 5.

7.3.2 Methods

7.3.2.1 Cell Culture

Please refer to chapters 2 and 5.

For the L-DOPA treatment, when cells reached about 65-70% confluence, the experiments were initiated by changing the medium followed by addition of various concentration L-DOPA, as indicated in the legends.

7.3.2.2 Immunocytochemistry

Please refer to chapters 2 and 5.

The primary antibodies were set at the following concentrations: rabbit polyclonal anti-rat DMT1+IRE, DMT1-IRE (1:500), rabbit anti-mouse FP1 (1:500) antibody (Alpha Diagnostic, USA), mouse anti-rat TfR (1:200) monoclonal antibody (BD Bioscience).

7.3.2.3 RNA Purification, Generation of Specific Probes, and Northern Blot Assay

Please refer to chapters 2 and 5.

^{32}P-labeled probes corresponding to positions 1755-2592 of DMT1+IRE (Genbank, AF008439), 1697-2031 of DMT1-IRE (Genbank, AF029757), 1298-1733 of FP1 (Genbank, AF394785) and 5-574 of TfR (M58040) was synthesized.

7.3.2.4 Western Blot Analysis

Please refer to chapters 2 and 5.

The dilutions rabbit anti-rat DMT1+IRE, DMT1-IRE1 polyclonal antibody, rabbit anti-mouse FP1 polyclonal antibody (Alpha Diagnostic, USA) are set at 1:5000; mouse anti-rat TfR monoclonal antibody (BD Bioscience) is 1:1000 and anti-rabbit

secondary antibody conjugated horseradish peroxide is 1:5000.

7.3.2.5 Calcein Loading of the Cells and Divalent Metal Transport Assay

Please refer to chapter 2 and 5.

C6 cells were grown to 65-70% confluence on poly-l-lysine coated plastic 96-well plates. These were then maintained at control condition and in the presence of 10, 30, 100 μM L-DOPA DMEM medium for 16 hours. Cells were washed twice times with medium and incubated with 125 nM CA-AM in serum-free medium, After incubation for 10 min at 37℃, excess calcein-AM was removed and the cells were washed twice with Hank's balance salt solution (HBSS, invitrogen, CA) at 37℃. For the kinetic fluorescence measurements, the BMG (Durham, NC, USA) Fluostar Galaxy fluorescence plate reader (λ_{ex} of 485 nm, λ_{em} of 520 nm, 37℃) equipped with excitation and emission probes was directed to the bottom of the plate. 100 μl HEPES was added and initial baseline fluorescence intensity data was collected. Then 0 and 8 μM ferrous ammonium sulfate (FAS) was added by pipetting 1 μl of stock aqueous FAS solution into the wells and gently mixing the solution with a pipette. The quenching of calcein fluorescence by divalent metals was measured every 5min for 30 min at 37℃. Data were normalized to the steady-state values of fluorescence before addition of the FAS.

7.3.3 Statistical Analysis

Please refer to chapter 3.

7.4 RESULTS

7.4.1 Identification of DMT1+IRE, DMT1-IRE, Ferroportin1 and Transferrin Receptor Protein in C6 Glioma Cells

Because DMT1, TfR and FP1 are the key proteins in iron metabolism (Qian and Shen, 2001), we immunostained the C6 cells grown on poly-l-lysine coated coverslips with antibodies against DMT1+IRE, DMT1-IRE, FP1 and TfR to determine gene expression. Immunoactive staining for TfR (Fig 7-1A), FP1 (Fig 7-1B), DMT1-IRE (Fig 7-1C) and DMT1+IRE (Fig 7-1D) was observed in C6 cells.

7.4.2 Effect of L-dopa on DMT1+IRE, DMT1-IRE and Transferrin Receptor mRNA Expression by C6 Glioma Cells

To determine whether L-dopa modulates DMT1+IRE, DMT1-IRE and TfR gene expression, C6 glioma cells grown in a 75 cm^2 flask were treated for 16 hours with 0 μM, 10 μM, 30 μM, 100 μM L-dopa. Northern blot analysis was quantified by densitometry and total RNA loading was corrected using β-actin expression. Representative Northern blot showing one mRNA band with expected molecular mass ~4.4kb, ~2.4kb and ~5 kb of DMT1+IRE, DMT1-IRE and TfR are presented in Fig 7-2. The modulation of gene expression demonstrated that treatment with different dilutions of L-dopa increased DMT1-IRE mRNA levels 4-fold (10 μM) and 3.5-fold (30 μM). Levels in the 100 μM treated group increased about 1.4-fold, but it

is not significant to control (Fig 7-2B). In contrast to DMT1-IRE, DMT1+IRE (Fig 7-2A) and TfR (Fig 7-2C) mRNA remained unchanged.

7.4.3 Influence of L-dopa on the DMT1+IRE, DMT1-IRE, Ferroportin1 and Transferrin Receptor Protein synthesis

The influence of L-dopa on distribution of the two isoforms of DMT1 and TfR was examined to elucidate the L-dopa function in iron transport. Both forms of DMT1 are proteins with 12 putative membrane-spanning domains that are presumed to be located at the cell membrane and/or within the endosomal fraction of the cell. Tf-TfR is a mainly iron uptake route in the most kinds of cell. Changes in the two forms of DMT1, FP1 and TfR proteins were induced by L-dopa concentrations ranging from 0 μM to 100 μM were detected by Western blots in C6 glioma cells. A single major band was observed with these antibodies, with an M_r of ~56 kDa for both isoforms of DMT1 (Fig. 7-3A, Fig. 7-3B), ~60 kDa for FP1 (Fig. 7-3C), ~90 kDa for TfR (Fig. 7-3D) and ~45 kDa for β-actin, which was in good agreement with the expected molecular weights based on published papers. As shown in Fig. 7-3B, the change of DMT1-IRE protein was induced by L-dopa concentrations greater than or equal to 0 μM, with significant induction occurring at concentrations of 5 μM, 10 μM, 30 μM. The maximum level of DMT1-IRE protein was induced by 10 μM L-dopa treatment. However, at L-dopa concentrations of both 60 μM and 100 μM, no effect of L-dopa on regulation of DMT1-IRE protein synthesis was observed. The expression of DMT1+IRE, FP1, TfR and control protein, β-actin, was unchanged throughout these experiments. Data from three independent experiments showed that the induction of DMT1-IRE protein was more than double in the case of 10 μM of

L-dopa treatment, and about 3-fold with 30 μM of L-dopa treatment. These results clearly reveal that in L-dopa treatment of C6 glioma cells the increase in DMT-IRE protein was paralleled by an increase in DMT-IRE mRNA. The optimum concentration of L-dopa ranged between 10 μM and 30 μM.

7.4.4 Effect of L-dopa Treatment on the C6 Glioma Cells Iron (II) Uptake

The acetoxymethyl ester of calcein (calcein-AM) is a nonfluorescent, membrane-permeate dye readily taken up by live cells. Once within the cytoplasm, calcein-AM is cleaved by cytoplasmic esterases, releasing the membrane-impermeate calcein fluorophore. Calcein fluorescence is stable and is quenched rapidly and stoichiometrically by ferrous ions. In order to confirm that the calcein method provides a valid measure of the ferrous uptake, a base line signal was obtained for normal conditions and non-ferrous cells (Fig 7-4A). This indicated fluorescence was steady in the 30 min recording. After stabilization of the fluorescence signal, 8 μM FAS was added to the untreated C6 glioma cells (B) and those given 10 μM (C), 30 μM (D), 100 μM (E) L-dopa incubation. Results show that calcein fluorescence was time-dependent quenched by FAS. There was no significant difference between the untreated and L-dopa treated group until 20 min. Significant quenching of fluorescence was observed after 20 min of incubation at 37 ℃ between the untreated group (B: -7.93% ± 0.81%, at 20 min; -9.15% ± 0.84%, at 25 min; -10.08% ± 1.78%, at 30 min) the 10 μM L-dopa treated group (C: -13.83% ± 1.59%, at 20 min; -15.53% ± 1.88%, at 25 min; -18.52% ± 1.26%, at 30 min) and the 30 μM L-dopa treated group (D: -12.81% ± 0.82%, at 20 min; -14.89% ± 1.09%, at

25 min; -17.23% ± 1.20%, at 30 min). There was no significant decrease in 100 μM L-dopa treated group. This indicates that L-dopa treatment increased the ferrous uptake in C6 glioma cells.

7.5 DISCUSSION

Important advances in the fields of physiology and pathophysiology of brain iron metabolism have been made with new findings on the role of DMT1, FP1, Heph, CP and TfR in brain iron transport. At least in some NDs, brain iron misregulation is an initial cause of neuronal death and recent studies suggest that this misregulation might be led by either genetic or non-genetic factors (Qian and Shen, 2001). Iron accumulation in the brain occurs in a number of NDs. The membrane TfR mediated endocytosis or internalization of Tf bound iron and the TfR is the major route of cellular iron uptake (Li et al., 2002; Li et al., 2003a). DMT1 is a glycosylated protein composed of 12 transmembrane domains that has been shown to act as an iron transporter either by itself, or in conjunction with TfRs in the endomembrane compartment. Ferroportin1 is a newly discovered transmembrane iron export protein. It plays a key role in Fe^{2+} transport across the basal membrane of enterocytes in the gut. It has been suggested that this protein may have the same role in Fe^{2+} transport across the abluminal membrane of the blood-brain barrier as in enterocytes. Our immunocytochemistry studies of DMT1+IRE, DMT1-IRE, TfR and FP1 with special antibody confirmed that C6 glioma cells were able to expression those proteins.

In the present study we investigated the regulation of the iron-uptake proteins TfR, DMT1+IRE, DMT1-IRE and the iron-release protein FP1 by L-dopa in C6 glioma

cells. As demonstrated by Northern blot and Western blot analyses, TfR, DMT1+IRE and FP1 mRNA expression and protein synthesis was not regulated by the concentrations of L-dopa. DMT1-IRE mRNA expression and protein synthesis, however, enhanced by varying concentration of the L-dopa the optimal being is 10 μM. Because of the significant correlation of DMT1-mRNA and protein expression at same concentration of L-dopa (r=0.927, P<0.001), the regulation of DMT1-IRE gene expression by L-dopa is likely to be at the transcriptional level. Mammalian DMT1 exists as two different isoforms resulting from alternative splicing of the 3' terminal exons. Utilization of the proximal polyadenylation site present in exon 16 gives rise to isoform I mRNAs, which contains a putative iron responsive element (IRE) in its 3' non-coding region. Alternative splicing using a 5' splice acceptor site present in exon 16 and the 3' splice site of exon 17 gives rise to isoform II mRNA devoid of IRE (Gunshin et al., 1997; Fleming et al., 1998; Tchernitchko et al., 2002). The DMT1 protein isoforms also differ in their last C-terminal 18 (DMT1+IRE) or 25 (DMT1-IRE) amino acids. The expression of DMT1 is highly inducible by iron deficiency (Trinder et al., 2000; Gambling et al., 2001; Zoller et al., 2002) and is suppressed by iron overload (Tandy et al., 2000) because of the role for the IRE in regulating mRNA stability in response to variations in cell iron status. However, very little results of regulation of DMT1-IRE gene expression were obtained. Our data show DMT1-IRE was able to regulate by L-dopa, but the mechanism need further study.

DMT1+IRE is predominantly expressed in epithelial cell lines (Canonne-Hergaux et al., 1999), whereas DMT1-IRE is expressed in the blood cell lines (Canonne-Hergaux et al., 2001a). In HEp-2 cells, GFP-tagged DMT1+IRE is

localized in late endosomes and lysosomes, whereas GFP-tagged DMT1-IRE is localized in early endosomes (Tabuchi et al., 2002). The DMT1-IRE is predominantly localized in the plasma membrane, early/recycling endosomes and the endoplasmic reticulum (Touret et al., 2003). Kinetic studies by surface labeling with [^{125}I]-labeled antibodies established that the fraction of endomembrane DMT1-IRE was approximately equal to that on the cell surface. The 2 components are in dynamic equilibrium: surface transporters are continuously internalized via a clathrin and dynamin-dependent process, while endosomal DMT1-IRE is recycled to the plasmalemma by a phosphatidylinositol 3-kinase-dependent exocytic process. This indicates DMT1-IRE is the entity responsible for transmembrane transport of the iron released from Tf to the early endosomal lumen (Touret et al., 2003). Our results support the proposal that increased DMT1-IRE contributes to the Tf-TfR mediated iron uptake in C6 glioma cells. After the ferrous was added, no significant difference was observed in the calcein fluorescence quenching in L-dopa treated cells compared to control in the initial 15min. This phase was perhaps due to NTBI uptake (such as DMT1+IRE or DMT1-IRE). After 20 min, the fluorescence quenching in the 10 and 30 μM treated groups was significantly faster than the control group, in line with the DMT1-IRE high expression in the two groups.

As described above, L-dopa treatment enhances DMT1-IRE gene expression and increases iron uptake in the C6 glioma cells, therefore, the data suggests that L-dopa treatment induces the Fenton reactions producing the more toxic hydroxyl radical (OH ·), which inflict oxidative damage on neurons (Jenner and Brin, 1998). However, the detailed mechanism requires further study.

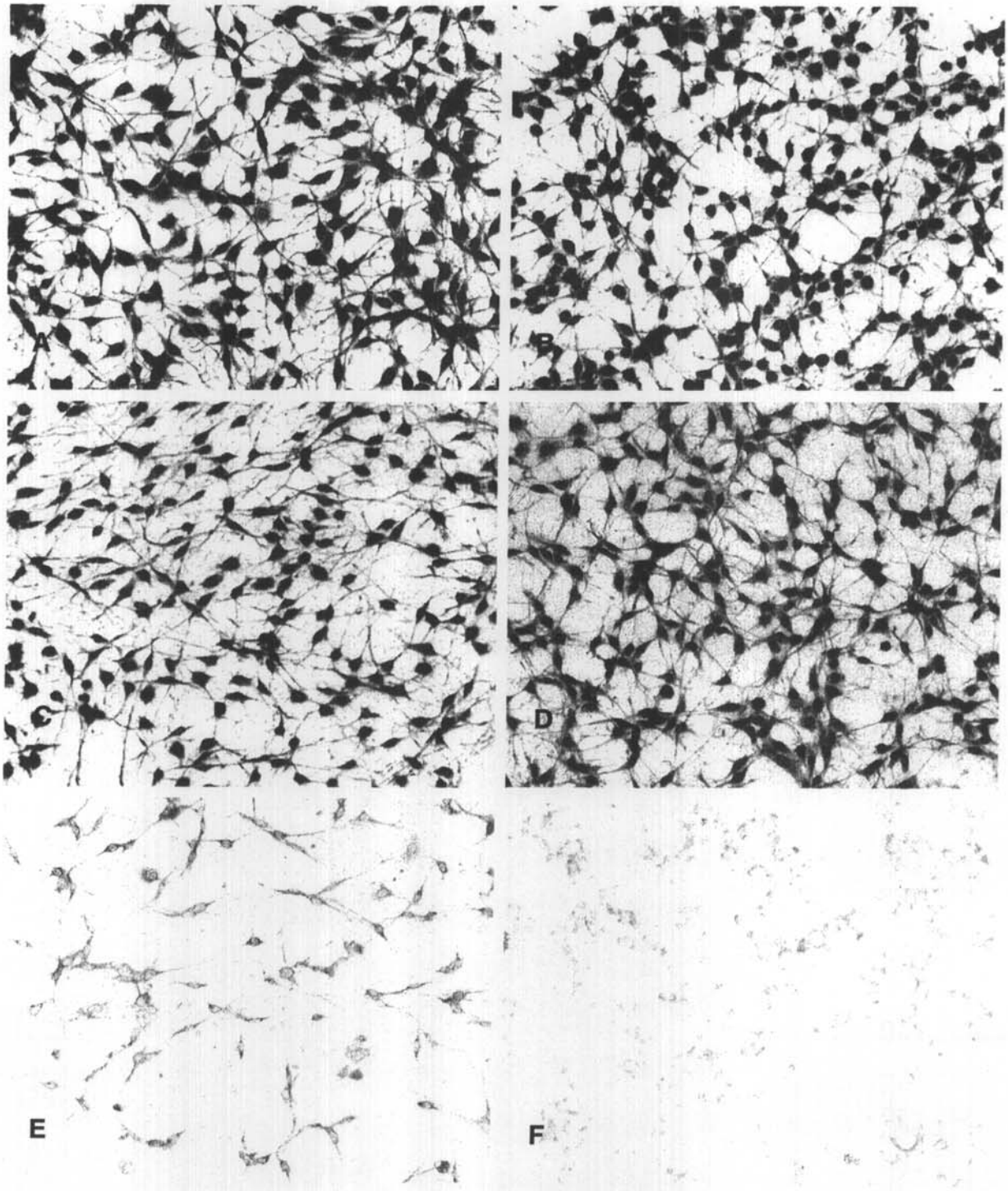

Figure 7-1. Immunocytochemical study of DMT1+IRE, DMT1-IRE, FP1 and TfR in C6 giloma cells. The cells (A), (B), (C) and (D) showed a marked positivity for TfR, FP1, DMT1-IRE and DMT1+IRE. Control images (E, the primary antibody instead of normal rabbit serum) and (F, the primary antibody instead of normal mouse serum) demonstrate no specific staining. Magnification = 400×.

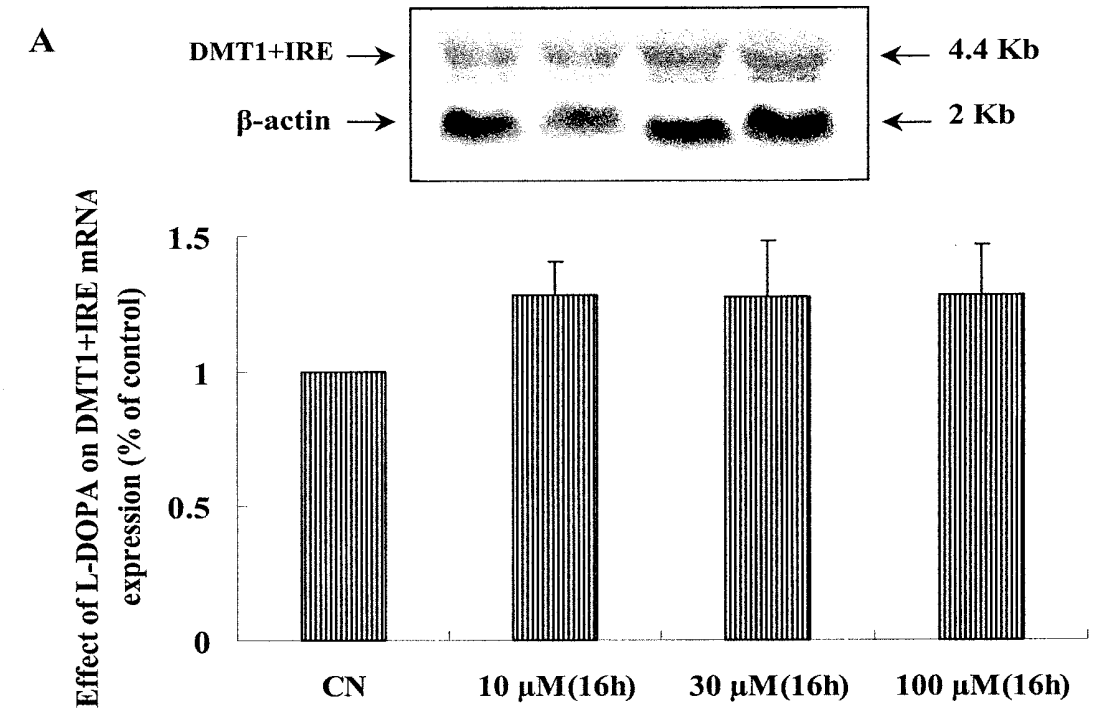
A
DMT1+IRE
β-actin
4.4 Kb
2 Kb
Effect of L-DOPA on DMT1+IRE mRNA expression (% of control)
1.5
1
0.5
0
CN
10 μM(16h)
30 μM(16h)
100 μM(16h)

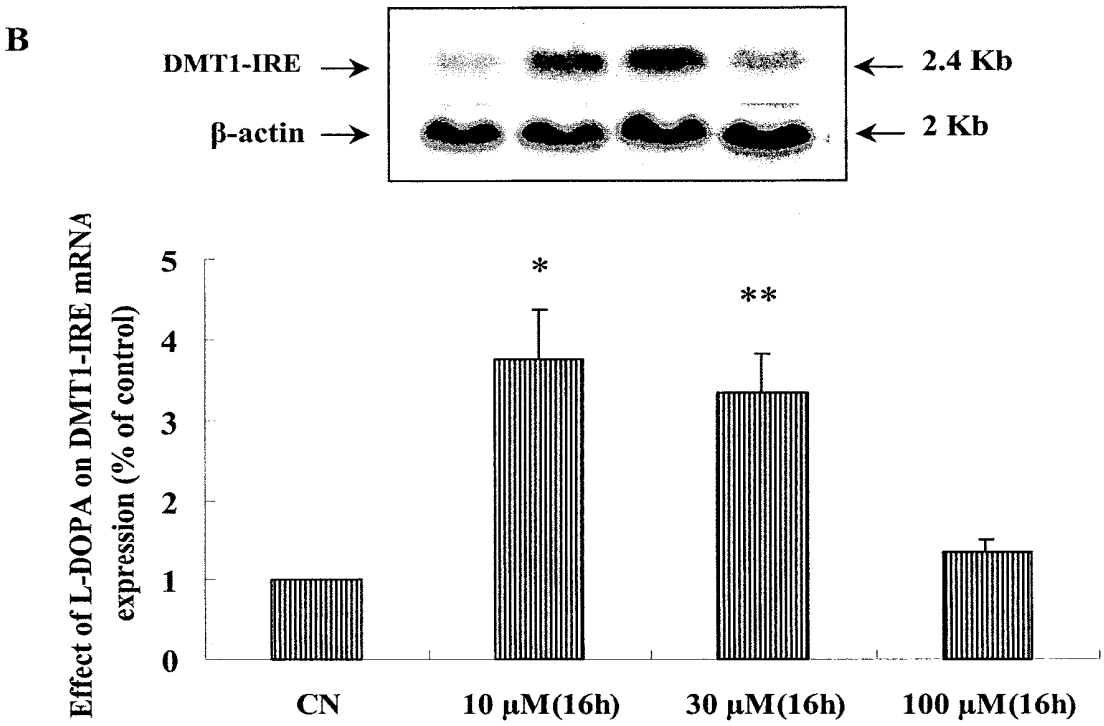
B
DMT1-IRE
β-actin
2.4 Kb
2 Kb
Effect of L-DOPA on DMT1-IRE mRNA expression (% of control)
5
4
3
2
1
0
*
**
CN
10 μM(16h)
30 μM(16h)
100 μM(16h)

C

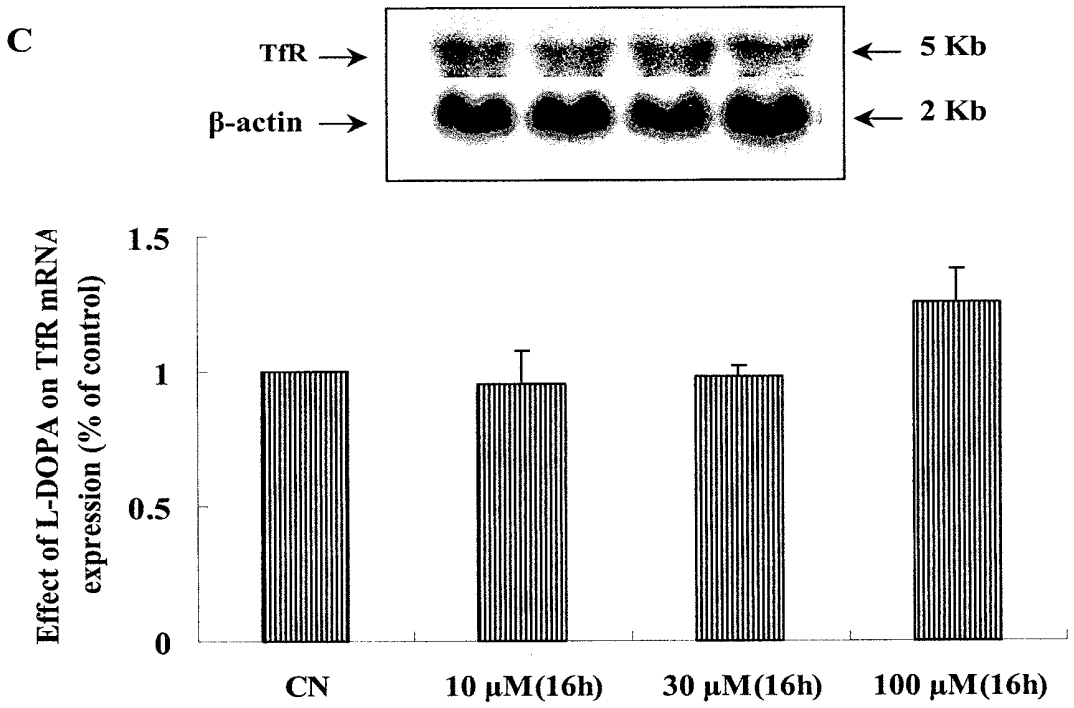
TfR
β-actin
5 Kb
2 Kb
Effect of L-DOPA on TfR mRNA expression (% of control)
1.5
1
0.5
0
CN
10 μM(16h)
30 μM(16h)
100 μM(16h)

Figure 7-2. Effect of L-dopa on DMT1+IRE (**A**), DMT1-IRE (**B**) and TfR (**C**) gene expression by C6 glioma cells. Total cellular RNA was isolated from C6 glioma cells treated without or with 10 μM, 30 μM, 100 μM L-dopa for 16 hours. 30 μg total RNA was were electrophoresed and transferred to Hybond-N^+ membrane as described in Materials and Methods. The Northern blot was hybridized with randomly primed ^{32}P-labeled probe for DMT1+IRE, DMT1-IRE or TfR and exposed to a phosphor screen for 8-24 hours for image analysis. To confirm equal loading of RNA, each blot was rehybridized with ^{32}P-labeled probe for β-actin. Shown are band intensities for ~4.4kb, 2.4-kb, 5kb and 2kb transcripts for DMT1+IRE (**A**), DMT1-IRE (**B**), TfR (**C**) and β-actin, respectively. *Lane 1*, untreated control; *lane 2-4*, 10 μM, 30 μM, 100 μM L-dopa treated for 16 hours. The radioactivity in bands for DMT1+IRE (**A**), DMT1-IRE (**B**) or TfR (**C**) was quantified using ImageQuant software (Molecular Dynamics, Sunnyvale, CA) and normalized to values obtained for β-actin. Data are means of % control ± SEM from 3 independent experiments. $*P < 0.05$, $**P < 0.01$ vs. control.

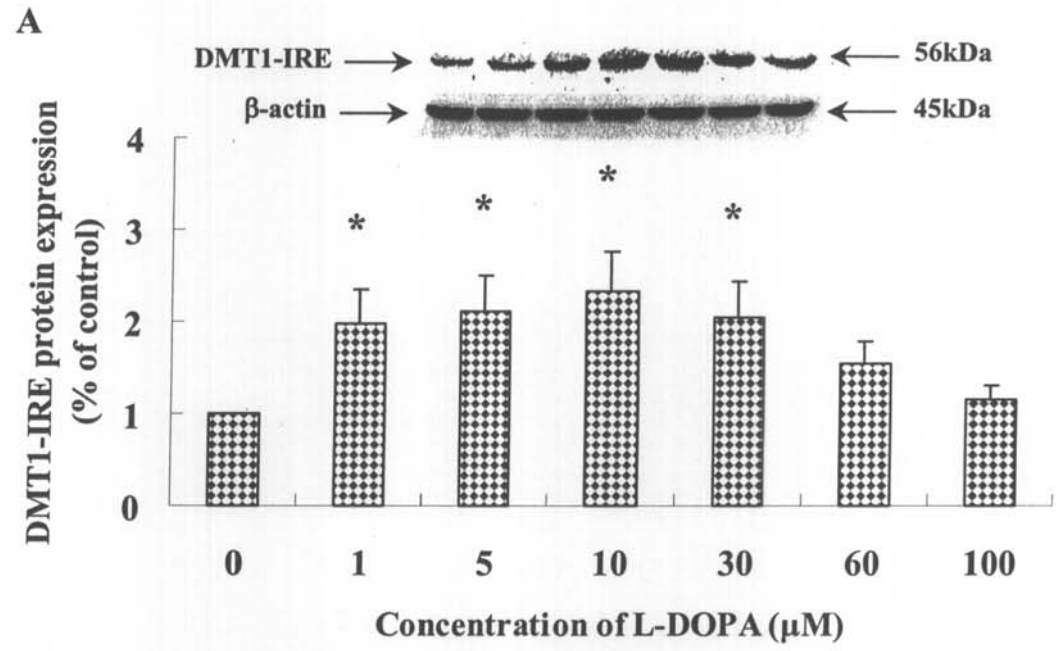
A
DMT1-IRE
β-actin
56kDa
45kDa
DMT1-IRE protein expression (% of control)
0
1
2
3
4
*
*
*
*
0
1
5
10
30
60
100
Concentration of L-DOPA (μM)

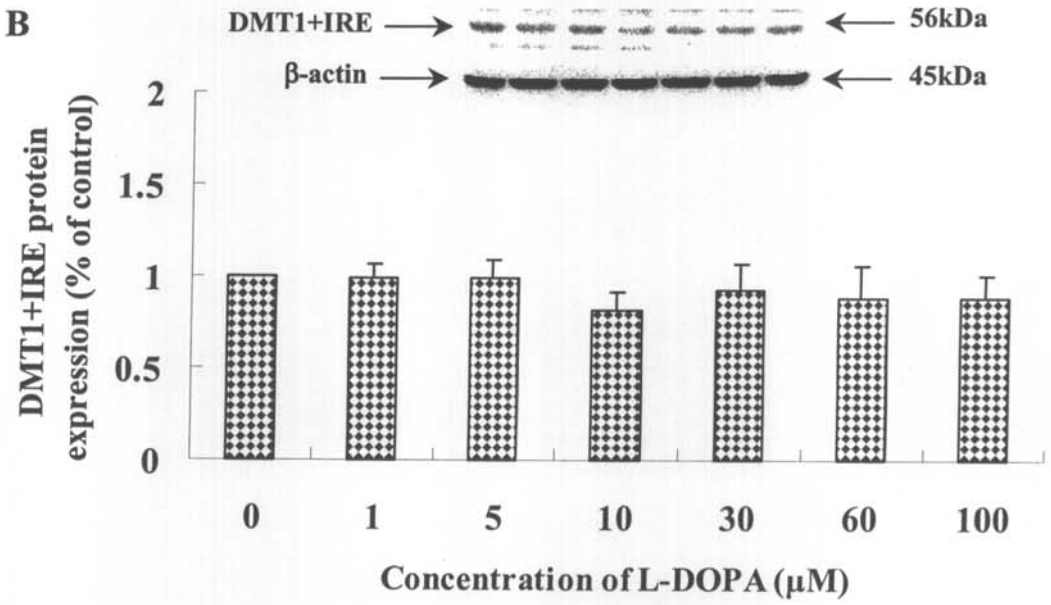
B
DMT1+IRE
β-actin
56kDa
45kDa
DMT1+IRE protein expression (% of control)
0
0.5
1
1.5
2
0
1
5
10
30
60
100
Concentration of L-DOPA (μM)

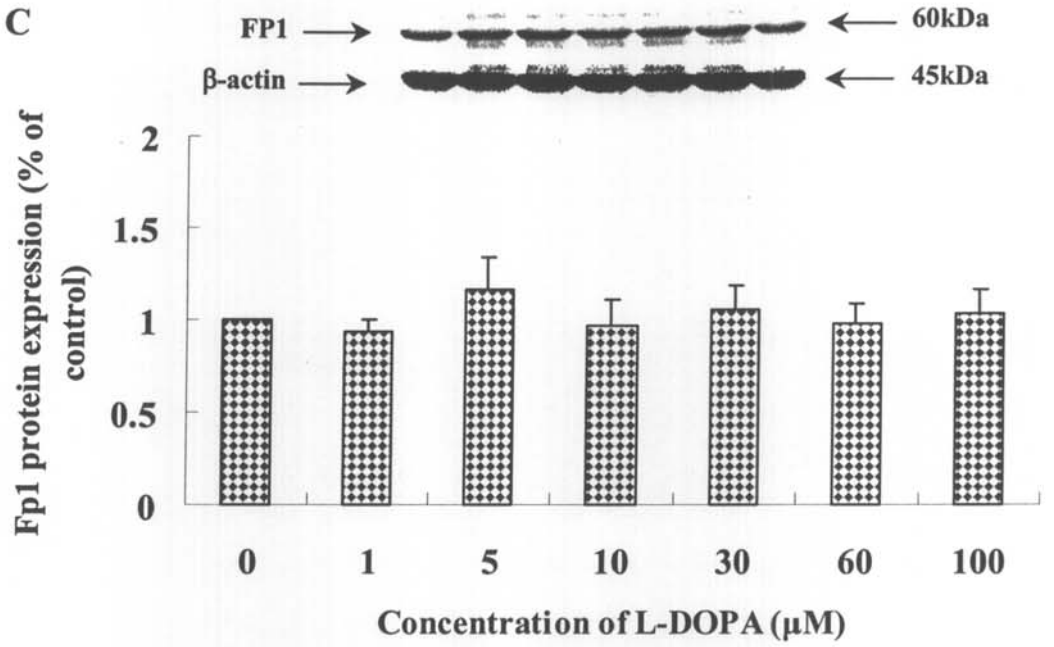
C
FP1
β-actin
60kDa
45kDa
Fp1 protein expression (% of control)
2
1.5
1
0.5
0
0
1
5
10
30
60
100
Concentration of L-DOPA (μM)

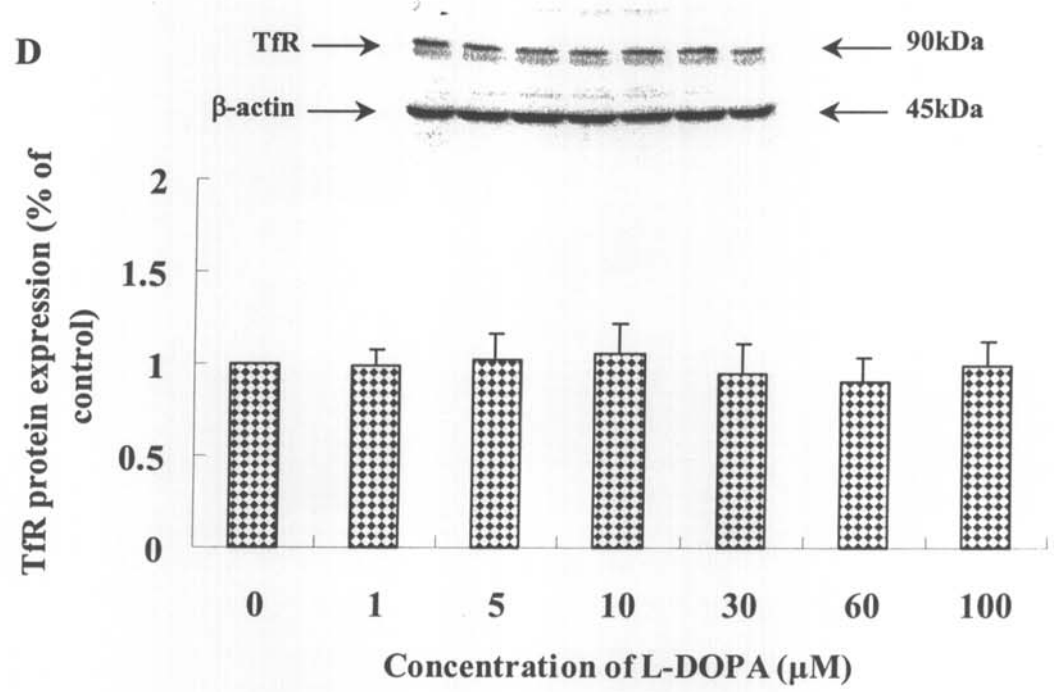
D
TfR
β-actin
90kDa
45kDa
TfR protein expression (% of control)
2
1.5
1
0.5
0
0
1
5
10
30
60
100
Concentration of L-DOPA (μM)

Figure 7-3. Effect of L-dopa on DMT1+IRE, DMT1-IRE, FP1 and TfR protein expression. Western blot analyses were performed as described in Materials and Methods. The *Mr* of ~65 kDa for DMT1+IRE (**A**) and DMT1-IRE (**B**), ~60 kDa for FP1 (**C**), ~90 kDa for TfR (**D**) appeared as single band on each gel, with the bands of β-actin corresponding to the expected molecular weight (45 kDa). The effect of L-dopa on DMT1+IRE (**A**), DMT1-IRE (**B**), FP1 (**C**), TfR (**D**) protein synthesis was tested with Western blot analysis. The experiments were performed in duplicate for three samples in each group. Expression values were normalized for β-actin and expressed as a percentage of control. Different letters above data bars indicate that these groups are statistically different from each other ($^*P < 0.05$).

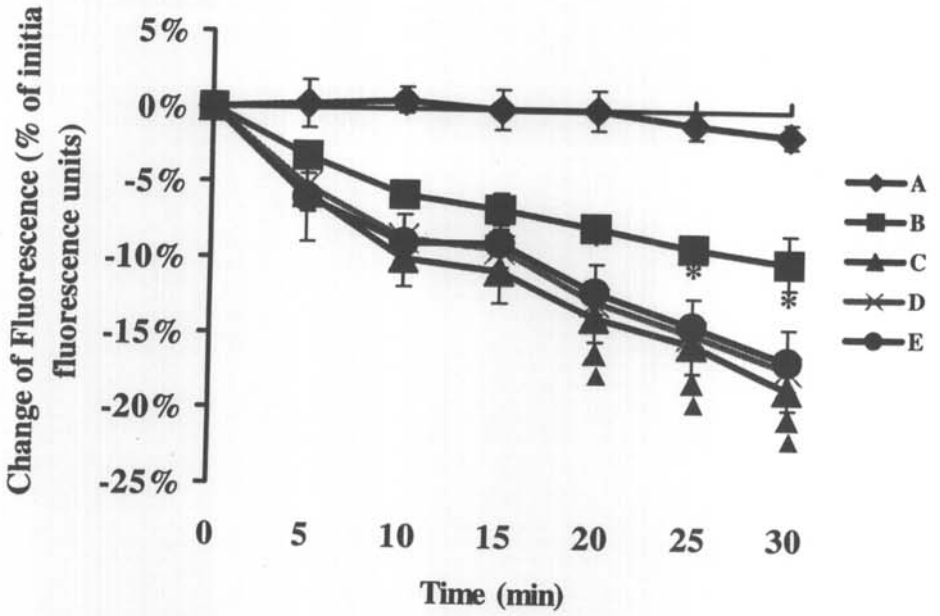

Figure 7-4. Effect of L-dopa on C6 glioma cells ferrous uptake. C6 glioma cells were treated with L-DOPA as described in Materials and Methods. For the kinetic fluorescence measurements on the BMG (Durham, NC, USA) Fluostar Galaxy fluorescence plate reader (λ_{ex} -of 485 nm, λ_{em} of 520 nm, 37℃) excitation and emission probes were directed to the bottom of the plate. 100 μl HEPES was added and initial baseline fluorescence intensity data was collected, 8 μM FAS was added by pipetting 1 μl of stock aqueous FAS solution into the 0 μM (**B**); 10 μM (**C**); 30 μM (**D**) and 100 μM (**E**) L-DOPA treated cell wells and gently mixing the solution. The quenching of calcein fluorescence by divalent metals was measured every 5min for 30 min. The change of fluorescence value has been normalized percentage to the steady-state values of fluorescence before addition of the FAS. The fluorescence assay for ferrous uptake by C6 cells performed in duplicate of three independent experiments. The data represent means ± SEM. Different letters near the traces indicate that the change of fluorescence is statistically different with the control (**A**) in different time: ▲ $P<0.05$, 10 μM (C), * $P<0.05$, 30 μM (D) L-DOPA treated group to control (B).

CHAPTER 8

THE EFFECT OF NEUROTRANSMITTER GAMMA-ANINOBUTYRIC ACID AND GLUTAMATE ON THE EXPRESSION OF IRON TRANSPORTERS

8.1 ABSTRACT

Iron appears widespread throughout the brain and has a specific and uneven distribution. The substantia nigra, ventral pallidum, globus pallidus and cerebellar nuclei are iron rich areas. In some NDs, iron is accumulated in the substantia nigra and globus pallidus. These areas receive GABA-containing efferents and have high concentrations of GABA and glutamic acid decarboxylase. This study examined the effect of GABA and glutamate on the gene expression of iron transporter proteins in C6 glioma cells. From Northern and Western blot analysis, 10 μM GABA treatment induced on increase in Heph gene expression and 10 μM glutamate treatment induced a decrease in Heph synthesis. TfR gene expression was suppressed by 100 μM GABA and 1, 100, 1000 μM glutamate treatment. Results from this study suggest neurotransmitter regulation of the iron metabolism is though the control of the iron transport proteins.

KEY WORDS

GABA, Glutamate, Iron Metabolism, Brain, Transferrin Receptor, Hephaestin, Ceruloplasmin, Ferroportin1, DMT1

8.2 INTRODUCTION

Iron is the most abundant trace metal in the brain (Beard et al., 1993b; Beard et al., 1993a). The importance of iron for normal neurological function has been well established. As in all cells, neurons and glia require iron for many aspects of their physiology, including electron transport, NADPH reductase activity, myelination of axons, and as a co-factor for several enzymes involved in neurotransmitter synthesis. Hence, an imbalance in brain iron results in dysfunction in iron-related metabolism (Gelman, 1995; Owen et al., 1996; Schipper, 1996). However, very little is known about the regulation of iron concentration in the central nervous system and about the mechanisms of iron uptake and release in brain cells. The concentration of iron in the brain is region dependent, the substantia nigra, ventral pallidum, globus pallidus and cerebellar nuclei being iron-rich areas (Hill and Switzer, 1984). At cellular level, the oligodendrocyte is the predominant cell type containing iron in the brain (Connor et al., 1990; Connor and Menzies, 1996). Some brain areas that are iron rich in adult rats are not iron rich in the neonatal and young rats (Connor et al., 1992; Erikson et al., 1997; Focht et al., 1997), but the reason(s) for the change of iron distribution in the developing brain is not clear (Qian and Shen, 2001). In humans, increased iron concentrations in the substantia nigra and accompanying SN neuronal loss occur in

several NDs, including Hallervorden-Spatz disease, multiple system atrophy and progressive supranuclear palsy (Dexter et al., 1991; Gibb, 1991). Iron is also significantly increased in the globus pallidus in Alzheimer's disease (AD) and Parkinson's disease (PD) (Loeffler et al., 1995). The striatum and the SN are two key components in the motor circuit relevant to movement disorders. As previous study exhibited, the substantia nigra and globus pallidus receive substantial innervation from the neostriatum, a considerable amount of which is GABAergic, and also receive excitatory (glutamatergic) efferents of the subthalamic nucleus (STN) (Wichmann and DeLong, 1996, 1999). Synaptic GABA is taken up by nerve endings, GABAergic perikarya, or by glial cells. Once taken up, GABA is transaminated by GABA-transaminase, producing succinate semialdehyde and glutamate (Hill, 1985). Glutamate is a highly abundant neurotransmitter in the striatum. The striatum receives major glutamatergic projections from most cortical areas (McGeorge and Faull, 1989) and from the thalamus (Lapper and Bolam, 1992). Release of dopamine from the terminals of the nigrostriatal projection appears to modulate the activity via two pathways: transmission over the direct pathway is facilitated via dopamine D1 receptors and transmission over the indirect pathway is inhibited via dopamine D2 receptors. The overall effect of striatal dopamine release is to reduce basal ganglia output, leading to increased activity of thalamocortical projection neurons (Wichmann and DeLong, 1996, 1999). There is considerable the overlap GABAergic and glutamatergic projections with the intense iron accumulated in substantia nigra pars reticulata and GP. Previous studies investigating the potential relationship between GABA and brain iron, Hill injected an inhibitor of GABA degradation into the GP and adjacent neostriatum and directly into the SN (Hill, 1985). These injections resulted in decreased substantia nigra pars reticulata iron staining two days

later, providing the first evidence that histochemical levels of brain iron are related to GABA utilization/metabolism. Shoham et al. (Shoham et al., 1992) reported that after unilateral microinjection of excitatory amino acids, kainate, or quinolinate to the anterior olfactory nucleus/ventral striatal region, an increase in histochemical iron concentration was observed in the ipsilateral ventral pallidum, the globus pallidus and the substantia nigra pars reticulata. After microinjection of ibotenate or quisqualate to the nucleus basalis of Meynert, iron also accumulated in the pars reticulata of substantia nigra. Sastry and Arendash (Sastry and Arendash, 1995) further investigated the progressive increase in both iron staining in the substantia nigra zona reticularis and iron concentration in the substantia nigra by neostriatum/globus palldus lesion. These results suggest that lose or dysfunction of striatonigral/striatopallidal GABAergic neurons in several NDs may result in an increase or redistribution of nigral iron, resulting in loss of substantia nigra neurons. However, what mechanism involved in the iron accumulation induced by neurotransmitters is not being performed.

Intracellular iron balance depends on the amount of iron taken up as well as on the amount of iron released by the cell (Qian and Wang, 1998; Qian and Shen, 2001). TfR mediated endocytosis or internalization of the complex of Tf bound iron and the TfR is the major route of cellular iron uptake (Li et al., 2002; Li et al., 2003b). DMT1 may be involved in translocation of iron from endosome to cytosol under physiological conditions (Su et al., 1998; Tabuchi et al., 2000; Touret et al., 2003). On other hand, the DMT1 may play an important role in iron transport across the apical surface of human intestinal Caco-2 cells (Tandy et al., 2000) and rat duodenal enterocytes (Trinder et al., 2000) in Tf-independent uptake of iron. CP is an

abundant plasma protein synthesized mainly in hepatocytes. A role for CP in iron efflux was first suggested in the 1960s, based on the observation that the ferroxidase activity of CP promoted iron incorporation into Tf (Osaki et al., 1966). This suggestion is supported by aceruloplasminemia (Gitlin, 1998) and animal model of aceruloplasminemia (Harris et al., 1999). Recent gene mapping studies have identified a CP homologue, Heph, which is expressed predominantly in the small intestine (Vulpe et al., 1999). Heph facilitates the transport of iron from enterocyte to plasma, but it is not a membrane transporter. Ferroportin1 (FP1) was recently identified as a duodenal iron export molecule (Donovan et al., 2000). The basolateral membrane of the duodenal is the primary iron regulatory site, FP1 and Heph may work together in iron transport from the enterocytes into the circulation. In other cell types, Ferroportin1 may work with CP, to load iron onto Tf to enhance the iron release from the cell (Fleming and Sly, 2001b). The current study is designed to determine the effect of neurotransmitters GABA and glutamate on the expression of iron transporters genes in C6 glioma cells.

8.3 MATERIALS AND METHODS

8.3.1 Materials

Please refer to chapters 2 and 7.

8.3.2 Methods

8.3.2.1 Cell Culture

Please refer to chapters 2 and 5.

When the cells reached about 65-70% confluence, the experiments were initiated by changing medium followed by addition of various concentrations GABA and glutamate as indicated in the figure legends.

8.3.2.2 RNA Purification, Generation of Specific Probes, and Northern Blot Assay

Please refer to chapters 2, 4, 5 and 7.

8.3.2.3 Western Blot Analysis

Please refer to chapters 2, 5 and 7.

The dilution of mouse anti-rat TfR monoclonal antibody (BD Bioscience) is 1:1000; rabbit anti-rat DMT1+IRE, DMT1-IRE1 polyclonal antibody, rabbit anti-mouse FP1 polyclonal antibody and rabbit anti-mouse Heph polyclonal antibody (Alpha Diagnostic, USA) is 1:5000; purified mouse anti CP IgG1 (BD Transduction Laboratories, BD Biosciences, USA) is 1:1000 and anti-rabbit secondary antibody conjugated horseradish peroxide is 1:5000.

8.3.3 Statistical Analysis

Please refer to chapter 3.

8.4 RESULTS

8.4.1 Effect of GABA and Glutamate on Transferrin Receptor mRNA Expression and Protein Synthesis in C6 Glioma Cells

To determine whether GABA and glutamate modulates TfR gene expression, C6 glioma cells grown in 75 cm^2 flask were treated for 16 hours with 0 μM, 10 μM, 100 μM, 1000 μM GABA and glutamate. Northern blot analysis was quantified by densitometry, and total RNA loading was corrected using β-actin expression. Representative Northern blot showed one mRNA band with the expected molecular mass ~5 kb is presented in Fig 8-1A. After being normalized to β-actin expression, the levels of TfR mRNA significantly decreased in all concentrations of glutamate-treated and in 100 μM GABA treated cells (Fig 8-1B). Western blot analysis detected the expression of the TfR protein synthesis in C6 glioma cells. A single major, M_r of ~90 kDa band was observed with TfR monoclonal antibody (Fig 8-1C). This is in good agreement with the expected molecular weight based on published papers. As shown in Fig 8-1D, the change of TfR protein synthesis induced by GABA and glutamate approximately paralleled changes of mRNA expression. Because the decreased protein is greater than mRNA, this is implies a post-regulation mechanism is involved in the TfR expression. At present, no data

was reported about the regulation of TfR gene expression, but investigators was found that the excitatory neurotransmitter glutamate (5 μM) increased TfR transcytosis during the Tf starvation period, whereas the inhibitory neurotransmitter GABA (10 μM) reduced it in the constant presence of Tf (Hemar et al., 1997). Since glutamate increases the efficiency of TfR transcytosis, ensuring iron uptake of the cell to perform the physiological function, it is possible decreasing the TfR protein synthesis. In our experiments, no Tf was added to the cell culture medium, low concentration of GABA showed no effect on TfR expression. Decreased TfR expression observed in high concentration (100 μM) of GABA, the mechanism requires further discussion.

8.4.2 Effect of GABA and Glutamate on DMT1-IRE and DMT1+IRE mRNAs Expression and Proteins Synthesis in C6 Glioma Cells

DMT1 is a proton-dependent cation transporter, which plays a central role in iron homeostasis. The DMT1+IRE mRNA contains an iron-responsive element (IRE) in its 3' UTR region, and its abundance is controlled by the prevailing concentration of intracellular iron (Canonne-Hergaux et al., 1999; Tandy et al., 2000; Yeh et al., 2000; Gunshin et al., 2001). DMT1+IRE is expressed in the apical membrane of duodenal enterocytes and in kidney epithelial cells (Gunshin et al., 1997; Burdo et al., 2001; Ferguson et al., 2001; Tallkvist et al., 2001). DMT1-IRE lacks the IRE and differs from DMT1+IRE at its C-terminus. It is expressed in non-epithelial cells and is particularly abundant in erythroid cells (Canonne-Hergaux et al., 2001b). Our previous study demonstrated that the two forms of DMT1 mRNA and protein

expression in rat heart is age-dependent and that both forms of DMT1 mRNAs both are regulated by iron at the post-transcriptional level only (Ke et al., 2003). The current data found that DMT1+IRE and DMT1-IRE mRNAs are expressed in C6 glioma cells, with a high ratio of DMT1-IRE to DMT1+IRE at both mRNA and protein levels. (Fig 8-2A, 8-2C; Fig 8-3A, 8-3C). A number of studies have reported that the ratio of DMT1+IRE to DMT1-IRE mRNA varies in different tissues. Like C6 glioma cells, the spleen, thymus, and pancreas have low ratios of DMT1+IRE to DMT1-IRE, whereas the heart, brain and intestine have high ratios of DMT1+IRE to DMT-IRE. The difference in expression of two forms of DMT1 mRNA may be due to the specificity of tissue (Ke et al., 2003). Northern blot analysis showed that the effect of GABA and glutamate on regulation of the two isoforms of DMT1 is different in C6 glioma cells (Fig 8-2B, Fig 8-3B): 1 μM glutamate significantly increased DMT1-IRE mRNA expression and 1 μM GABA decreased it, however, the DMT1+IRE mRNA expression remained unchanged. Western blot analysis of the synthesis of the two forms of DMT1 proteins found a similar pattern of regulation between DMT1-IRE, DMT1+IRE mRNAs and proteins: low concentration of glutamate increased the DMT1-IRE protein synthesis and GABA suppressed it; DMT1+IRE protein showed no significant change after treatment with GABA and glutamate. This suggests that the regulation of DMT1-IRE mainly exists at transcriptional level. The possibility of the post-transcriptional regulation cannot be excluded.

8.4.3 GABA and Glutamate Has Little Effect on Ferroportin1 mRNA Expression and Protein Synthesis in C6 Glioma Cells

Ferroportin1 is a newly discovered transmembrane iron export protein. It plays a key role in Fe^{2+} transport across the basal membrane of enterocytes in the gut (Donovan et al., 2000). We investigated the expression of ferroportin1 protein in different brain regions, including cortex, hippocampus, striatum and substantia nigra, in developing male Sprague-Dawley rats. The results provided direct evidence for the existence of ferroportin1 protein in the rat brain (Jiang et al., 2002). In present study, Northern blot and Western blot analysis were performed to determine FP1 mRNA expression and protein synthesis in C6 glioma cells. These results showed that FP1 mRNA and protein were in the cell line (Fig 8-4A, Fig 8-4C), suggesting that this protein may play a role in the cells iron metabolism. As an iron exporter, FP1 may also play a role in iron release from some types of brain cell, keeping iron balance within the cells (Qian and Shen, 2001). In this study, we analyzed the effect of GABA and glutamate on FP1 mRNA expression and protein synthesis. However, no significant difference was found between GABA and glutamate treated groups and control group, either at the mRNA level or the protein level ($P>0.05$, Fig 8-4B and Fig 8-4D). FP1 mRNA contains a consensus IRE motif in its 5'UTR. An IRE/IRP-dependent iron-regulatory pathway for the FP1 gene appears to exist in the rat heart (Chapter 6) and in lung cells (Yang et al., 2002). In duodenal entreocytes, however, the iron-regulatory pathway is IRE/IRP-independent (Abboud and Haile, 2000; Martini et al., 2002; Chen et al., 2003a). Knowledge about the regulation of FP1 gene expression by other factors is limited. The neurotransmitters GABA and glutamate were not involved in the regulation of FP1 mRNA expression and protein synthesis.

8.4.4 Effect of GABA and Glutamate on Ceruloplasmin, Hephaestin Gene Expression in C6 Glioma Cells

As shown in Fig. 8-5A and Fig. 8-6A, the expression of Heph and CP mRNA was tested by Northern blot. Heph mRNA (~5 kb) and CP mRNA (~4 kb) were detected and the molecular sizes were consistent to previous reports (Fleming and Gitlin, 1990; Vulpe et al., 1999). Expression of Heph and CP proteins was determined by immunoblotting. As shown in Fig 8-5C, a major component of ~110 kDa immunoactive band of Heph was observed. This molecular weight is lower than that published by Anderson (Anderson et al., 2002b). To our knowledge, this is the first report on the Heph protein expression in C6 glioma cells as well as in the neurons of rat brain (chapter 4) and myocyte of rat heart (chapter 6). As shown in Fig 8-6C, we also detected a *Mr* ~150 kDa CP immunoactive band consistent with the expected molecular weight (Patel and David, 1997; Patel et al., 2000). The CP expressed by C6 glioma cells is likely to be the glycosylphosphatidylinositol (GPI) anchor form, which may play a role similar to the secreted form in oxidizing ferrous iron (Patel and David, 1997; Jeong and David, 2003) and in antioxidant defense (Mittal et al., 2003).

Next, the effect of GABA and glutamate on Heph and CP expression was analysed. mRNA levels relative to β-actin for each transcript from independent samples are shown in Fig 8-5B and Fig 8-6B. The transcript level of Heph mRNA was significantly decreased in the 1 μM glutamate treated group and increased in the 1 μM GABA treated group but the high concentrations of GABA and glutamate had little effect on Heph mRNA expression. CP mRNA level was significantly decreased

only in high concentrations GABA and increased with rising the glutamate concentrations. As illustrated in Fig 8-5D, the pattern of regulation of Heph protein synthesis was identical with the regulation of mRNA expression in the glutamate and the GABA treated groups. Heph protein synthesis was significantly enhanced by 1 μM GABA and suppressed by 1 μM glutamate. Surprising results was observed in Fig 8-6D; neither GABA nor glutamate influenced CP protein synthesis in C6 glioma cells.

8.5 DISCUSSION

This work provides direct evidence for the existence of TfR, DMT1+IRE, DMT1-IRE, FP1, Heph and CP in C6 glioma cell. Although our understanding of iron transport and regulation of iron levels in hematopoetic tissue, macrophages and enterocytes in the gut has grown, there is little direct evidence for the molecular mechanisms underlying iron transport across neural cell membranes in the CNS (Burdo and Connor, 2003). Iron uptake in neural cells could occur via Tf and/or non-Tf mediated mechanisms. TfRs are expressed by oligodendrocytes, neurons and astrocytes (Qian et al., 1999a). However, Tf levels in the CSF is extremely low (0.1-0.28 μM/L in human) (Bradbury, 1997), suggesting that under normal conditions, mediated-mediated uptake may not be significant and non-mediated-mediated mechanisms are likely to be involved in iron influx into cells in the brain (Qian and Ke, 2001). In the present study, showed that TfR and DMT1 are expressed in the C6 glioma cells and low concentrations of glutamate increased DMT1-IRE expression and decreased TfR expression. GABA, on the other hand, suppressed DMT1-IRE and no effect on TfR expression. However, DMT1+IRE is

not regulated by two neurotransmitters. The results imply that low concentration of GABA may decrease iron influx. The function of glutamate on increased DMT1-IRE expression and the efficiency of TfR transcytosis maybe enhance the cell iron uptake. But the further metabolism cannot be explained according to the present results. FP1 plays a key role in Fe^{2+} transport across the basal membrane of enterocytes in the gut (Donovan et al., 2000). Our previous results provided direct evidence for the existence of FP1 protein in the rat brain (Jiang et al., 2002). Confocal microscopy of cultured astrocytes with double-immunofluorescence labeling show that FP1 is colocalized with GPI-CP in the surface of astrocytes, and the expression of FP1 alone is insufficient to allow iron efflux in the absence of GPI-CP in cultured $CP^{-/-}$ mice brain astrocytes. The requirement of GPI-CP for iron efflux from astrocytes indicates that oxidation of ferrous iron is an essential step of iron transported across the cell membrane via the FP1 (Jeong and David, 2003). However, the studies of Mukhopadhyay CK et al. (Mukhopadhyay et al., 1998), Attieh ZK et al. (Attieh et al., 1999) and support the possibility that CP plays a role in iron influx into the cells. Our study (Qian et al., 2001a; Xie et al., 2002) found that CP plays a role both in iron efflux from and in iron influx into the brain cells via its ferroxidase activity. The precise biological role of CP remains unclear despite many decades of investigation (Qian and Ke, 2001). A recent study indicates that the ferroxidase activity of the CP homologue Heph may be involved in the transfer of iron across the basolateral membrane (Vulpe et al., 1999). Our study shows that Heph is mainly expressed in the neuronal cell membrane (chapter 4) and CP is mainly expressed in the gliocyte membrane (chapter 3), suggesting the two kinds of ferroxidase may play an important role in mobilizing iron out of the neuron and gliocyte. The present studies showed the GABA and glutamate did not regulate FP1 and CP proteins; Heph

expression was increased by treatment with the 1 μM GABA and decreased by treatment with 1 μM glutamate. These results provide the basis for understanding the effect of GABA and glutamate on iron metabolism.

The previous study supports an important regulatory role for striatonigral and pallidonigral GABAergic neurons in iron homeostasis within the substantia nigra's zona reticularis (Sastry and Arendash, 1995). Injecting gamma-vinyl GABA (GVG) into the striatum and globus pallidus reduced the accumulation of iron in the ventral pallidum and in the substantia nigra – the target sites for GABAergic efferents (Hill, 1985). However, destruction of the striatal/pallidal innervation to the substantia nigra's zona reticularis disrupts iron homeostasis, resulting in a redistribution and/or accumulation of iron in the substantia nigra's zona reticularis and consequent substantia nigra's zona reticularis neurodegeneration. This suggests that loss or dysfunction of striatonigral/striatopallidal GABAergic neurons in several NDs including Hallervorden-Spatz syndrome, progressive supranuclear palsy, multiple system atrophy, and PD, may result in an increase or redistribution of nigral iron to cause loss of substantia nigra neurons (Sastry and Arendash, 1995). In addition, microinjection of excitatory amino acids to the anterior olfactory nucleus/ventral striatal region showed an increase in histochemical iron concentration in the ipsilateral ventral pallidum, the islands of calleja, the globus pallidus, the entopeduncular nucleus and the ventral thalamus (Shoham et al., 1992). In this regard, GABA would seem to suppress iron accumulation while excitatory amino acids increase iron influx, but the molecular mechanism is unclear.

Our experiments demonstrated that the iron transporters TfR, DMT1+IRE, DMT1-IRE, FP1, Dcytb, CP, and Heph are present in the cortex, hippocampus, striatum and substantia nigra and provide direct evidence for understanding iron metabolism in the brain. *In vitro*, we found that low concentrations of GABA suppressed the DMT1-IRE and enhanced the Heph gene expression in the C6 glioma cells. Glutamate increased DMT1-IRE and down-regulated the Heph gene expression in the C6 glioma cells. We suggest that the repressive neurotransmitter GABA increases iron efflux by decreasing the DMT1-IRE and increasing the Heph gene expression. The excitatory neurotransmitter glutamate, on the other hand, induces the iron accumulation. In CNS, the abnormal synthesis and release of GABA and glutamate is one of the possible reasons breakdowns in brain iron homeostasis and neuron damage in some neurodegenerative diseases. Further investigations are needed to clarify the effect of GABA and glutamate on the iron transporters *in vivo* and on brain iron transport and balance.

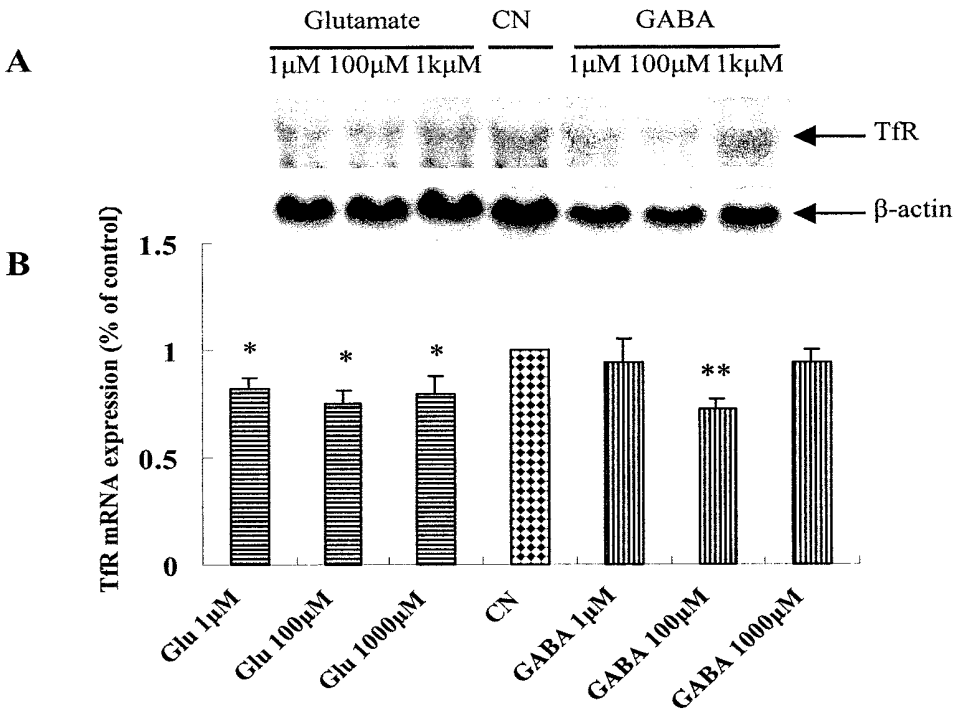
A
Glutamate
CN
GABA
1μM 100μM 1kμM
1μM 100μM 1kμM
TfR
β-actin
B
TfR mRNA expression (% of control)
1.5
1
0.5
0
*
*
*
**
Glu 1μM
Glu 100μM
Glu 1000μM
CN
GABA 1μM
GABA 100μM
GABA 1000μM

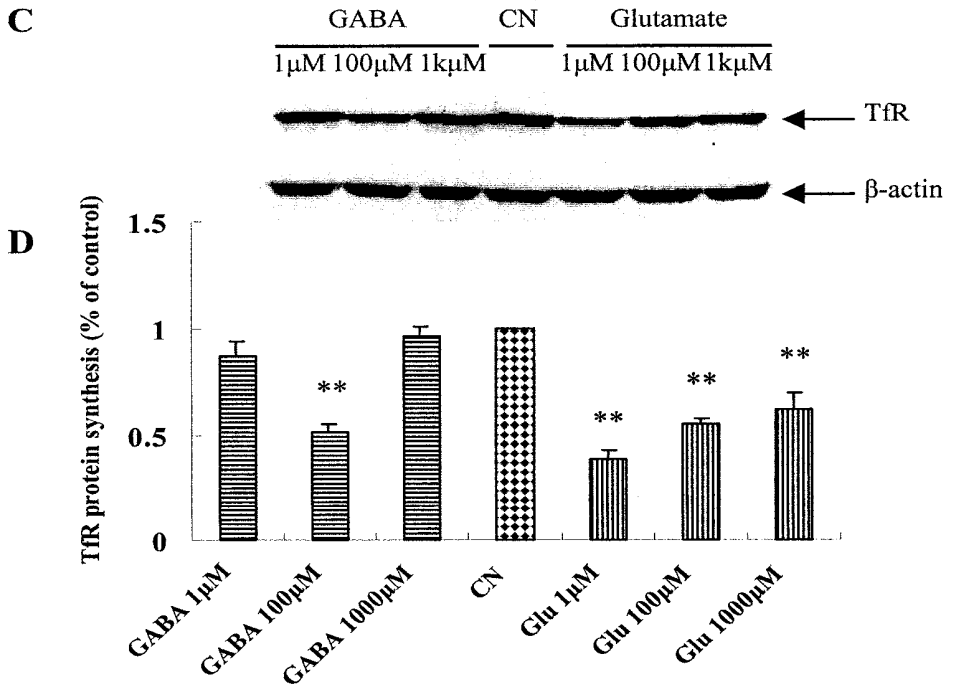
C
GABA
CN
Glutamate
1μM 100μM 1kμM
1μM 100μM 1kμM
TfR
β-actin
D
TfR protein synthesis (% of control)
1.5
1
0.5
0
**
**
**
**
GABA 1μM
GABA 100μM
GABA 1000μM
CN
Glu 1μM
Glu 100μM
Glu 1000μM

Figure 8-1. Effect of L-glutamate (Glu) and gamma-aminobutyric acid (GABA) on TfR mRNA expression and protein synthesis in C6 glioma cells. TfR mRNA levels were determined by Northern blot analysis using 30 μg of total RNA as described in Methods. Western blots analysis was performed to determine TfR protein levels using 40 μg of protein as described in Methods. Samples from the C6 glioma cells were exposed to Glu (1 μM, 100 μM, 1000 μM), GABA (1 μM, 100 μM, 1000 μM) and medium alone for 16 hours. **A:** representative blots of TfR and β-actin mRNA. Note at the right indicates the approximate molecular weight of TfR and β-actin mRNAs. **B:** relative expression of TfR gene in C6 glioma cells. Levels of mRNA are expressed in relation to β-actin expression. The data represent means of % control ± SEM of 3 separate experiments. **C:** representative Western blots for TfR. Note at the right indicates the approximate molecular weight of TfR and β-actin proteins. D: relative TfR protein synthesis in C6 glioma cells. TfR protein levels were quantified using LumiAnalyst Image Analysis software and densitometry values were normalized to β-actin. Data are means of % control ± SEM from 6 independent experiments. *$P<0.05$, **$P<0.01$ vs. control.

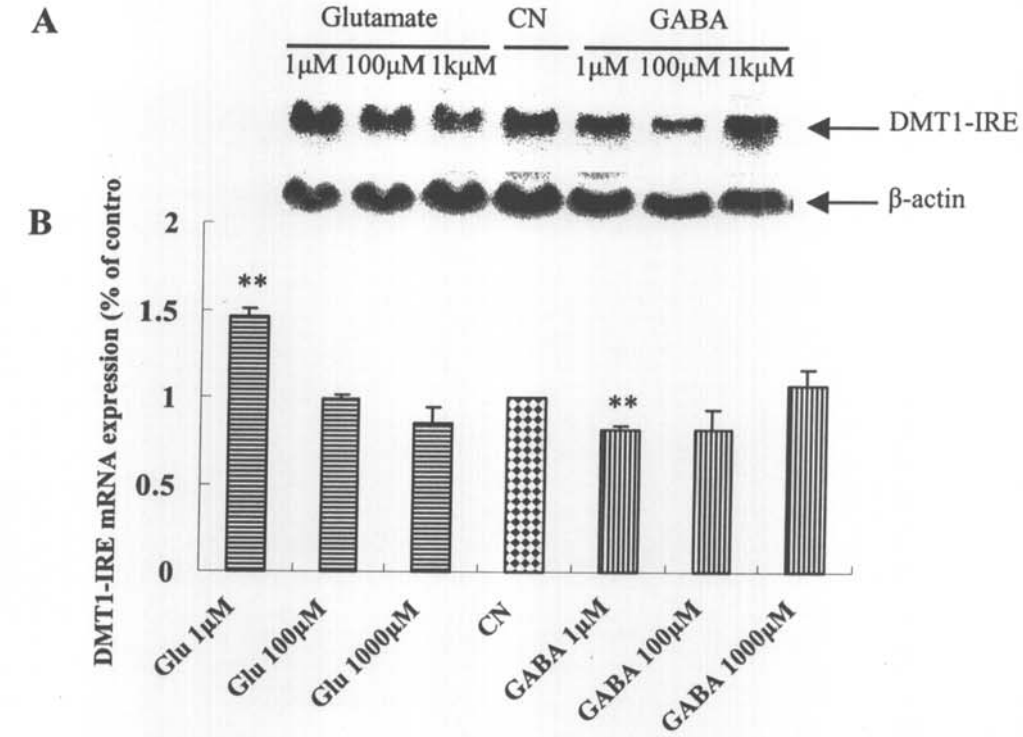
A
Glutamate
CN
GABA
1μM 100μM 1kμM
1μM 100μM 1kμM
DMT1-IRE
β-actin
B
DMT1-IRE mRNA expression (% of contro
2
1.5
1
0.5
0
**
**
Glu 1μM
Glu 100μM
Glu 1000μM
CN
GABA 1μM
GABA 100μM
GABA 1000μM

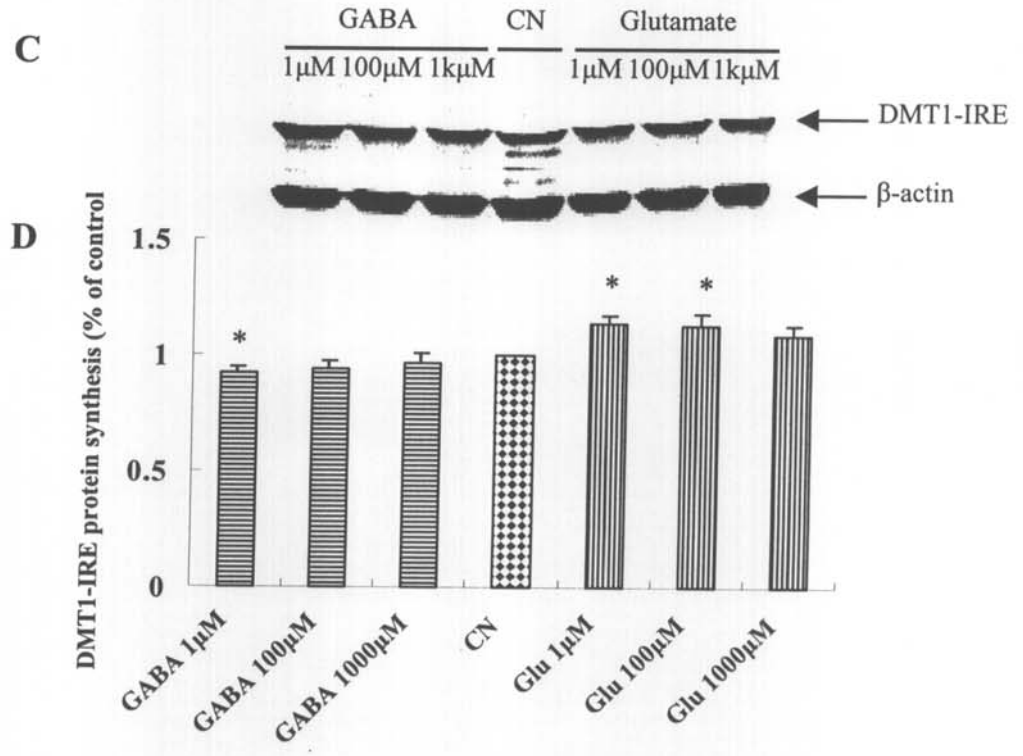
C
GABA
CN
Glutamate
1μM 100μM 1kμM
1μM 100μM 1kμM
DMT1-IRE
β-actin
D
DMT1-IRE protein synthesis (% of control
1.5
1
0.5
0
*
*
*
GABA 1μM
GABA 100μM
GABA 1000μM
CN
Glu 1μM
Glu 100μM
Glu 1000μM

Figure 8-2. Effect of L-glutamate (Glu) and gamma-aminobutyric acid (GABA) on DMT1-IRE mRNA expression and protein synthesis in C6 glioma cells. DMT1-IRE mRNA levels was determined by Northern blot analysis using 30 μg of total RNA as described in Methods. Western blots analysis was performed to determine DMT1-IRE protein levels using 40 μg of protein as described in Methods. Samples from the C6 glioma cells were exposed to Glu (1 μM, 100 μM, 1000 μM), GABA (1 μM, 100 μM, 1000 μM) and medium alone for 16 hours. **A:** representative blots of DMT1-IRE and β-actin mRNA. Note at the right indicates the approximate molecular weight of DMT1-IRE and β-actin mRNAs. **B:** relative expression of DMT1-IRE gene in C6 glioma cells. Levels of mRNA are expressed in relation to β-actin expression. The data represent means of % control ± SEM of 3 separate experiments. **C:** representative Western blots for DMT1-IRE. Note at the right indicates the approximate molecular weight of DMT1-IRE and β-actin proteins. **D:** relative DMT1-IRE protein synthesis in C6 glioma cells. DMT1-IRE protein levels were quantified using LumiAnalyst Image Analysis software and densitometry values were normalized to β-actin. Data are means of % control ± SEM from 6 independent experiments. *$P<0.05$, **$P<0.01$ vs. control.

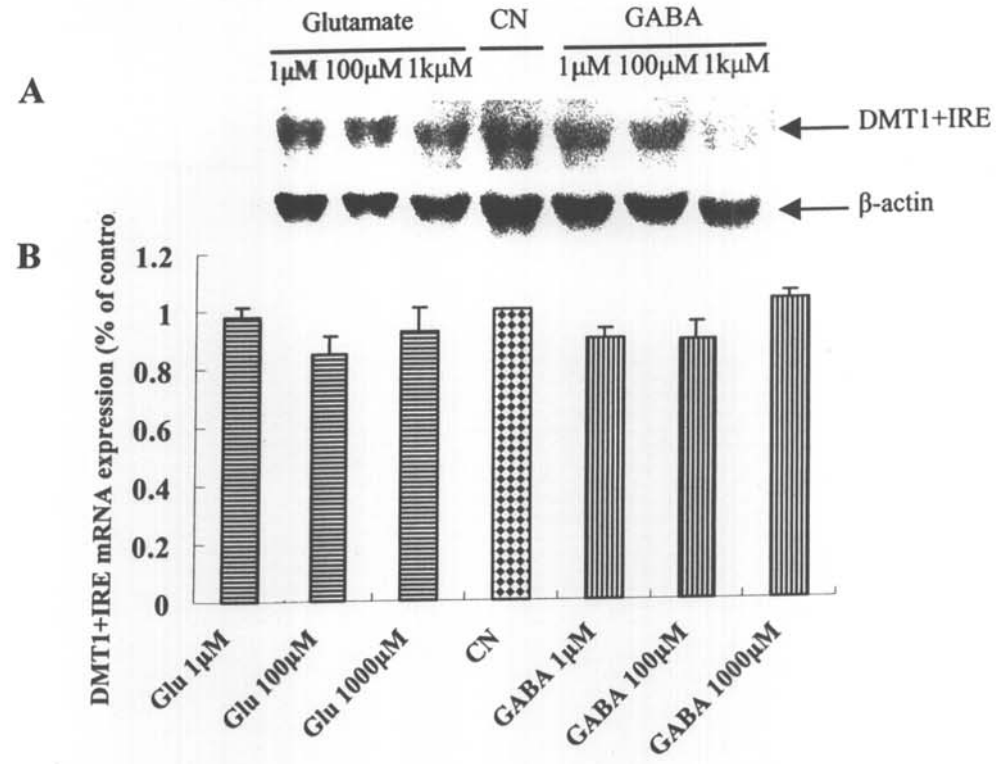
A
Glutamate
CN
GABA
1μM 100μM 1kμM
1μM 100μM 1kμM
DMT1+IRE
β-actin
B
DMT1+IRE mRNA expression (% of contro
1.2
1
0.8
0.6
0.4
0.2
0
Glu 1μM
Glu 100μM
Glu 1000μM
CN
GABA 1μM
GABA 100μM
GABA 1000μM

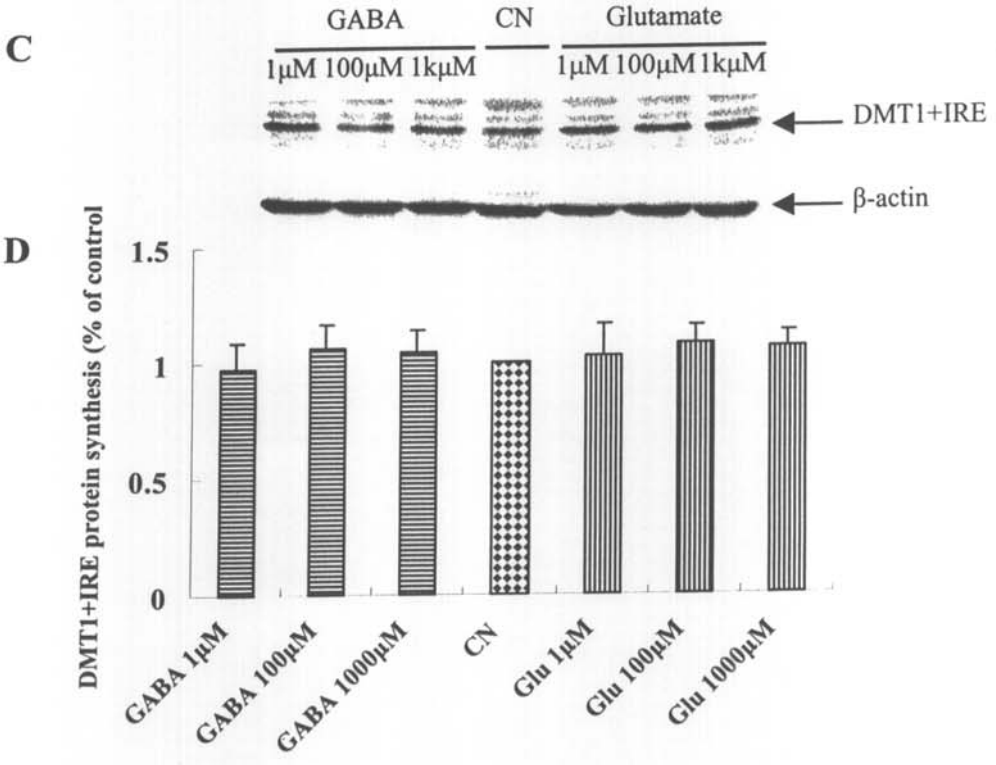
C
GABA
CN
Glutamate
1μM 100μM 1kμM
1μM 100μM 1kμM
DMT1+IRE
β-actin
D
DMT1+IRE protein synthesis (% of control
1.5
1
0.5
0
GABA 1μM
GABA 100μM
GABA 1000μM
CN
Glu 1μM
Glu 100μM
Glu 1000μM

Figure 8-3. Effect of L-glutamate (Glu) and gamma-aminobutyric acid (GABA) on DMT1+IRE mRNA expression and protein synthesis in C6 glioma cells. DMT1+IRE mRNA levels were determined by Northern blot analysis using 30 μg of total RNA as described in Methods. Western blots analysis was performed to determine DMT1+IRE protein levels using 40 μg of protein as described in Methods. Samples from the C6 glioma cells were exposed to Glu (1 μM, 100 μM, 1000 μM), GABA (1 μM, 100 μM, 1000 μM) and medium alone for 16 hours. **A:** representative blots of DMT1+IRE and β-actin mRNA. Note at the right indicates the approximate molecular weight of DMT1+IRE and β-actin mRNAs. **B:** relative expression of DMT1+IRE gene in C6 glioma cells. Levels of mRNA are expressed in relation to β-actin expression. The data represent means % control ± SEM of 3 separate experiments. **C:** representative Western blots for DMT1+IRE. Note at the right indicates the approximate molecular weight of DMT1+IRE and β-actin proteins. **D:** relative DMT1+IRE protein synthesis in C6 glioma cells. DMT1+IRE protein levels were quantified using LumiAnalyst Image Analysis software and densitometry values were normalized to β-actin. Data are means % control ± SEM from 6 independent experiments.

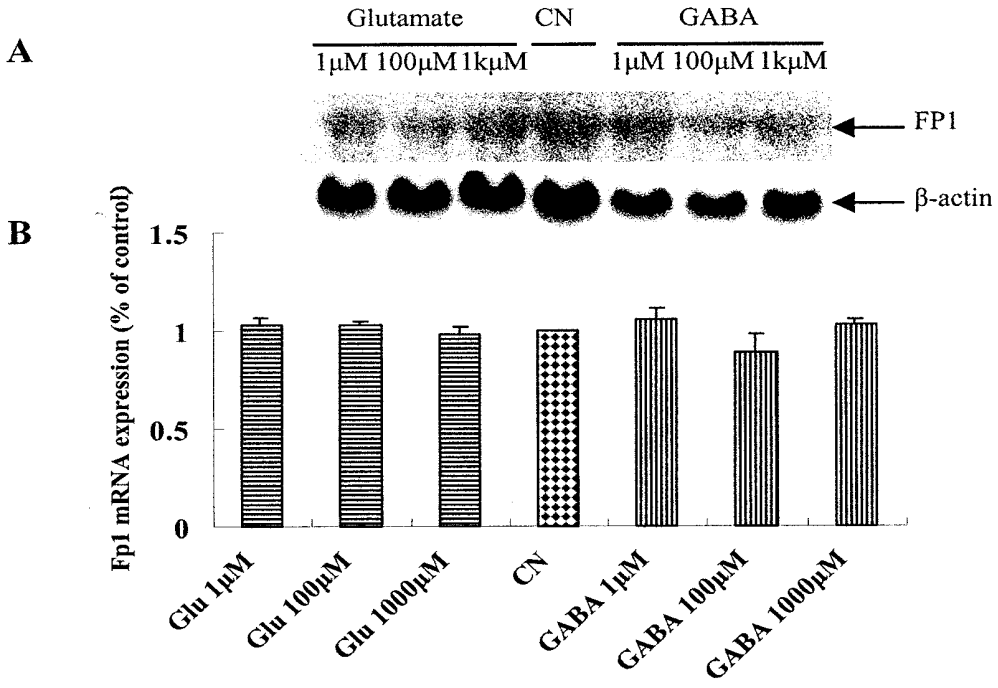
A
Glutamate
CN
GABA
1μM 100μM 1kμM
1μM 100μM 1kμM
FP1
β-actin
B
Fp1 mRNA expression (% of control)
1.5
1
0.5
0
Glu 1μM
Glu 100μM
Glu 1000μM
CN
GABA 1μM
GABA 100μM
GABA 1000μM

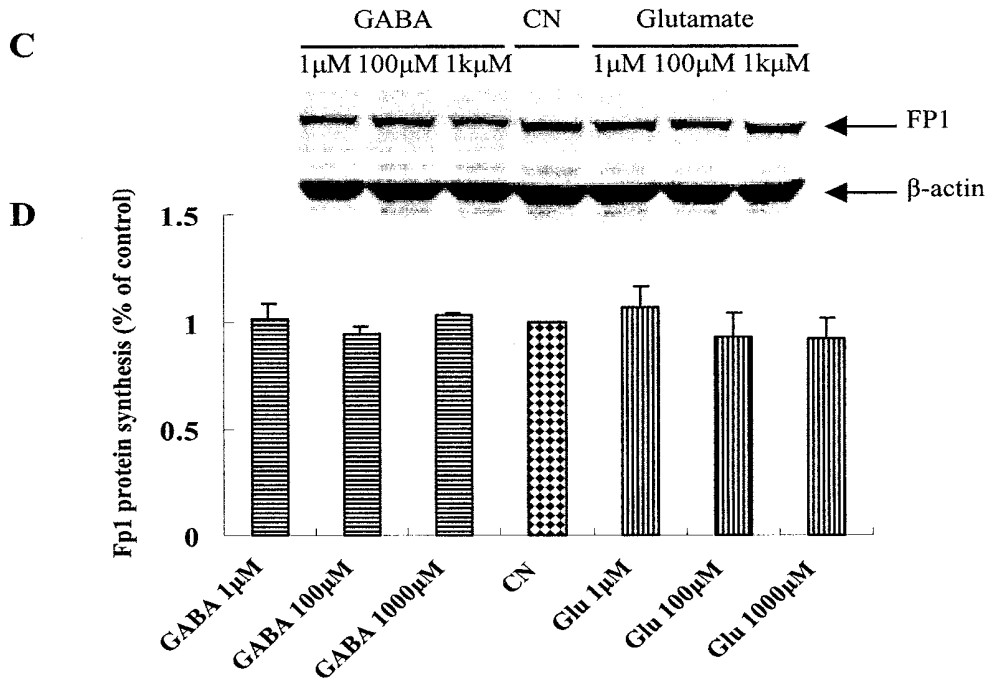
C
GABA
CN
Glutamate
1μM 100μM 1kμM
1μM 100μM 1kμM
FP1
β-actin
D
Fp1 protein synthesis (% of control)
1.5
1
0.5
0
GABA 1μM
GABA 100μM
GABA 1000μM
CN
Glu 1μM
Glu 100μM
Glu 1000μM

Figure 8-4. Effect of L-glutamate (Glu) and gamma-aminobutyric acid (GABA) on FP1 mRNA expression and protein synthesis in C6 glioma cells. FP1 mRNA levels were determined by Northern blot analysis using 30 μg of total RNA as described in Methods. Western blots analysis was performed to determine FP1 protein levels using 40 μg of protein as described in Methods. Samples from the C6 glioma cells were exposed to Glu (1 μM, 100 μM, 1000 μM), GABA (1 μM, 100 μM, 1000 μM) and medium alone for 16 hours. **A:** representative blots of FP1 and β-actin mRNA. Note at the right indicates the approximate molecular weight of FP1 and β-actin mRNAs. **B:** relative expression of FP1 gene in C6 glioma cells. Levels of mRNA are expressed in relation to β-actin expression. The data represent means % control ± SEM of 3 separate experiments. **C:** representative Western blots for FP1. Note at the right indicates the approximate molecular weight of FP1 and β-actin proteins. **D:** relative FP1 protein synthesis in C6 glioma cells. FP1 protein levels were quantified using LumiAnalyst Image Analysis software and densitometry values were normalized to β-actin. Data are means % control ± SEM from 6 independent experiments.

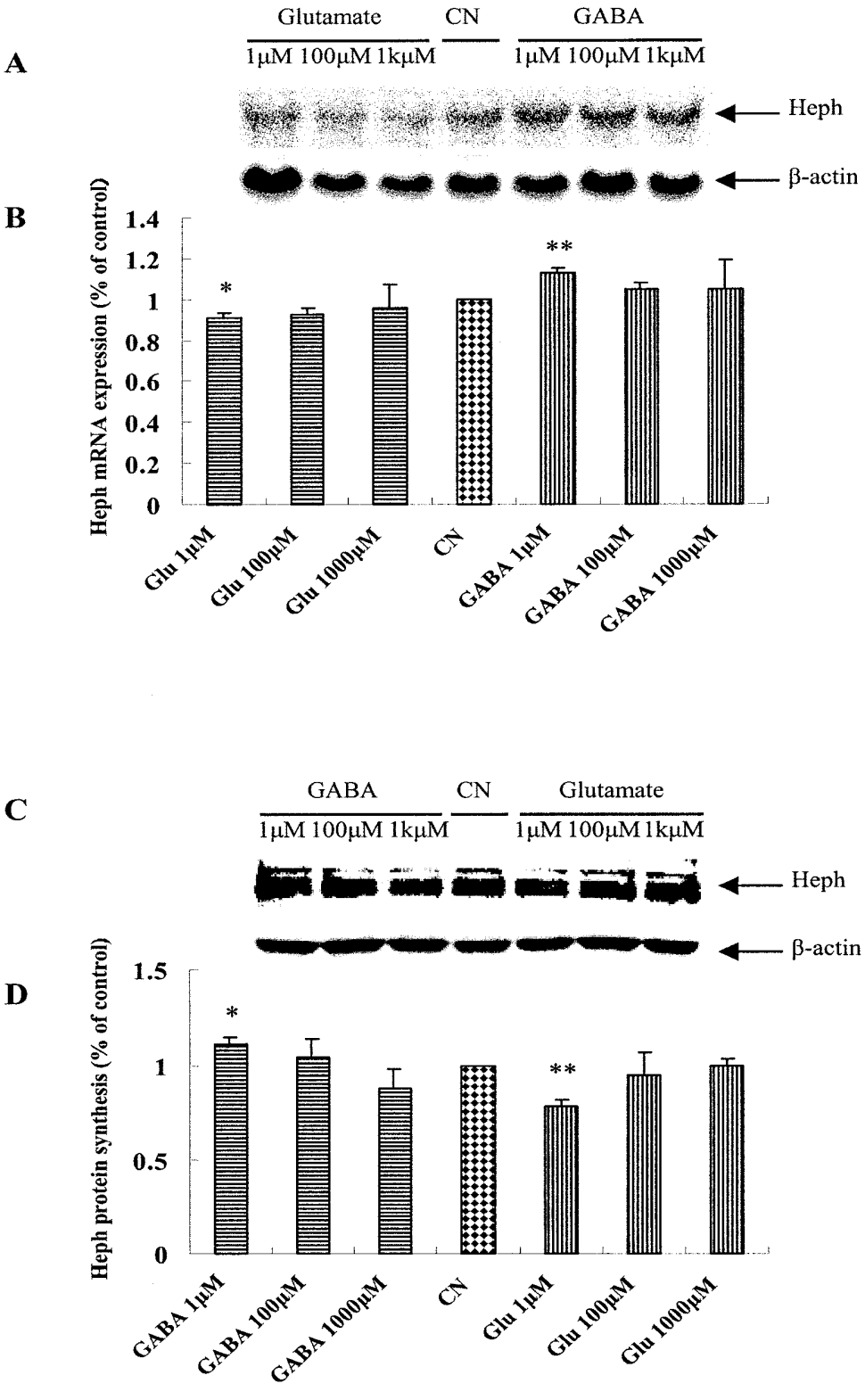
A
Glutamate
CN
GABA
1μM 100μM 1kμM
1μM 100μM 1kμM
Heph
β-actin
B
Heph mRNA expression (% of control)
1.4
1.2
1
0.8
0.6
0.4
0.2
0
*
**
Glu 1μM
Glu 100μM
Glu 1000μM
CN
GABA 1μM
GABA 100μM
GABA 1000μM
C
GABA
CN
Glutamate
1μM 100μM 1kμM
1μM 100μM 1kμM
Heph
β-actin
D
Heph protein synthesis (% of control)
1.5
1
0.5
0
*
**
GABA 1μM
GABA 100μM
GABA 1000μM
CN
Glu 1μM
Glu 100μM
Glu 1000μM

Figure 8-5. Effect of L-glutamate (Glu) and gamma-aminobutyric acid (GABA) on Heph mRNA expression and protein synthesis in C6 glioma cells. Heph mRNA levels were determined by Northern blot analysis using 30 μg of total RNA as described in Methods. Western blots analysis was performed to determine Heph protein levels using 40 μg of protein as described in Methods. Samples from the C6 glioma cells were exposed to Glu (1 μM, 100 μM, 1000 μM), GABA (1 μM, 100 μM, 1000 μM) and medium alone for 16 hours. **A:** representative blots of Heph and β-actin mRNA. Note at the right indicates the approximate molecular weight of Heph and β-actin mRNAs. **B:** relative expression of Heph gene in C6 glioma cells. Levels of mRNA are expressed in relation to β-actin expression. The data represent means % control ± SEM of 3 separate experiments. **C:** representative Western blots for Heph. Note at the right indicates the approximate molecular weight of Heph and β-actin proteins. **D:** relative Heph protein synthesis in C6 glioma cells. Heph protein levels were quantified using LumiAnalyst Image Analysis software and densitometry values were normalized to β-actin. Data are means % control ± SEM from 6 independent experiments. *$P<0.05$, **$P<0.01$ vs. control.

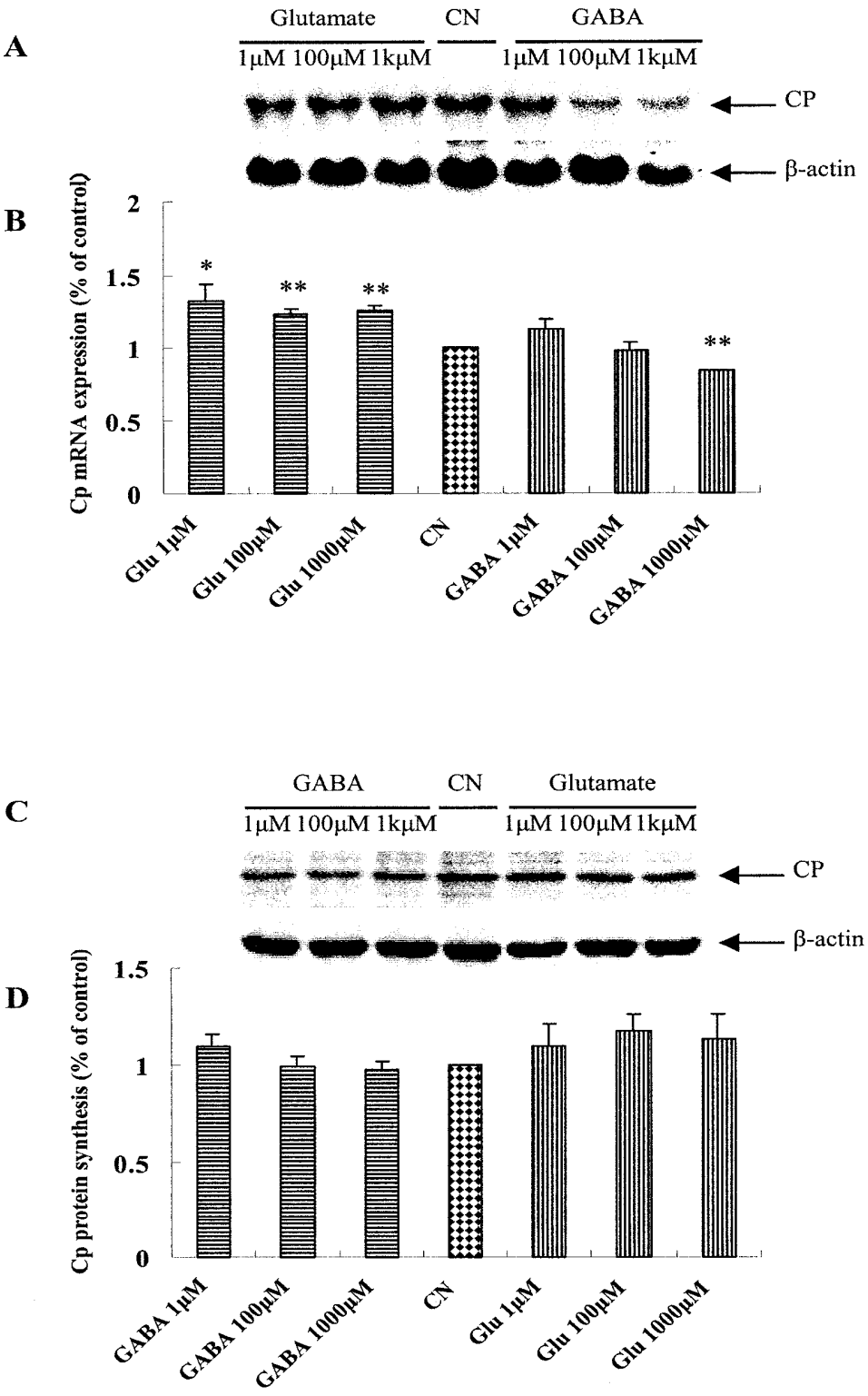
A
Glutamate
CN
GABA
1μM 100μM 1kμM
1μM 100μM 1kμM
CP
β-actin
B
Cp mRNA expression (% of control)
2
1.5
1
0.5
0
*
**
**
**
Glu 1μM
Glu 100μM
Glu 1000μM
CN
GABA 1μM
GABA 100μM
GABA 1000μM
C
GABA
CN
Glutamate
1μM 100μM 1kμM
1μM 100μM 1kμM
CP
β-actin
D
Cp protein synthesis (% of control)
1.5
1
0.5
0
GABA 1μM
GABA 100μM
GABA 1000μM
CN
Glu 1μM
Glu 100μM
Glu 1000μM

Figure 8-6. Effect of L-glutamate (Glu) and gamma-aminobutyric acid (GABA) on CP mRNA expression and protein synthesis in C6 glioma cells. CP mRNA levels were determined by Northern blot analysis using 30 μg of total RNA as described in Methods. Western blots analysis was performed to determine CP protein levels using 40 μg of protein as described in Methods. Samples from the C6 glioma cells were exposed to Glu (1 μM, 100 μM, 1000 μM), GABA (1 μM, 100 μM, 1000 μM) and medium alone for 16 hours. **A:** representative blots of CP and β-actin mRNA. Note at the right indicates the approximate molecular weight of CP and β-actin mRNAs. **B:** relative expression of CP gene in C6 glioma cells. Levels of mRNA are expressed in relation to β-actin expression. The data represent means % control ± SEM of 3 separate experiments. **C:** representative Western blots for CP. Note at the right indicates the approximate molecular weight of CP and β-actin proteins. **D:** relative CP protein synthesis in C6 glioma cells. CP protein levels were quantified using LumiAnalyst Image Analysis software and densitometry values were normalized to β-actin. Data are means % control ± SEM from 6 independent experiments. *$P<0.05$, **$P<0.01$ vs. control

Chapter 9

GENERAL DISCUSSION

Iron is essential for virtually all types of cells and organisms. The significance of timely delivery of normal amounts of iron to the brain is manifested in the number of devastating neurological consequences associated with too little or too much iron. Brain iron deficiency during development results in chronic neurological impairment (Beard, 2003). High iron concentrations in the brains of patients and the discovery of mutations in the genes associated with iron metabolism in the brain suggest that iron misregulation plays a part in neuronal death in some neurodegenerative disorders such as Alzheimer's, Parkinson's, and Huntington's diseases and Hallervorden-Spatz syndrome (Qian and Shen, 2001). The disrupted expression or function of proteins involved in iron metabolism increases the concentration of iron in the brain. Disturbances can happen at several stages in iron metabolism, including uptake and release, storage, intracellular metabolism and regulation (Ke and Ming Qian, 2003). There is good agreement that iron influx occurs by means of receptor-mediated uptake of iron-Tf at the brain barriers and on the hypothesis of additional iron 'uptake' proteins, including DMT1, LfR and p97 (Qian and Wang, 1998), there are little knowledge about iron release from the brain cells. CP is the first protein known to enhance iron release from the cell due to its ferroxidase activity (Osaki et al., 1966; Gitlin, 1999). However, accumulated evidence shows that addition of CP to cells *in vitro* results in enhanced iron uptake rather then iron release in HepG2 (Mukhopadhyay et al., 1998), K562 (Attieh et al., 1999) and BT325 brain glioma cell (Qian et al., 2001a; Xie et al., 2002). Therefore the role of CP in the iron

homeostasis has yet to be determined. Heph, a newly discovered CP homologue, has been suggested to be necessary for iron egress from the enterocytes into circulation but its distribution and the effect on brain iron metabolism have not been identified.

The experiments described in chapter 3 and 4 demonstrated that the difference in cellular and regional distribution of CP and Heph in the rat brain. Immunohistochemistry study showed that both CP and Heph were found in the cortex, hippocampus, striatum and substantia nigra. Like CP mRNA distribution (Klomp et al., 1996; Klomp and Gitlin, 1996; Patel and David, 1997; Patel et al., 2000), cell-specific positive staining of CP was mainly detected in glial cells, predominantly in glial of surrounding the microvasculature, in adult rat brain CP was also found in ependymal cells lining the ventricles, the choroid plexus and the leptomeningeal cells. But specific immunoactive staining was rarely observed in neurons. However, heavy Heph staining was observed on neuron membranes and/or bodies. The expression of this protein was also detected in the glia, vascular endothelial cells and ependymal cells. The character of CP and Heph distribution suggested that they might play a physiological role in iron release from these cells. Previous results showed that FP1 is expressed in the brain (Burdo et al., 2001; Jiang et al., 2002). In line with a current hypothesis that FP1 (Donovan et al., 2000) and Heph (Vulpe et al., 1999), is required for exporting iron from enterocytes into the blood stream, we propose that iron release from brain cells, including, neurons may be mediated by a FP1/Heph pathway. Heph, acting as a putative ferroxidase (Anderson et al., 2002b), may oxidize Fe^{2+} to Fe^{3+} and subsequently load Fe^{3+} on to Tf or other iron carrier in the brain. The localization of CP in leptomeningeal cells suggests that this protein plays a role in antioxidant defense along the surface of the

postnatal CNS, possibly by detoxifying the cerebrospinal fluid (Mittal et al., 2003). In the chapter 5, the data suggest that the levels of CP in CSF and GPI-CP in the membrane do not lead to any significant change in iron release from normal iron or iron-loaded C6 glioma cells. These findings are similar to the effects observed with high concentrations of CP in BT325 cells (Qian et al., 2001a), in HepG2 (Mukhopadhyay et al., 1998) and in K-562 cells (Attieh et al., 1999). These results suggest that the antioxidant effect of CP is more important then its role of iron homeostasis. We propose that Heph plays a key role in iron release at physiological condition in the CNS.

Iron is abundant in the brain and has a distinct regional and cellular pattern of distribution (Connor and Menzies, 1995). Iron is most highly concentrated in the globus pallidus and substantia nigra, followed by the caudate nucleus and the putamen in the normal brain (Hill and Switzer, 1984). As mentioned in the introduction, the increase in iron and CP levels of patients with neurodegenerative disease occurs in distinct regions of the brain, including striatum, substantia nigra, hippocampus and cortex. In order to study the regulation of CP and Heph gene expression *in vivo*, we studied the effect of iron status on CP and Heph mRNA expression and protein synthesis in the striatum, substantia nigra, hippocampus and cortex of rat brain. Our results showed that iron status had no effect on CP mRNA expression in cortex, hippocampus and striatum. The only affected region is the substantia nigra – the area with the most severe lipid perocidantion – where iron overload enhances CP gene expression and iron deficiency suppresses the process (Migliore et al., 2002; Patel et al., 2002; Ryu et al., 2002; Jenner, 2003). However, iron status has a significant effect on Heph mRNA expression as well as protein

synthesis in different brain regions. The positive correlation of iron status and Heph gene expression was observed in cortex and hippocampus but inverse correlation was observed in striatum and substantia nigra. These results imply that Heph may play a key role in cellular iron balance and may be essential for iron release from brain cells. Ceruloplasmin, on the other hand, may play a critical role in preventing damage from free radicals injury (Chen et al., 2003b). The different patterns in the responses of CP, Heph mRNA and protein expression to the iron content in different brain regions show that the effect of iron on CP and Heph is regionally specific.

In vitro, iron status did not have any effect on CP mRNA expression in C6 glioma cells. At the protein level, CP protein synthesis was suppressed in iron-treated cells and promoted in those treated with DFO and high concentration of BP. This result suggests that CP gene expression is regulated at the post-transcriptional level. The different patterns of protein regulation in the substantia nigra *in vivo* and in C6 glioma cells *in vitro* imply multiple principles maybe involved. The effect of iron levels and oxidative stress on CP gene expression is difference *in vivo* and *in vitro*. Oxidative stress may play a dominant role (then iron levels) in the regulation of CP gene expression *in vivo*, but *in vitro*, the iron levels are main factor to regulate the CP gene expression. In primary culture cortical astrocytes, the pattern of the regulation of Heph was observed as the same as that *in vivo*: iron status induced both mRNA expression and protein synthesis. These data suggest that Heph is strongly regulated at the translational level. But further work is necessary to understand this aspect.

In the current study, we found that CP and Heph expression in the brain changed in cortex, hippocampus, striatum and substantia nigra during brain development. This pattern of regulation exists at both at mRNA and protein levels. We also found that the same pattern expressed between the CP and Heph in the cortex and hippocampus. But while CP gene expression in the striatum and substantia nigra along with rat development, Heph levels in those regions increased to PND 21 and then decreased. Because oxidative stress rises in substantia nigra and striatum along with rat development, the results imply the CP gene is sensitive to oxidative stress (Martin et al., 1998; Groc et al., 2001). To our knowledge, this is the first report on Heph expression in the brain of developing male Sprague-Dawley rats. Using a polyclonal antibody raised against an 18-amino acid peptide in the C-terminus of rat Heph, two bands with approximate relative molecular weight of 165 kDa and 106 kDa, rather than the expected 155 kDa or 135 kDa band, were detected in the brain in this study (Frazer et al 1999, 2001, 2003). This may imply the presence of different mechanisms involved in the post-translational modification of the full size Heph protein in the brain and the tissues outside brain. It is highly likely that the proteins of 165 kDa and 106 kDa in the brain we found in this study might be the post-translationally modified form of Heph. Interestingly, Heph was not expressed in the neonatal rat brain. Heph of both molecular weights were observed at postnatal weeks 3 and 9, but only the 106 kDa Heph was found in the postnatal weeks 28. This result implies that Heph is a developmental gene, but the process needs to be further examined. Based on the changes observed in brain iron distribution during development, brains iron increases with age and reaches its maximum values at the age of 30-40 years in humans and 4-5 weeks postnatal in rats (Hu and Connor, 1996); Hpeh gene expression in rats is the highest at 3 weeks, after which the level

stabilizes, we propose that Heph is predominantly involved in iron homeostasis in the brain.

At present, it is unclear why two membrane-bound copper oxidases are present in the brain. Syed et al (2002) suggested that they might have different substrates or activities or those two proteins are trafficked to different cellular compartments. However, based on the location and expression form of ceruloplasmin and Heph in the brain, we suggested that these two proteins might play their role in different location in the brain. CP might be necessary for Fe^{2+}, after it crosses the abluminal membrane of the BBB endothelial cells probably via ferroportin1, to be oxidized to Fe^{3+} (Jeong and David 2003, Patel et al 2000, Qian and Shen 2001, Qian and Ke 2001, Patel et al 2002), while Heph might have the same function in iron efflux from other brain cells including neuron, glia, and ependymal cells. Future research on this possibility is needed.

In addition, we found that both CP mRNA and protein respond to changes in iron concentration in the rat heart. This pattern is similar to that observed in the HepG2 cell line (Mukhopadhyay et al., 1998; Mukhopadhyay et al., 2000). However, iron status does not affect either the levels of plasma CP, or CP mRNA expression in the liver (Huang and Shaw, 2002; Strube et al., 2002; Tran et al., 2002). Thus, the regulation of CP by iron status is peculiar to different organ, tissue and kind of cell. It is clear that the transcriptional regulation of CP expression by iron deficiency may be activated by hypoxia-inducible factor (HIF) (Mukhopadhyay et al., 1998; Attieh et al., 1999). HIF-1α and HIF-1β are known to bind to the CP gene promoter HRE (Mukhopadhyay et al., 2000). In the heart, Heph expression responds dramatically to

iron status; both mRNA and protein was down regulated either in iron sufficiency or in iron deficiency. Previous studies found variations in iron status had an insignificant effect on Heph expression in the duodenum (Frazer et al., 2001; Rolfs et al., 2002; Yamamoto et al., 2002; Frazer et al., 2003), whereas studies by Sakakibara and Aoyama showed dietary iron-deficiency boosts Heph mRNA levels in the small intestine of rats (Sakakibara and Aoyama, 2002). A recent study confirmed that Heph mRNA and protein levels correlate with systemic rather than local iron status in enterocytes (Chen et al., 2003a). Systemic iron deficiency enhances Heph expression and sufficiency suppresses it. How to explain the different regulation of Heph in the brain areas and heart? It is not known whether this can be attributed to regional or tissue differences in sensitivity to system iron concentrations, which are related to the functions of different kinds of cell and organs. According to the Chen et al results, it is not only Heph but also FP1 mRNA levels responsive to systemic levels of iron (Chen et al., 2003a). In the present study, we did not detect this pattern of FP1 gene expression in the heart. Given our published studies and the results of DMT1 gene expression response to iron in the brain and heat (Ke et al., 2003), this implies the specific construction and function of cells and organs make the different effect of iron status on the FP1, DMT1, CP and Heph genes expression. However, the precise reason needs to be clarified.

The CP and Heph mRNA do not contain an IRE structure; therefore, the IRE-IRP regulation system has no effect on their genes expression at the post-transcriptional level. In contrast, the post-transcriptional regulation by iron status involved in CP protein synthesis in brain substantia nigra *in vivo* and in C6 glioma cells *in vitro*. The mechanism requires further study. Transcriptional regulation of Heph gene

expression was observed both brain and heart. It is critical to investigate the promoter and enhancer involved in the Heph gene to identify the molecular mechanisms involved.

FP1 mRNA contains a consensus IRE motif in its 5'UTR, and our results indicate the heart FP1 is regulated by iron status at the post-transcription level, there is no evidence that IRE plays a role in FP1 regulation in the intestine (Abboud and Haile, 2000). However, how FP1 gene expression is regulated by iron status at the transcriptional level, the precise mechanism needs to be further determined.

We have identified Heph distribution in the brain and proposed Heph protein plays a key role in iron release in neurons and in other brain cells, including the glia, vascular endothelial cells and ependymal cells. This role may be mediated by an FP1/Heph pathway, but direct evidence has not been obtained. Further study will focus on the function of Heph protein in the iron release and its correlation with the role of FP1.

How the brain signals for shifts in iron homeostasis in response to changes in brain iron requirements is poorly understood. But recent evidence suggests that the liver-derived peptide, hepcidin, is a strong candidate for the signaling molecule to regulate the body iron metabolism (Park et al., 2001), clues us on the possibility that hepcidin is also a signal peptide to regulate brain iron homeostasis. Recent results demonstrated that the expression of iron transport molecules is altered simultaneously in all mature enterocytes by serum hepcidin level, therefore regulating iron absorption in the duodenum to control body iron homeostasis (Frazer

and Anderson, 2003). In the CNS, blood brain barrier is similar to the barrier of duodenum. At least 9 kinds of iron transport proteins -- Heph, CP, DMT1, Tf, TfR, FP1, p97, HFE, Lf – have been identified in the brain, based on our present study, published results (Jiang et al., 2002) and the studies of others (Patel and David, 1997; Qian and Wang, 1998; Burdo et al., 2001; Burdo and Connor, 2003). Where are the hepcidin or other factor(s) that regulate iron transport proteins expressed in the brain? What are the mechanisms while hepcidin and other factors regulate iron homeostasis in the brain? Further study is needed.

As mentioned in chapter 8, a new concept of regulation of brain iron homeostasis was reviewed -- neurotransmitters probably regulate brain iron metabolism by controlling the expression of iron transporters.

Iron has a distinct regional and cellular pattern of distribution (Connor and Menzies, 1995). The reason for this heterogenous distribution probably involves differences in oxidative metabolism and in neurotransmitter concentration (Burdo and Connor, 2003). However, how neurotransmitters regulate distribution remains unclear.

The striatum and the substantia nigra are two key areas in iron accumulation in the brain, and where iron content is most greatly altered in NDs. The two areas are also critical brain regions relevant to movement disorders. As previous study showed, the substantia nigra and globus pallidus receive substantial innervation from the neostriatum, a considerable amount of which is GABAergic and also receive excitatory (glutamatergic) efferents of the subthalamic nucleus (STN) (Wichmann and DeLong, 1996, 1999). Glutamate is a highly abundant neurotransmitter in the

striatum. The striatum receives major glutamatergic projections from most cortical areas (McGeorge and Faull, 1989) and from the thalamus (Lapper and Bolam, 1992). Dopamine released from substantia nigra is mainly to modulate the functions of striatum (Wichmann and DeLong, 1996, 1999). Substantia nigra zona reticularis and GP regions of high iron accumulation, receive dense GABAergic and glutamatergic projections. Previous studies investigating the potential relationship between GABA and brain iron (Hill, 1985; Shoham et al., 1992) (Sastry and Arendash, 1995) suggest that loss or dysfunction of striatonigral/striatopallidal GABAergic neurons in several NDs may result in an increase or redistribution of nigral iron. Abnormally high levels of iron induced the oxidative stress widely believed to be associated with neuronal death, including the death of dopaminergic neurons (Sayre et al 1999). Both GABA and glutamate pathways have been implicated in several nervous system disorders. Dysfunction of the glutamatergic pathway has been suggested in Huntington's disease (Albin et al. 1990; Calabresi et al. 1999), Alzheimers disease (Chalmers et al. 1990) and epilepsy (Sherwin, 1999). Damage to dopaminergic neurons plays an important role in Parkinson's disease. Therefore, GABA, glutamine and dopamine are the key neurotransmitters in the regulation of iron metabolism.

Heph, CP, DMT1, FP1 and TfR are the key proteins regulating body iron homeostasis. Our experiments demonstrated that TfR, DMT1+IRE, DMT1-IRE, FP1, CP, and Heph are present in the rat brain and provide direct evidence for understanding iron metabolism in the brain. In chapter 8, we showed that low concentrations of GABA suppressed DMT1-IRE and enhanced Heph gene expression, while glutamate boosted the DMT1-IRE levels and suppressed the Heph gene expression in C6 glioma cells. The results suggest that the repressive

neurotransmitter GABA decreases iron influx by suppressing the DMT1-IRE and enhancing the Heph gene expression. In contrast, the excitatory neurotransmitter glutamate induces iron accumulation. In the chapter 7, the data showed that DMT1-IRE gene expression was up-regulated by L-dopa treatment; the iron uptake was increased in the C6 glioma cells. This implies that L-dopa treatment probably increases cells iron uptake and induces the Fenton reactions to produce that generate the toxic hydroxyl radical (OH ·) causing neuron oxidative damage. Iron accumulation in the striatum and substantia nigra may be related to the role of dopamine.

Nevertheless, further study is required. The effects of GABA and glutamate on iron transporters *in vivo* as well as the mechanisms of regulation and the function of neurotransmitters in iron homeostasis in normal brain cells need further investigation.

In summary, increased brain iron triggers a cascade of events that lead to neurodegeneration. Better understanding of the process of iron regulation in the brain, the proteins important in this process, and the effects of iron misregulation could help to treat or prevent NDs. Our present study provides new evidence to elucidate the process.

ABBREVIATIONS

AD	Alzheimer's disease
ApoTf	apotransferrin
BBB	Blood brain barrier
BP	Bathophenanthroline disulfonate
CA-AM	Calcein acetoxymethyl ester
CHO	Chinese hamster ovary
CN	Control
CNS	Central nervous system
CP	Ceruloplasmin
CSF	Cerebrospinal fluid
ddH_2O	Double distilled water
Dcytb	Duodenal cytochrome b
DCT1	Divalent cation transport 1
DFO	Desferrioxamine
DMT1	Divalent metal transport 1
FP1	Ferroportin1
GFAAS	Graphite furnace atomic absorption spectrophotometry
GPI	Gglycosylphosphatidylinositol
Hb	Hemoglobin
HBSS	Hank's balanced salt solution
Hct	Hematocrit
HD	Huntington's disease
HF	High concentration dietary iron feeding rats

HH	Hereditary hemochromatosis
H_2O_2	Hydrogen peroxide
Heph	Hephaestin
Hippo	Hippocampus
HSS	Hallervorden-Spatz Syndrome
IF	Interstitial fluid
IL	Interleukin
IRE	Iron response element
IREG1	Iron-regulated transporter 1
IRP	Iron regulatory protein
Lf	Lactoferrin or lactotransferrin
LF	Low concentration dietary iron feeding rats
LfR	Lactoferrin receptor or lactotransferrin receptor
MAO	Monoamine oxidase
mk mouse	Microcytic anemia mouse
MRI	Magnetic resonance imaging
MTP1	Metal transport protein 1
NDs	Neurodegenerative diseases
NHI	Non-heme iron
NO	Nitric oxide
Nramp2	Natural resistance-associated macrophage protein 2
NTBI	Non-transferrin-bound iron
p97(MTF)	Melanotransferrin
PD	Parkinson's disease
PDZ	postsynaptic density-95 (PSD-95)/discs large (Dlg)/zona

	occludens-1 (ZO-1)
PND	Postnatal day
Tf	Transferrin
ROS	Reactive oxygen species
RT-PCR	Reverse transcriptase-mediated polymerase chain reaction
SD rats	Sprague-Dawley rats
SN	Substantia nigra
Tf-Fe	Transferrin-bond iron
TfR(1,2)	Transferrin receptor (1 and 2)
TIBC	Total iron-binding capacity
UIBC	Unsaturated iron-binding capacity
wt	Weight

REFERENCE

Abboud S, Haile DJ (2000) A novel mammalian iron-regulated protein involved in intracellular iron metabolism. J Biol Chem 275:19906-19912.

Aessopos A, Farmakis D, Karagiorga M, Voskaridou E, Loutradi A, Hatziliami A, Joussef J, Rombos J, Loukopoulos D (2001) Cardiac involvement in thalassemia intermedia: a multicenter study. Blood 97:3411-3416.

Aisen P, Enns C, Wessling-Resnick M (2001) Chemistry and biology of eukaryotic iron metabolism. Int J Biochem Cell Biol 33:940-959.

Aldred AR, Dickson PW, Marley PD, Schreiber G (1987a) Distribution of transferrin synthesis in brain and other tissues in the rat. J Biol Chem 262:5293-5297.

Aldred AR, Grimes A, Schreiber G, Mercer JF (1987b) Rat ceruloplasmin. Molecular cloning and gene expression in liver, choroid plexus, yolk sac, placenta, and testis. J Biol Chem 262:2875-2878.

Al-Timimi DJ, Dormandy TL (1977) The inhibition of lipid autoxidation by human caeruloplasmin. Biochem J 168:283-288.

Anderson BF, Baker HM, Dodson EJ, Norris GE, Rumball SV, Waters JM, Baker EN (1987) Structure of human lactoferrin at 3.2-A resolution. Proc Natl Acad Sci U S A 84:1769-1773.

Anderson GJ, Frazer DM, McKie AT, Vulpe CD (2002a) The ceruloplasmin homolog hephaestin and the control of intestinal iron absorption. Blood Cells Mol Dis 29:367-375.

Anderson GJ, Frazer DM, McKie AT, Wilkins SJ, Vulpe CD (2002b) The expression and regulation of the iron transport molecules hephaestin and IREG1:

implications for the control of iron export from the small intestine. Cell Biochem Biophys 36:137-146.

Anderson GJ, Murphy TL, Cowley L, Evans BA, Halliday JW, McLaren GD (1998) Mapping the gene for sex-linked anemia: an inherited defect of intestinal iron absorption in the mouse. Genomics 48:34-39.

Andrews NC (1999a) Disorders of iron metabolism. N Engl J Med 341:1986-1995.

Andrews NC (1999b) The iron transporter DMT1. Int J Biochem Cell Biol 31:991-994.

Andrews NC (2000) Iron homeostasis: insights from genetics and animal models. Nat Rev Genet 1:208-217.

Andrews NC, Levy JE (1998) Iron is hot: an update on the pathophysiology of hemochromatosis. Blood 92:1845-1851.

Andrews NC, Fleming MD, Gunshin H (1999) Iron transport across biologic membranes. Nutr Rev 57:114-123.

Arnaud P, Gianazza E, Miribel L (1988) Ceruloplasmin. Methods Enzymol 163:441-452.

Atanasiu RL, Stea D, Mateescu MA, Vergely C, Dalloz F, Briot F, Maupoil V, Nadeau R, Rochette L (1998) Direct evidence of caeruloplasmin antioxidant properties. Mol Cell Biochem 189:127-135.

Attieh ZK, Mukhopadhyay CK, Seshadri V, Tripoulas NA, Fox PL (1999) Ceruloplasmin ferroxidase activity stimulates cellular iron uptake by a trivalent cation-specific transport mechanism. J Biol Chem 274:1116-1123.

Avrameas S, Uriel J (1966) [Method of antigen and antibody labelling with enzymes and its immunodiffusion application]. C R Acad Sci Hebd Seances Acad Sci D 262:2543-2545.

Bannerman RM, Cooper RG (1966) Sex-linked anemia: a hypochromic anemia of mice. Science 151:581-582.

Barnabe N, Zastre JA, Venkataram S, Hasinoff BB (2002) Deferiprone protects against doxorubicin-induced myocyte cytotoxicity. Free Radic Biol Med 33:266-275.

Bartzokis G, Tishler TA (2000) MRI evaluation of basal ganglia ferritin iron and neurotoxicity in Alzheimer's and Huntingon's disease. Cell Mol Biol (Noisy-le-grand) 46:821-833.

Beard J (2003) Iron deficiency alters brain development and functioning. J Nutr 133:1468S-1472S.

Beard J, Erikson KM, Jones BC (2003) Neonatal iron deficiency results in irreversible changes in dopamine function in rats. J Nutr 133:1174-1179.

Beard JL, Connor JR, Jones BC (1993a) Iron in the brain. Nutr Rev 51:157-170.

Beard JL, Connor JD, Jones BC (1993b) Brain iron: location and function. Prog Food Nutr Sci 17:183-221.

Beaumont C (2000) [Intracellular iron metabolism]. Bull Acad Natl Med 184:313-323; discussion 323-314.

Benkovic SA, Connor JR (1993) Ferritin, transferrin, and iron in selected regions of the adult and aged rat brain. J Comp Neurol 338:97-113.

Berenshtein E, Mayer B, Goldberg C, Kitrossky N, Chevion M (1997) Patterns of mobilization of copper and iron following myocardial ischemia: possible predictive criteria for tissue injury. J Mol Cell Cardiol 29:3025-3034.

Bloch B, Popovici T, Chouham S, Levin MJ, Tuil D, Kahn A (1987) Transferrin gene expression in choroid plexus of the adult rat brain. Brain Res Bull 18:573-576.

Boll MC, Sotelo J, Otero E, Alcaraz-Zubeldia M, Rios C (1999) Reduced ferroxidase activity in the cerebrospinal fluid from patients with Parkinson's disease. Neurosci Lett 265:155-158.

Bomford A (2002) Genetics of haemochromatosis. Lancet 360:1673-1681.

Bradbury MW (1997) Transport of iron in the blood-brain-cerebrospinal fluid system. J Neurochem 69:443-454.

Breuer W, Epsztejn S, Cabantchik ZI (1995a) Iron acquired from transferrin by K562 cells is delivered into a cytoplasmic pool of chelatable iron(II). J Biol Chem 270:24209-24215.

Breuer W, Epsztejn S, Millgram P, Cabantchik IZ (1995b) Transport of iron and other transition metals into cells as revealed by a fluorescent probe. Am J Physiol 268:C1354-1361.

Bridle KR, Frazer DM, Wilkins SJ, Dixon JL, Purdie DM, Crawford DH, Subramaniam VN, Powell LW, Anderson GJ, Ramm GA (2003) Disrupted hepcidin regulation in HFE-associated haemochromatosis and the liver as a regulator of body iron homoeostasis. Lancet 361:669-673.

Burdo JR, Connor JR (2003) Brain iron uptake and homeostatic mechanisms: an overview. Biometals 16:63-75.

Burdo JR, Martin J, Menzies SL, Dolan KG, Romano MA, Fletcher RJ, Garrick MD, Garrick LM, Connor JR (1999) Cellular distribution of iron in the brain of the Belgrade rat. Neuroscience 93:1189-1196.

Burdo JR, Menzies SL, Simpson IA, Garrick LM, Garrick MD, Dolan KG, Haile DJ, Beard JL, Connor JR (2001) Distribution of divalent metal transporter 1 and metal transport protein 1 in the normal and Belgrade rat. J Neurosci Res 66:1198-1207.

Byrnes V, Ryan E, O'Keane C, Crowe J (2000) Immunohistochemistry of the Hfe protein in patients with hereditary hemochromatosis, iron deficiency anemia, and normal controls. Blood Cells Mol Dis 26:2-8.

Cabiscol E, Belli G, Tamarit J, Echave P, Herrero E, Ros J (2002) Mitochondrial Hsp60, resistance to oxidative stress and the labile iron pool are closely connected in Saccharomyces cerevisiae. J Biol Chem 27:27.

Calabrese L, Malatesta F, Barra D (1981) Purification and properties of bovine caeruloplasmin. Biochem J 199:667-673.

Calabrese L, Carbonaro M, Musci G (1988) Chicken ceruloplasmin. Evidence in support of a trinuclear cluster involving type 2 and 3 copper centers. J Biol Chem 263:6480-6483.

Camaschella C, Roetto A, Cali A, De Gobbi M, Garozzo G, Carella M, Majorano N, Totaro A, Gasparini P (2000) The gene TFR2 is mutated in a new type of haemochromatosis mapping to 7q22. Nat Genet 25:14-15.

Canonne-Hergaux F, Gruenheid S, Ponka P, Gros P (1999) Cellular and subcellular localization of the Nramp2 iron transporter in the intestinal brush border and regulation by dietary iron. Blood 93:4406-4417.

Canonne-Hergaux F, Zhang AS, Ponka P, Gros P (2001a) Characterization of the iron transporter DMT1 (NRAMP2/DCT1) in red blood cells of normal and anemic mk/mk mice. Blood 98:3823-3830.

Canonne-Hergaux F, Levy JE, Fleming MD, Montross LK, Andrews NC, Gros P (2001b) Expression of the DMT1 (NRAMP2/DCT1) iron transporter in mice with genetic iron overload disorders. Blood 97:1138-1140.

Casaril M, Capra F, Marchiori L, Gabrielli GB, Nicoli N, Corso F, Baracchino F, Corrocher R (1989) Serum copper and ceruloplasmin in early and in advanced

hepatocellular carcinoma: diagnostic and prognostic relevance. Tumori 75:498-502.

Casey JL, Di Jeso B, Rao K, Rouault TA, Klausner RD, Harford JB (1988) The promoter region of the human transferrin receptor gene. Ann N Y Acad Sci 526:54-64.

Cazzola M, Huebers HA, Sayers MH, MacPhail AP, Eng M, Finch CA (1985) Transferrin saturation, plasma iron turnover, and transferrin uptake in normal humans. Blood 66:935-939.

Chahine R, Mateescu MA, Roger S, Yamaguchi N, de Champlain J, Nadeau R (1991) Protective effects of ceruloplasmin against electrolysis-induced oxygen free radicals in rat heart. Can J Physiol Pharmacol 69:1459-1464.

Chen H, Su T, Attieh ZK, Fox TC, McKie AT, Anderson GJ, Vulpe CD (2003a) Systemic regulation of HEPHAESTIN and IREG1 revealed in studies of genetic and nutritional iron deficiency. Blood 1:1.

Chen J, Maltby KM, Miano JM (2001) A novel retinoid-response gene set in vascular smooth muscle cells. Biochem Biophys Res Commun 281:475-482.

Chen L, Dentchev T, Wong R, Hahn P, Wen R, Bennett J, Dunaief JL (2003b) Increased expression of ceruloplasmin in the retina following photic injury. Mol Vis 9:151-158.

Chen YY, Ho KP, Xia Q, Qian ZM (2002) Hydrogen peroxide enhances iron-induced injury in isolated heart and ventricular cardiomyocyte in rats. Mol Cell Biochem 231:61-68.

Chowrimootoo GF, Ahmed HA, Seymour CA (1996) New insights into the pathogenesis of copper toxicosis in Wilson's disease: evidence for copper incorporation and defective canalicular transport of caeruloplasmin. Biochem J

315:851-855.

Connor JR, Benkovic SA (1992) Iron regulation in the brain: histochemical, biochemical, and molecular considerations. Ann Neurol 32:S51-61.

Connor JR, Menzies SL (1995) Cellular management of iron in the brain. J Neurol Sci 134:33-44.

Connor JR, Menzies SL (1996) Relationship of iron to oligodendrocytes and myelination. Glia 17:83-93.

Connor JR, Menzies SL, St Martin SM, Mufson EJ (1990) Cellular distribution of transferrin, ferritin, and iron in normal and aged human brains. J Neurosci Res 27:595-611.

Connor JR, Tucker P, Johnson M, Snyder B (1993) Ceruloplasmin levels in the human superior temporal gyrus in aging and Alzheimer's disease. Neurosci Lett 159:88-90.

Connor JR, Snyder BS, Beard JL, Fine RE, Mufson EJ (1992) Regional distribution of iron and iron-regulatory proteins in the brain in aging and Alzheimer's disease. J Neurosci Res 31:327-335.

Connor JR, Pavlick G, Karli D, Menzies SL, Palmer C (1995) A histochemical study of iron-positive cells in the developing rat brain. J Comp Neurol 355:111-123.

Conrad ME, Umbreit JN, Moore EG, Hainsworth LN, Porubcin M, Simovich MJ, Nakada MT, Dolan K, Garrick MD (2000) Separate pathways for cellular uptake of ferric and ferrous iron. Am J Physiol Gastrointest Liver Physiol 279:G767-774.

Cousins RJ, Leinart AS (1988) Tissue-specific regulation of zinc metabolism and metallothionein genes by interleukin 1. Faseb J 2:2884-2890.

Crowe A, Morgan EH (1992) Iron and transferrin uptake by brain and cerebrospinal

fluid in the rat. Brain Res 592:8-16.

Daffada AA, Young SP (1999) Coordinated regulation of ceruloplasmin and metallothionein mRNA by interleukin-1 and copper in HepG2 cells. FEBS Lett 457:214-218.

Daimon M, Yamatani K, Igarashi M, Fukase N, Kawanami T, Kato T, Tominaga M, Sasaki H (1995) Fine structure of the human ceruloplasmin gene. Biochem Biophys Res Commun 208:1028-1035.

Dal-Pizzol F, Klamt F, Frota ML, Jr., Andrades ME, Caregnato FF, Vianna MM, Schroder N, Quevedo J, Izquierdo I, Archer T, Moreira JC (2001) Neonatal iron exposure induces oxidative stress in adult Wistar rat. Brain Res Dev Brain Res 130:109-114.

Danzeisen R, Ponnambalam S, Lea RG, Page K, Gambling L, McArdle HJ (2000) The effect of ceruloplasmin on iron release from placental (BeWo) cells; evidence for an endogenous Cu oxidase. Placenta 21:805-812.

Danzeisen R, Fosset C, Chariana Z, Page K, David S, McArdle HJ (2002) Placental ceruloplasmin homolog is regulated by iron and copper and is implicated in iron metabolism. Am J Physiol Cell Physiol 282:C472-478.

Davis W, Chowrimootoo GF, Seymour CA (1996) Defective biliary copper excretion in Wilson's disease: the role of caeruloplasmin. Eur J Clin Invest 26:893-901.

de Arriba Zerpa GA, Saleh MC, Fernandez PM, Guillou F, Espinosa de los Monteros A, de Vellis J, Zakin MM, Baron B (2000) Alternative splicing prevents transferrin secretion during differentiation of a human oligodendrocyte cell line. J Neurosci Res 61:388-395.

de Silva D, Aust SD (1992) Stoichiometry of Fe(II) oxidation during

ceruloplasmin-catalyzed loading of ferritin. Arch Biochem Biophys 298:259-264.

de Valk B, Marx JJ (1999) Iron, atherosclerosis, and ischemic heart disease. Arch Intern Med 159:1542-1548.

Deaglio S, Capobianco A, Cali A, Bellora F, Alberti F, Righi L, Sapino A, Camaschella C, Malavasi F (2002) Structural, functional, and tissue distribution analysis of human transferrin receptor-2 by murine monoclonal antibodies and a polyclonal antiserum. Blood 100:3782-3789.

Del Principe D, Menichelli A, Colistra C (1989) The ceruloplasmin and transferrin system in cerebrospinal fluid of acute leukemia patients. Acta Paediatr Scand 78:327-328.

Denizot F, Lang R (1986) Rapid colorimetric assay for cell growth and survival. Modifications to the tetrazolium dye procedure giving improved sensitivity and reliability. J Immunol Methods 89:271-277.

Dexter DT, Carayon A, Javoy-Agid F, Agid Y, Wells FR, Daniel SE, Lees AJ, Jenner P, Marsden CD (1991) Alterations in the levels of iron, ferritin and other trace metals in Parkinson's disease and other neurodegenerative diseases affecting the basal ganglia. Brain 114:1953-1975.

DiSilvestro RA, Barber EF, David EA, Cousins RJ (1988) An enzyme-linked immunoadsorbent assay for rat ceruloplasmin. Biol Trace Elem Res 17:1-9.

Dixon JS, Greenwood M, Lowe JR (1988) Caeruloplasmin concentration and oxidase activity in polyarthritis. Rheumatol Int 8:11-14.

Donovan A, Brownlie A, Zhou Y, Shepard J, Pratt SJ, Moynihan J, Paw BH, Drejer A, Barut B, Zapata A, Law TC, Brugnara C, Lux SE, Pinkus GS, Pinkus JL, Kingsley PD, Palis J, Fleming MD, Andrews NC, Zon LI (2000) Positional

cloning of zebrafish ferroportin1 identifies a conserved vertebrate iron exporter. Nature 403:776-781.

Duffy SJ, Biegelsen ES, Holbrook M, Russell JD, Gokce N, Keaney JF, Jr., Vita JA (2001) Iron chelation improves endothelial function in patients with coronary artery disease. Circulation 103:2799-2804.

Dupic F, Fruchon S, Bensaid M, Loreal O, Brissot P, Borot N, Roth MP, Coppin H (2002) Duodenal mRNA expression of iron related genes in response to iron loading and iron deficiency in four strains of mice. Gut 51:648-653.

Dwork AJ, Schon EA, Herbert J (1988) Nonidentical distribution of transferrin and ferric iron in human brain. Neuroscience 27:333-345.

Edwards JA, Bannerman RM (1970) Hereditary defect of intestinal iron transport in mice with sex-linked anemia. J Clin Invest 49:1869-1871.

Edwards JA, Hoke JE (1972) Defect of intestinal mucosal iron uptake in mice with hereditary microcytic anemia. Proc Soc Exp Biol Med 141:81-84.

el Hage Chahine JM, Pakdaman R (1995) Transferrin, a mechanism for iron release. Eur J Biochem 230:1102-1110.

Enns CA, Sussman HH (1981) Physical characterization of the transferrin receptor in human placentae. J Biol Chem 256:9820-9823.

Epsztejn S, Kakhlon O, Glickstein H, Breuer W, Cabantchik I (1997) Fluorescence analysis of the labile iron pool of mammalian cells. Anal Biochem 248:31-40.

Erikson KM, Pinero DJ, Connor JR, Beard JL (1997) Regional brain iron, ferritin and transferrin concentrations during iron deficiency and iron repletion in developing rats. J Nutr 127:2030-2038.

Escriou V, Laporte F, Garin J, Brandolin G, Vignais PV (1994) Purification and physical properties of a novel type of cytochrome b from rabbit peritoneal

neutrophils. J Biol Chem 269:14007-14014.

Espinosa de los Monteros A, Zhang M, Gordon MN, Kumar S, Scully SA, de Vellis J (1990) The myelin-deficient rat mutant: partial recovery of oligodendrocyte maturation in vitro. Dev Neurosci 12:326-339.

Farcich EA, Morgan EH (1992) Diminished iron acquisition by cells and tissues of Belgrade laboratory rats. Am J Physiol 262:R220-224.

Faucheux BA, Nillesse N, Damier P, Spik G, Mouatt-Prigent A, Pierce A, Leveugle B, Kubis N, Hauw JJ, Agid Y, et al. (1995) Expression of lactoferrin receptors is increased in the mesencephalon of patients with Parkinson disease. Proc Natl Acad Sci U S A 92:9603-9607.

Feder JN, Gnirke A, Thomas W, Tsuchihashi Z, Ruddy DA, Basava A, Dormishian F, Domingo R, Jr., Ellis MC, Fullan A, Hinton LM, Jones NL, Kimmel BE, Kronmal GS, Lauer P, Lee VK, Loeb DB, Mapa FA, McClelland E, Meyer NC, Mintier GA, Moeller N, Moore T, Morikang E, Wolff RK, et al. (1996) A novel MHC class I-like gene is mutated in patients with hereditary haemochromatosis. Nat Genet 13:399-408.

Ferguson CJ, Wareing M, Ward DT, Green R, Smith CP, Riccardi D (2001) Cellular localization of divalent metal transporter DMT-1 in rat kidney. Am J Physiol Renal Physiol 280:F803-814.

Fishman JB, Rubin JB, Handrahan JV, Connor JR, Fine RE (1987) Receptor-mediated transcytosis of transferrin across the blood-brain barrier. J Neurosci Res 18:299-304.

Fitch CA, Song Y, Levenson CW (1999) Developmental regulation of hepatic ceruloplasmin mRNA and serum activity by exogenous thyroxine and dexamethasone. Proc Soc Exp Biol Med 221:27-31.

Fleet JC, Wang L, Vitek O, Craig BA, Edenberg HJ (2003) Gene expression profiling of Caco-2 BBe cells suggests a role for specific signaling pathways during intestinal differentiation. Physiol Genomics 13:57-68.

Fleming MD, Romano MA, Su MA, Garrick LM, Garrick MD, Andrews NC (1998) Nramp2 is mutated in the anemic Belgrade (b) rat: evidence of a role for Nramp2 in endosomal iron transport. Proc Natl Acad Sci U S A 95:1148-1153.

Fleming MD, Trenor CC, 3rd, Su MA, Foernzler D, Beier DR, Dietrich WF, Andrews NC (1997) Microcytic anaemia mice have a mutation in Nramp2, a candidate iron transporter gene. Nat Genet 16:383-386.

Fleming RE, Gitlin JD (1990) Primary structure of rat ceruloplasmin and analysis of tissue-specific gene expression during development. J Biol Chem 265:7701-7707.

Fleming RE, Sly WS (2001a) Hepcidin: a putative iron-regulatory hormone relevant to hereditary hemochromatosis and the anemia of chronic disease. Proc Natl Acad Sci U S A 98:8160-8162.

Fleming RE, Sly WS (2001b) Ferroportin mutation in autosomal dominant hemochromatosis: loss of function, gain in understanding. J Clin Invest 108:521-522.

Fleming RE, Whitman IP, Gitlin JD (1991) Induction of ceruloplasmin gene expression in rat lung during inflammation and hyperoxia. Am J Physiol 260:L68-74.

Fleming RE, Migas MC, Holden CC, Waheed A, Britton RS, Tomatsu S, Bacon BR, Sly WS (2000) Transferrin receptor 2: continued expression in mouse liver in the face of iron overload and in hereditary hemochromatosis. Proc Natl Acad Sci U S A 97:2214-2219.

Fleming RE, Ahmann JR, Migas MC, Waheed A, Koeffler HP, Kawabata H, Britton RS, Bacon BR, Sly WS (2002) Targeted mutagenesis of the murine transferrin receptor-2 gene produces hemochromatosis. Proc Natl Acad Sci U S A 99:10653-10658.

Focht SJ, Snyder BS, Beard JL, Van Gelder W, Williams LR, Connor JR (1997) Regional distribution of iron, transferrin, ferritin, and oxidatively-modified proteins in young and aged Fischer 344 rat brains. Neuroscience 79:255-261.

Fortna RR, Watson HA, Nyquist SE (1999) Glycosyl phosphatidylinositol-anchored ceruloplasmin is expressed by rat Sertoli cells and is concentrated in detergent-insoluble membrane fractions. Biol Reprod 61:1042-1049.

Frazer DM, Anderson GJ (2003) The orchestration of body iron intake: how and where do enterocytes receive their cues? Blood Cells Mol Dis 30:288-297.

Frazer DM, Vulpe CD, McKie AT, Wilkins SJ, Trinder D, Cleghorn GJ, Anderson GJ (2001) Cloning and gastrointestinal expression of rat hephaestin: relationship to other iron transport proteins. Am J Physiol Gastrointest Liver Physiol 281:G931-939.

Frazer DM, Wilkins SJ, Becker EM, Vulpe CD, McKie AT, Trinder D, Anderson GJ (2002) Hepcidin expression inversely correlates with the expression of duodenal iron transporters and iron absorption in rats. Gastroenterology 123:835-844.

Frazer DM, Wilkins SJ, Becker EM, Murphy TL, Vulpe CD, McKie AT, Anderson GJ (2003) A rapid decrease in the expression of DMT1 and Dcytb but not Ireg1 or hephaestin explains the mucosal block phenomenon of iron absorption. Gut 52:340-346.

Gambling L, Danzeisen R, Gair S, Lea RG, Charania Z, Solanky N, Joory KD, Srai SK, McArdle HJ (2001) Effect of iron deficiency on placental transfer of iron

and expression of iron transport proteins in vivo and in vitro. Biochem J 356:883-889.

Ganz T (2003) Hepcidin, a key regulator of iron metabolism and mediator of anemia of inflammation. Blood 27:27.

Gelman BB (1995) Iron in CNS disease. J Neuropathol Exp Neurol 54:477-486.

Gerber MR, Connor JR (1989) Do oligodendrocytes mediate iron regulation in the human brain? Ann Neurol 26:95-98.

Gerlach M, Ben-Shachar D, Riederer P, Youdim MB (1994) Altered brain metabolism of iron as a cause of neurodegenerative diseases? J Neurochem 63:793-807.

Gerstein M, Anderson BF, Norris GE, Baker EN, Lesk AM, Chothia C (1993) Domain closure in lactoferrin. Two hinges produce a see-saw motion between alternative close-packed interfaces. J Mol Biol 234:357-372.

Gibb WR (1991) Neuropathology of the substantia nigra. Eur Neurol 31:48-59.

Giometto B, Bozza F, Argentiero V, Gallo P, Pagni S, Piccinno MG, Tavolato B (1990) Transferrin receptors in rat central nervous system. An immunocytochemical study. J Neurol Sci 98:81-90.

Gitlin JD (1988) Transcriptional regulation of ceruloplasmin gene expression during inflammation. J Biol Chem 263:6281-6287.

Gitlin JD (1998) Aceruloplasminemia. Pediatr Res 44:271-276.

Gitlin JD (1999) The sky blue protein. J Lab Clin Med 134:431-432.

Gitlin JD, Schroeder JJ, Lee-Ambrose LM, Cousins RJ (1992) Mechanisms of caeruloplasmin biosynthesis in normal and copper-deficient rats. Biochem J 282:835-839.

Goldstein IM, Kaplan HB, Edelson HS, Weissmann G (1979) A new function for

ceruloplasmin as an acute-phase reactant in inflammation: a scavenger of superoxide anion radicals. Trans Assoc Am Physicians 92:360-369.

Gordon N (2003) Iron deficiency and the intellect. Brain Dev 25:3-8.

Graham DG (1978) Oxidative pathways for catecholamines in the genesis of neuromelanin and cytotoxic quinones. Mol Pharmacol 14:633-643.

Griffiths WJ, Cox TM (2003) Co-localization of the mammalian hemochromatosis gene product (HFE) and a newly identified transferrin receptor (TfR2) in intestinal tissue and cells. J Histochem Cytochem 51:613-624.

Groc L, Bezin L, Foster JA, Jiang H, Jackson TS, Weissmann D, Levine RA (2001) Lipid peroxidation-mediated oxidative stress and dopamine neuronal apoptosis in the substantia nigra during development. Neurochem Int 39:127-133.

Gruenheid S, Canonne-Hergaux F, Gauthier S, Hackam DJ, Grinstein S, Gros P (1999) The iron transport protein NRAMP2 is an integral membrane glycoprotein that colocalizes with transferrin in recycling endosomes. J Exp Med 189:831-841.

Grunblatt E, Mandel S, Youdim MB (2000) Neuroprotective strategies in Parkinson's disease using the models of 6-hydroxydopamine and MPTP. Ann N Y Acad Sci 899:262-273.

Gu M, Gash MT, Cooper JM, Wenning GK, Daniel SE, Quinn NP, Marsden CD, Schapira AH (1997) Mitochondrial respiratory chain function in multiple system atrophy. Mov Disord 12:418-422.

Guerrini R, Capasso A, Marastoni M, Bryant SD, Cooper PS, Lazarus LH, Temussi PA, Salvadori S (1998) Rational design of dynorphin A analogues with delta-receptor selectivity and antagonism for delta- and kappa-receptors. Bioorg Med Chem 6:57-62.

Gunshin H, Mackenzie B, Berger UV, Gunshin Y, Romero MF, Boron WF, Nussberger S, Gollan JL, Hediger MA (1997) Cloning and characterization of a mammalian proton-coupled metal-ion transporter. Nature 388:482-488.

Gunshin H, Allerson CR, Polycarpou-Schwarz M, Rofts A, Rogers JT, Kishi F, Hentze MW, Rouault TA, Andrews NC, Hediger MA (2001) Iron-dependent regulation of the divalent metal ion transporter. FEBS Lett 509:309-316.

Gutteridge JM (1983) Antioxidant properties of caeruloplasmin towards iron- and copper-dependent oxygen radical formation. FEBS Lett 157:37-40.

Haidari M, Javadi E, Sanati A, Hajilooi M, Ghanbili J (2001) Association of increased ferritin with premature coronary stenosis in men. Clin Chem 47:1666-1672.

Haile DJ (1999) Regulation of genes of iron metabolism by the iron-response proteins. Am J Med Sci 318:230-240.

Han O, Wessling-Resnick M (2002) Copper repletion enhances apical iron uptake and transepithelial iron transport by Caco-2 cells. Am J Physiol Gastrointest Liver Physiol 282:G527-533.

Han O, Fleet JC, Wood RJ (1999) Reciprocal regulation of HFE and NNamp2 gene expression by iron in human intestinal cells. J Nutr 129:98-104.

Hannuksela J, Parkkila S, Waheed A, Britton RS, Fleming RE, Bacon BR, Sly WS (2003) Human platelets express hemochromatosis protein (HFE) and transferrin receptor 2. Eur J Haematol 70:201-206.

Harris ZL, Durley AP, Man TK, Gitlin JD (1999) Targeted gene disruption reveals an essential role for ceruloplasmin in cellular iron efflux. Proc Natl Acad Sci U S A 96:10812-10817.

Harris ZL, Takahashi Y, Miyajima H, Serizawa M, MacGillivray RT, Gitlin JD

(1995) Aceruloplasminemia: molecular characterization of this disorder of iron metabolism. Proc Natl Acad Sci U S A 92:2539-2543.

Hellman NE, Kono S, Miyajima H, Gitlin JD (2002) Biochemical analysis of a missense mutation in aceruloplasminemia. J Biol Chem 277:1375-1380.

Hemar A, Olivo JC, Williamson E, Saffrich R, Dotti CG (1997) Dendroaxonal transcytosis of transferrin in cultured hippocampal and sympathetic neurons. J Neurosci 17:9026-9034.

Hilewicz-Grabska M, Zgirski A, Krajewski T, Plonka A (1988) Purification and partial characterization of goose ceruloplasmin. Arch Biochem Biophys 260:18-27.

Hill JM (1985) Iron concentration reduced in ventral pallidum, globus pallidus, and substantia nigra by GABA-transaminase inhibitor, gamma-vinyl GABA. Brain Res 342:18-25.

Hill JM, Switzer RC, 3rd (1984) The regional distribution and cellular localization of iron in the rat brain. Neuroscience 11:595-603.

Hill JM, Ruff MR, Weber RJ, Pert CB (1985) Transferrin receptors in rat brain: neuropeptide-like pattern and relationship to iron distribution. Proc Natl Acad Sci U S A 82:4553-4557.

Horwitz LD, Rosenthal EA (1999) Iron-mediated cardiovascular injury. Vasc Med 4:93-99.

Horwitz LD, Sherman NA, Kong Y, Pike AW, Gobin J, Fennessey PV, Horwitz MA (1998) Lipophilic siderophores of Mycobacterium tuberculosis prevent cardiac reperfusion injury. Proc Natl Acad Sci U S A 95:5263-5268.

Hough CD, Cho KR, Zonderman AB, Schwartz DR, Morin PJ (2001) Coordinately up-regulated genes in ovarian cancer. Cancer Res 61:3869-3876.

Hu J, Connor JR (1996) Demonstration and characterization of the iron regulatory protein in human brain. J Neurochem 67:838-844.

Huang HL, Shaw NS (2002) Role of hypolipidemic drug clofibrate in altering iron regulatory proteins IRP1 and IRP2 activities and hepatic iron metabolism in rats fed a low-iron diet. Toxicol Appl Pharmacol 180:118-128.

Hubert N, Hentze MW (2002) Previously uncharacterized isoforms of divalent metal transporter (DMT)-1: implications for regulation and cellular function. Proc Natl Acad Sci U S A 99:12345-12350.

Huebers H, Csiba E, Huebers E, Finch CA (1985) Molecular advantage of diferric transferrin in delivering iron to reticulocytes: a comparative study. Proc Soc Exp Biol Med 179:222-226.

Huebers HA, Finch CA (1987) The physiology of transferrin and transferrin receptors. Physiol Rev 67:520-582.

Huebers HA, Josephson B, Huebers E, Csiba E, Finch CA (1984) Occupancy of the iron binding sites of human transferrin. Proc Natl Acad Sci U S A 81:4326-4330.

Hunter HN, Fulton DB, Ganz T, Vogel HJ (2002) The solution structure of human hepcidin, a peptide hormone with antimicrobial activity that is involved in iron uptake and hereditary hemochromatosis. J Biol Chem 277:37597-37603.

Ide T, Tsutsui H, Hayashidani S, Kang D, Suematsu N, Nakamura K, Utsumi H, Hamasaki N, Takeshita A (2001) Mitochondrial DNA damage and dysfunction associated with oxidative stress in failing hearts after myocardial infarction. Circ Res 88:529-535.

Ilyin G, Courselaud B, Troadec MB, Pigeon C, Alizadeh M, Leroyer P, Brissot P, Loreal O (2003) Comparative analysis of mouse hepcidin 1 and 2 genes:

evidence for different patterns of expression and co-inducibility during iron overload. FEBS Lett 542:22-26.

Iwanska S, Strusinska D (1978) Copper metabolism in different states of erythropoiesis activity. Acta Physiol Pol 29:465-474.

Jaeger JL, Shimizu N, Gitlin JD (1991) Tissue-specific ceruloplasmin gene expression in the mammary gland. Biochem J 280:671-677.

Jefferies WA, Brandon MR, Hunt SV, Williams AF, Gatter KC, Mason DY (1984) Transferrin receptor on endothelium of brain capillaries. Nature 312:162-163.

Jefferies WA, Food MR, Gabathuler R, Rothenberger S, Yamada T, Yasuhara O, McGeer PL (1996) Reactive microglia specifically associated with amyloid plaques in Alzheimer's disease brain tissue express melanotransferrin. Brain Res 712:122-126.

Jenner P (2003) Oxidative stress in Parkinson's disease. Ann Neurol 53:S26-36; discussion S36-28.

Jenner PG, Brin MF (1998) Levodopa neurotoxicity: experimental studies versus clinical relevance. Neurology 50:S39-43; discussion S44-38.

Jeong SY, David S (2003) GPI-anchored ceruloplasmin is required for iron efflux from cells in the central nervous system. J Biol Chem 12:12.

Jiang DH, Ke Y, Cheng YZ, Ho KP, Qian ZM (2002) Distribution of ferroportin1 protein in different regions of developing rat brain. Dev Neurosci 24:94-98.

Kalaria RN, Sromek SM, Grahovac I, Harik SI (1992) Transferrin receptors of rat and human brain and cerebral microvessels and their status in Alzheimer's disease. Brain Res 585:87-93.

Kalmovarin N, Friedrichs WE, O'Brien HV, Linehan LA, Bowman BH, Yang F (1991) Extrahepatic expression of plasma protein genes during inflammation.

Inflammation 15:369-379.

Kaplan J (1996) Metal transport and unsafe sanctuary sites. J Clin Invest 98:3-4.

Kaplan J (2002) Mechanisms of cellular iron acquisition: another iron in the fire. Cell 111:603-606.

Kaplan J, Kushner JP (2000) Mining the genome for iron. Nature 403:711, 713.

Kawabata H, Germain RS, Vuong PT, Nakamaki T, Said JW, Koeffler HP (2000) Transferrin receptor 2-alpha supports cell growth both in iron-chelated cultured cells and in vivo. J Biol Chem 275:16618-16625.

Kawabata H, Nakamaki T, Ikonomi P, Smith RD, Germain RS, Koeffler HP (2001) Expression of transferrin receptor 2 in normal and neoplastic hematopoietic cells. Blood 98:2714-2719.

Kawabata H, Yang R, Hirama T, Vuong PT, Kawano S, Gombart AF, Koeffler HP (1999) Molecular cloning of transferrin receptor 2. A new member of the transferrin receptor-like family. J Biol Chem 274:20826-20832.

Kawanami T, Kato T, Daimon M, Tominaga M, Sasaki H, Maeda K, Arai S, Shikama Y, Katagiri T (1996) Hereditary caeruloplasmin deficiency: clinicopathological study of a patient. J Neurol Neurosurg Psychiatry 61:506-509.

Ke Y, Ming Qian Z (2003) Iron misregulation in the brain: a primary cause of neurodegenerative disorders. Lancet Neurol 2:246-253.

Ke Y, Chen YY, Chang YZ, Duan XL, Ho KP, Jiang de H, Wang K, Qian ZM (2003) Post-transcriptional expression of DMT1 in the heart of rat. J Cell Physiol 196:124-130.

Ke YC, YY.Chang, YZ.Duan, XL.Ho, KP.Jiang, DH.Wang, K.Qian, ZM (2003) Post-Transcriptional Expression of DMT1 in the Heart of Rat. Journal of

cellular physiology.

Kennard ML, Richardson DR, Gabathuler R, Ponka P, Jefferies WA (1995) A novel iron uptake mechanism mediated by GPI-anchored human p97. Embo J 14:4178-4186.

Klipstein-Grobusch K, Koster JF, Grobbee DE, Lindemans J, Boeing H, Hofman A, Witteman JC (1999) Serum ferritin and risk of myocardial infarction in the elderly: the Rotterdam Study. Am J Clin Nutr 69:1231-1236.

Klomp LW, Gitlin JD (1996) Expression of the ceruloplasmin gene in the human retina and brain: implications for a pathogenic model in aceruloplasminemia. Hum Mol Genet 5:1989-1996.

Klomp LW, Farhangrazi ZS, Dugan LL, Gitlin JD (1996) Ceruloplasmin gene expression in the murine central nervous system. J Clin Invest 98:207-215.

Kluge H, Hartmann W, Mertins B, Wieczorek V (1986) Correlation between protein data in normal lumbar CSF and morphological findings of choroid plexus epithelium: a biochemical corroboration of barrier transport via tight junction pores. J Neurol 233:195-199.

Knopfel M, Schulthess G, Funk F, Hauser H (2000) Characterization of an integral protein of the brush border membrane mediating the transport of divalent metal ions. Biophys J 79:874-884.

Koschinsky ML, Chow BK, Schwartz J, Hamerton JL, MacGillivray RT (1987) Isolation and characterization of a processed gene for human ceruloplasmin. Biochemistry 26:7760-7767.

Koutsilieri E, Scheller C, Grunblatt E, Nara K, Li J, Riederer P (2002) Free radicals in Parkinson's disease. J Neurol 249:II1-5.

Krack P, Poepping M, Weinert D, Schrader B, Deuschl G (2000) Thalamic, pallidal,

or subthalamic surgery for Parkinson's disease? J Neurol 247:II122-134.

Krause A, Neitz S, Magert HJ, Schulz A, Forssmann WG, Schulz-Knappe P, Adermann K (2000) LEAP-1, a novel highly disulfide-bonded human peptide, exhibits antimicrobial activity. FEBS Lett 480:147-150.

Laine F, Ropert M, Lan CL, Loreal O, Bellissant E, Jard C, Pouchard M, Le Treut A, Brissot P (2002) Serum ceruloplasmin and ferroxidase activity are decreased in HFE C282Y homozygote male iron-overloaded patients. J Hepatol 36:60-65.

Lamb DJ, Leake DS (1994) Acidic pH enables caeruloplasmin to catalyse the modification of low-density lipoprotein. FEBS Lett 338:122-126.

Lapper SR, Bolam JP (1992) Input from the frontal cortex and the parafascicular nucleus to cholinergic interneurons in the dorsal striatum of the rat. Neuroscience 51:533-545.

Latunde-Dada GO, Van der Westhuizen J, Vulpe CD, Anderson GJ, Simpson RJ, McKie AT (2002) Molecular and functional roles of duodenal cytochrome B (dcytb) in iron metabolism. Blood Cells Mol Dis 29:356-360.

Le NT, Richardson DR (2002) Ferroportin1: a new iron export molecule? Int J Biochem Cell Biol 34:103-108.

Lee GR, Nacht S, Lukens JN, Cartwright GE (1968) Iron metabolism in copper-deficient swine. J Clin Invest 47:2058-2069.

Lee PL, Gelbart T, West C, Halloran C, Beutler E (1998) The human Nramp2 gene: characterization of the gene structure, alternative splicing, promoter region and polymorphisms. Blood Cells Mol Dis 24:199-215.

Leibman A, Aisen P (1979) Distribution of iron between the binding sites of transferrin in serum: methods and results in normal human subjects. Blood 53:1058-1065.

Levin LA, Geszvain KM (1998) Expression of ceruloplasmin in the retina: induction after optic nerve crush. Invest Ophthalmol Vis Sci 39:157-163.

LeVine SM, Macklin WB (1990) Iron-enriched oligodendrocytes: a reexamination of their spatial distribution. J Neurosci Res 26:508-512.

Levy JE, Jin O, Fujiwara Y, Kuo F, Andrews NC (1999) Transferrin receptor is necessary for development of erythrocytes and the nervous system. Nat Genet 21:396-399.

Li H, Qian ZM (2002) Transferrin/transferrin receptor-mediated drug delivery. Med Res Rev 22:225-250.

Li H, Sun H, Qian ZM (2002) The role of the transferrin-transferrin-receptor system in drug delivery and targeting. Trends Pharmacol Sci 23:206-209.

Li H, Li F, Sun H, Qian ZM (2003a) Membrane-inserted conformation of transmembrane domain4 of divalent metal transporter. Biochem J 19.

Li H, Li F, Sun H, Qian ZM (2003b) Membrane-inserted conformation of transmembrane domain 4 of divalent-metal transporter. Biochem J 372:757-766.

Lieu PT, Heiskala M, Peterson PA, Yang Y (2001) The roles of iron in health and disease. Mol Aspects Med 22:1-87.

Linder MC, Moor JR (1977) Plasma ceruloplasmin. Evidence for its presence in and uptake by heart and other organs of the rat. Biochim Biophys Acta 499:329-336.

Linder MC, Zerounian NR, Moriya M, Malpe R (2003) Iron and copper homeostasis and intestinal absorption using the Caco2 cell model. Biometals 16:145-160.

Liu Y, Peterson DA, Kimura H, Schubert D (1997) Mechanism of cellular 3-(4,5-dimethylthiazol-2-yl)-2,5-diphenyltetrazolium bromide (MTT) reduction. J Neurochem 69:581-593.

Loeffler DA, Sima AA, LeWitt PA (2001) Ceruloplasmin immunoreactivity in

neurodegenerative disorders. Free Radic Res 35:111-118.

Loeffler DA, DeMaggio AJ, Juneau PL, Brickman CM, Mashour GA, Finkelman JH, Pomara N, LeWitt PA (1994) Ceruloplasmin is increased in cerebrospinal fluid in Alzheimer's disease but not Parkinson's disease. Alzheimer Dis Assoc Disord 8:190-197.

Loeffler DA, Connor JR, Juneau PL, Snyder BS, Kanaley L, DeMaggio AJ, Nguyen H, Brickman CM, LeWitt PA (1995) Transferrin and iron in normal, Alzheimer's disease, and Parkinson's disease brain regions. J Neurochem 65:710-724.

Loeffler DA, LeWitt PA, Juneau PL, Sima AA, Nguyen HU, DeMaggio AJ, Brickman CM, Brewer GJ, Dick RD, Troyer MD, Kanaley L (1996) Increased regional brain concentrations of ceruloplasmin in neurodegenerative disorders. Brain Res 738:265-274.

Logan JI (1996) Hereditary deficiency of ferroxidase (aka caeruloplasmin). J Neurol Neurosurg Psychiatry 61:431-432.

Loske C, Gerdemann A, Schepl W, Wycislo M, Schinzel R, Palm D, Riederer P, Munch G (2000) Transition metal-mediated glycoxidation accelerates cross-linking of beta-amyloid peptide. Eur J Biochem 267:4171-4178.

Lynch T, Cherny RA, Bush AI (2000) Oxidative processes in Alzheimer's disease: the role of abeta-metal interactions. Exp Gerontol 35:445-451.

Machonkin TE, Musci G, Zhang HH, Bonaccorsi di Patti MC, Calabrese L, Hedman B, Hodgson KO, Solomon EI (1999) Investigation of the anomalous spectroscopic features of the copper sites in chicken ceruloplasmin: comparison to human ceruloplasmin. Biochemistry 38:11093-11102.

Mainero A, Aguilar A, Rodarte B, Pedraza-Chaverri J (1996) Rabbit ceruloplasmin:

purification and partial characterization. Prep Biochem Biotechnol 26:217-228.

Malecki EA, Devenyi AG, Beard JL, Connor JR (1999) Existing and emerging mechanisms for transport of iron and manganese to the brain. J Neurosci Res 56:113-122.

Manis J (1971) Intestinal iron-transport defect in the mouse with sex-linked anemia. Am J Physiol 220:135-139.

Manolis A, Cox DW (1980) Purification of rat ceruloplasmin. characterization and comparison with human ceruloplasmin. Prep Biochem 10:121-132.

Manthorpe M, Adler R, Varon S (1979) Development, reactivity and GFA immunofluorescence of astroglia-containing monolayer cultures from rat cerebrum. J Neurocytol 8:605-621.

Martin WR, Ye FQ, Allen PS (1998) Increasing striatal iron content associated with normal aging. Mov Disord 13:281-286.

Martini LA, Tchack L, Wood RJ (2002) Iron treatment downregulates DMT1 and IREG1 mRNA expression in Caco-2 cells. J Nutr 132:693-696.

Mash DC, Pablo J, Flynn DD, Efange SM, Weiner WJ (1990) Characterization and distribution of transferrin receptors in the rat brain. J Neurochem 55:1972-1979.

Mason DY, Sammons R (1978) Alkaline phosphatase and peroxidase for double immunoenzymatic labelling of cellular constituents. J Clin Pathol 31:454-460.

Mazumder B, Fox PL (1999) Delayed translational silencing of ceruloplasmin transcript in gamma interferon-activated U937 monocytic cells: role of the 3' untranslated region. Mol Cell Biol 19:6898-6905.

McGeorge AJ, Faull RL (1989) The organization of the projection from the cerebral cortex to the striatum in the rat. Neuroscience 29:503-537.

McKie AT, Marciani P, Rolfs A, Brennan K, Wehr K, Barrow D, Miret S, Bomford

A, Peters TJ, Farzaneh F, Hediger MA, Hentze MW, Simpson RJ (2000) A novel duodenal iron-regulated transporter, IREG1, implicated in the basolateral transfer of iron to the circulation. Mol Cell 5:299-309.

McKie AT, Barrow D, Latunde-Dada GO, Rolfs A, Sager G, Mudaly E, Mudaly M, Richardson C, Barlow D, Bomford A, Peters TJ, Raja KB, Shirali S, Hediger MA, Farzaneh F, Simpson RJ (2001) An iron-regulated ferric reductase associated with the absorption of dietary iron. Science 291:1755-1759.

Medda R, Cara N, Floris G (1987) Horse plasma ceruloplasmin molecular weight and subunit analysis. Prep Biochem 17:447-454.

Migliore L, Petrozzi L, Lucetti C, Gambaccini G, Bernardini S, Scarpato R, Trippi F, Barale R, Frenzilli G, Rodilla V, Bonuccelli U (2002) Oxidative damage and cytogenetic analysis in leukocytes of Parkinson's disease patients. Neurology 58:1809-1815.

Miskimins WK, McClelland A, Roberts MP, Ruddle FH (1986) Cell proliferation and expression of the transferrin receptor gene: promoter sequence homologies and protein interactions. J Cell Biol 103:1781-1788.

Mittal B, Doroudchi MM, Jeong SY, Patel BN, David S (2003) Expression of a membrane-bound form of the ferroxidase ceruloplasmin by leptomeningeal cells. Glia 41:337-346.

Miura T, Muraoka S, Ogiso T (1993) Adriamycin-induced lipid peroxidation of erythrocyte membranes in the presence of ferritin and the inhibitory effect of ceruloplasmin. Biol Pharm Bull 16:664-667.

Miyajima H, Nishimura Y, Mizoguchi K, Sakamoto M, Shimizu T, Honda N (1987) Familial apoceruloplasmin deficiency associated with blepharospasm and retinal degeneration. Neurology 37:761-767.

Mollgard K, Stagaard M, Saunders NR (1987) Cellular distribution of transferrin immunoreactivity in the developing rat brain. Neurosci Lett 78:35-40.

Mollgard K, Dziegielewska KM, Saunders NR, Zakut H, Soreq H (1988) Synthesis and localization of plasma proteins in the developing human brain. Integrity of the fetal blood-brain barrier to endogenous proteins of hepatic origin. Dev Biol 128:207-221.

Moos T (1996) Immunohistochemical localization of intraneuronal transferrin receptor immunoreactivity in the adult mouse central nervous system. J Comp Neurol 375:675-692.

Moos T, Morgan EH (1998a) Evidence for low molecular weight, non-transferrin-bound iron in rat brain and cerebrospinal fluid. J Neurosci Res 54:486-494.

Moos T, Morgan EH (1998b) Kinetics and distribution of [59Fe-125I]transferrin injected into the ventricular system of the rat. Brain Res 790:115-128.

Moos T, Morgan EH (2000) Transferrin and transferrin receptor function in brain barrier systems. Cell Mol Neurobiol 20:77-95.

Moos T, Morgan EH (2002) A morphological study of the developmentally regulated transport of iron into the brain. Dev Neurosci 24:99-105.

Moos T, Trinder D, Morgan EH (2000) Cellular distribution of ferric iron, ferritin, transferrin and divalent metal transporter 1 (DMT1) in substantia nigra and basal ganglia of normal and beta2-microglobulin deficient mouse brain. Cell Mol Biol (Noisy-le-grand) 46:549-561.

Moos T, Oates PS, Morgan EH (2001) Expression of transferrin mRNA in rat oligodendrocytes is iron-independent and changes with increasing age. Nutr Neurosci 4:15-23.

Morell AG, Irvine RA, Sternlieb I, Scheinberg IH, Ashwell G (1968) Physical and chemical studies on ceruloplasmin. V. Metabolic studies on sialic acid-free ceruloplasmin in vivo. J Biol Chem 243:155-159.

Morgan EH (1983) Effect of pH and iron content of transferrin on its binding to reticulocyte receptors. Biochim Biophys Acta 762:498-502.

Morgan EH (1988) Membrane transport of non-transferrin-bound iron by reticulocytes. Biochim Biophys Acta 943:428-439.

Morris CM, Candy JM, Bloxham CA, Edwardson JA (1990) Brain transferrin receptors and the distribution of cytochrome oxidase. Biochem Soc Trans 18:647-648.

Morris CM, Candy JM, Oakley AE, Taylor GA, Mountfort S, Bishop H, Ward MK, Bloxham CA, Edwardson JA (1989) Comparison of the regional distribution of transferrin receptors and aluminium in the forebrain of chronic renal dialysis patients. J Neurol Sci 94:295-306.

Morris CM, Candy JM, Keith AB, Oakley AE, Taylor GA, Pullen RG, Bloxham CA, Gocht A, Edwardson JA (1992) Brain iron homeostasis. J Inorg Biochem 47:257-265.

Mukhopadhyay CK, Ehrenwald E, Fox PL (1996) Ceruloplasmin enhances smooth muscle cell- and endothelial cell-mediated low density lipoprotein oxidation by a superoxide-dependent mechanism. J Biol Chem 271:14773-14778.

Mukhopadhyay CK, Attieh ZK, Fox PL (1998) Role of ceruloplasmin in cellular iron uptake. Science 279:714-717.

Mukhopadhyay CK, Mazumder B, Fox PL (2000) Role of hypoxia-inducible factor-1 in transcriptional activation of ceruloplasmin by iron deficiency. J Biol Chem 275:21048-21054.

Musci G, Bonaccorsi di Patti MC, Calabrese L (1993a) The state of the copper sites in human ceruloplasmin. Arch Biochem Biophys 306:111-118.

Musci G, Polticelli F, Calabrese L (1999) Structure/function relationships in ceruloplasmin. Adv Exp Med Biol 448:175-182.

Musci G, Bonaccorsi di Patti MC, Fagiolo U, Calabrese L (1993b) Age-related changes in human ceruloplasmin. Evidence for oxidative modifications. J Biol Chem 268:13388-13395.

Musci G, Carbonaro M, Adriani A, Lania A, Galtieri A, Calabrese L (1990) Unusual stability properties of a reptilian ceruloplasmin. Arch Biochem Biophys 279:8-13.

Nakamura K, Endo F, Ueno T, Awata H, Tanoue A, Matsuda I (1995) Excess copper and ceruloplasmin biosynthesis in long-term cultured hepatocytes from Long-Evans Cinnamon (LEC) rats, a model of Wilson disease. J Biol Chem 270:7656-7660.

Nakane PK, Pierce GB, Jr. (1967) Enzyme-labeled antibodies for the light and electron microscopic localization of tissue antigens. J Cell Biol 33:307-318.

Nemeth E, Valore EV, Territo M, Schiller G, Lichtenstein A, Ganz T (2003) Hepcidin, a putative mediator of anemia of inflammation, is a type II acute-phase protein. Blood 101:2461-2463.

Nicolas G, Bennoun M, Devaux I, Beaumont C, Grandchamp B, Kahn A, Vaulont S (2001) Lack of hepcidin gene expression and severe tissue iron overload in upstream stimulatory factor 2 (USF2) knockout mice. Proc Natl Acad Sci U S A 98:8780-8785.

Nicolas G, Chauvet C, Viatte L, Danan JL, Bigard X, Devaux I, Beaumont C, Kahn A, Vaulont S (2002) The gene encoding the iron regulatory peptide hepcidin is

regulated by anemia, hypoxia, and inflammation. J Clin Invest 110:1037-1044.

Okuyama E, Yamamoto R, Ichikawa Y, Tsubaki M (1998) Structural basis for the electron transfer across the chromaffin vesicle membranes catalyzed by cytochrome b561: analyses of cDNA nucleotide sequences and visible absorption spectra. Biochim Biophys Acta 1383:269-278.

Olson JE, Holtzman D (1980) Respiration in rat cerebral astrocytes from primary culture. J Neurosci Res 5:497-506.

Osaki S (1966) Kinetic studies of ferrous ion oxidation with crystalline human ferroxidase (ceruloplasmin). J Biol Chem 241:5053-5059.

Osaki S, Johnson DA, Frieden E (1966) The possible significance of the ferrous oxidase activity of ceruloplasmin in normal human serum. J Biol Chem 241:2746-2751.

Oshiro S, Kawahara M, Kuroda Y, Zhang C, Cai Y, Kitajima S, Shirao M (2000) Glial cells contribute more to iron and aluminum accumulation but are more resistant to oxidative stress than neuronal cells. Biochim Biophys Acta 1502:405-414.

Owen AD, Schapira AH, Jenner P, Marsden CD (1996) Oxidative stress and Parkinson's disease. Ann N Y Acad Sci 786:217-223.

Owen D, Kuhn LC (1987) Noncoding 3' sequences of the transferrin receptor gene are required for mRNA regulation by iron. Embo J 6:1287-1293.

Pan Y, Katula K, Failla ML (1996) Expression of ceruloplasmin gene in human and rat lymphocytes. Biochim Biophys Acta 1307:233-238.

Pan Y, DeFay T, Gitschier J, Cohen FE (1995) Proposed structure of the A domains of factor VIII by homology modelling. Nat Struct Biol 2:740-744.

Pardridge WM, Eisenberg J, Yang J (1987) Human blood-brain barrier transferrin

receptor. Metabolism 36:892-895.

Park CH, Valore EV, Waring AJ, Ganz T (2001) Hepcidin, a urinary antimicrobial peptide synthesized in the liver. J Biol Chem 276:7806-7810.

Parkkila S, Waheed A, Britton RS, Bacon BR, Zhou XY, Tomatsu S, Fleming RE, Sly WS (1997) Association of the transferrin receptor in human placenta with HFE, the protein defective in hereditary hemochromatosis. Proc Natl Acad Sci U S A 94:13198-13202.

Patel BN, David S (1997) A novel glycosylphosphatidylinositol-anchored form of ceruloplasmin is expressed by mammalian astrocytes. J Biol Chem 272:20185-20190.

Patel BN, Dunn RJ, David S (2000) Alternative RNA splicing generates a glycosylphosphatidylinositol-anchored form of ceruloplasmin in mammalian brain. J Biol Chem 275:4305-4310.

Patel BN, Dunn RJ, Jeong SY, Zhu Q, Julien JP, David S (2002) Ceruloplasmin regulates iron levels in the CNS and prevents free radical injury. J Neurosci 22:6578-6586.

Percival SS, Harris ED (1990) Copper transport from ceruloplasmin: characterization of the cellular uptake mechanism. Am J Physiol 258:C140-146.

Pereira AC, Cuoco MA, Mota GF, da Silva FF, Freitas HF, Bocchi EA, Soler JM, Mansur AJ, Krieger JE (2001) Hemochromatosis gene variants in patients with cardiomyopathy. Am J Cardiol 88:388-391.

Persijn JP, van der Slik W, Riethorst A (1971) Determination of serum iron and latent iron-binding capacity (LIBC). Clin Chim Acta 35:91-98.

Picard V, Govoni G, Jabado N, Gros P (2000) Nramp 2 (DCT1/DMT1) expressed at the plasma membrane transports iron and other divalent cations into a

calcein-accessible cytoplasmic pool. J Biol Chem 275:35738-35745.

Pigeon C, Ilyin G, Courselaud B, Leroyer P, Turlin B, Brissot P, Loreal O (2001) A new mouse liver-specific gene, encoding a protein homologous to human antimicrobial peptide hepcidin, is overexpressed during iron overload. J Biol Chem 276:7811-7819.

Pinero DJ, Hu J, Connor JR (2000a) Alterations in the interaction between iron regulatory proteins and their iron responsive element in normal and Alzheimer's diseased brains. Cell Mol Biol (Noisy-le-grand) 46:761-776.

Pinero DJ, Li NQ, Connor JR, Beard JL (2000b) Variations in dietary iron alter brain iron metabolism in developing rats. J Nutr 130:254-263.

Pinkerton PH, Bannerman RM (1967) Hereditary defect in iron absorption in mice. Nature 216:482-483.

Ponka P, Lok CN (1999) The transferrin receptor: role in health and disease. Int J Biochem Cell Biol 31:1111-1137.

Puchkova LV, Aleinikova TD, Zakharova ET, Konopistseva LA, Tsymbalenko NV, Gaitskoki VS (1994) [Regulation of biosynthesis of molecular forms of ceruloplasmin in rat ontogenesis]. Biokhimiia 59:1304-1311.

Qian ZM, Morgan EH (1990) Effect of lead on the transport of transferrin-free and transferrin-bound iron into rabbit reticulocytes. Biochem Pharmacol 40:1049-1054.

Qian ZM, Morgan EH (1991) Effect of metabolic inhibitors on uptake of non-transferrin-bound iron by reticulocytes. Biochim Biophys Acta 1073:456-462.

Qian ZM, Morgan EH (1992) Changes in the uptake of transferrin-free and transferrin-bound iron during reticulocyte maturation in vivo and in vitro.

Biochim Biophys Acta 1135:35-43.

Qian ZM, Tang PL (1995) Mechanisms of iron uptake by mammalian cells. Biochim Biophys Acta 1269:205-214.

Qian ZM, Wang Q (1998) Expression of iron transport proteins and excessive iron accumulation in the brain in neurodegenerative disorders. Brain Res Brain Res Rev 27:257-267.

Qian ZM, Ke Y (2001) Rethinking the role of ceruloplasmin in brain iron metabolism. Brain Res Brain Res Rev 35:287-294.

Qian ZM, Shen X (2001) Brain iron transport and neurodegeneration. Trends Mol Med 7:103-108.

Qian ZM, Pu YM, Tang PL, Wang Q (1998) Transferrin-bound iron uptake by the cultured cerebellar granule cells. Neurosci Lett 251:9-12.

Qian ZM, To Y, Tang PL, Feng YM (1999a) Transferrin receptors on the plasma membrane of cultured rat astrocytes. Exp Brain Res 129:473-476.

Qian ZM, Tsoi YK, Ke Y, Wong MS (2001a) Ceruloplasmin promotes iron uptake rather than release in BT325 cells. Exp Brain Res 140:369-374.

Qian ZM, Xiao DS, Ke Y, Liao QK (2001b) Increased nitric oxide is one of the causes of changes of iron metabolism in strenuously exercised rats. Am J Physiol Regul Integr Comp Physiol 280:R739-743.

Qian ZM, Li H, Sun H, Ho K (2002) Targeted Drug Delivery via the Transferrin Receptor-Mediated Endocytosis Pathway. Pharmacol Rev 54:561-587.

Qian ZM, Xiao DS, Tang PL, Yao FY, Liao QK (1999b) Increased expression of transferrin receptor on membrane of erythroblasts in strenuously exercised rats. J Appl Physiol 87:523-529.

Qian ZM, Liao QK, To Y, Ke Y, Tsoi YK, Wang GF, Ho KP (2000)

Transferrin-bound and transferrin free iron uptake by cultured rat astrocytes. Cell Mol Biol (Noisy-le-grand) 46:541-548.

Reilly CA, Aust SD (1998) Iron loading into ferritin by an intracellular ferroxidase. Arch Biochem Biophys 359:69-76.

Richardson DR, Ponka P (1997) The molecular mechanisms of the metabolism and transport of iron in normal and neoplastic cells. Biochim Biophys Acta 1331:1-40.

Roetto A, Totaro A, Piperno A, Piga A, Longo F, Garozzo G, Cali A, De Gobbi M, Gasparini P, Camaschella C (2001) New mutations inactivating transferrin receptor 2 in hemochromatosis type 3. Blood 97:2555-2560.

Rolfs A, Bonkovsky HL, Kohlroser JG, McNeal K, Sharma A, Berger UV, Hediger MA (2002) Intestinal expression of genes involved in iron absorption in humans. Am J Physiol Gastrointest Liver Physiol 282:G598-607.

Rosei MA, Foppoli C, Wang XT, Coccia R, Mateescu MA (1998) Production of melanins by ceruloplasmin. Pigment Cell Res 11:98-102.

Roskams AJ, Connor JR (1994) Iron, transferrin, and ferritin in the rat brain during development and aging. J Neurochem 63:709-716.

Roth JA, Horbinski C, Feng L, Dolan KG, Higgins D, Garrick MD (2000) Differential localization of divalent metal transporter 1 with and without iron response element in rat PC12 and sympathetic neuronal cells. J Neurosci 20:7595-7601.

Roy CN, Andrews NC (2001) Recent advances in disorders of iron metabolism: mutations, mechanisms and modifiers. Hum Mol Genet 10:2181-2186.

Russell ES (1979) Hereditary anemias of the mouse: a review for geneticists. Adv Genet 20:357-459.

Ryan TP, Grover TA, Aust SD (1992) Rat ceruloplasmin: resistance to proteolysis and kinetic comparison with human ceruloplasmin. Arch Biochem Biophys 293:1-8.

Ryden L (1972) Comparison of polypeptide-chain structure of four mammalian ceruloplasmins by gel filtration in guanidine hydrochloride solutions. Eur J Biochem 28:46-50.

Ryu JK, Shin WH, Kim J, Joe EH, Lee YB, Cho KG, Oh YJ, Kim SU, Jin BK (2002) Trisialoganglioside GT1b induces in vivo degeneration of nigral dopaminergic neurons: role of microglia. Glia 38:15-23.

Saenko EL, Skorobogat'ko OV, Tarasenko P, Romashko V, Zhuravetz L, Zadorozhnaya L, Senjuk OF, Yaropolov AI (1994) Modulatory effects of ceruloplasmin on lymphocytes, neutrophils and monocytes of patients with altered immune status. Immunol Invest 23:99-114.

Sakakibara S, Aoyama Y (2002) Dietary iron-deficiency up-regulates hephaestin mRNA level in small intestine of rats. Life Sci 70:3123-3129.

Salzer JL, Lovejoy L, Linder MC, Rosen C (1998) Ran-2, a glial lineage marker, is a GPI-anchored form of ceruloplasmin. J Neurosci Res 54:147-157.

Sampath P, Mazumder B, Seshadri V, Fox PL (2003) Transcript-selective translational silencing by gamma interferon is directed by a novel structural element in the ceruloplasmin mRNA 3' untranslated region. Mol Cell Biol 23:1509-1519.

Sanger F, Nicklen S, Coulson AR (1992) DNA sequencing with chain-terminating inhibitors. 1977. Biotechnology 24:104-108.

Sastry S, Arendash GW (1995) Time-dependent changes in iron levels and associated neuronal loss within the substantia nigra following lesions within the

neostriatum/globus pallidus complex. Neuroscience 67:649-666.

Sato M, Schilsky ML, Stockert RJ, Morell AG, Sternlieb I (1990) Detection of multiple forms of human ceruloplasmin. A novel Mr 200,000 form. J Biol Chem 265:2533-2537.

Schapira AH, Mann VM, Cooper JM, Dexter D, Daniel SE, Jenner P, Clark JB, Marsden CD (1990) Anatomic and disease specificity of NADH CoQ1 reductase (complex I) deficiency in Parkinson's disease. J Neurochem 55:2142-2145.

Schipper HM (1996) Astrocytes, brain aging, and neurodegeneration. Neurobiol Aging 17:467-480.

Senra Varela A, Lopez Saez JJ, Quintela Senra D (1997) Serum ceruloplasmin as a diagnostic marker of cancer. Cancer Lett 121:139-145.

Seshadri V, Fox PL, Mukhopadhyay CK (2002) Dual role of insulin in transcriptional regulation of the acute phase reactant ceruloplasmin. J Biol Chem 277:27903-27911.

Shike H, Lauth X, Westerman ME, Ostland VE, Carlberg JM, Van Olst JC, Shimizu C, Bulet P, Burns JC (2002) Bass hepcidin is a novel antimicrobial peptide induced by bacterial challenge. Eur J Biochem 269:2232-2237.

Shoham S, Wertman E, Ebstein RP (1992) Iron accumulation in the rat basal ganglia after excitatory amino acid injections--dissociation from neuronal loss. Exp Neurol 118:227-241.

Shreffler DC, Brewer GJ, Gall JC, Honeyman MS (1967) Electrophoretic variation in human serum ceruloplasmin: a new genetic polymorphism. Biochem Genet 1:101-115.

Simovich MJ, Conrad ME, Umbreit JN, Moore EG, Hainsworth LN, Smith HK

(2002) Cellular location of proteins related to iron absorption and transport. Am J Hematol 69:164-170.

Simuni T, Stern MB (1999) Does levodopa accelerate Parkinson's disease? Drugs Aging 14:399-408.

Sipe JC, Lee P, Beutler E (2002) Brain iron metabolism and neurodegenerative disorders. Dev Neurosci 24:188-196.

Sofic E, Riederer P, Heinsen H, Beckmann H, Reynolds GP, Hebenstreit G, Youdim MB (1988) Increased iron (III) and total iron content in post mortem substantia nigra of parkinsonian brain. J Neural Transm 74:199-205.

Song Y, Levenson CW (1997) Regulation of ceruloplasmin by retinoic acid in the developing rat. Int J Vitam Nutr Res 67:141-144.

St Pierre TG, Richardson DR, Baker E, Webb J (1992) A low-spin iron complex in human melanoma and rat hepatoma cells and a high-spin iron(II) complex in rat hepatoma cells. Biochim Biophys Acta 1135:154-158.

Starcher B, Hill CH (1966) Isolation and characterization of induced ceruloplasmin from chicken serum. Biochim Biophys Acta 127:400-406.

Strube YN, Beard JL, Ross AC (2002) Iron deficiency and marginal vitamin A deficiency affect growth, hematological indices and the regulation of iron metabolism genes in rats. J Nutr 132:3607-3615.

Stuart KA, Anderson GJ, Frazer DM, Powell LW, McCullen M, Fletcher LM, Crawford DH (2003) Duodenal expression of iron transport molecules in untreated haemochromatosis subjects. Gut 52:953-959.

Su MA, Trenor CC, Fleming JC, Fleming MD, Andrews NC (1998) The G185R mutation disrupts function of the iron transporter Nramp2. Blood 92:2157-2163.

Subramaniam VN, Summerville L, Wallace DF (2002) Molecular and cellular

characterization of transferrin receptor 2. Cell Biochem Biophys 36:235-239.

Sullivan JL, Zacharski LR (2001) Hereditary haemochromatosis and the hypothesis that iron depletion protects against ischemic heart disease. Eur J Clin Invest 31:375-377.

Swaiman KF (1991) Hallervorden-Spatz syndrome and brain iron metabolism. Arch Neurol 48:1285-1293.

Swaiman KF (2001) Hallervorden-Spatz syndrome. Pediatr Neurol 25:102-108.

Swaiman KF, Machen VL (1985) Iron uptake by glial cells. Neurochem Res 10:1635-1644.

Syed BA, Beaumont NJ, Patel A, Naylor CE, Bayele HK, Joannou CL, Rowe PS, Evans RW, Srai SK (2002) Analysis of the human hephaestin gene and protein: comparative modelling of the N-terminus ecto-domain based upon ceruloplasmin. Protein Eng 15:205-214.

Tabuchi M, Yoshimori T, Yamaguchi K, Yoshida T, Kishi F (2000) Human NRAMP2/DMT1, which mediates iron transport across endosomal membranes, is localized to late endosomes and lysosomes in HEp-2 cells. J Biol Chem 275:22220-22228.

Tabuchi M, Tanaka N, Nishida-Kitayama J, Ohno H, Kishi F (2002) Alternative splicing regulates the subcellular localization of divalent metal transporter 1 isoforms. Mol Biol Cell 13:4371-4387.

Tacchini L, Fusar Poli D, Bernelli-Zazzera A, Cairo G (2002) Transferrin receptor gene expression and transferrin-bound iron uptake are increased during postischemic rat liver reperfusion. Hepatology 36:103-111.

Taher A, Sheikh-Taha M, Koussa S, Inati A, Neeman R, Mourad F (2001) Comparison between deferoxamine and deferiprone (L1) in iron-loaded

thalassemia patients. Eur J Haematol 67:30-34.

Takahashi N, Ortel TL, Putnam FW (1984) Single-chain structure of human ceruloplasmin: the complete amino acid sequence of the whole molecule. Proc Natl Acad Sci U S A 81:390-394.

Takahashi Y, Miyajima H, Shirabe S, Nagataki S, Suenaga A, Gitlin JD (1996) Characterization of a nonsense mutation in the ceruloplasmin gene resulting in diabetes and neurodegenerative disease. Hum Mol Genet 5:81-84.

Tallkvist J, Bowlus CL, Lonnerdal B (2001) DMT1 gene expression and cadmium absorption in human absorptive enterocytes. Toxicol Lett 122:171-177.

Tandy S, Williams M, Leggett A, Lopez-Jimenez M, Dedes M, Ramesh B, Srai SK, Sharp P (2000) Nramp2 expression is associated with pH-dependent iron uptake across the apical membrane of human intestinal Caco-2 cells. J Biol Chem 275:1023-1029.

Tchernitchko D, Bourgeois M, Martin ME, Beaumont C (2002) Expression of the two mRNA isoforms of the iron transporter Nrmap2/DMTI in mice and function of the iron responsive element. Biochem J 363:449-455.

Thomas C, Oates PS (2002) IEC-6 cells are an appropriate model of intestinal iron absorption in rats. J Nutr 132:680-687.

Thomas T, Macpherson A, Rogers P (1995) Ceruloplasmin gene expression in the rat uterus. Biochim Biophys Acta 1261:77-82.

Thompson K, Menzies S, Muckenthaler M, Torti FM, Wood T, Torti SV, Hentze MW, Beard J, Connor J (2003) Mouse brains deficient in H-ferritin have normal iron concentration but a protein profile of iron deficiency and increased evidence of oxidative stress. J Neurosci Res 71:46-63.

Tong X, Kawabata H, Koeffler HP (2002) Iron deficiency can upregulate expression

of transferrin receptor at both the mRNA and protein level. Br J Haematol 116:458-464.

Torrance JD, Bothwell TH (1968) A simple technique for measuring storage iron concentrations in formalinised liver samples. S Afr J Med Sci 33:9-11.

Touret N, Furuya W, Forbes J, Gros P, Grinstein S (2003) Dynamic traffic through the recycling compartment couples the metal transporter Nramp2 (DMT1) with the transferrin receptor. J Biol Chem 30:30.

Townsend A, Drakesmith H (2002) Role of HFE in iron metabolism, hereditary haemochromatosis, anaemia of chronic disease, and secondary iron overload. Lancet 359:786-790.

Tran T, Ashraf M, Jones L, Westbrook T, Hazegh-Azam M, Linder MC (2002) Dietary iron status has little effect on expression of ceruloplasmin but alters that of ferritin in rats. J Nutr 132:351-356.

Trinder D, Zak O, Aisen P (1996) Transferrin receptor-independent uptake of differic transferrin by human hepatoma cells with antisense inhibition of receptor expression. Hepatology 23:1512-1520.

Trinder D, Oates PS, Thomas C, Sadleir J, Morgan EH (2000) Localisation of divalent metal transporter 1 (DMT1) to the microvillus membrane of rat duodenal enterocytes in iron deficiency, but to hepatocytes in iron overload. Gut 46:270-276.

Tuomainen TP, Punnonen K, Nyyssonen K, Salonen JT (1998) Association between body iron stores and the risk of acute myocardial infarction in men. Circulation 97:1461-1466.

Tzonou A, Lagiou P, Trichopoulou A, Tsoutsos V, Trichopoulos D (1998) Dietary iron and coronary heart disease risk: a study from Greece. Am J Epidemiol

147:161-166.

Udenfriend S, Kodukula K (1995) Prediction of omega site in nascent precursor of glycosylphosphatidylinositol protein. Methods Enzymol 250:571-582.

van Rensburg SJ, Potocnik FC, De Villiers JN, Kotze MJ, Taljaard JJ (2000) Earlier age of onset of Alzheimer's disease in patients with both the transferrin C2 and apolipoprotein E-epsilon 4 alleles. Ann N Y Acad Sci 903:200-203.

Venakteshwara Rao M, Khanijo SK, Chande RD, Chouhan SS, Bisarya BN (1975) Serum ceruloplasmin in iron deficiency anaemia. J Assoc Physicians India 23:571-576.

Vidal S, Belouchi AM, Cellier M, Beatty B, Gros P (1995) Cloning and characterization of a second human NRAMP gene on chromosome 12q13. Mamm Genome 6:224-230.

Vogt TM, Blackwell AD, Giannetti AM, Bjorkman PJ, Enns CA (2003) Heterotypic interactions between transferrin receptor and transferrin receptor 2. Blood 101:2008-2014.

Vulpe CD, Kuo YM, Murphy TL, Cowley L, Askwith C, Libina N, Gitschier J, Anderson GJ (1999) Hephaestin, a ceruloplasmin homologue implicated in intestinal iron transport, is defective in the sla mouse. Nat Genet 21:195-199.

Waheed A, Parkkila S, Saarnio J, Fleming RE, Zhou XY, Tomatsu S, Britton RS, Bacon BR, Sly WS (1999) Association of HFE protein with transferrin receptor in crypt enterocytes of human duodenum. Proc Natl Acad Sci U S A 96:1579-1584.

Wang GL, Jiang BH, Rue EA, Semenza GL (1995a) Hypoxia-inducible factor 1 is a basic-helix-loop-helix-PAS heterodimer regulated by cellular O2 tension. Proc Natl Acad Sci U S A 92:5510-5514.

Wang R, Zhang L, Mateescu MA, Nadeau R (1995b) Ceruloplasmin: an endogenous depolarizing factor in neurons? Biochem Biophys Res Commun 207:599-605.

Wang XS, Ong WY, Connor JR (2002) A light and electron microscopic study of divalent metal transporter-1 distribution in the rat hippocampus, after kainate-induced neuronal injury. Exp Neurol 177:193-201.

Wardrop SL, Richardson DR (1999) The effect of intracellular iron concentration and nitrogen monoxide on Nramp2 expression and non-transferrin-bound iron uptake. Eur J Biochem 263:41-49.

Wardrop SL, Wells C, Ravasi T, Hume DA, Richardson DR (2002) Induction of Nramp2 in activated mouse macrophages is dissociated from regulation of the Nramp1, classical inflammatory genes, and genes involved in iron metabolism. J Leukoc Biol 71:99-106.

Weiner AL, Cousins RJ (1983) Hormonally produced changes in caeruloplasmin synthesis and secretion in primary cultured rat hepatocytes. Relationship to hepatic copper metabolism. Biochem J 212:297-304.

Weinstein DA, Roy CN, Fleming MD, Loda MF, Wolfsdorf JI, Andrews NC (2002) Inappropriate expression of hepcidin is associated with iron refractory anemia: implications for the anemia of chronic disease. Blood 100:3776-3781.

Wessling-Resnick M (2000) Iron transport. Annu Rev Nutr 20:129-151.

West AP, Jr., Bennett MJ, Sellers VM, Andrews NC, Enns CA, Bjorkman PJ (2000) Comparison of the interactions of transferrin receptor and transferrin receptor 2 with transferrin and the hereditary hemochromatosis protein HFE. J Biol Chem 275:38135-38138.

West AP, Jr., Giannetti AM, Herr AB, Bennett MJ, Nangiana JS, Pierce JR, Weiner LP, Snow PM, Bjorkman PJ (2001) Mutational analysis of the transferrin

receptor reveals overlapping HFE and transferrin binding sites. J Mol Biol 313:385-397.

Wichmann T, DeLong MR (1996) Functional and pathophysiological models of the basal ganglia. Curr Opin Neurobiol 6:751-758.

Wichmann T, DeLong MR (1999) Oscillations in the basal ganglia. Nature 400:621-622.

Wolf PL (1982) Ceruloplasmin: methods and clinical use. Crit Rev Clin Lab Sci 17:229-245.

Xie JX, Tsoi YK, Chang YZ, Ke Y, Qian ZM (2002) Effects of ferroxidase activity and species on ceruloplasmin mediated iron uptake by BT325 cells. Brain Res Mol Brain Res 99:12-16.

Xu J, Ling EA (1994) Studies of the ultrastructure and permeability of the blood-brain barrier in the developing corpus callosum in postnatal rat brain using electron dense tracers. J Anat 184:227-237.

Yamaguchi-Iwai Y, Dancis A, Klausner RD (1995) AFT1: a mediator of iron regulated transcriptional control in Saccharomyces cerevisiae. Embo J 14:1231-1239.

Yamamoto K, Yoshida K, Miyagoe Y, Ishikawa A, Hanaoka K, Nomoto S, Kaneko K, Ikeda S, Takeda S (2002) Quantitative evaluation of expression of iron-metabolism genes in ceruloplasmin-deficient mice. Biochim Biophys Acta 1588:195-202.

Yang F, Wang X, Haile DJ, Piantadosi CA, Ghio AJ (2002) Iron increases expression of iron-export protein MTP1 in lung cells. Am J Physiol Lung Cell Mol Physiol 283:L932-939.

Yang F, Friedrichs WE, deGraffenried L, Herbert DC, Weaker FJ, Bowman BH,

Coalson JJ (1996) Cellular expression of ceruloplasmin in baboon and mouse lung during development and inflammation. Am J Respir Cell Mol Biol 14:161-169.

Yeh KY, Yeh M, Watkins JA, Rodriguez-Paris J, Glass J (2000) Dietary iron induces rapid changes in rat intestinal divalent metal transporter expression. Am J Physiol Gastrointest Liver Physiol 279:G1070-1079.

Yoshida K, Furihata K, Takeda S, Nakamura A, Yamamoto K, Morita H, Hiyamuta S, Ikeda S, Shimizu N, Yanagisawa N (1995) A mutation in the ceruloplasmin gene is associated with systemic hemosiderosis in humans. Nat Genet 9:267-272.

Young SP, Bomford A, Williams R (1984) The effect of the iron saturation of transferrin on its binding and uptake by rabbit reticulocytes. Biochem J 219:505-510.

Zahs KR, Bigornia V, Deschepper CF (1993) Characterization of "plasma proteins" secreted by cultured rat macroglial cells. Glia 7:121-133.

Zaitsev VN, Zaitseva I, Papiz M, Lindley PF (1999) An X-ray crystallographic study of the binding sites of the azide inhibitor and organic substrates to ceruloplasmin, a multi-copper oxidase in the plasma. J Biol Inorg Chem 4:579-587.

Zaman AK, Fujii S, Sawa H, Goto D, Ishimori N, Watano K, Kaneko T, Furumoto T, Sugawara T, Sakuma I, Kitabatake A, Sobel BE (2001) Angiotensin-converting enzyme inhibition attenuates hypofibrinolysis and reduces cardiac perivascular fibrosis in genetically obese diabetic mice. Circulation 103:3123-3128.

Zoller H, Theurl I, Koch R, Kaser A, Weiss G (2002) Mechanisms of iron mediated regulation of the duodenal iron transporters divalent metal transporter 1 and

ferroportin 1. Blood Cells Mol Dis 29:488-497.

Zywicke HA, van Gelderen P, Connor JR, Burdo JR, Garrick MD, Dolan KG, Frank JA, Bulte JW (2002) Microscopic R2* mapping of reduced brain iron in the Belgrade rat. Ann Neurol 52:102-105.